MICROARRAY ANALYSIS OF DIFFERENTIAL EXPRESSION OF GENES IN SHOOT APEX AND YOUNG LEAF OF ENGLISH IVY (*HEDERA HELIX* L. CV. GOLDHEART)

Seung-Geuk Shin

A Dissertation

Submitted to the Graduate College of Bowling Green
State University in partial fulfillment of
the requirements for the degree of

DOCTOR OF PHILOSOPHY

August 2010

Committee:

Dr. Scott O. Rogers, Advisor

Dr. Kit C. Chan
Graduate Faculty Representative

Dr. Carmen F. Fioravanti

Dr. Helen Michaels

Dr. Paul F. Morris

ABSTRACT

Scott O. Rogers, Advisor

Shoot apical meristems (SAMs) of higher plants maintain a population of pluripotent cells which continue to divide throughout the life of plant and provide cells for development of all the above-ground organs after embryogenesis. Since the plant is sessile, maintenance of stem cells in the SAM and appropriate differentiation are crucial for the plants to adapt to the changing environments. Shoot apex of the plant is the very tip of the shoot, in which the SAM resides. To analyze the differential gene expression patterns between the shoot apex and the very young leaf, transcriptomes from the two tissue types of a variegated variety of English ivy (*Hedera helix* L. cv. Goldheart) plants, were hybridized on *Arabidopsis thaliana* cDNA microarrays, using cross-species hybridization (CSH). Among 11,255 cDNA probes excluding 'BLANK' and 'bad' spots, 2,597 features produced signals that were greater than background levels, which constitutes 23% of the total number of usable probes on the microarray. One hundred seventy four genes were expressed statistically differentially (fold change >=2 and p=0.05). Of these, 60 were in the shoot apex and 114 were in the young leaf. Functional categorization based on the genome/protein databases and a pathway analysis revealed some of the tissue-specific biological processes and identified some of the genes involved. The annotated and/or predicted roles of those genes in the tissue-specific biological processes were described and discussed in relation to the plant development.

I dedicate this dissertation to my parents, wife and daughter.
Without their patience, encouragement, support, and most of all love, the completion of this work would not have been possible.

ACKNOWLEDGEMENTS

This dissertation would not be complete without expressing the deepest appreciation to my academic advisor, Professor Scott Orland Rogers, who continually and patiently supported me from the initiation to the end of this research project. Without his guidance and persistent help this dissertation would not have been possible.

I would like to thank my dissertation committee members, Professor Carmen F. Fioravanti, Professor Helen Michaels and Professor Paul F. Morris whose productive suggestions and recommendations broadened my view on the subject. In addition, I thank Professor Kit C. Chan, the Graduate Faculty Representative, who warmly welcomed and chaired committee meetings.

Special thanks are reserved for the late Muwydang Sir Chang Il Soon, who reopened my eyes to the world of the life.

TABLE OF CONTENTS

LIST OF TABLES

LIST OF FIGURES

PART 1. INTRODUCTION

1.1 Postembryogenic Development and Apical Meristems in Plants

Higher plants continue to form organs throughout their lives after embryogenesis. Postembryonic development enables plants to adapt to the varying conditions of the surrounding environment with greater plasticity (Walbot, 1996). This is essential for plants to compensate their sessile life style, since they cannot avoid adverse environments as do motile animals (Twyman, 2003). During embryogenesis, two meristematic tissues, the shoot apical meristem (SAM) and the root apical meristem (RAM), are established and organized at opposite ends of plant embryo. Plant postembryonic development depends on the activity of these two meristems. The shoot and root systems of the adult plants are elaborated gradually through the activities of these meristematic tissues after germination of the seed (Steeves and Sussex, 1989). These meristems are composed of a group of cells that have the potential to produce virtually all types of tissues and organs. The SAM consists of a group of pluripotent cells lying distal to the youngest leaf primordium at the apex of plant stems (Cutter, 1965) and serves as the initiation site of all major shoot structures, including axillary apical meristems. The SAM produces the shoot system, which is composed of iterative modules, called phytomers, each consists of a node at which a leaf (or leaves) and axillary meristem(s) are attached, and a subtending internode (Figure 1-1 on page 2). The SAM maintains totipotency and produces phytomers repeatedly throughout the life of a plant, which can be as long as thousands of years in some trees (Brunstein and Yamaguchi, 1992; Schulman, 1958).

1.2 Concepts of Shoot Apical Meristem

In 1759 Caspar Wolff first recognized that the new tissues and leaves arise from a particular area at the apex of the shoot (Tooke and Battey, 2003). He described the leaf initiation site as ‘the convex, juicy and translucent vegetation surface’ and also observed the leaf primordia in different developmental stages around the leaf initiation site (Figure 1-2 on page 3). A century later Nägeli (1858) introduced the term ‘meristem’, from the Greek word *merizein*, meaning *to divide*, to describe a group of plant cells that are always capable of division. He also made the first accurate account of apical initial cells in some of the seedless vascular plants, where a single apical cell divides into two daughter cells, one of which remains as an apical initial cell while the other is added to the meristematic tissue in a relatively peripheral position. Although he also extended his

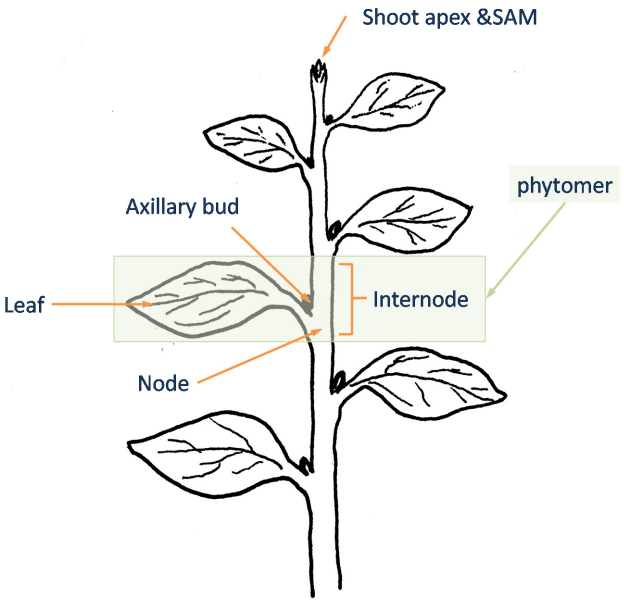

Figure 1-1. Illustration of a vegetative shoot showing phytomers. A phytomer of a leaf (or leaves) attached at a node, a subtending internode and an axillary meristem (lateral bud) at the base of the leaf. The shoot apical meristem (SAM) is located at the apex of the shoot.

apical initial cell concept to the meristems of higher vascular plants, this interpretation subsequently turned out not to be accurate (Tooke and Battey, 2003). While the concept of apical cells pertains to descriptions of the SAM of seedless vascular plants, currently the most widely accepted concepts describing angiosperm shoot apical meristem are 'tunica-corpus' organization and apical zonation (Brand *et al*., 2001; Clowes, 1961; Scofield and Murray, 2006; Steeves and Sussex, 1989).

Hanstein (1868) first proposed the histogen concept of meristem organization and function in the flowering plant. According to this concept, three meristem layers are recognized in the apical meristem: the outermost *dermatogen*, the middle *periblem*, and the innermost *plerome* (Figure 1-3 on page 3). The *dermatogen* layer exhibits only anticlinal divisions and gives rise to the epidermis of all parts of the plant. The *periblem* layer also displays anticlinal divisions with occasional periclinal divisions to form the cortex of the plant. The *plerome* gives rise to the central cylinder (vascular tissues and pith) of the plant through both anticlinal and periclinal divisions. Although his interpretation, in which each layer gives rise to a specific portion of the plant, was once widely accepted and was applied to both the SAM and the RAM, it is now largely disappeared in description of SAM organization, but continues to be used to some extent in description of RAM (Steeves, 2006).

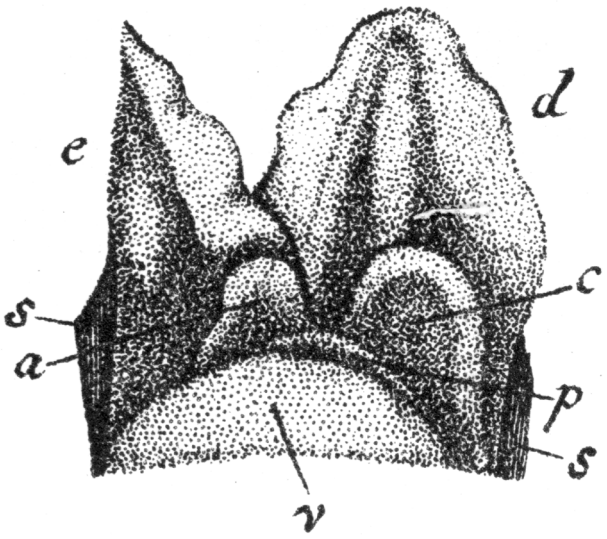

Figure 1-2. The *punctum vegetationis* ('point of vegetation') depicted by Caspar Wolff. Diagram and translated description were adopted from Tooke and Battey (2003): 'The tip was peeled and all leaves were removed from the front view, so that it is possible to see the vegetation point. Leaves were not removed from the back to demonstrate their attachment to the vegetation surface.' (***v***) 'The convex, juicy and translucent vegetation surface.' (***p***) 'The first leaf to appear, with its concave inner surface adjacent to the vegetation surface. The consistency of this leaf is barely more substantial than a viscous fluid.' (***a***) 'A different leaf, which is larger and more substantial than the previous.' (***c***) 'A leaf which has already developed a surrounding edge.' (**e**) 'Half a leaf.' (***d***) 'Complete leaf.'

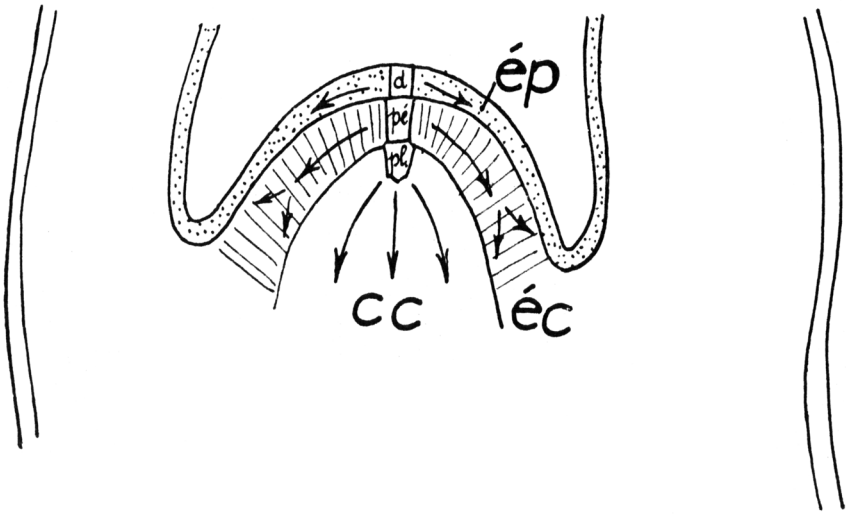

Figure 1-3. Hanstein's description of an angiosperm apical meristem. Three histogenic meristem layers were described: *dermatogen* (*d*), *periblem* (*pe*), and *plerome* (*pl)*, which give rise to the epidermis (***ép***), cortex (***éc***), and central cylinder (***cc***), respectively (Buvat, 1952).

Later, Schmidt (1924) proposed a new concept of apical organization known as ‘tunica-corpus’ organization, in which the SAM was described as stratified cell layers consisting of a ‘tunica’ and ‘corpus’ based on the orientation of cell divisions in the layer (Figure 1-4 on page 5; Tooke and Battey, 2003). The tunica consists of one to several superficial layers that cover the underlying central core, called the corpus. These two distinguished regions reflect the result of their cell division patterns. In the tunica, cell divisions are exclusively or predominantly anticlinal, so that all new cell walls are formed perpendicular to the surface of the SAM. As a result, progeny cells of the tunica remain in the layer and the tunica maintains a stratified appearance. On the other hand, cell divisions in the corpus region occur in multiple directions including both anticlinal and periclinal (parallel to the surface of the SAM), as well as oblique, so that progeny cells of the corpus form a mass of cells underlying the tunica. This description applied typically to flowering plants, but it has been extended to some gymnosperm species as well (Steeves, 2006). Schmidt’s interpretation of apical organization was the same general idea of Hanstein’s layers that were formed by different directions of cell division planes. However, while Hanstein postulated that specific portions of the plants rose from different layers, Schmidt thought that the contribution of the tunica layers and the corpus to each part of the plant was variable, but interdependent (Rogers, 1980).

While the tunica-corpus concept was gaining acceptance, a new concept emerged in France, first postulated by Plantefol (1947) and developed by Buvat (1955), based on the mitotic activity of the cells in the shoot apex. In this concept of SAM, the center of the shoot meristem consisting of topmost cells of the tunica and corpus remains essentially inactive and playing no part in organogenesis or histogenesis during vegetative phase of development, as named *méristème d’ attente* (waiting or resting meristem; Figure 1-5 on page 5). This distal inert region becomes active and functional only with the onset of flowering and forms a terminal flower or inflorescence. Leaf primordia originate in the region surrounding the *méristème d’ attente*. This developmental or formative region was named *anneau initial* (initiating ring) and characterized by active cell division and therefore considered to be a self-sustaining tissue. While the distal part of the corpus and tunica (*méristème d’ attente*) is inactive during the vegetative phase, the lower part of the corpus, the subtending *méristème medullaire* (medullary meristem), contributes to the elongation of the shoot by participating in the internodal elongation of the axis of the actively growing leaf primordia. This concept was originally applied to dicotyledonous plants but was later extended to monocotyledonous plants and eventually to some gymnosperms and seedless vascular plants. Although this concept was appealing to some investigators, opponents of this interpretation disagreed on that specific cells in the summit of the SAM were set aside early in development

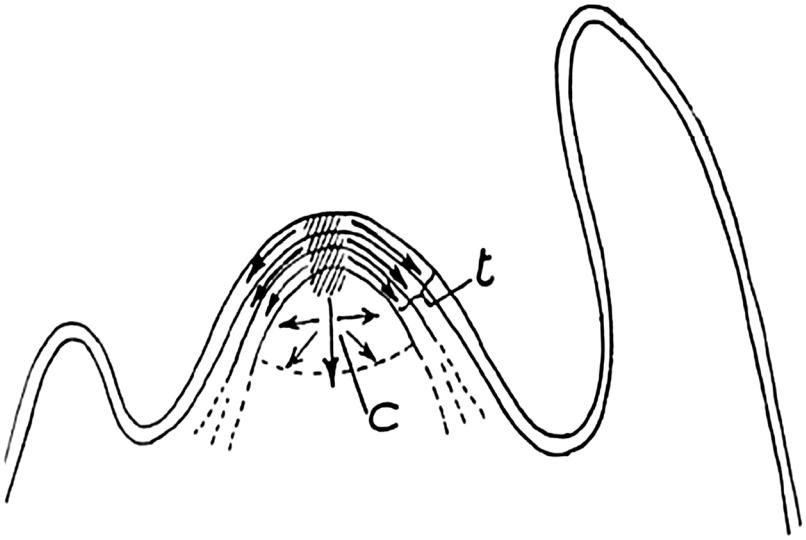

Figure 1-4. Schmidt's tunica-corpus organization of the shoot apical meristem. In the tunica (t), cell division is anticlinal, so that progeny cells remain in the same layer. In the corpus (c), cell division is periclinal or non-directional, forming a mass of progeny underneath the tunica layer (Buvat, 1952). Arrows indicate the direction of cell proliferation.

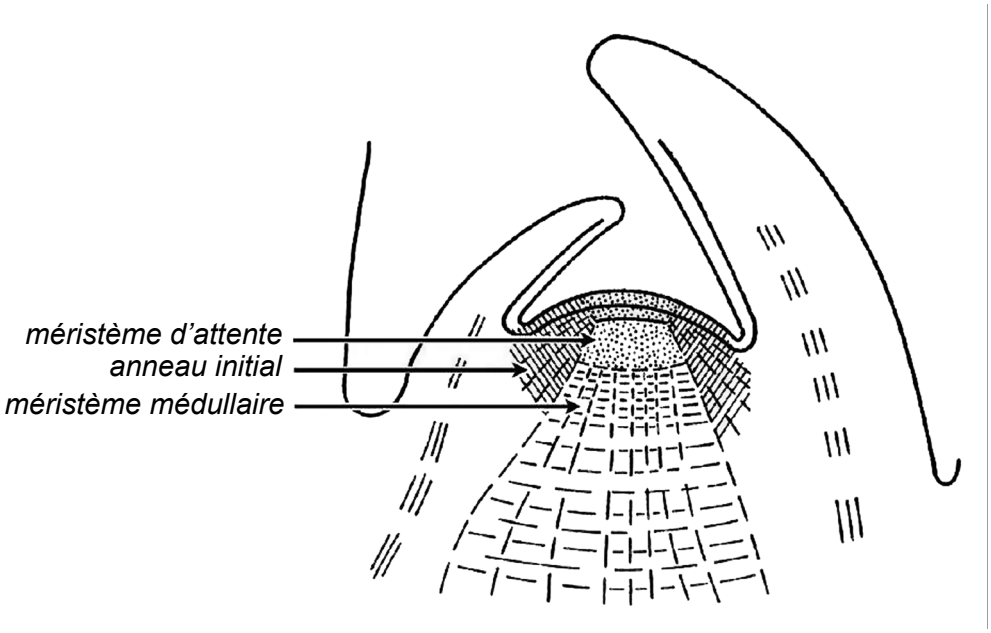

Figure 1-5. Buvat's concept of shoot apical meristem. A diagrammatic representation of an angiosperm shoot apex showing the *méristème d'attente*, *anneau initial* and *méristème médullaire* (Buvat, 1955).

solely to provide the initial cells for reproductive structures later (Steeves and Sussex, 1989). Based on histological observation of mitotic figures in the shoot apex and other aspects, Wardlaw (1957) showed that cells in the summit of the shoot apex divide to contribute to all of the organs and tissues of the shoot, vegetative or reproductive (Irish and Sussex, 1992).

1.2.1 Zonation Patterns in Shoot Apical Meristems

In both gymnosperms (Foster, 1938) and angiosperms (Gifford, 1954; Popham and Chan, 1950), cytological and histochemical differences have been observed between cells in different regions of the tunica and corpus. Foster (1938), and Popham and Chan (1950) described five zones in the SAMs of *Ginkgo* (Figure 1-6 on page 7) and *Chrysanthemum* (Figure 1-7 on page 7), respectively. However, three regions of different cytohistochemical patterns are generally recognized in angiosperms (Bäurle and Laux, 2003): central zone (CZ), peripheral zone (PZ) and rib zone (RZ) (Figure 1-8 on page 8).

The CZ consists of infrequently dividing cells located at the summit of the SAM. Those cells are relatively large and have diffuse nuclei that stain lightly. The CZ harbors a population of pluripotent and self-renewing cells that serve as a source for new cells for other regions. These cells are relatively larger and with poorly defined cell walls compared to other cells within the same zone, and referred to as apical initials, or collectively the apical initial zone (Rogers and Bonnett, 1989). The apical initials, later have been referred to as ‘stem cells’ first by Francis (1992) and, more explicitly by Hudson and Goodrich (1997), reflecting their functional similarity to stem cells in animals. Surrounding the CZ is the PZ, which includes the tunica layers outside of the axial zone, where rapidly dividing cells differentiate into leaf primordia and outer stem tissues. The cells in PZ are small and have densely staining nuclei and darkly staining cytoplasm. The underlying RZ is the region of the corpus responsible for generating the inner stem tissues. Cells of the RZ are enlarging, usually with large vacuoles, and become larger as they mature into pith further from the SAM.

Considering both the tunica-corpus organization and the zonation patterns, the SAM can be envisioned as having clonally distinct layers of cells that are sub-divided into three broadly defined functional zones, which are distinguished by cell sizes, nuclear sizes, and staining patterns, reflecting differences in the extent of cell division or cellular activity in different regions of SAM. (Clark, 1997; Kerstetter *et al*., 1997; Lyndon, 1998; Medford, 1992; Steeves and Sussex, 1989).

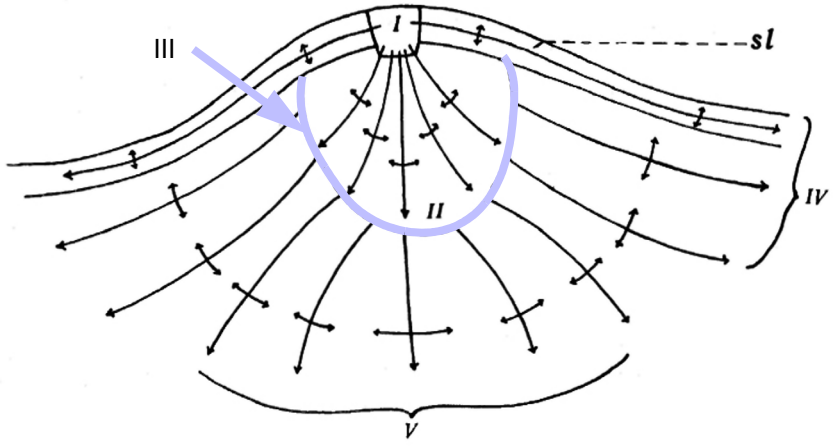

Figure 1-6. Foster's cytohistological zones and their mode of growth in *Ginkgo* shoot apical meristem. Zone I, apical initial cells, from which by anticlinal and periclinal divisions respectively the surface layer (sl) and the internal tissue of the growing point originate. Zone II is the mass of slowly dividing central mother cells. The lateral and basal margins of the group of central mother cells (indicated by the broken U-shaped light-blue outline pointed by the arrow) constitute Zone III, which was not shown in the original diagram. This marginal region is characterized by the smaller size and frequent division of its cells. From this transition zone, the peripheral subsurface layers (Zone IV) and rib meristem (Zone V) arise. The points and lengths of arrows represent the direction and relative amount of growth (Foster, 1938).

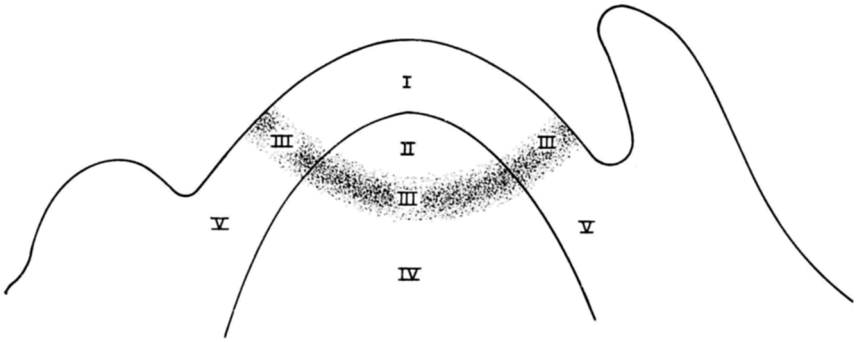

Figure 1-7. Cytohistological zonation pattern in *Chrysanthemum*. I, Mantle layers; II, central mother cell zone; III, cambion-like zone (not always present); IV, rib meristem; V, peripheral zone (Popham and Chan, 1950).

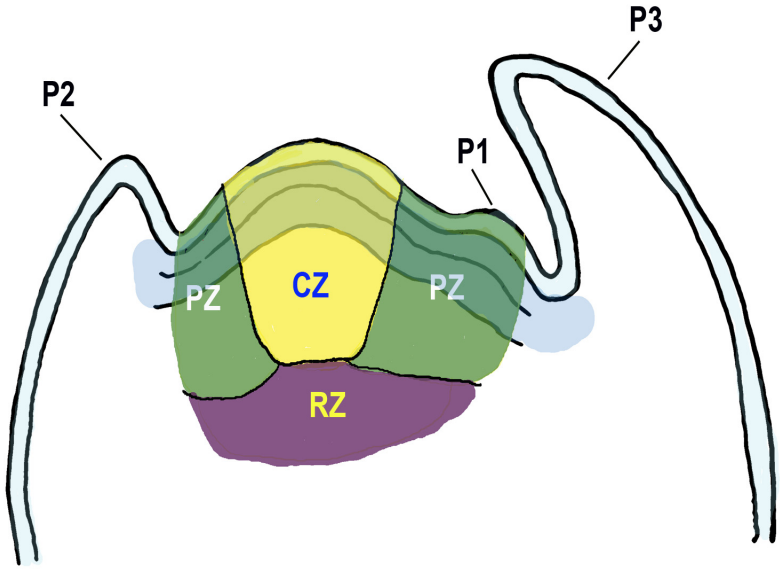

Figure 1-8. A schematic diagram showing cytohistological zonation in angiosperm shoot apical meristem. CZ, central zone residing at the summit of the SAM; PZ, peripheral zone surrounding CZ; RZ, rib zone or rib meristem underneath the CZ. P1, P2, P3: the youngest, the second youngest and the third youngest leaf primordium, respectively.

1.2.2 Experimental Analyses on Shoot Apical Meristem

The concepts of layered organization and zonation pattern were shown to be functionally valid by experimental analyses, such as microsurgery (reviewed in: Cutter, 1965; Steeves and Sussex, 1989), mitotic counts (Lyndon, 1970a; Lyndon, 1970b; Stewart and Dermen, 1970), radioisotope labeling (Brown *et al*., 1964; Sussex and Rosenthal, 1973), and chimeric analysis (Rogers and Bonnet, 1989; Tilney-Bassett, 1986). In microsurgery experiments, punctures or ablations were made to destroy some of the meristem cells, incisions were made to separate the meristem from other regions, or to divide the meristem into parts longitudinally. When cells in the central zone were punctured or ablated so that the supposed initials were destroyed, growth from the punctured meristem was aborted and one or more new meristems were formed on the flanks of the original apex and the new meristem initiated new leaf primordia. If the central apical meristem was isolated from the flanking tissues by several deep vertical incisions, it was capable of continued normal growth and development. If an apical meristem was divided longitudinally into a number of parts, some or all of parts regenerated new functional apical meristems and each

initiated new leaf primordia (Pilkington, 1929). All of these observations in microsurgical experiments indicate that cells of the central zone are capable of autonomous development and suppression of precocious outgrowth of the flanking regions (reviewed in: Cutter, 1965; Steeves and Sussex, 1989). When entire apical meristems or parts of meristems were excised and cultured on artificial growth media, they produced shoots with normal morphology, indicating the information required for formation and development of a shoot with its lateral organs and cell types exists within the apical meristem (Ball, 1960; Wetmore, 1953). Although there is variation in the nutrient requirements of different species (Cutter, 1965), the ability of the excised shoot apex to develop normal morphology also indicates the high level of autonomy of the SAM.

Mitotic counts and DNA labeling have been used to measure cell division occurring in different regions of the shoot apex, and showed that the rate of cell division in the central zone is much lower than that in the peripheral zones (Brown *et al*., 1964; Lyndon, 1970a; Lyndon, 1970b; Sussex and Rosenthal, 1973). The low mitotic activities of the distal-most cells of the central zone indicated that they were the ultimate source of all cells in the SAM (Laufs *et al*., 1998b; Lyndon, 1970a; Lyndon, 1970b; Stewart and Dermen, 1970). Radioisotope labeling studies, where ^{3}H-thymidine was used as an indicator of DNA synthesis and thus subsequent cell division, showed that the cells in the summit of the central zone were dividing slowly but apparently contribute cells to the surrounding region, and eventually to the vegetative shoot (Brown *et al*., 1964; Sussex and Rosenthal, 1973). The use of various staining techniques (Corson and Gifford, 1969), measurement of cell size (Lyndon and Cunninghame, 1986), and other observations that reflect the degree of activity have generally supported this conclusion (Steeves and Sussex, 1989).

The chimeric analysis provided means to trace each meristem layer to the differentiated cells in the shoot. Chimeric plants are composed of tissue with distinctive cellular markers such as chromosome number (polyploidy) and loss of chloroplast pigments (albino) (Tilney-Bassett, 1986). Chimeras can be produced by radiation, chemical treatment, somatic mutation, or plastid segregation to induce phenotypic cellular markers. There are three types of chimeric tissues: periclinal, sectorial and mericlinal (Figure 1-9 on page 10). Periclinal chimeras are formed when a mutation is restricted in one or more layers of the apex and affects the entire layer(s). As a consequence, the affected progeny cells form different layer(s) parallel with the unaffected layer(s). Sectorial chimeras have mutations in a section encompassing multiple layers of the apex. The cells that are derived from the mutated cells form a segment in multiple layers. Sectorial chimeras are stable and persist for several nodes and internodes (Steeves and Sussex, 1989). In mericlinal chimeras, a mutation is limited within a section in one layer of the apex, and the mutated

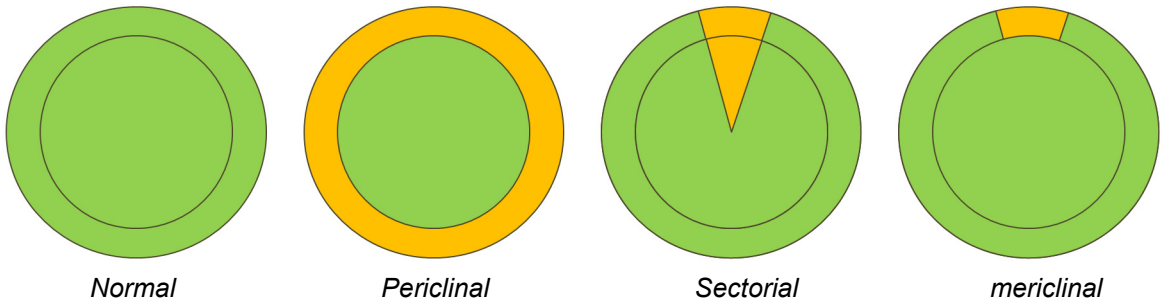

Figure 1-9. Diagrammatic cross-sectional views of different types of chimeras in plant shoots. Green represents normal green tissue and the orange regions are composed of albino cells. Black circles indicate the boundary or outline of different layers. Drawn based on Tilney-Bassett (1986).

cells occur in a single layer on one side of the plant only. This type of the chimera is not sable and does not persists very long. By tracing the lineage of the progeny cells having cellular markers (*i.e.*, mutated traits) in the periclinal chimera, it is possible to demonstrate the presence of initial cells in angiosperm shoot meristems (Tilney-Bassett, 1986). The clonal analysis using chimeric plants supports the concept that the apex consists of distinct layers and each layer has its own group of initial cells that give rise to all cells in the layer (Rogers and Bonnett, 1989).

In the angiosperm SAM, the stratified tunica and corpus are described as three clonally distinct cell layers, which reflect the cell division patterns in each layer (Figure 1-10 on page 11). The tunica is distinguished in two layers; an outer single cell layer designated as L1 and an inner layer, L2, which can be more than one cell layer. The cell mass of underlying corpus is designated L3 (Brand *et al*., 2001; Satina and Blakeslee, 1941). It was shown that progeny cells of the anticlinally dividing initial cells in the outermost layer of the tunica (L1) remain in the same layer and differentiate exclusively into the epidermal layer. The underlying layer(s) of the tunica (L2), in which cells divide predominantly anticlinally, as well as periclinally at lower frequency, generates subepidermal cortex, some of the vascular tissue and the gametes. Cells in the corpus (L3), which divide periclinally and anticlinally, as well as obliquely, give rise to the pith and most of the vascular tissues. This early allocation of cells in the meristem into separate clonal cell layers supports the concept that the layers of the meristem are distinct and that each has its own small group of initial cells, suggesting a cell-lineage-dependent mechanisms of development (Rogers and Bonnett, 1989). This is true as long as the daughter cells stay in the layer from which they are derived. Although the chimeric sectors in the meristem may last for many years in perennials, they are displaced ultimately, suggesting that the initials are not permanent although they may function for

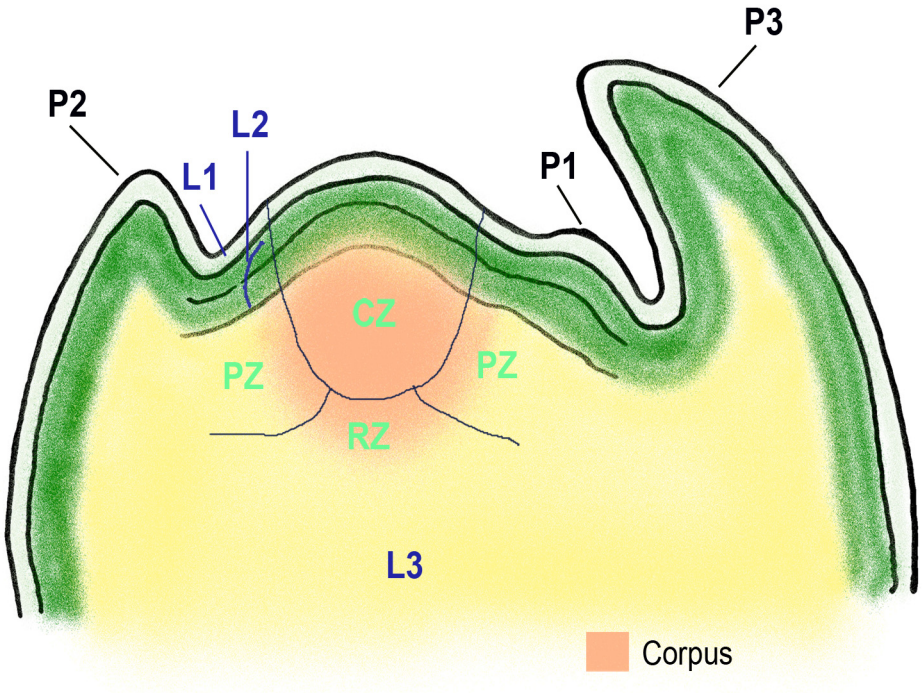

Figure 1-10. Shoot apical meristem showing three clonally distinct cell layers. L1 (white) and L2 (green) represent tunica layers whereas L3 represents the corpus (pink region). CZ, central zone; PZ, peripheral zone. P1, the youngest leaf primordium; P2, the second youngest leaf primordium; P3, the third youngest leaf primordium.

a long time. Also, studies using genetic mosaics showed that the development of each clonal layer is flexible and adjustable to the changes of cell proliferation occurring in other layers (Szymkowiak and Sussex, 1996). When an initial cell in L1 divides periclinally, the daughter cell is displaced from the layer and is incorporated into the underlying layer, adopting the fate of its new position as an L2 cell. This suggests that the position of a cell, and not its clonal origin, determines the ultimate fate of the cell (Irish, 1991; Poethig, 1989; Rogers and Bonnett, 1989; Satina et al., 1940; Satina and Blakeslee, 1941; Szymkowiak and Sussex, 1996).

1.2.3 Integration of Layers and Zones in Development

To sustain growth and to assure proper functioning and survival of a plant, the establishment and maintenance of zones and layers of the SAM are essential. Adequate proliferation of stem cells, proper differentiation of derived cells and formation of organs must be properly coordinated among these zones and layers. During development, all three layers (L1, L2, L3) of the SAM contribute cells to newly formed organs, indicating that the rate of cell proliferation and the

specification of cell fate are to be coordinated among the layers (Brand *et al*., 2001).

A division of an initial cell in each cell layer results in two daughter cells. The daughter cell that stays in the apical position remains pluripotent and functions as the initial cell. By contrast, the daughter cell more distant from the apex is incorporated into the central zone and recruited into the peripheral zone or the rib meristem, where it ultimately undergoes differentiation. While a cell cannot move and its position is fixed at the time of division, the position of the daughter cell shifts further away from its mother cell. As the positions of daughter cells shift as a result of successive divisions, gene expression in the cell also changes depending on the fate of the cell. This implies that cells in the SAM appropriately determine their gene expression based on signal exchanges with others in the meristem, not on a lineage-specific predisposition of cell fate (Carles and Fletcher, 2003; Szymkowiak and Sussex, 1996).

There can be two main routes by which meristem cells in the SAM can communicate with each other to coordinate their development. One way of the intercellular communication appears to involve transfer of signal molecules, such as RNA and proteins (including transcription factors) to neighboring cells through symplastic continuity *via* plasmodesmata (Kim *et al*., 2005b; Lucas, 1995). It has been shown that cells in zones and layers in the SAM form rather separate symplastic domains (Gisel *et al*., 1999; Rinne and van der Schoot, 1998; Rinne *et al*., 2001). The cells in a domain are effectively coupled, allowing facilitated exchange of molecules, whereas the exchange between cells of different domains may be less efficient (Bayer *et al*., 2008). A second way of communication between cells in the SAM is signaling through the intercellular space, apoplast. Mobile molecules secreted by one cell can be recognized by specific receptors on another cell's surface. The signaling pathway that covers the different layers or gene expression domains is a candidate for this type of communication in the SAM (Doerner, 1999; Fletcher and Meyerowitz, 2000).

1.2.4 Gene Expression Domains in Shoot Apical Meristem

The availability of a variety of mutants from model plants, such as *Arabidopsis*, rice and maize, along with various molecular genetic analysis techniques, led to identification of specific genes that are expressed only in a certain meristem zone and controlling various aspects of shoot development (reviewed in: Brand *et al*., 2001; Steeves, 2006; Tooke and Battey, 2003; Veit, 2006). Many of these genes encode putative transcriptional regulators, controlling the expression of downstream genes. Although it is not clear if the gene expression domains and the cytohistochemical zonation correspond exactly, especially at the boundaries of the zonation,

many genes have their expression domains in one region or another in the SAM, suggesting that the cytohistologically distinct zones within the SAM may be characterized by distinct patterns of gene expression. By using *Arabidopsis* mutants that have altered SAM morphology, genes that are expressed in specific zones in the SAM, or in the whole SAM, but not in differentiating cells, have been identified (Figure 1-11; Brand *et al*., 2001).

CLAVATA3 (*CLV3*) is expressed in a small region in the L1 and L2 layers at the summit of the SAM, and these cells are considered as the initial cells for the shoot (Fletcher *et al*., 1999). Underneath the *CLV3* expression, *CLV1* and *CLV2* are expressed in most cells of L3, but absent in L1 and L2 layers (Clark, 1997). *WUSCHEL* (*WUS*) is expressed in a small number of the lower cells within the corpus below the *CLV3* expression domain, barely overlapping with *CLV1/CLV2* expression domain (Laux *et al*., 1996; Mayer *et al*., 1998). The *CLV1CLV2* domain is much broader than *WUS* domain laterally and apically. Since the *WUS*-expressing cells within the RZ

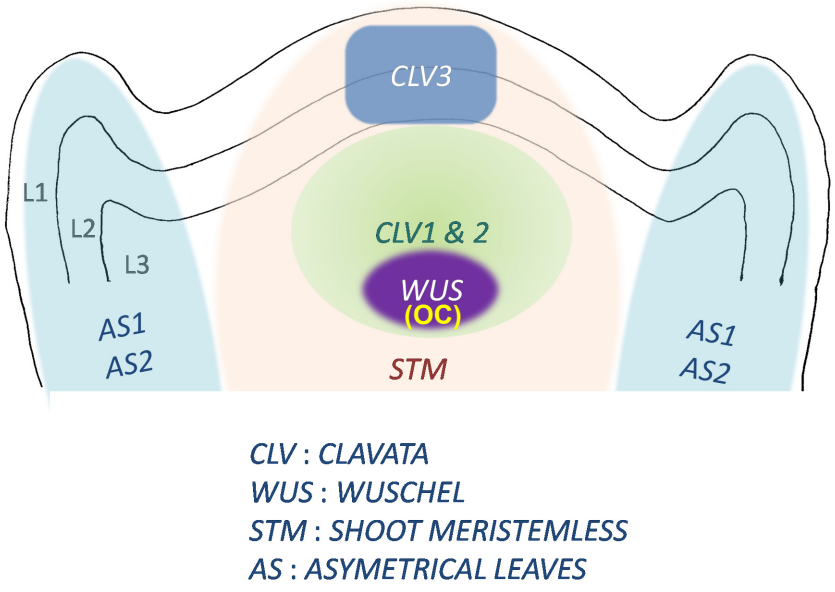

Figure 1-11. Schematic diagram showing expression domains of shoot apex-specific genes in a wild-type *Arabidopsis* shoot apical meristem. *STM* (light pink) is expressed throughout the apical meristem, but not in the differentiating region, where *AS1* and *AS2* (light blue) are predominantly expressed. The *CLV3* expression domain (blue) is largely restricted to a small number of cells in L1 and L2 layers, whereas *CLV1* and *CLV2* (light green) are exclusively expressed in most cells of the L3 layer (Clark *et al*., 1997). *WUS* expression (purple) is in the lower cells of the L3 layer beneath the *CLV* expression domain (red; Mayer *et al*., 1998) and the *WUS*-expressing cell domain is also referred to as organizing center (OC) (Mayer et al., 1998).

signal to its overlying *CLV*-expressing cells, specifying them as pluripotent stem cells in the CZ, the *WUS* expression domain is referred to as an organizing center (OC) of the SAM (Mayer et al., 1998). A KNOTTED1-like HOMEOBOX (KNOX) gene *SHOOTMERISTEMLESS* (*STM*) is expressed throughout the CZ and the PZ of the SAM but not at the sites of primordia specification within the PZ, indicating that *STM* expression is either specifically activated in the meristem, or repressed in those cells that will differentiate into organ primordia (Barton and Poethig, 1993; Long and Barton, 1998; Long *et al*., 1996). *ASYMMETRIC LEAVES* genes (*AS1* and *AS2*) are expressed in founder cells of the primordium and negatively interact with *STM* to maintain the SAM/primordium boundary. While *STM* restricts *AS1* expression from cells in the SAM, *AS1* and *AS2* prevent *STM* expression in founder cells in the primordium (Fletcher, 2002).

1.2.5 Cell Proliferation and Maintenance of SAM

While cells that make up the CZ of the SAM continuously divide and transit away from the apex into the peripheral region for differentiation, the size and organization of the SAM are preserved (Ball, 1974; Brand *et al*., 2001; Evans and Barton, 1997; Silk and Erickson, 1979). To maintain the SAM as an integrated unit in size and organization, it is essential to ensure that a stable population of stem cells is maintained in the SAM while their progeny are recruited into differentiation in a timely manner so that the rates of proliferation and recruitment of cells are precisely balanced (Clark, 1997; Meyerowitz, 1997). It appears that the balance between these two processes is achieved by a combination of negative and positive interactions between genes and gene products in different zones within the meristem, as well as between meristem genes and genes expressed in differentiating regions (Figure 1-12 on page 15; Fletcher, 2002).

The maintenance and function of the stem cells in the SAM appears to be regulated by three regulatory gene actions7 1) the *CLAVATA* signal transduction pathway maintains stem cell identity by controlling the recruitment of stem cell into differentiation, 2) the feedback loop of the *CLV* and *WUS* genes maintains the balance between the central reservoir of stem cell population and recruitment of differentiating cells, 3) the combined activities of homeodomain genes prevent stem cells from premature differentiation (Carles and Fletcher, 2003; Clark *et al*., 1996).

When cells become displaced from the meristem center, they lose stem cell identity first and then undergo differentiation. The transition from stem cell to differentiating cell is regulated by the *CLAVATA* receptor kinase signal transduction pathway, which involves actions of all three *CLV* genes (*CLV1, CLV2* and *CLV3*). Mutations in any of these delays the recruitment of stem cells into differentiation and gradually accumulates meristem cells, resulting in an enlarged meristem with

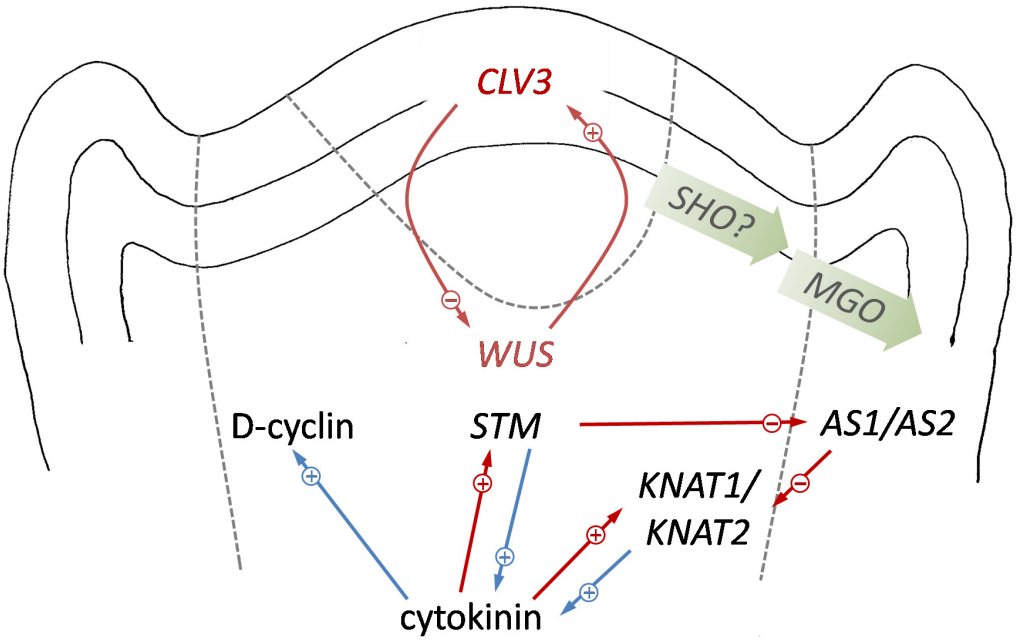

Figure 1-12. A schematic diagram showing the hypothesized regulation of cell identity across the *Arabidopsis* shoot apex. In the central zone of the meristem (CZ), a positive signal from *WUSCHELL* (*WUS*) specifies stem cell identity and maintains the *CLAVATA3* (*CLV3*) expression domain to a narrow region in the deeper layers of the meristem. The signal from *CLV3* limits the expression domain of *WUS* to a small region within the corpus. Putative *Arabidopsis* homologs of the rice gene *SHOOT ORGANIZATION* (*SHO*) are proposed to regulate the rate of cell transition from the CZ to the peripheral zone (PZ). The *MGOUN* genes (*MGO1* and *MGO2*), which are expressed at the outer margin of the PZ, promote the transition of cells from the PZ into the leaf primordium. When mutated, these genes result in defective organ formation (Laufs *et al*., 1998a). The plant hormone cytokinin is proposed to stimulate mitotic activity in the SAM by elevating the levels of D-type cyclins. Cytokinin is also proposed to increase the expression of *STM*, *KNOTTED1-LIKE* genes *KNAT1* and *KNAT2*, which concomitantly appear to promote cytokinin accumulation. *ASYMMETRIC LEAVES* genes (*AS1* and *AS2*) are expressed in founder cells of the primordium and negatively interact with *STM*, *KNAT1* and *KNAT2* to maintain the SAM/primordium boundary. *STM* restricts *AS1* expression from cells in the SAM, while *AS1* and *AS2* prevent *KNAT1* and *KNAT2* expression in founder cells in the primordium (Fletcher, 2002). The brown arrows indicate regulation of the gene expression, and the blue ones represent metabolic regulation. The + and - signs in the circles indicate positive and negative regulations, respectively.(Redrawn from Fletcher, 2002.)

expanded CZ (Bäurle and Laux, 2003; Williams and Fletcher, 2005). By continuously turning stem cells into differentiating cells, *CLV* genes limit the stem cell population to an adequate number (Clark *et al*., 1993; Clark *et al*., 1996).

The balance between stem cell maintenance and recruitment for differentiation, and thus the homeostasis of the SAM, is regulated by a feedback loop involving the *CLV* gene expressing stem cell domain and the *WUS* gene expression domain underneath, which is also called organizing center (OC) (Figure 1-13; Hobe *et al*., 2001). Signals from the *WUS*-expressing OC maintains stem cell identity by promoting the expression of the *CLV3* in the overlying CZ cells. In response, the *CLV3* gene produces a putative ligand to activate a receptor kinase complex that includes CLV1 and CLV2, which are expressed in the RZ cells (Clark et al., 1997; Fletcher *et al*., 1999; Ni and Clark, 2006; Trotochaud *et al*., 1999). The activated CLV1/CLV2 complex represses the expression of the transcription factor WUS and thereby limits the *WUS* expression domain within the RZ. By this regulatory feedback loop, the size of the stem cell population can continuously be checked and kept constant during development. Over-expression of *WUS* promotes *CLV3* expression (Schoof *et al*., 2000), suggesting that CLV3 may control the size of stem cell domain by regulating its own expression levels through a feedback interaction between *CLV3*-expressing

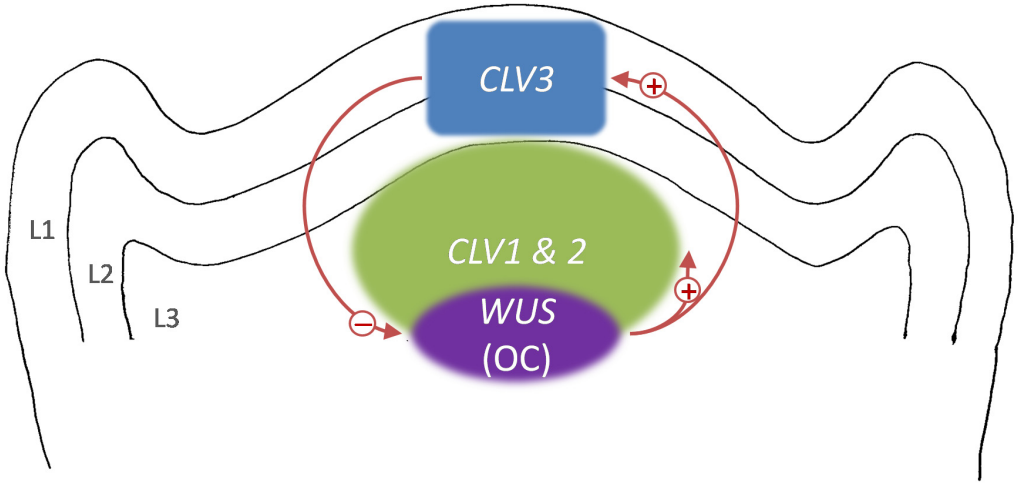

Figure 1-13. Homeostasis of stem cells *via* feedback regulation in the Arabidopsis shoot apical meristem. *CLV3* is expressed in the layers L1 and L2, and activates the CLV1/CLV2 receptor complex underneath. Activity of the CLV pathway represses transcription and/or function of WUS in the organizing center (OC), and possibly other genes. WUS promotes stem cell fate in the overlying cells, and also promotes expression of the *CLV* genes in their respective domains. Together, these gene functions establish a feedback loop with negative and positive interactions for the control of stem cell fate in the SAM (Adapted from: Groß-Hardt and Laux, 2001; Hobe *et al*., 2001).

stem cell domain in the CZ and the *WUS*-expressing OC in the RZ (Xie et al., 2009). While the mutations in the *CLV* genes result in an expanded stem-cell domain and enlarged SAMs (Bäurle and Laux, 2003; Fletcher *et al*., 1999; Kayes and Clark, 1998; Trotochaud *et al*., 1999; Williams and Fletcher, 2005), mutation in the *WUS* results in depletion of stem cells and loss of SAM activity (Laux *et al*., 1996). The misspecified stem cells in *wus* mutants do not become integrated into organs, indicating that WUS functions as a positive regulator of stem cell identity rather than as a repressor of organ formation (Laux et al., 1996).

Mutations in the *SHOOT MERISTEMLESS* (*STM*) genes, of which expression is restricted in the meristem, result in failure to produce a functional SAM and stops growing after formation of ectopic organ in the meristem center. This observation indicates that maintenance of shoot meristem activity also involves mechanisms that implement the expression of SAM-specific genes as well as repress the formation and outgrowth of organs in the meristem domain (Clark et al., 1996; Endrizzi et al., 1996). STM has been proposed to function in maintenance of cell proliferation by repressing the activity of ASYMMETRIC LEAVES1 (AS1), a MYB domain containing protein which is expressed at the sites of primordia specification within the PZ (Byrne et al., 2002). The genetic interaction between *stm* and *clv* mutants has revealed that *stm* mutations can dominantly suppress *clv* phenotypes indicating that the *stm* phenotype is sensitive to the levels of CLV activity. It has been proposed that these genes play related but opposing roles in the regulation of cell proliferation and/or differentiation in SAMs (Clark *et al*., 1996). Based on the genetic interactions between STM and WUS it has been suggested that they perform independent functions. While WUS is required to specify stem-cells in the CZ, STM is required to suppress differentiation throughout the SAM dome and thus allowing the proliferation of stem cell daughters within the PZ (Brand et al., 2002; Gallois et al., 2002; Lenhard et al., 2002).

1.3 *Hedera helix* as An Experimental Plant

English ivy (*Hedera helix* L.) is distinguished from other plant species in that it maintains a vegetative state for many years without a transition to the reproductive state. *Hedera helix* plants in the vegetative phase have several traits different from those in the reproductive phase (Table 1-1 on page 18). In *H. helix* plants, transition from vegetative to reproductive phase appears to be initiated by factors intrinsic to the shoot apical meristem (Poethig, 1990) although detailed molecular analyses have not been performed. The exceptionally long vegetative state of English ivy is advantageous in studying leaf development for several reasons: 1) genetically uniform specimens can be obtained repeatedly from a single plant for a long time before any floral

Table 1-1. Different features in vegetative and reproductive phases of English ivy (*Hedera helix*)[a].

Traits	Vegetative	Reproductive
Leaf shape	lobed or incised	entire, ovate
Phyllotaxy	alternate	spiral
Plastochron	1 week	2 week
Growth habit	plagiotropic (prostrate)	orthotropic (upright)
Internodes	long	short
Anthocyanin pigment in stems	present	absent
Adventitious roots	present	absent
Rooting	easy	difficult

[a.] Adapted from Poethig (1990).

gene becomes involved in the process; 2) mericlinal sectors of variegated variety, such as *H. helix* cv. Goldheart, can be followed during growth of many nodes before the onset of flowering or dormancy; and 3) *H. helix* possesses vegetative buds and maintains a perennial life cycle, which are lacking in the well-characterized model plant species, such as *Arabidopsis* and other crop species. Thus, it is suitable for studying the global expression of genes associated with regulating dormancy and growth of vegetative buds, which has not been studied in detail.

1.3.1 Organization of Shoot Apical Meristem in *H. helix*

As in many angiosperm shoot apical meristems, English ivy (*Hedera helix* L.) has a stratified organization of the cell layers into a tunica and a corpus. The tunica of *H. helix* consists of three superficial layers that cover the underlain corpus, designated as T1, T2 and T3, respectively. (Figure 1-14 on page 20; Rogers and Bonnett, 1989). In the SAM of *H. helix*, cytohistological zonation is also apparent: the central zone, peripheral zones and rib meristem. Inside the central zone, apical initial cells (AI) are located at or near the longitudinal axis of the apex, which is pear-shaped, 2-3 cells in diameter, and extending through the tunica layers and several cells deep into the corpus. The total depth of apical initial zone was 6-10 cells (Figure 1-15 on page 20; Rogers and Bonnett, 1989). The region of apical initial zone described in *H. helix* has close resemblance to the *CLV*/*WUS* expression domain in the *Arabidopsis* shoot apical meristem (shown in Figure 1-11 on page 13), suggesting that the cytohistological characteristics may be the reflection of gene function in that particular region.

1.3.2 Variegation Patterns and Cell Lineage

In the shoot apical meristem of *H. helix* plants, the L1 layer forms exclusively the single layer of epidermis throughout the entire plant. The L2 layer forms the outer parts of the stem, petioles, and leaf margins, and the L3 layer forms the interior portion of the stem, parts of petioles, and the central parts of the leaf blade (Figure 1-16 on page 21; Rogers and Bonnett, 1989). The 'Goldheart' variety of English ivy (*H. helix* L. cv. Goldheart) exhibits a unique variegation pattern on its leaves. It is a mericlinal chimera with white (albino) patches in the center of the leaf blade and green margins, which arise from the mutated L3 histogenic layers with normal L1 and L2 layer. In the plants with chimeric variegation, it was shown that a mutation occurs in the nuclear gene that affects assembly of thylakoid membrane, causing a lack of chlorophyll (Evenari, 1989; Kirk and Tilney-Bassett, 1978; Manenti and Tedesco, 1971; Sakamoto, 2003; Tilney-Bassett, 1986). It has been shown that the white leaf sectors in the variegated leaf of *Arabidopsis thaliana* are comprised of viable cells with undifferentiated plastids (Kato *et al*., 2007). Since the L1 constitutes exclusively epidermis, in which only the guard cells contain chloroplasts, the appearance of the variegation pattern is not affected by mutations in the L1 layer.

In the 'Goldheart' variety of ivy plants, there are three major types of leaf patterns: 1) fully green leaves; 2) leaves in which only half of the center is white; and 3) leaves with completely white centers (Figure 1-17 on page 21). Changes in the pattern on one side of the stem axis are independent of changes on the other side. This pattern is fairly stable and predictable such that most leaves exhibit the same variegation pattern as the leaves produced immediately previous to them on the same side of the stem axis. However, some display changes in variegation pattern, indicating a displacement of the cells of L3 layer (corpus) by the cells of L2 layer. For example, if a phenotypically white cell of L3 is displaced by a phenotypically green cell of L2 in the apical initial zone can lead to the loss of the variegation; or, *vice versa*. This displacement sometimes causes an instability and reorganization of the central region of the shoot apex, occasionally leading to selection of a new initial cell, as indicated by a persistent pattern change.

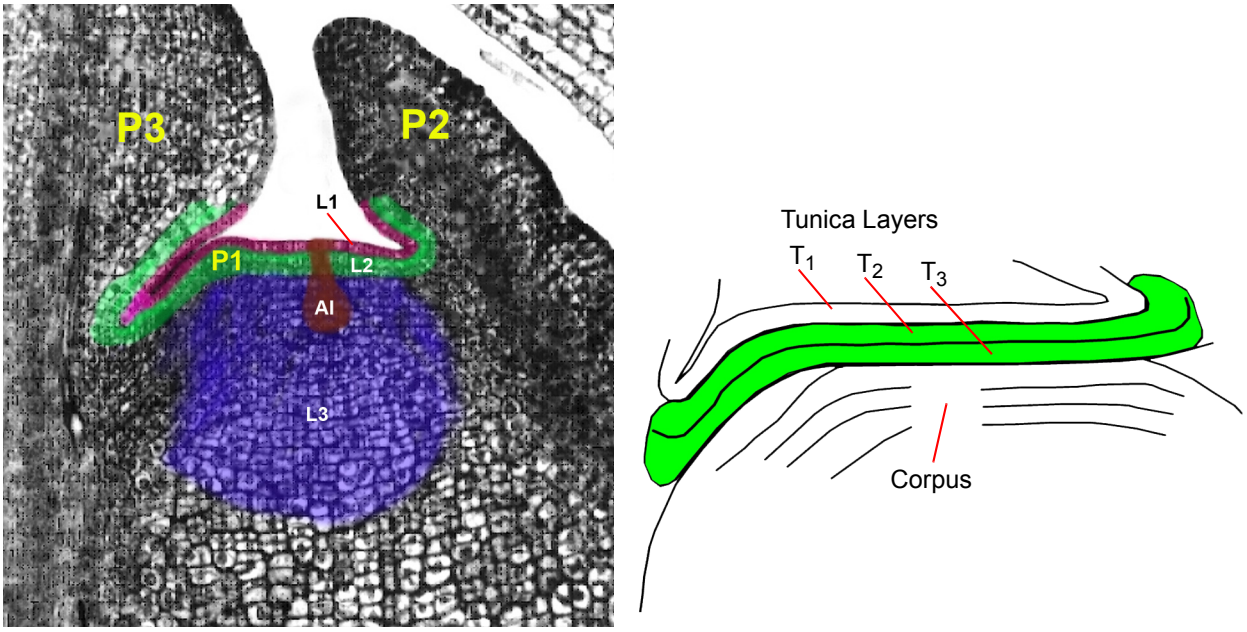

Figure 1-14. Tunica-corpus arrangement of the *H. helix* shoot apex. The L1 consists of 1 layer (T_1), whereas the L2 consists of two layers (T_2, and T_3) in the *H. helix* shoot apex (Rogers and Bonnett, 1989).

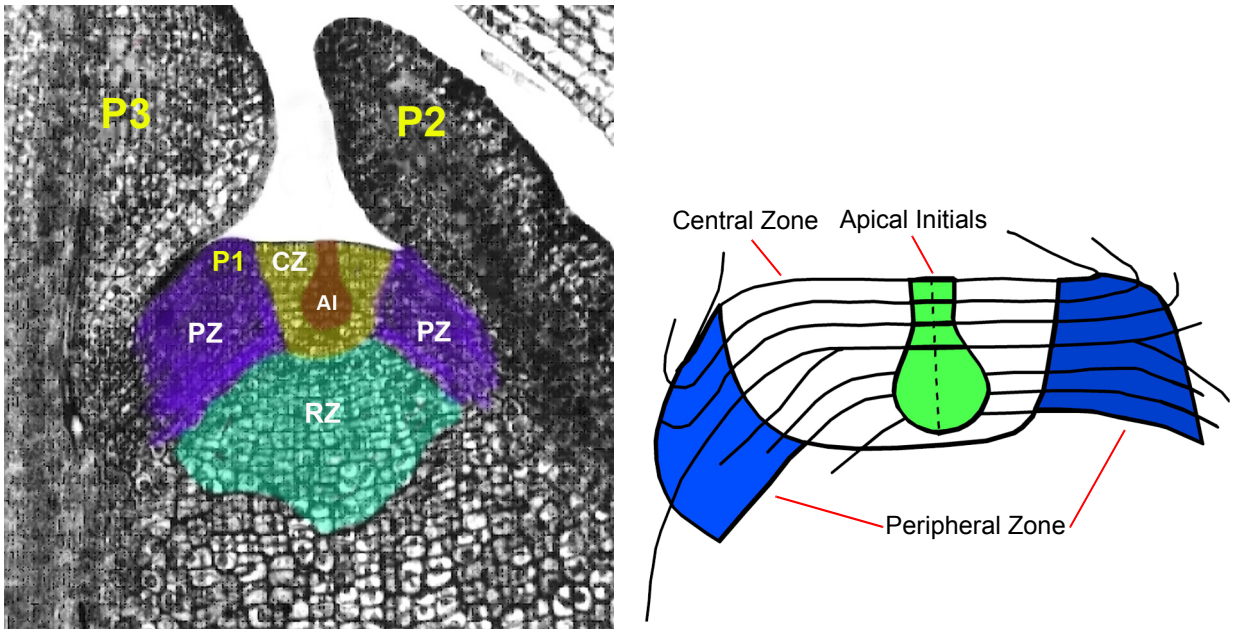

Figure 1-15. Zonation pattern of shoot apical meristem of *H. helix*. Leaf primordia (P1, P2, P3) and various zones within shoot apical meristem are shown: peripheral zone (PZ), where new organs are formed, the central zone (CZ), where a population of stem cells are located, and rib zone (RZ), which gives rise to inner tissue of the stem. Notably in the diagram on the right, the apical initial zone (AI) does not reside at the center of the shoot meristem, but is located off the center away from the location where a new primordium develops (Rogers and Bonnett, 1989).

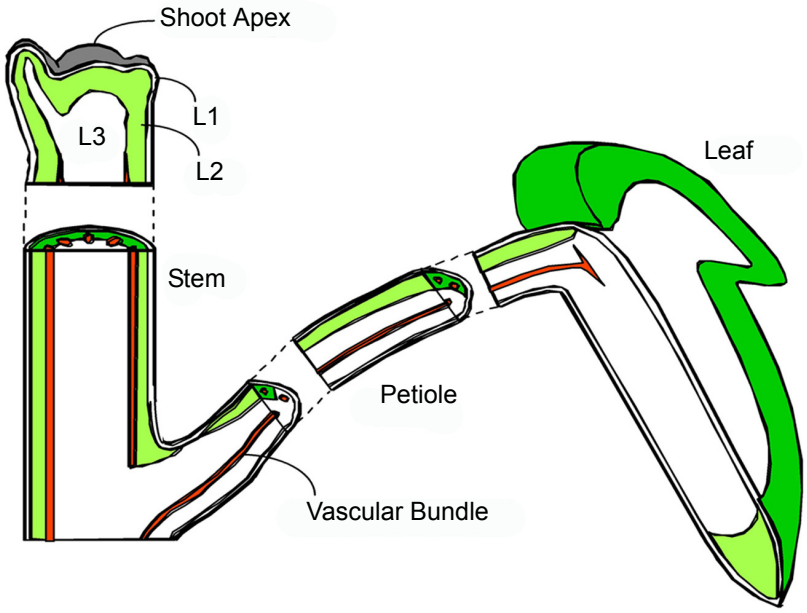

Figure 1-16. Histogenic layers and ontogeny of variegated leaf tissues of *H. helix*. L1 histogenic layer forms single layer of epidermis, L2 forms the outer parts of the stem, petioles, and leaf margins, and L3 forms the interior portion of the stem, parts of petioles, and the central parts of the leaf blade. The white patch in the center of the leaf blade is derived from the cells in L3 that have a mutation in a nuclear gene (Rogers, 1980).

Figure 1-17. Portions of vegetative shoots of *H. helix* L. cv. Goldheart showing various patterns of variegation. Left, no variegation; Middle, leaves on the left side of the shoot have white patch on the left half of the leaf blade, and those on the right side have the mirror image of the pattern on the left; Right, leaves on both side of the shoot axis have white patches at the center of the leaf blades.

1.4 Cross-species Microarray Hybridization For Transcript Profiling

1.4.1 Types of Microarrays

A microarray consists of a number of microscopic spots of cDNA or oligonucleotide probes that are permanently affixed on a platform in such an arrangement that the position of each probe is identifiable. Microarray platforms are usually glass microscope slides, nylon membranes or silicon chips (Schena, 2003). In the cDNA microarrays, the probes consist of cDNA or small fragments of PCR products, of which sequences are identified completely or partially. These are synthesized and then spotted (or printed) onto a glass or nylon support (Pariset *et al*., 2009). In oligonucleotide microarrays, the probes are short sequences designed to match the part of protein encoding sequences of genes. The oligonucleotide arrays are produced either by spotting the pre-synthesized oligos on the glass or nylon support (inkjet depositing technology; Hughes *et al*., 2001) as in Agilent microarrays (http://www.agilent.com) or by synthesizing the probes *in situ* on a chip by a light-directed process (photolithography; Tan *et al*., 2003) as those produced by Affymetrix (http://www.affymetrix.com; Pease *et al*., 1994) or Roche Nimblegen (http://www.nimblegen.com; Nuwaysir *et al*., 2002).

Microarrays quantify gene expression level based on the relative intensities of fluorescent dyes that correspond to the amount of mRNA in the sample. In a typical experiment using spotted microarrays, which have either full-length cDNA or oligonucleotide probes on glass or nylon support, two sets of cDNA targets, each generated through reverse transcriptation of expressed mRNA of the sample and labeled with a unique fluorescent dye, are hybridized simultaneously to the probes on a microarray. The competitive hybridization of two differentially labeled target sets provides means for the measurement of the transcript levels from each sample by comparing the relative intensities of fluorescence from two dyes in each spot. The intensity levels are generally presented as a set of ratios between the two samples for each spot on the microarray reflecting the fold-difference in the gene expression levels between the two samples (Buckley, 2007; Schena, 2003). Since two different fluorescent dyes are employed and the intensities of the dyes are measured in different channels (excitation wavelengths), this type of microarray is referred to as a two-color or two-channel microarray. In the experiment using the silicon-chip based oligonucleotide microarray, such as Affymetrix GeneChip (http://affymetrix.com), each of target sets from samples (usually fluorescently labeled mRNA rather than cDNA) is hybridized to separate chips. Since the target sets are labeled with the same fluorescent dye and the intensity of fluorescence from each chip is measured in one fixed channel, this type of microarray is referred to as a single-color or single-channel microarray.

1.4.2 Single-species and Cross-species Hybridization of Microarrays

Microarrays are widely recognized as a significant technical advance, which provide a powerful means for analyzing the genome-scale expression of thousands of genes in a single experiment. Using microarrays, genes that are tissue-specific and/or involved in metabolic pathways in response to environmental stimuli can be identified. However, the application of this technique has been limited to a small number of well-characterized model species. For the majority of microarray studies using model species, the fluorescently labeled targets are generated from the same species that also provides the probes on the microarray. This method is referred to as single-species or species-specific hybridization (SSH).

A growing number of studies are utilizing heterologous array hybridization, where microarrays generated from a well-characterized species are used to examine gene expression in a related extant species (Bar-Or *et al.*, 2007a; Bar-Or *et al.*, 2007b; Eddy and Storey, 2007; Renn *et al*., 2004). This method is termed cross-species hybridization (CSH). The advantage of the cross-species hybridization is that it avoids expenses necessary for the fabrication of the novel microarrays for the new species of interest, including generation of cDNA clones and expressed sequence tag (EST) data (Buckley, 2007). The use of microarray-based heterologous hybridization technique recently has been gaining feasibility in its use, especially in the field of comparative environmental genomics, where broad scale gene expression patterns are compared among different species to discover the evolutionarily conserved mechanisms and the genomic responses to environmental stimuli (Bar-Or *et al.*, 2007a; Bar-Or *et al.* 2007b; Buckely, 2007; Castilho *et al*., 2009; Eddy and Storey, 2008; Kassahn *et al*., 2008; Renn *et al*., 2004). However, the usefulness of CSH is applied only when reasonably broad areas of homology are compared and the lengths of probes in use are sufficiently long that small inter-species differences in the nucleotide sequences would not obscure the analytical results (Adjaye *et al*., 2004).

In the plant community, availability of extensive sequence information had been limited to *Arabidopsis* (*Arabidopsis* Genome Initiative, 2000) and rice (Goff *et al*., 2002; Yu *et al.*, 2002), and the majority of broad-scale gene expression profiling using microarray had been limited to these species. However, with the advent of second generation sequencing technology, the list of the plant species with known genome sequences has been expanding rapidly (Figure 1-18 on page 25) in recent years. The increased availability of sequenced genomes in different species, the rapid development of EST and the advance of heterologous hybridization microarray techniques make it possible to incorporate transcriptional information into comparative genomics studies of the species with little genomic sequence data. Microarray-based heterologous

hybridization techniques have been successfully applied for gene expression profiling of closely related species in the plant families such as Brassicaceae (Becher *et al*., 2004; Kang *et al*., 2008) and Solanaceae (Bagnaresi *et al*., 2008; Fei *et al*., 2004; Moore *et al*., 2005), as well as among distantly related species, such as leafy spurge (*Euphobia esula*), poplar (*Populus deltoides*) and wild oat (*Avena fatua*) (Horvath *et al*., 2003).

1.4.3 Factors Involved in Microarray-based Heterologous Hybridization

Various factors may affect the effectiveness of microarray-based heterologous hybridization, including such variables as the inter-species sequence diversity, the nature and length of the cDNA probes in the microarray used and the experimental design employed (Buckley, 2007).

Sequence divergence influences the hybridization between the probes on the microarray and the targets from the samples, and therefore it is crucial to distinguish differences in detected intensity levels that reflect actual differential gene expression and those that result from sequence mismatches. With increasing phylogenetic divergence, the number of features on a microarray that can effectively hybridize to the targets from other species is expected to decrease as the sequence divergence between the species increases, resulting in the reduction of effective size of a given microarray (Buckley, 2007). The lengths of probes affixed on the platform also has profound effects on the efficiency of hybridization between two species. Heterologous hybridization to oligonucleotide microarrays, which generally consist of short cDNA probes (70-mer), is only effective for analyzing gene expression in closely related species (Bagnaresi *et al*., 2008). The experimental design also affects the efficiency of hybridization when a microarray prepared from a species is used to compare gene expression profiles among different sample species. The different levels of sequence homology between the probe species and each target species affect the resulting gene expression values. This might introduce a bias and it becomes more difficult to distinguish the actual differential gene expression from the effect of sequence mismatches, which becomes more variable as the level of sequence divergence increases between the sample and the reference species and among sample species. In the experiments where this kind of bias arising from sequence divergence is expected, uncertainties in the interpretation of the results could be reduced by including only highly homologous genes and/or best matching annotation, when genomic data are available for target species comparable to probe species (*e.g.*, potato *vs.* tomato; Bagnaresi *et al*., 2008; Bar-Or *et al*., 2006). The sequence divergence does not add bias when different tissue samples or samples subjected to different environmental stimuli are from single target species.

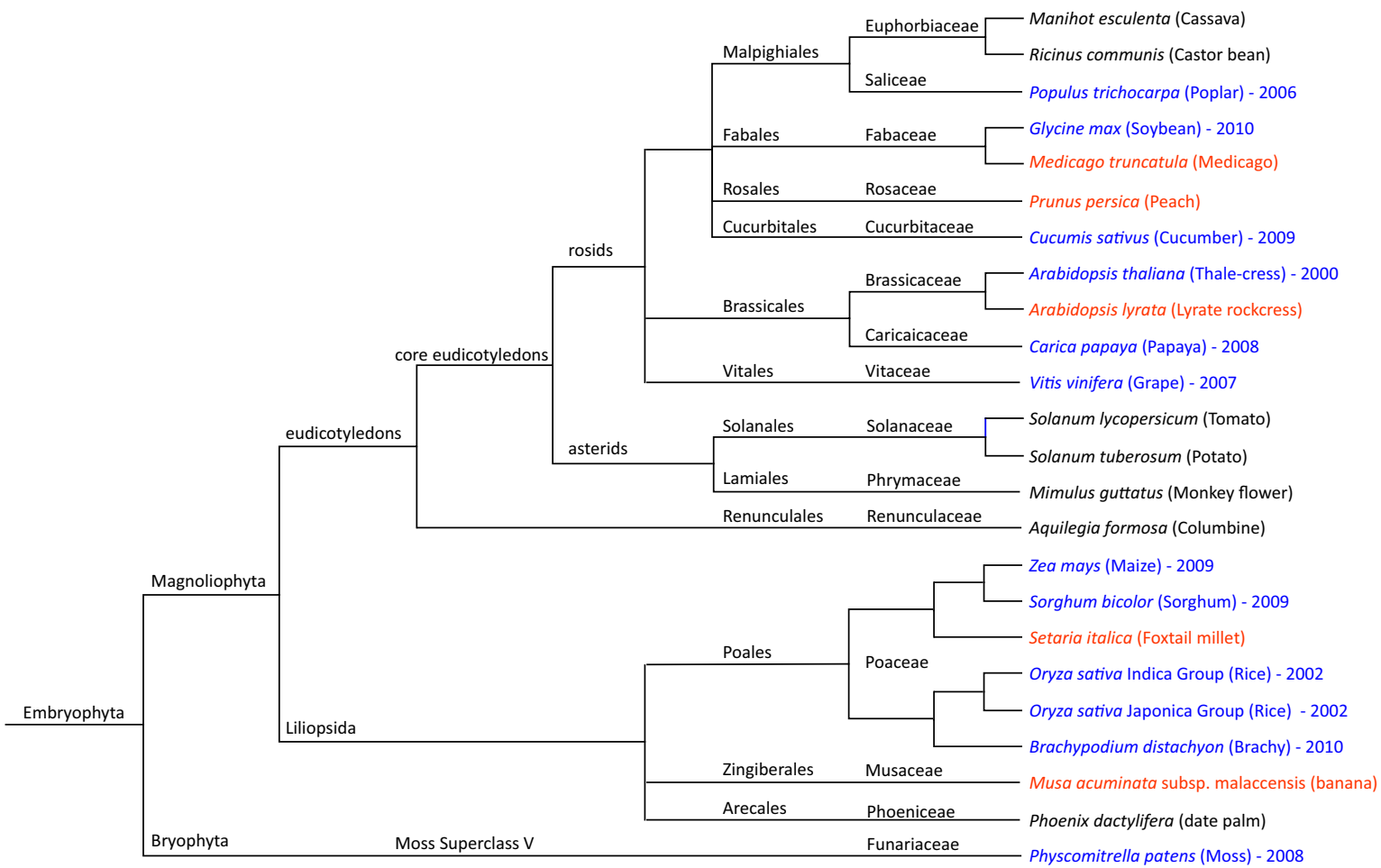

Figure 1-18. Cladogram showing the species of which genomes were sequenced or in progress. Drawn based on the sequenced plant genome information at CoGepedia (http://synteny.cnr.berkeley.edu/wiki/index.php/Sequenced_plant_genomes). The taxonomy tree file was generated at Interactive Tree of Life (http://itol.embl.de/index.shtml) using NCBI taxonomy data retrieved from http://www.ncbi.nlm.nih.gov/sites/entrez?db=taxonomy and is based on rRNA sequences. Tree was constructed using Dendroscope software (http://www-ab.informatik.uni-tuebingen.de/software/dendroscope/; Huson *et al*., 2007). As of April 10, 2010, the genomes of 10 plant species (blue font) including a moss were sequenced and published (year indicated for each). The genome sequences of 7 plant species (black) are incomplete, but sequence data are available. The genome sequencing for 5 species (red) is known to be underway, but not published or released.

1.5 Microarray in Studies of SAM

Mutant analyses have identified quite a large number of genes that are involved in the maintenance of the totipotent stem cell population in the central region and in the organ differentiation in the peripheral region of the SAM, some of which are known to be conserved among plant species (Bäurle and Laux, 2003; Bowman and Floyd, 2008; Carles and Fletcher, 2003). However, these genetic approaches, often relying on the knockout mutation in the gene of a function, have limitations since many genes have genetically and functionally redundant alleles that may mask the phenotype of any loss-of-function mutation in an allele. In addition, mutagenic approach for specific functions of essential genes are unsuitable, if the mutations are lethal (Bouche and Bouchez, 2001). Furthermore, loss- or gain-of-function mutation in one gene may affect the entire network of the interacting cells (Reddy and Meyerowitz, 2005). Thus, it is unlikely that genetic approaches alone can elucidate the entire network of the regulatory pathways controlling growth, division and differentiation of cells in the SAM.

Microarray technology is a suitable tool for analyzing the global expression of numerous genes in a single experiment by comparing the transcriptomes from multiple sources (Schena et al., 1995). In this study, global differential gene expression patterns in the shoot apex and young leaf of *H. helix* cv. Goldheart were compared. cDNA microarray-based heterologous hybridization technique with an *A. thaliana* cDNA microarrays was employed, which allows simultaneous display of thousands of gene products in non-model plant species. The focus of the study was screening the shoot apex-specific genes, and identifying those that might be involved in the underlying regulatory pathways for the SAM function in relation to the cell types, cell lineages and initiation of leaf primordia, which is essential to understand the roles of the SAM in a more coherent picture of the gene network involved.

One of the difficulties involved in the experiments to detect genome-wide expression of shoot apex-specific genes in *Arabidopsis* has been the separation and collection of uniform shoot apex tissue, due to its small size. Laser capture microdissection (LCM) allows the isolation of specific cell types from tissue sections, and has been applied for the studies of global gene expression profiling using microarray technology for the SAM (Emrich *et al*., 2007; Ohtsu *et al*., 2007). While the cost of the LCM equipment and the technical issues (such as reproducibility and validity) involved in the amplification of small amount of mRNA sample become another challenge to be resolved (Clement-Ziza *et al*., 2009; Li *et al*., 2005b; Nygaard *et al*., 2005), the heterologous hybridization of targets from other plant species with larger shoot apex, such as *H. helix,* to *Arabidopsis* cDNA microarrays could be a cost-effective alternative to cope with this problem.

PART 2. MATERIALS AND METHODS

2.1 Plant Material

2.1.1 Starting Plant Stock

Ten variegated ivy (*Hedera helix* L. cv. Goldheart) plants, which were assured by the vendor to have been propagated from single plant, were obtained locally (Chuck Hafner's Farmers Market, Syracuse, NY) and transferred in plastic pots (4" diameter) containing a 1:1:1 mixture of perlite, vermiculite and MiracleGro® Professional Potting Mix (Scotts Co., Marysville, OH). The potted plants were maintained under a greenhouse bench, where they were partially shaded, in the greenhouse at the State University of New York College of Environmental Science and Forestry (SUNY ESF), Syracuse, New York. About three months after transplanting, when root systems were stabilized and shoots resumed growing vigorously, the main shoots of the plants were cut off and new shoots were grown from the lateral buds at the first, second or third node from the ground. These new shoots were used for propagation by stem cutting (Figure 2-1 on page 29, A).

2.1.2 Propagation by Stem Cutting

After one growing season, stem cuttings were prepared separately from each plant. Stem segments of 10-15 cm in length, containing 3-5 nodes, were cut using sharp razor blades. After removing the leaves at the lowest node, the base of the cuttings were soaked in an indol-3-butyric acid (IBA, # 57310; Sigma-Aldrich, St. Louis, MO) solution at 1000 ppm for one minute, powdered with Captan® 50% WP (Bonide Products, Inc. Oriskany, NY), and then immediately inserted into the holes pre-made in a 1:1 mixture of perlite and vermiculite (Horticultural Grade; Conrad Fafard, Inc., Agawam, MA). Stem cuttings were kept for about 1½ months until they produced new root and shoot systems under humid conditions maintained by a mist system. More than 95% of the total cuttings rooted successfully and 13-27 new plants per stock were produced for further propagation (Figure 2-1 on page 29, B). Plants were grown in the greenhouse at SUNY ESF for about 10 weeks until they produced 15-20 nodes. They were watered regularly and fertilized with MiracleGro® All Purpose Plant Food (Scotts Co., Marysville, OH) as needed following the manufacturer's recommendation. To control aphids and white flies, Ortho® Isotox® Insect Killer (Scotts Co., Marysville, OH) was sprayed periodically following the manufacturer's instruction.

Using the newly established ivy plant stock, the second stem cutting propagation was carried

out in the same way as described previously. To ensure genetic homogeneity of sample plants, only the batch that was in the largest number and relatively uniform in the size was selected. A total of 135 plants were obtained by the second stem cutting from 13 of the 27 plants propagated from single plants from the initial batch (Figure 2-1 on page 29, C).

2.1.3 Re-establishment of Plant Batches

About 100 plants were transferred to Bowling Green State University (BGSU), Bowling Green, Ohio. Shoots were cut back and new shoots were grown from about 60 plants (Figure 2-1, D), which were previously propagated by stem cuttings from a single plant. A new batch of 193 plants was established by stem cuttings from 16 plants (Figure 2-1 on page 29, E). Stem cutting was carried out in the same way as described above, except for the cutting treatment, where the cuttings were treated with Hormex® Rooting Powder No. 1 (Brooker Chemical, Chatsworth, CA) containing 0.1% indol-3-butyric acid (IBA) in talc powder. Another batch of 574 plants was propagated from another 40 *H. helix* cv. Goldheart plants (Figure 2-1 on page 29, E). Cuttings were treated with Hormex® Rooting Powder No.1 (Brooker Chemical, Chatsworth, CA), and rooted on OASIS® WEDGE® System (Cat. #5644; Smithers-Oasis U.S.A., Kent, OH), a rooting medium formulated to assure a high soil moisture content. A month later, the plants which rooted in the wedge media were transferred to 5½" square plastic pots containing a fertilized soil mixture. Plants were watered and fertilized as needed and pesticides were applied as needed to control white flies and aphids. More than 400 plants, which originated from single plant, were maintained in the greenhouse throughout the period of sampling.

2.2 Sample Tissue Preparation

2.2.1 Tissue Collection

Samples of shoot apices and young leaves always were collected from actively growing healthy shoots. And, after sampling, the shoots were cut back leaving 2-3 nodes, at which a new shoot was grown for the next sampling. A shoot tip containing a shoot apex and a young leaf subtending the shoot apex was excised from each of 250 plants (Figure 2-2 on page 31, A) and immediately flash-frozen in liquid nitrogen. The jar containing liquid nitrogen and shoot tip specimens was capped loosely and transferred to a Styrofoam box containing dry ice. After all of the liquid nitrogen evaporated completely, the jar containing the shoot tip samples was capped tightly and transferred to the laboratory for further dissection. The shoot tips were stored in a -80°C freezer

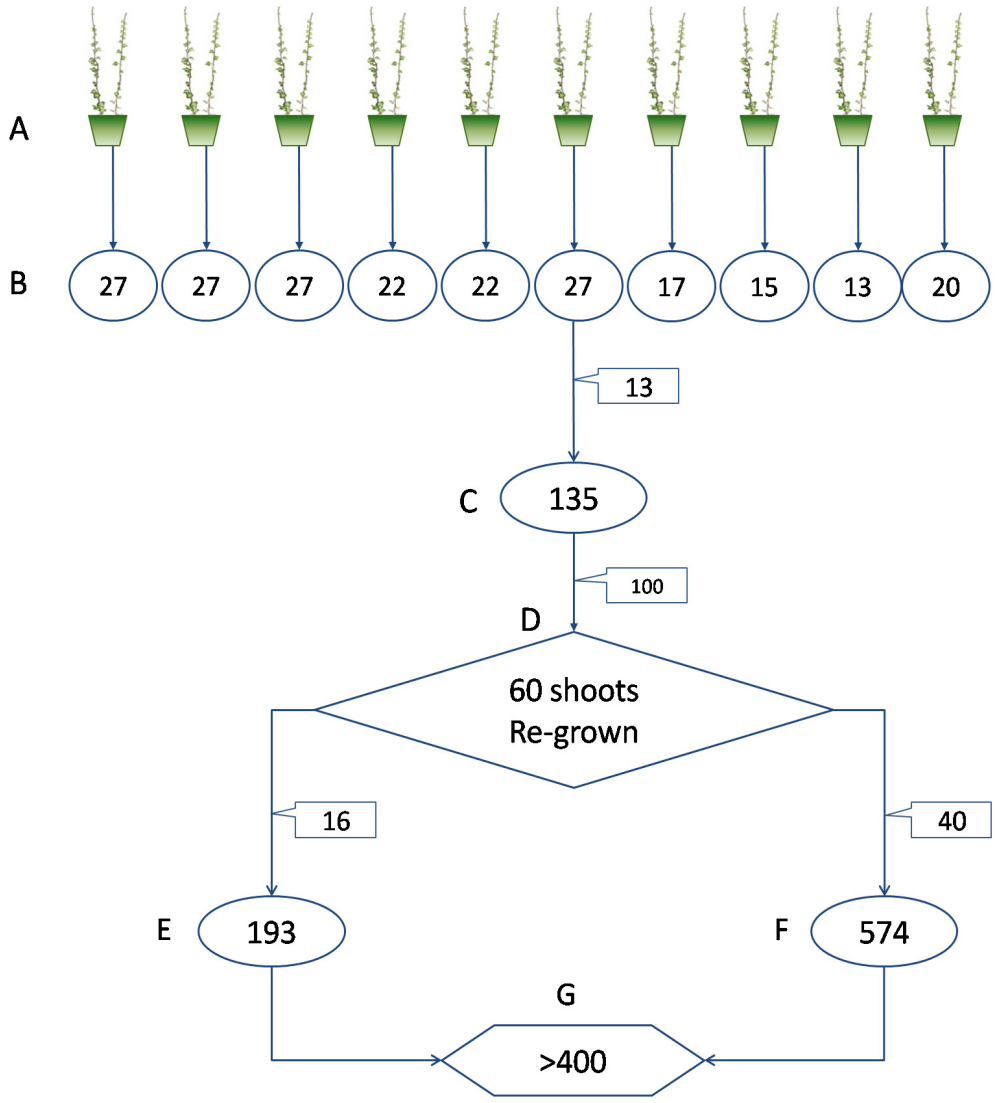

Figure 2-1. Clonal lineage of sample plants propagated by stem cuttings. The numbers in the circles are the quantities of plants produced by stem cutting, while the numbers in the call-out boxes are the quantities of the stock plants from which the stem cuttings were obtained. A: Starting plant stock, 10 plants obtained locally. B: The first batch of plants produced by stem cuttings from each of the starting stock. C: The second batch consisting of 135 plants, which were obtained from 13 of 27 plants propagated from a single plant. D: Out of 135 plants in the second batch, 100 were transferred to BGSU and 60 new shoots were re-grown. E: Among 60 plants with newly grown shoots, 16 were used to produce the third batch of 193 plants. F: Another 40 plants were used for stem cutting of the fourth batch consisting of 574 plants. G: More than 400 plants, which were propagated from a single stock plant, were maintained for sampling.

until they were dissected into apex and leaf specimens. During dissection, the shoot tips were kept submerged in liquid nitrogen to prevent formation of frost.

For dissecting, a shoot tip was placed on an aluminum block chilled by dry ice-95% ethanol bath under a dissecting microscope. Starting from the largest one, three young leaves were excised at the leaf base without petioles using a pair of fine-pointed forceps (Inox #5; Dumont S.A., Switzerland) and a scalpel with blade #11 (Feather Safety Razor Co., Osaka, Japan). The excised leaf samples were collected separately in insulated plastic jars containing liquid nitrogen according to their developmental stages, as follows (Figure 2-2 on page 31, B):

1. Young leaf #3: the smallest completely unfolded leaf with leaf blade larger than 1 cm in length.
2. Young leaf #2: partially or completely folded, but not covering the shoot apex; used for total RNA extraction in this experiment.
3. Young leaf #1: completely folded and enclosing the shoot apex.

After collecting the young leaf specimens, the apex specimens were excised and collected in a separate jar containing liquid nitrogen. Each apex specimen typically included the shoot apical meristem, leaf primordia and the first two emerging leaves; the first leaf had its concave adaxial surface adjacent to the primordium, and the second leaf, at the opposite side of the first leaf, had a leaf blade edge bending over and covering the apical dome. A total of 230 shoot apices and 100-115 young leaves were collected by dissection. The tissue samples were stored in a -80°C freezer until isolation of total RNA.

All of the instruments and containers used for collection and dissection were RNase-free and the entire sampling procedure was carried out in an RNase-free environment, whenever possible. The instruments and containers were cleaned with RNaseAway™ (Cat. #10328011; Invitrogen, Carlsbad, CA) or RNaseZap® (Cat. #9780; Applied Biosystems/Ambion, Austin, TX), rinsed with diethyl pyrocarbonate (DEPC; Cat. #D5758; Sigma-Aldrich, St. Louis, MO)-treated RNase-free water (Sambrook and Russell, 2001), and subsequently with 100% ethanol. The dust-free bench top was sprayed with one of the RNase decontamination agents and wiped with Kimtech Science® KimWipes® Delicate Task Wipers (Cat. # 34256; Kimtech Science, Roswell, GA). After wiping with the wipes moistened with DEPC-treated RNase-free water, the surface was wipe-dried using the same type of wipes.

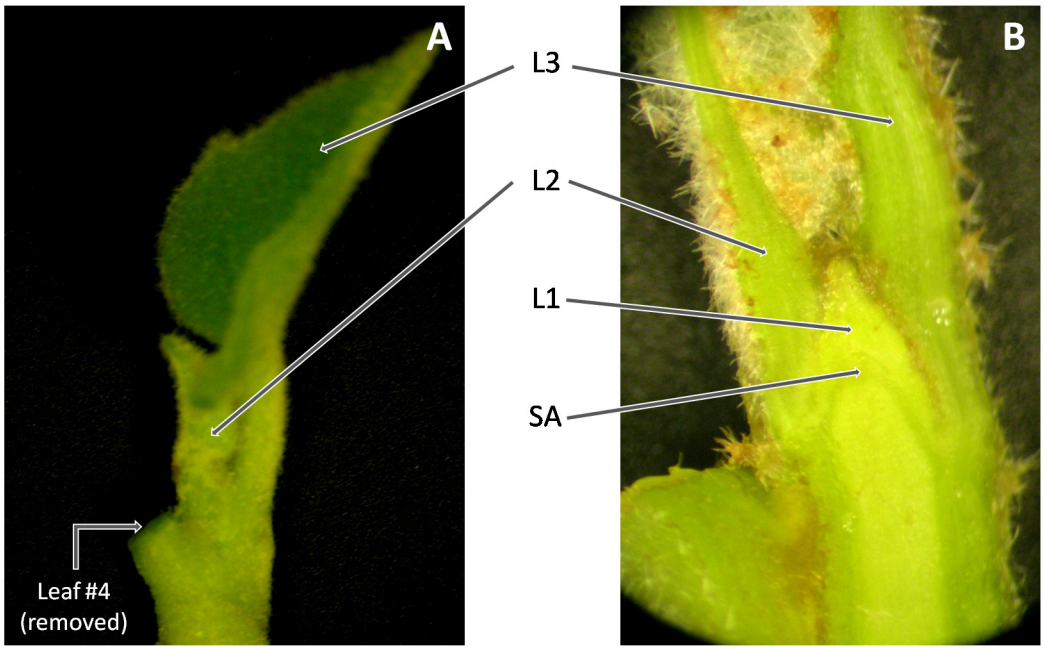

Figure 2-2. Sampling scheme for shoot apices and young leaves. A, a *Hedera helix* shoot tip showing the first unfolded leaf (L3), and the younger leaf (L2), which was used as the young leaf specimen without petiole. Leaf #4 was removed at the time of shoot tip sample collection in the greenhouse. B, Longitudinal view of hand-section of the shoot tip showing the shoot apex (SA), the enclosing leaf #1 (L1), leaf #2 (L2) and leaf #3 (L3). Leaf #2 was cut through mid-veins of the blade; and leaf #3, through the center of the petiole. The typical shoot apex sample included small developing young leaves, leaf primordia and the apical dome, which were enclosed by the Leaf #1. Leaf #1 was not included in the shoot apex sample.

2.2.2 Grinding Tissue Samples

For the extraction of total RNA, the shoot apices and young leaf samples were ground into fine powder. Frozen samples were ground in liquid nitrogen in RNase-free 15 ml BD Falcon™ polystyrene conical tubes (Cat. #352095, BD Biosciences, San Jose, CA) using an RNase-free Kontes® Chlorotrifluoroethylene (CTFE)/Stainless Steel Pellet Pestle® for 1.5 ml Tube (Cat. # 749515-0000; Kimble-Kontes, Vineland, NJ) attached to a cordless rotary tool (Dremel® Minimite 750, 4.8V; Robert Bosch Tool Corp., Racine, WI). The lower portion of the tube containing tissue sample was kept in liquid nitrogen, and the sample inside was slightly covered with liquid nitrogen to eliminate frictional heat between the tissue, pestle and tube wall. When the tissue was ground to fine powder suitable for the extraction of total RNA, it was pale green in color and dispersed readily in slowly swirled liquid nitrogen, forming aggregates, which eventually settled on the

bottom of the tube as a uniform layer of talc-like powder. After grinding, the tube containing liquid nitrogen and tissue powder was loosely capped and placed on dry ice at a 45 degree angle to evaporate the liquid nitrogen without excessive boiling and splashing. When all of the liquid nitrogen evaporated, the tube was capped tightly and kept at -80°C until RNA isolation.

2.3 Total RNA Extraction and Purification

Total RNA was extracted from the ground tissue samples of shoot apex and young leaf sample. To maximize the yield of isolated total RNA at the highest purity possible, total RNA was extracted with Trizol Reagent® (Cat.#155960; Invitrogen, Carlsbad, CA; Chomczynski and Mackey, 1995). The RNA-containing aqueous phase was separated using Phase Lock Gel™ (PLG, Heavy; Cat. # 95515404-5 or # 95515407-0; Eppendorf North America, Westbury, NY) and purified using RNeasy® Midi columns (Cat. #75142; Qiagen, Valencia, CA) in combination with RNase-free DNase (Cat. #79254; Qiagen, Valencia, CA) treatments.

2.3.1 Extraction

The frozen sample powder of shoot apices and young leaves were transferred into 15 ml or 50 ml BD Falcon™ polystyrene conical tubes (Cat. #352095 or #352073, BD Biosciences, San Jose, CA), which were pre-weighed and pre-chilled in liquid nitrogen. After the approximate volume of the sample and the net tissue weights were determined, approximately 10X sample volume of Trizol Reagent® was added to each tube (Table 2-1 on page 33). The reagent stored at 4°C, was warmed to 35-40°C in a water bath before being added to prevent freezing when it was added to the frozen tissue. Immediately after adding the reagent, the mixture was homogenized thoroughly using an RNase-free Kontes® Chlorotrifluoroethylene (CTFE)/Stainless Steel Pellet Pestle® For 0.5 ml Tube (Cat. #749515-0500; Kimble-Kontes, Vineland, NJ) attached to a Pellet Pestle Cordless Motor (#749540-0000; Kimble-Kontes, Vineland, NJ), and then incubated at room temperature for 6 minutes with vortexing every 2 minutes.

Chloroform (0.2 volumes relative to Trizol Reagent®) was added to each tube containing tissue-Trizol® homogenate, and the contents were mixed thoroughly to form a homogeneous suspension by vortexing. The tissue-Trizol® homogenate/chloroform mixture was transferred into pre-spun PLG tubes (Heavy; Cat. # 95515404-5 or # 95515407-0; Eppendorf North America, Westbury, NY) and mixed thoroughly by shaking vigorously. To separate the organic and the aqueous phases, 1.5 ml aliquots of Trizol homogenate/chloroform mixture were transferred into each of

Table 2-1. Amounts of tissue and reagents used for total RNA extraction and volume of retrieved aqueous phase.

Samples	Wt. of Tissue (mg)	Vol. of Tissue (ml)	Vol. of Trizol (ml)[a]	Vol. of Chloroform (ml)	Vol. of Retrieved Aqueous Phase (ml)
Shoot Apex	478	0.84	8.4	1.7	4.4
Young Leaf	974	1.70	17.0	3.4	9.0

[a.] The volume of 1g tissue powder was about 1.75 ml and 10X tissue volume of Trizol reagent was used (17.5 ml Trizol Reagent®/gram sample). The volume of chloroform added was 1/5 volume of Tizol Reagent added.

pre-spun 2.0 ml PLG tubes and mixed thoroughly by shaking vigorously. The PLG tubes were centrifuged at maximum speed (13,200 rpm) on a microcentrifuge (Model 5415D; Eppendorf North America, Westbury, NY) for 15 minutes to separate the phases. To keep the temperature of the PLG tubes low, dry ice was placed around and on the centrifuge. Immediately after centrifugation, the RNA-containing aqueous phase was pipetted off and pooled in a fresh RNase-free 15 ml BD Falcon™ polystyrene conical tube (Cat. #352095, BD Biosciences, San Jose, CA) for each sample.

2.3.2 Purification

To purify total RNA from the pooled aqueous phase, an equal volume of 70% ethanol was added slowly to the retrieved aqueous phase and mixed thoroughly by inverting the tube repeatedly. The first 4 ml aliquot of the mixture was pipetted into a RNA-binding column placed in a collection tube, which was supplied in the RNeasy® Midi kit (Cat. #75142; Qiagen, Valencia, CA). The column was centrifuged for 5 minutes at maximum speed (4750 rpm ± 2%) on a bench-top centrifuge with a swing-bucket rotor (Centrific™ Model 225; Fisher Scientific, Springfield, NJ). After the centrifugation, flow-through in the collection tube was discarded. Centrifugation was repeated using the same RNA-binding column for the rest of the mixture.

DNase I digestion was carried out using the RNase Free DNase Set (Cat. #79254; Qiagen, Valencia, CA) following the manufacturer's protocol. Briefly, the total RNA-bound RNeasy® silica-gel membrane in the binding column was washed with 2 ml RW1 buffer, which was included in the RNeasy® Midi kit, by centrifugation for 5 minutes at maximum speed. After applying 160 µl of the incubation mixture containing approximately 55 Kunitz units of DNase I directly onto the RNeasy®

silica-gel membrane, the reaction was incubated on the bench top at room temperature for 15 minutes. After DNase I digestion, the RNeasy® membrane was washed by two successive loadings of 2.5 ml RPE buffer supplied in the RNeasy® Midi kit and centrifugation for 2 minutes each at the maximum speed using the same centrifuge as in the RNA binding step described above. To dry the RNeasy® silica-gel membrane, the tubes were centrifuged for additional 3 minutes at maximum speed following the second centrifugation.

Total RNA was eluted by applying two 100 µl aliquots of non-DPEC treated RNase-free water supplied in the RNeasy® Midi Kit. After adding each aliquot of eluent, tubes were incubated for 5 minutes at room temperature and then centrifuged at maximum speed for 3 minutes. Using water in the second elution results in a higher yield of total RNA while using the first eluate as an eluent increases the concentration of total RNA with lower yields (Qiagen, 2001). To obtain a higher total RNA yield, a second elution step was performed using another volume of RNase-free water, rather than using the first eluate as the eluent to increase the concentration of total RNA.

2.3.3 Storage, Quantitation and Determination of Quality of Total RNA

The total RNA solutions were transferred to 1.5 ml microcentrifuge tubes with screw caps and kept frozen in a -80°C freezer, until needed. The quantity and purity of total RNA purified with RNeasy® Midi columns were assessed by spectrophotometry using 100 µl quartz cuvettes in a spectrophotometer (Model DU-600; Beckman, Fullerton, CA). For measurements of concentrations, the total RNA eluates were diluted in deionized water and the absorbance was measured at 260 nm with 320 nm background correction. RNA concentration was calculated by the equation:

$$(A_{260} - A_{320}) \times 40 \text{ mg/ml} \qquad \text{(EQ. 2-1)}$$

which is based on an extinction coefficient calculated for RNA in water (Qiagen, 2001). As the relationship between the absorbance and concentration is reliable only when the absorbance readings are in the range between 0.15-1 (or possibly 1.2), dilutions were made so that the absorbance readings of the diluted sample was within this range.

For determination of the purity of RNA, the total RNA samples were diluted in 0.1X TE (10 mM Tris-HCl, pH 7.5), and the spectrophotometer was calibrated with the same solution (Wilfinger *et al*., 1997). Absorbance was measured at 260 and 280 nm with 320 nm background correction. The

ratio (A_{260} - A_{320})/(A_{280} - A_{320}) was calculated to estimate the purity of RNA with respect to contaminating protein that absorb in the UV. The programmed routine in the equipment did not calculated the ratio (A_{260} - A_{320})/(A_{230} - A_{320}), which is an estimation of carbohydrate contaminants. The integrity of total RNA were verified by the ratio between *25S* and *18S* ribosomal RNA on a denaturing agarose gel electrophoresis (Imbeaud *et al*., 2005; Kleber and Kehr, 2006), which was run using the protocol and reagents described in the NorthernMax® Kit manual (Cat. #1940; Applied Biosystems/Ambion, Austin, TX) and SYBR® Green II RNA gel stain (Cat. #S-7564; Invitrogen, Carlsbad, CA).

2.4 Labeling cDNA Targets with Fluorescent Dyes

To prepare fluorescently labeled cDNA targets, an indirect labeling method was used (Russell *et al*., 2009). In this method, amino-modified nucleotides are incorporated into the first-strand cDNA by reverse transcriptase PCR (RT-PCR) using total RNA from tissue samples as templates. Subsequently, fluorescent dyes containing a reactive succinimidyl ester (NHS) group are reacted with the primary amine groups in the amino-modified nucleotide for dye coupling. Meanwhile, in a direct labeling method, a dye-conjugated nucleotide is directly incorporated into the first-strand cDNA during RT-PCR. While direct labeling method is simple and rapid, labeling efficiency is low due to large size of the dye molecules, and there is an incorporation bias caused by the difference in the molecular sizes between two dyes. For example, cDNA is labeled at higher efficiency by cyanine 3 (Cy3) than by cyanine 5 (Cy5). Indirect labeling is advantageous in that the labeling efficiency is higher because amino-modified nucleotides, which are much smaller in size, are incorporated into cDNA instead of nucleotides coupled to bulky dye molecules. Also, dye-incorporation bias is much smaller in the indirect labeling method than the direct labeling method because the reactivity of the primary amine group in the amino-modified nucleotides is similar for both Cy3 and Cy5.

2.4.1 Synthesis of Amino-Modified cDNA

Amino-modified nucleotides were incorporated into cDNA targets using SuperScript III reverse transcriptase and poly-d(T) primers provided in the SuperScript™ Indirect cDNA labeling System (Cat. #L1014-02; Invitrogen, Carlsbad, CA) following the manufacturer's instructions (Invitrogen Life Technologies, 2004). Two amino-modified nucleotides, an aminoallyl-modified nucleotide and an aminohexyl-modified nucleotide, were incorporated with other dNTPs. Equal amounts of total RNA from shoot apices or young leaf samples were used as RNA templates in each reaction.

Since the concentrations of the eluted total RNA of shoot apices and young leaves were different, the volumes of total RNA added to the reactions were adjusted to balance the amount of RNA template between two samples. Template/primer mixture tubes were prepared as in Table 2-2. Four reaction tubes were prepared for each sample, and a control reaction, in which an RNA ladder was used as template, was included to determine the efficiency of the labeling procedure. To denature RNA templates, the template/primer mixture tubes were incubated at 70°C for 5 minutes, and then placed on ice for at least 1 minute for primer annealing. To continue with first-stand cDNA synthesis reaction, the reaction mixture including amino-modified nucleotides (Table 2-3 on page 37) was added to each template/primer mixture tube and mixed.

Tubes containing the reaction mixture were incubated at 46°C for 3 hours using a thermocycler (Mastercycler® Gradient; Eppendorf N.A., Westbury, NY) to synthesize first-strand cDNA with amino-modified nucleotides incorporated. Immediately after stopping the cDNA synthesis reaction by heating the tubes at 94°C for 2-3 minutes, RNA templates were hydrolyzed by adding 15 µl of 1 N NaOH and incubating for 10 minutes at 70°C. Subsequently, the reaction mixture was neutralized by adding 15 µl of 1 N HCl.

Table 2-2. Components of template/primer mixture added for each reaction for first-strand cDNA synthesis.

Components	Amount to add for Sample (µl)		
	Shoot Apex	**Young Leaf**	**Control**
Total RNA (20 µg)	7.5	13	-
Control HeLa RNA (1 µg/µl)	-	-	1
Anchored Oligo$(dT)_{20}$ Primer (2.5 µg/µl)	2	2	2
Random hexamer primers (0.5 µg/µl)	-	-	1
Non-DEPC-treated water	8.5	3.0	14
Total Volume	**18**	**18**	**18**

Table 2-3. Components of reaction mixture added to each reaction for first-strand cDNA synthesis.

Component	Volume (µl)
5X First-Strand buffer[a]	6
0.1 M DTT in water	1.5
dNTP mix (including amino-modified nucleotides)[b]	1.5
RNaseOUT™ (40 U/µl)	1
SuperScript™ III RT (400 U/µl)[c]	2
DEPC-treated water	18
Final Volume	**30**

[a.] Contained 250 mM Tris-HCl (pH 8.3, room temp.), 375 mM KCl and 15 mM $MgCl_2$.

[b.] dATP, dGTP, dCTP, dTTP, one aminoallyl-modified nucleotide, and one aminohexyl-modified nucleotide at optimal concentrations in DEPC-treated water.

[c.] 400 U/µl in 20 mM Tris-HCl (pH 7.5), 100 mM NaCl, 0.1 mM EDTA, 1 mM DTT, 0.01% (v/v) NP-40 and 50% (v/v) glycerol.

2.4.2 Purification of Amino-Modified cDNA

The amino-modified cDNA was purified to remove unincorporated dNTPs and hydrolyzed RNA templates using a QIAquick PCR Purification Kit (Cat. #28104; Qiagen, Valencia, CA) by following the procedures in the accompanying manual with some modifications. Instead of using EB buffer in the kit for elution, the amino-modified cDNA was eluted in the dye-coupling buffer (0.1 M sodium bicarbonate, pH 9.0), which was the buffer used in the subsequent labeling steps. The quality of purified amino-modified cDNA was assessed by agarose gel electrophoresis and ethidium bromide staining.

2.4.3 Concentrating Amino-Modified cDNA

The purified amino-modified cDNA solutions were concentrated using Microcon® YM-30 Centrifugal Filter Units (Cat. #42410; Millipore, Billerica, MA) to accommodate the whole amount of cDNA in the labeling reaction. For each tissue sample, two aliquots of 100 µl amino-modified cDNA solution were transferred into two separate filter units. To obtain a final volume of 5 µl, the filter units placed in the collection tubes were centrifuged for 6 minutes at 13,200 rpm on a microcentrifuge (Model 5415D, Eppendorf North America, Westbury, NY). When the recovered volume was less than 5 µl, coupling buffer (0.1 M $NaHCO_3$, pH 9.0) was added to make the final volume 5 µl before the conjugation reaction with fluorescent dye.

2.4.4 Labeling Amino-Modified cDNA by Dye Conjugation

Subsequent to synthesis, purification and concentration, the amino-modified cDNA's were coupled with mono-functional forms of fluorescent dyes for labeling the target cDNA. Alexa Fluor® 555 and Alexa Fluor® 647 Reactive Dye Decapacks (Cat. #A-32755; Invitrogen, Carlsbad, CA) were used for labeling. For dye-swap (dye-flip or fluor-flip), two sets of fluorescently labeled cDNA targets were prepared (Table 2-4). One set consisted of shoot apex cDNA labeled with Alexa Fluor® 555 and young leaf cDNA labeled with Alexa Fluor® 647. The other set consisted of the same cDNA targets, but labeled with the opposite fluors (Figure 2-3 on page 39).

To couple fluorescent dye to the amino-modified first-stand cDNA, dyes were prepared by adding 2 µl of moisture-free DMSO directly to each of 4 dye vials; two containing Alexa Fluor® 555, and the other two containing Alexa Fluor® 647. The whole content of each dye vial was pipetted into each tube containing amino-modified cDNA target, such that one of two cDNA targets from each sample tissue was coupled with Alexa Fluor® 555 and the other with 647. To bring the final reaction volume to 10 µl, 3 µl of coupling buffer (0.1 M $NaHCO_3$, pH 9.0) was added and mixed. The contents in the tube were mixed well and incubated at room temperature in the dark for 1 hour and 20 minutes.

Table 2-4. cDNA target sets labeled fluorescently with dye-swap.

Labeled cDNA Target Sets	Source of cDNA Targets	Labeling Dyes Used	Fluorescence Color
Target Set 1	Shoot apex	Alexa Fluor® 555	Green
	Young leaf	Alexa Fluor® 647	Red
Target Set 2	Shoot apex	Alexa Fluor® 647	Red
	Young leaf	Alexa Fluor® 555	Green

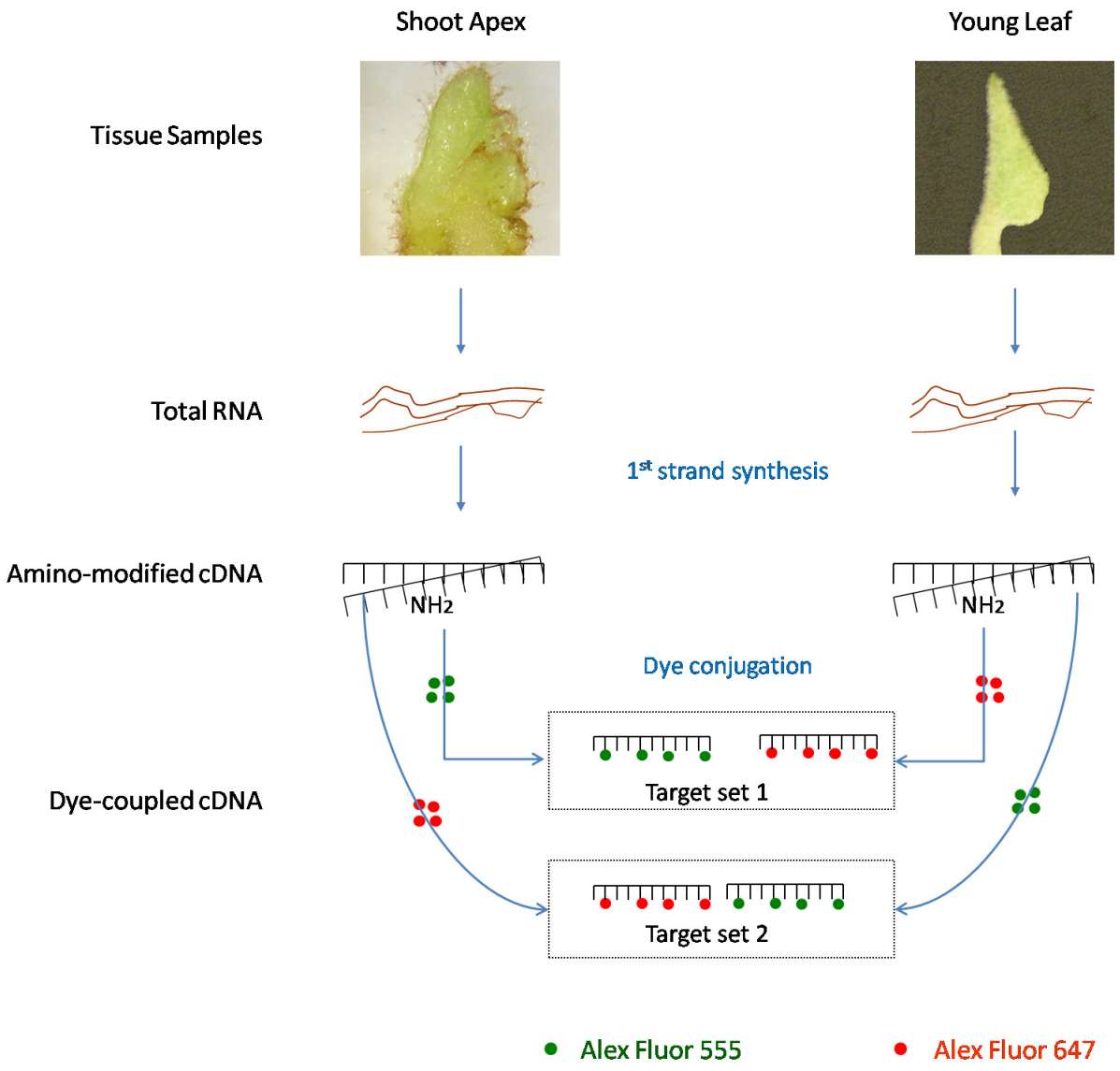

Figure 2-3. A schematic diagram showing preparation of fluorescently labeled cDNA targets. Total RNA was isolated from each sample tissue. Using total RNA as template, amino-modified 1st-stand cDNA was synthesized. The amino-modified cDNA solution from each sample was divided in half. For dye-swap, shoot apex cDNA target was labeled with Alexa Fluor® 555, and young leaf cDNA with 647 in a target set. In the other target set, dyes were coupled reversely; i.e., shoot apex cDNA target was labeled with Alexa Fluor® 647, and young leaf cDNA with 555.

2.4.5 Purification, Quantitation and Concentration of Labeled cDNA Targets

The fluorescently labeled cDNA targets were purified to remove any un-reacted dye using a QIAquick PCR Purification Kit (Cat. #28104; Qiagen, Valencia, CA). To calculate the total amounts of the amino-modified and the fluorescently labeled cDNA, respectively, in the purified target samples, absorbances were measured at 260 mn, 320 nm, 550 nm, 650 mn and 750 nm using a 'Multiple Wavelength Mode' in a Beckman DU-600 spectrophotometer (Beckman, Fullerton, CA). The labeled cDNA elutes were diluted in deionized water and measured in quartz cuvettes.

Total amounts of amino-modified cDNA were determined using the following formula:

$$\text{Amino-modified cDNA (ng)} = (A_{260}–A_{320}) \times 37 \text{ ng/µl} \times 90 \text{ µl (elution volume)} \quad \text{(EQ. 2-2)}$$

The amounts of fluorescently labeled dyes were calculated using the following formulas:

$$\text{Alexa Fluor}^{®} 555 \text{ (pmole)} = (A_{550}–A_{650})/0.15 \times 90 \text{ µl (elution volume)} \quad \text{(EQ. 2-3)}$$

$$\text{Alexa Fluor}^{®} 647 \text{ (pmole)} = (A_{650}–A_{750})/0.24 \times 90 \text{ µl (elution volume)} \quad \text{(EQ. 2-4)}$$

Labeling efficiency was assessed by comparing the yield of fluorescently labeled cDNA to the total yield of cDNA as described in the accompanied manual in the cDNA labeling system (Invitrogen Life Technology, 2004). After the spectrophotometry for labeling efficiency assessment, the purified labeled cDNA was concentrated using a Microcon® YM-30 Centrifugal Filter Unit (Cat. #42410; Millipore, Billerica, MA) to an appropriate volume (11 µl) to accommodate in the total volume of hybridization mixture (36 µl), as recommended by the array manufacturer (W.M. Keck Foundation Biotechnology Resource Lab at Yale University, New Haven, CT, USA). The prepared cDNA targets were kept in each tube separately on ice until mixed in the hybridization mixture.

2.5 Hybridization of Labeled cDNA Targets on Array Probes

2.5.1 Description of cDNA Microarray

Two *Arabidopsis thaliana* cDNA microarray slides (AR12K, serial #980 and #981; W.M. Keck Foundation Biotechnology Resource Lab at Yale University, New Haven, CT, USA) were used for the cross-species hybridization. Each array contained 11,960 expressed sequence tags (ESTs) generated from lambda PRL-2 cDNA library, which was cloned in the Plant Research Laboratory (PRL) at Michigan State University, East Lansing, MI, and made available from the *Arabidopsis*

Biological Resource Center (ABRC) at The Ohio State University (http://www.biosci.ohio-state.edu/~plantbio/Facilities/abrc/abrchome.htm). The clones were prepared from the mixture of four types of tissues of the Columbia wild type of *A. thaliana* (L.) Heynh.: 1) etiolated seedlings; 2) roots; 3) rosette plants of various ages; 4) stems, flowers, and siliques at all stages from floral initiation to mature seeds (Newman *et al*., 1994). The cDNA probes were printed in 32-pin conformations on 1 inch x 3 inch glass slides. Each array contained 32 subarrays in a 4 x 8 block format, and each block had 16 rows and 24 columns. Among a total of 12,288 array spots, 328 spots were blank without properly identified ESTs deposited.

2.5.2 Denaturation and Prehybridization of Arrays

For an optimal hybridization of cDNA targets onto the microarrays, the probes on the microarrays were denatured and prehybridized prior to the target hybridization as described below. Since the printed cDNA probes were double-stranded and the array slides were delivered without denaturation during post-print processing, the cDNA probes on the array slides were denatured to create single-stranded cDNA probes before hybridization with the labeled targets as described below. The denaturation of cDNA probes was immediately followed by prehybridization. The purpose of prehybridization was to coat the surface of the glass to block any sites on which the fluorescently labeled target cDNA might bind nonspecifically and produce background signal (Anderson, 1995). The prehybridization solution contained a blocking agent, a detergent and random-sheared foreign DNA, which is heterologous to both labeled cDNA targets and printed probes on the array slide so as to minimize nonspecific binding of labeled cDNA targets to the slide (Table 2-5 on page 42).

Denaturation and prehybridization were carried out according to the microarray manufacturer's recommended protocol with some modification to adapt the availability of equipment. Briefly, 36 µl of prehybridization solution was placed on each array slide, covered with a clean standard glass coverslip (22 x 50 mm), and laid on the *In situ* Adapter (Cat. #950007052; Eppendorf N.A., Westbury, NY), which in turn was fit onto the metal block of a thermocycler (Mastercycler® Gradient; Eppendorf N.A., Westbury, NY). Before placing the slide on the adapter, a thin layer of water was spread, to ensure even heat transfer. The thermocycler was programmed to heat the block to 76°C for 2 minutes and then to hold the temperature at 50°C.

Immediately after the temperature dropped to 50°C, the slides were transferred into aluminum hybridization chambers (Cat. #DT-1001; Die-Tech, San Jose, CA; Table 2-4 on page 42) and 300 µl of pre-warmed chamber buffer (Table 2-6 on page 43) was added in the grooves and reservoirs

Table 2-5. Ingredients of prehybridization solution.

Ingredient	Stock Conc.	Vol. Added (µl)	Final Conc.
Formamide[a]	99.5%	60	48%
SSPE[b]	20X	20	3.2X
SDS[c]	10%	5	0.4%
Denhardt's[d]	50X	5	2X
Salmon sperm ssDNA[e]	10 mg/ml	2	0.177 mg/ml
ddH_2O	-	33	-
Total Volume		**125**	

a. Molecular biology grade (Cat. #47671; Sigma-Aldrich, St. Louis, MO)

b. 20X SSPE (Saline-Sodium phosphate-EDTA) solution consisted of 3 M NaCl, 200 mM sodium phosphate and 20 mM EDTA in nuclease-free water. About 6.5 ml of 10 N NaOH was used to adjust the pH to 7.4. Solution was autoclaved and sterile filtered (0.2 µm).

c. Sodium dodecyl sulfate, molecular biology grade (Cat. # L4390; Sigma-Aldrich, St. Louis, MO)

d. Denhardt 's Solution (Denhardt, 1966) is a mixture of blocking agents used in hybridization protocols. The solution contained 1% Ficoll (Type 400, molecular biology grade; Cat. #F2637; Sigma-Aldrich, St. Louis, MO), 1% polyvinylpyrrolidone (Cat. #F2637; Sigma-Aldrich, St. Louis, MO), and 1% bovine serum albumin (Cat. #A2764; Sigma-Aldrich, St. Louis, MO) in nuclease-free water. The prepared solution was sterile filtered (0.2 µm).

e. Randomly shredded foreign DNA (Cat. #15632-011; Invitrogen, Carlsbad, CA), which is hetetologous to the labeled target cDNA.

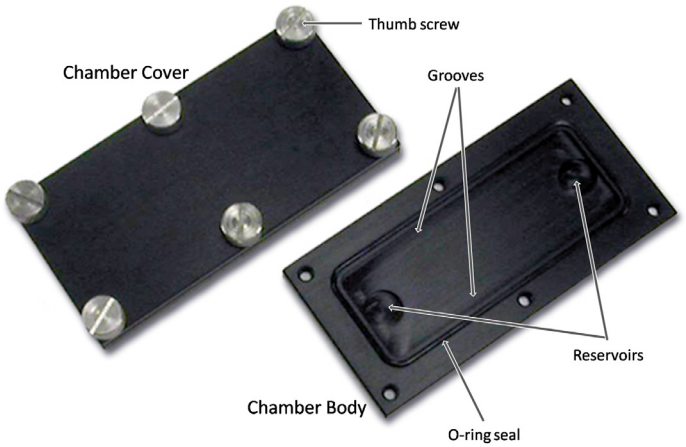

Figure 2-4. Die-Technology hybridization chamber model DT-1001. Grooves and reservoirs are for chamber buffer to keep moisture in the chamber during incubation for prehybridization or hybridization. Capacity of each groove and reservoir are 50 and 100 µl, respectively, holding 300 µl total. (Labels added to a downloaded picture from http://www.die-technology.com/images/p_DT-1001_big.jpg)

Table 2-6. Ingredients of hybridization chamber buffer.

Ingredient[a]	Stock Conc.	Vol. Added (µl)	Final Conc.
Formamide	99.5%	460	23%
SSC	20X	320	3.2X
ddH_2O	-	1220	-
Total Volume		**2000**	

[a.] For the ingredient details, refer to table footnotes of Table 2-5 on page 42

of each hybridization chamber to prevent evaporation of prehybridization solution from the slides. After tightening the thumb screws evenly, the hybridization chambers were placed horizontally in a 50°C water bath. After the array slides were incubated for 1 hour, the slides were carefully and quickly taken out of the hybridization chamber and immediately transferred to a glass Couplin jar (Cat. # 900570; Wheaton Sci. Prod., Millville, NJ) containing distilled-deionized water.

After the coverslips floated off the slide into the water, the array slides were carefully lifted avoiding contacts with the coverslips so as not to scratch the array, and were transferred to another Couplin jar containing fresh water. Prehybridization buffer was removed by gently agitating in the water for 2 minutes. The slides were then dehydrated by placing in 70% ethanol followed by 100% for 2 minutes each. The residual alcohol was evaporated in the air and the slides were kept in a vacuum-sealed canister (FOODSAVER® Round Canister, Cat. #T16-0032; Jarden Corp., Rye, NY) containing dust-free desiccants (DriCan® Reusable Desiccating Canister, Cat. #19950; Ted Pella, Inc., Redding, CA) while hybridization mixtures were being prepared. According to the array manufacturer, removal of the prehybridization buffer results in a more uniform and reproducible hybridization (W.M. Keck Foundation Biotechnology Resource Lab at Yale University, 2006). Denaturation and prehybridization of cDNA probes on the slide were carried out while preparing the hybridization mixture (described in the next section, “2.5.3 Preparation of Hybridization Mixtures”), so that the labeled target could be applied immediately as soon as it was ready.

2.5.3 Preparation of Hybridization Mixtures

To compensate for dye-related bias, which is commonly observed in the two-color microarray platform, dye-swap experimental design was used. In this experiment, one array was co-hybridized with shoot apex and young leaf cDNA targets that were labeled with Alexa Fluor® 555 (fluoresces green) and Alexa Fluor® 647 (fluoresces red), respectively. In a second co-hybridization, the dyes of the two samples were switched.

To prepare the two sets of hybridization mixture, 22.2 µl hybridization buffer (Table 2-7) and 1.4 µl blocking solution (Table 2-8 on page 45) were added in each of two separate 0.5 ml microcentrifuge tubes. The blocking solution was intended to inactivate reactive groups remaining on glass microarray slide surface. It reduces background noise while maintaining full signal intensities for DNA microarray applications according to the microarray manufacturer (W.M. Keck Foundation Biotechnology Resource Lab at Yale University).

Into one of the two microcentrifuge tubes containing hybridization buffer and blocking solution, the shoot apex cDNA labeled with Alexa Fluor® 555 and young leaf cDNA labeled with Alexa Fluor® 647 were added. Into the other, shoot-apex and young leaf cDNA with reversed fluorophores were added (Table 2-9 on page 45). The total volume of the hybridization mixture was 36 µl.

Table 2-7. Ingredients of hybridization buffer solution.

Ingredient[a]	Stock Conc.	Vol. Added (µl)	Final Conc.
Formamide	99.9%	78.5	62.8%
SSPE	20X	31.5	5X
SDS	20%	5	0.8%
Denhardt's	50X	10	4X
Total Volume		**125**	

[a.] For the ingredient details, refer to table footnotes of Table 2-5 on page 42

Table 2-8. Ingredients of blocking solution.

Ingredient	Stock Conc.	Vol. Added (µl)	Final Conc.
Poly dA[a]	1 mg/ml	100	2 mg/ml
tRNA[b]	25 mg/ml	5	4 mg/ml
Mouse Cot1 DNA[c]	1 mg/ml	500	10 mg/ml
Total Volume[d]		**605**	

a. Poly(2'-deoxyadenylic acid) sodium salt (Cat. #81342; Sigma-Aldrich, St. Louis, MO)

b. Yeast tRNA (Lyophilized; Cat. #15401011; Invitrogen, Carlsbad, CA)

c. Mouse Cot-1 DNA® (Cat. #18440016; Invitrogen, Carlsbad, CA) was predominantly 50 to 300 bp in size and enriched for repetitive DNA sequences such as the B1, B2, and L1 family members. Mouse Cot-1 DNA® is commonly used to block non-specific hybridization in microarray screening.

d. After mixing the ingredients, ethanol precipitated and re-suspended in 50 µl of filtered sterile ddH_2O. The blocking solution was diluted with the same volume of 20X SSPE, when the hybridization mixture was prepared.

Table 2-9. Ingredients of hybridization mixture.

Ingredients	Vol. Added (µl)
20X SSPE[a]	1.4
Hybridization Buffer[b]	22.2
Blocking Solution[c]	1.4
Labeled cDNA Targets	11.0
Total Volume	**36.0**

a. For the ingredient details, refer to table footnotes of Table 2-5 on page 42

b. See Table 2-7 on page 44 for ingredients of hybridization buffer.

c. See Table 2-8 on page 45 for ingredients of blocking solution.

2.5.4 Denaturation of cDNA Targets & Hybridization

The fluorescently labeled cDNA targets in the hybridization mixture were denatured at 90°C for 3 minutes on a thermocycler (Mastercycler® Gradient; Eppendorf N.A., Westbury, NY) and kept at 42°C until applied on the array slides. After mixing well by repeated pipetting, each of the hybridization mixtures was applied on each cDNA array slide with dye-swap (Table 2-10 and Figure 2-5 on page 47) carefully so as not to create bubbles, and covered with clean standard 22 x 50 mm glass cover slips. (The array was 18 x 36 mm in size and could be covered under 22 x 40 mm coverslip; but, it was not large enough to hold 36 µl mixture.) After transferring the slides into the aluminum hybridization chambers (Cat. #DT-1001; Die-Tech, San Jose, CA), chamber buffer was added, as previously described in the section, "2.5.2 Denaturation and Prehybridization of Arrays" on page 41. The hybridization chambers were sealed by tightening the thumb screws, placed horizontally and incubated in a water bath at 42°C for 9 hours for hybridization.

Table 2-10. Array identification number and dye-swapped cDNA targets co-hybridized on each array.

Array Slides	Source Tissue of cDNA Targets	Fluorophores Used	Fluorescence Color
Array 1	Shoot apex	Alexa Fluor® 555	Green
	Young leaf	Alexa Fluor® 647	Red
Array 2	Shoot apex	Alexa Fluor® 647	Red
	Young leaf	Alexa Fluor® 555	Green

2.6 Washing and Drying Hybridized Microarray

While hybridization was in progress, a series of wash solutions containing saline-sodium citrate (SSC) and sodium dodecyl sulfate (SDS) in decreasing concentrations (Table 2-11 on page 48) was prepared in glass staining dishes (Slide Staining Dish with Removable Rack, Cat. #900200; Wheaton Sci. Prod., Millville, NJ) and pre-warmed at 32°C in a water bath, which was 10°C below the hybridization temperature.

After hybridization, while maintaining the level, the hybridization chambers were transferred onto a slide warmer, which was set to the same temperature as for hybridization. After the moisture on the outside of the hybridization chamber was wiped dry (especially in the gap between

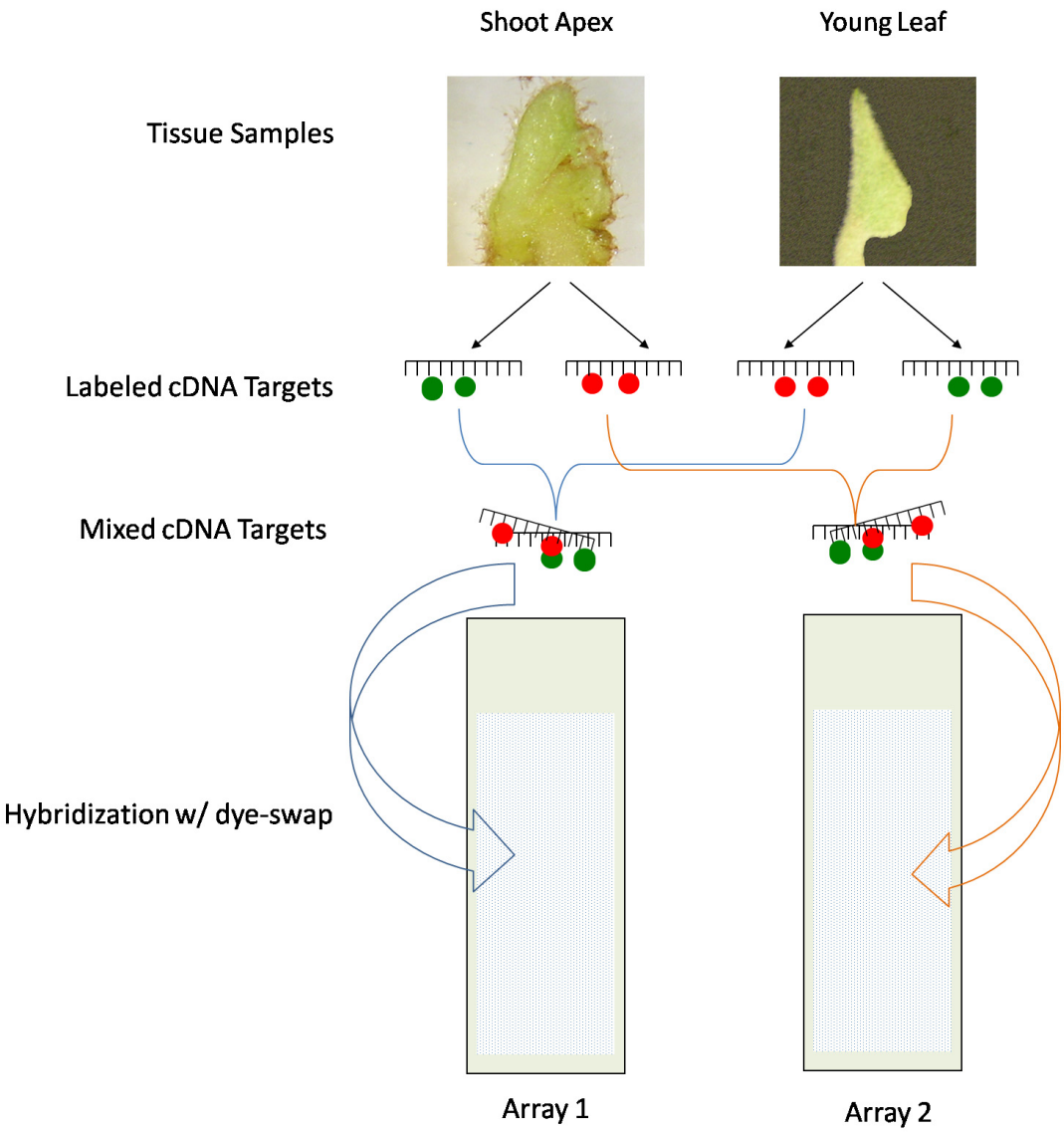

Figure 2-5. A schematic diagram showing hybridization in dye-swap design. Array probes on each array slide were hybridized with cDNA targets that were oppositely labeled. In Array 1, shoot apex cDNA target labeled with Alexa Fluor® 555 and young leaf cDNA target labeled with Alexa Fluor® 647 were co-hybridized, while in Array 2, shoot apex cDNA target labeled with Alexa Fluor® 647 and young leaf cDNA target labeled with Alexa Fluor® 555 were co-hybridized.

Table 2-11. Concentrations of ingredients in wash buffer series.

Wash Buffer Series	Ingredients[a]
Wash #1	2X SSC / 0.1% SDS
Wash #2	0.2X SSC / 0.1% SDS
Wash #3 & #4	0.2X SSC

[a.] For the ingredient details, refer to table footnotes of Table 2-5 on page 42

the upper and lower pieces of the chamber that were created by the thickness of the O-ring seal), the thumb screws were unfastened and the cover of the hybridization chamber was carefully prised open using a blade of the coverslip forceps. With the slide still in the hybridization chamber, the cover slip was removed with a fine forceps and the slide was placed as quickly as possible in the first wash dish containing 2X SSC and 0.1% SDS. Slides were washed for 10 minutes with gentle shaking, and transferred to the second wash dish containing 0.2X SSC and 0.1% SDS. After washing in the same way as in the first wash, the slides were transferred to the third wash dish containing 0.2X SSC, but no SDS, and washed for 10 minutes with gentle shaking. Finally, the last wash step was repeated with a fresh solution in another wash dish to ensure all residual SDS was removed.

To dry the slides, each slide was separately placed with printed side down in 50 ml BD Falcon™ polystyrene conical tubes (Cat. #352073, BD Biosciences, San Jose, CA) separately and spun at 1000 rpm for 5 minutes on a bench-top centrifuge with a swing-bucket rotor (Centrific™ Model 225; Fisher Scientific, Springfield, NJ). Dry slides were placed in a vacuum-sealed canister (FOODSAVER® Round Canister, Cat. #T16-0032; Jarden Corp., Rye, NY) containing dust-free desiccants (DriCan® Reusable Desiccating Canister, Cat. #19950; Ted Pella, Inc., Redding, CA) to transport to Laboratory of Genomics Bioinformatics & Proteomics, University of Toledo Health Science Campus, where scans were performed (described below).

2.7 Scanning Array Slides and Image Analysis

2.7.1 Scanning for Image Acquisition

Prepared array slides were scanned using a two-channel confocal microarray scanner (ScanArray®) and quantitated by the scanner's dedicated software (ProScanArray® Express v.3.0.0; ProSAE), which were bundled in a PerkinElmer™ Microarray Analysis System (PerkinElmer Life and Analytical Sciences, Shelton, CT). To achieve optimal fluorescence

intensity, the photomultiplier tube (PMT) gain was set at 80% of the maximum for both Alexa Fluor® 555 and Alexa Fluor® 647. The laser power for scanning was limited to 80% for Alexa Fluor® 555 and 84% for Alexa Fluor® 647, respectively, to reflect the difference in fluorescing capacity of the two dyes, while minimizing the photo-bleaching effects (PerkinElmer Life Sciences Inc., 2002). After laser focusing and balancing of the two channels, scans were conducted at a resolution of at 10 μm. For each array scan, two separate 16-bit Tagged Image File Format (TIFF) images were produced and combined together to produce a composite image.

2.7.2 Array Spot Recognition ('Gridding')

For spot recognition, the grid was defined using the GAL (GenePix® Array List) file, which was provided by the array manufacturer (file name: AR12K-768+.gal; W.M. Keck Foundation Biotechnology Resource Lab at Yale University, New Haven, CT). The format of the GAL file was originally implemented by Molecular Devices (Union City, CA) and the file describes the dimension and position of blocks, the layout of spots, and the names and identifiers of the printed cDNA associated with each spot (Molecular Devices Inc., 2001; Zhai, 2001). During the spot finding procedure, the ProSAE software recognizes spots in 5 different classes of the spots based on the quality of the spots, ranging from 1 to 5. Flag code 1 indicates a spot that was 'not found'; flag code 2, 'found'; flag code 3, 'good'; flag code 4, 'bad'; and flag code 5, 'absent', which is not a spot on the array format. The flag code 2 was not seen because if the spot was found, it was either good or bad spot. Based on the flags, the 'gridding' process was repeated until the maximum number of spots on the array matched with the grid and recognized as good spots. As a final step of the spot finding procedure, the spots with artifacts, such as dust particles or scratches, were marked as 'bad' and they were excluded from data analysis.

2.7.3 Array Spot Segmentation

After grids were properly placed, segmentation was carried out, in which foreground (spots) and background on the scanned images were defined and the pixel intensity data within the array spots were extracted. The 'adaptive circle segmentation' method was chosen in the ProSAE software. In this segmentation method, the program tries to find the edges of a spot and draws a circle around the spot, and what is inside the circle is the foreground (spots), and areas outside of the circle are background (Weeraratna and Taub, 2007). This method allows for the radius to be adapted to the spot shape and more accurate segmentation, compared to the 'fixed circle segmentation', in which spots are assumed to be circular with fixed radii (Li *et al*., 2005c;

Nagarajan, 2003; Rueda and Qin, 2004; Rueda and Qin, 2005; Wu *et al*., 2005).

2.7.4 Quantitation of Array Spot

After segmentation, the color information in the array spots were quantitated into intensity data. Background-corrected spot intensities were obtained by using a 'local background correction' method, where the mean intensity of pixels in the background was subtracted from the mean intensity of those in the spot.

2.8 Data Analysis

2.8.1 Selection of Data

Using the background-corrected mean spot intensity data, which were generated by ProSAE software, the patterns of differential gene expression in shoot apices and young leaves were analyzed. For analyses, data from spots that were marked as 'bad' were excluded from further analysis. Among 12,288 spots on each array, 336 were marked as "BLANK" in the GAL file supplied by the array manufacturer, and they were also excluded. "BLANK" means that AIG Locus link or gene description have not been found for the corresponding GenBank Accession.

When background-subtracted spot intensities became negative, those were regarded as missing values and excluded from the data analysis (Hovatta *et al*., 2005). If a spot had negative spot intensity in a channel, all other corresponding spots across the channels and arrays also were excluded from the data analysis.

2.8.2 Log Transformation and Normalization of Data

The spot intensity data were imported into GeneSpring GX software (Version 10; Agilent Technologies, Inc., Santa Clara CA, USA) and the data were transformed to their $\log_2$ values followed by Quantile normalization. A $\log_2$ transformation converts the expression values into an intuitive linear scale that represents two-fold differences (Alba *et al*., 2004). Quantile normalization makes the distribution of expression values of both channels and all samples in an experiment the same (Bolstad *et al*., 2003; Yang and Thorne, 2003). Thus, after the quantile normalization, all statistical parameters (*i.e.*, mean, median and percentiles) of the sample become identical. Quantile normalization reduces variance between arrays, thus overcoming the differences among the arrays that are caused by non-biological factors, including dye-bias (Ewens and Grant, 2005; Hovatta et al., 2005). Quantile normalization was performed by the following steps (Agilent Technologies Inc., 2008; Mayer and Glasbey, 2005):

1. The spot intensity values of each sample were sorted in ascending order and placed next to each other.
2. Each column was sorted in ascending order. The mean of the sorted order across all samples was taken so that each row in the sorted matrix had value equal to the previous mean.
3. The modified matrix, as obtained in the previous step, was rearranged to have the same ordering as the input matrix.

2.8.3 Selection of Differentially Expressed Genes

The final step in the data analysis was to identify the genes that were differentially expressed in the shoot apices and the young leaves with biological and statistical significance. To screen the genes that were differentially expressed in the two tissue types with a test for statistical significance, an unpaired t-test was used since the expression levels of a gene in the shoot apex *versus* the young leaf are independent from each other (Glantz, 2005). The critical significance level (*p*-value cutoff) was 0.05. To reduce the number of false positives, which are the genes that are called significant by chance alone, the Benjamini and Hochberge False Discovery Rate (FDR) procedure (Benjamini and Hochberge, 1995) was applied to the data set screened by t-test.

For screening the genes that were biologically differentially expressed in the two tissue types, the gene was considered differentially expressed when the $\log_2$ ratio in the spot intensity level between the two tissue types was greater than 1 (*i.e.*, fold ratio ≥ 2.0).

To facilitate finding differentially expressed genes under the given criteria, the data set was filtered on a ‘volcano plot’ using GeneSpring GX software, in which the fold-difference of expression level and corresponding *p*-value are plotted for easy identification of genes that fall into the biological and statistical selection criteria given above. The Benjamini and Hochberge FDR was the least stringent among the multiple testing procedures available in the GeneSpring GX software and provides a good balance between discovery of statistically significant genes and limitation of false positive occurrences (Dudoit *et al.*, 2002). Other methods include the Bonferroni procedure (Bonferroni, 1936), the Bonferroni Step-down (also called Holm’s method or a sequential rejection method; Holm, 1979) and the Westfall-Young method, in order of their stringencies (Dudoit and van der Laan, 2007).

2.8.4 Verification of Differential Expression of Genes

Instead of using RT real-time PCR (RT-rt-PCR) to verify the expression levels of the genes that were predominantly expressed in a tissue type, two microarray data exploring tools were used: the 'electronic Northerns (e-Northern) with Expression Browser'(Toufighi *et al*., 2005) and the 'electronic Fluorescent Pictograph (eFP) Browser'. They are available from the Botany Array Resource (BAR; http:// www.bar.utoronto.ca/), and used to explore the expression levels with data sets obtained from other gene expression experiments (Winter *et al*., 2007).

In the e-Northerns, the Expression Browser is used to explore how genes of interest are being expressed, with the gene expression data sets accumulated in the BAR database or public data sets from the AtGenExpress Consortium. Using this tool, a list of 163 AGI locus identifiers of the genes that were preferentially expressed in the shoot apex (60) or the young leaf (103) was queried in order to determine if the set of genes is up-regulated or down-regulated in a particular tissue type across all the experiments in the BAR database or in projects from the AtGenExpress Consortium.

The eFP Browser provides a pictographic representation of the experimental expression data based on the expression levels among different plant parts and the developmental stages in the large-scale data sets from the BAR and the AtGenExpress Consortium (Goda *et al.*, 2008; Kilian *et al*., 2007; Schmid *et al*., 2005). Using AGI locus identifiers of 163 genes (60 from the shoot apex and 103 from the young leaf), eFPs were produced to explore the expression level of each gene in the data sets in the BAR and the AtGenExpress Consortium databases.

2.9 Functional Analysis of Differentially Expressed Genes

2.9.1 Cluster Analysis

To identify and group together the genes that were similarly expressed and infer any biological significance of the group of genes, cluster analyses were carried out using two methods provided by GeneSpring GX: hierarchical clustering and K-mean clustering. In hierarchical clustering, the co-regulated genes were grouped by distance matrix calculated based on the Euclidian distance. Hierarchical clustering does not distribute data into a fixed number of clusters, but produce a grouping hierarchy so that most similar entities are merged together to form a cluster.

In contrast to hierarchical clustering, in K-mean clustering, genes are partitioned into a fixed number (k) of clusters such that, genes within a cluster are similar, while those across clusters are dissimilar. Based on the number of clusters obtained from the hierarchical clustering analyses, K-

mean clustering was also carried out to compare the outcomes between the two clustering methods. To begin with K-mean clustering, genes were randomly assigned to four distinct clusters and average expression vector was computed for each cluster based on the Euclidean distance as in hierarchical clustering analyses. For every gene, the algorithm then computed the distance to all expression vectors, and moved the gene to that cluster whose expression vector was closest to it. The entire process was repeated iteratively until no genes can be reassigned to a different cluster, or 50 iterations were reached.

2.9.2 Functional Annotation

Differentially expressed genes in either tissue type were categorized based on the functional annotations. Since GenBank accession numbers for ESTs (Expressed Sequence Tags) were used to identify the array features in the GAL file provided by the array manufacturer, they were first converted (mapped) into AGI (*Arabidopsis* Genome Initiative) locus identifiers using an 'association' file downloaded from the TAIR ftp site (ftp://ftp.arabidopsis.org/home/tair/Genes/TAIR9_genome_release/). These locus identifiers were used for subsequent query and retrieval of the gene descriptions from The *Arabidopsis* Information Resource (TAIR; Berardini et al., 2004; http://www.arabidopsis.org/tools/bulk/go/index.jsp).

Using the GO Slim Classification for Plants at TAIR, the genes that were statistically differentially expressed in the shoot apex or the young leaf were functionally categorized. The TAIR GO slim is a reduced set of GO terms from the Gene Ontology (GO; The Gene Ontology Consortium, 2000; http://www. geneontology.org/), which has been tailored to Arabidopsis. While the GO slim is useful for a broad view of a large set of genes, it does not provide detailed GO terms for the functional categorization of the genes, and was not very informative for the relatively small gene set detected in this study. On the other hand, a subset of the TAIR Genome (Release 9) with matching locus identifiers, which was downloaded to obtain the low-level GO terms for the detailed functional categorization, contained only the lowest level GO terms. Based on the lowest level GO terms, which describe the specific function of a given gene, the gene set screened in this study were divided into too many functional categories, each containing no more than a few genes. Since the high- or low-level GO categories resulted in too broad or too narrow functional categorization, intermediate level GO terms were retrieved manually using the individual link to each GO terms in the TAIR genome database.

The genes were then categorized manually and described based on the three GO vocabularies, each providing a specific type of information about the gene or protein: (i) the

pertinent biological processes, (ii) its specific molecular function, and (iii) its cellular localization. To fine-tune the categorization the gene products were also queried in the protein databases, such as the Universal Protein Knowledgebase (UniProtKB; The UniProt Consortium, 2009; http://www.uniprot.org/) and the Munich Information Center for Protein Sequences (MIPS; Mewes *et al*., 2008; http://mips.helmholtz-muenchen.de/). The functional role of the uncharacterized gene products in these databases were predicted based on their occurrences of their functional domains provided in the InterPro database (Hunter *et al*., 2009; http://www.ebi.ac.uk/interpro/) and supporting publications.

2.9.3 Pathway Analysis

In order to determine a biologically meaningful inter-relations among the genes that were statistically differentially expressed in the shoot apex and in the young leaf, respectively, pathway analyses were carried out in GeneSpring GX using the parameters set as in Table 2-12 on page 54.

Table 2-12. Parameter values used for pathway analysis in GeneSpring GX.

Parameters	Value
Pathway analysis	Expand Interactions
Relations score	9
Relation types chosen	Expression, Binding, Regulation, Promoter Binding, Transport, Member, Metabolism, Protein Modification
Entity local connectivity	2
Entity types chosen	Process, Family, Complex, Function, Protein, Small Molecule, Enzyme
Limit results	by Local to Global Connectivity Ratio
Limit results to	50 new entities

PART 3. RESULTS

3.1 Yield and Quality of Total RNA and Amino-Modified cDNA

When the yield and purity of genomic DNA-free total RNA isolated from the shoot apex and the young leaf samples were determined by spectrometry, the concentration of total RNA obtained from shoot apices was approximately 1.7 times higher than that of young leaves (Table 3-1). The ratios between absorbance readings measured at 260 nm and 280 nm were 2.1 in both samples, indicating that the purity of the isolated total RNA samples was adequate for use in the microarray application (Kleber and Kehr, 2006; Qiagen, 2001).

Table 3-1. Concentrations of total RNA isolated from shoot apex and young leaf samples determined by spectrophotometry, and the ratios of absorbance readings (A_{260}/A_{280}).

Samples	Conc. of Total RNA (µg/µl)	A_{260}/A_{280}
Shoot Apex	2.6	2.1
Young Leaf	1.5	2.1

The quality and integrity of the total RNA were also assessed using formaldehyde denaturing agarose gel electrophoresis (Figure 3-1 on page 56).The electrophoretogram of total RNA samples clearly showed sharp heavy bands of high-concentration corresponding to large and small ribosomal subunits, respectively, and the large subunit rRNA band appeared far more abundant than the small subunit rRNA band, demonstrating that the samples were intact and non-degraded (Imbeaud *et al*., 2005). Also, a smear of mRNAs in various molecular weights indicated no signs of degradation of total RNA. Other ribosomal RNA bands, which were visible in the mature leaf samples (Figure S-1 on page 120 in “Supplementary Data”), were not positively detectable in the shoot apex or the young leaf sample. The 5S rRNA, tRNA, and other low-molecular-weight RNAs (<200 nucleotides), which make up 15-20% of total RNA, are not retained by RNeasy® column (Cat. #75142; Qiagen, Valencia, CA). Genomic DNA contamination was not detected; it is visible as a very high molecular weight band, if any.

The quality of the amino-modified first-strand cDNA synthesized from total RNA templates was assessed by standard agarose gel electrophoresis (Figure 3-2 on page 56). On the agarose gel, first-strand cDNA products appeared as a smear with some distinctive bands, indicating the presence of relatively abundant mRNA species at certain sizes. Although the equal amounts of total RNA templates were added in both reactions, the bands of first-strand cDNA derived from

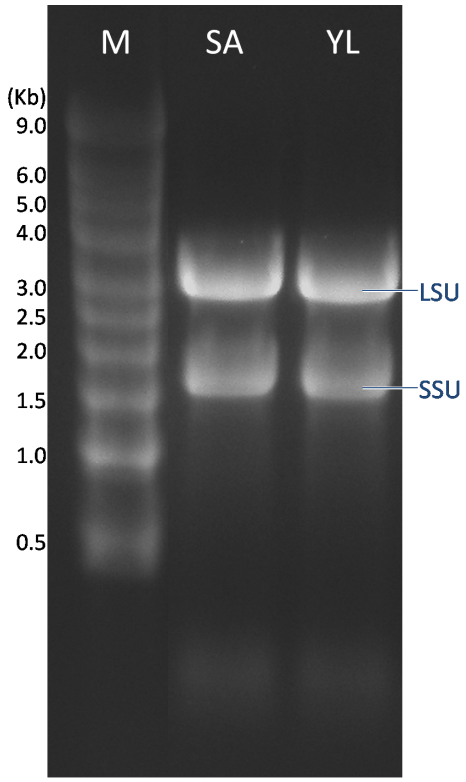

Figure 3-1. Formaldehyde denaturing agarose gel electrophoresis of total RNA. Total RNA samples from shoot apex (SA) and young leaf (YL) were loaded on the formaldehyde denaturing agarose gel (1.2%) containing SYBR® Green II RNA Gel Stain (0.1 µl/ml; Cat. #S7564; Invitrogen, Carlsbad, CA), and run in 1X MOPS buffer along with RNA Millennium™ Size Markers (Cat. #7151; Ambion, Austin, TX). (M).

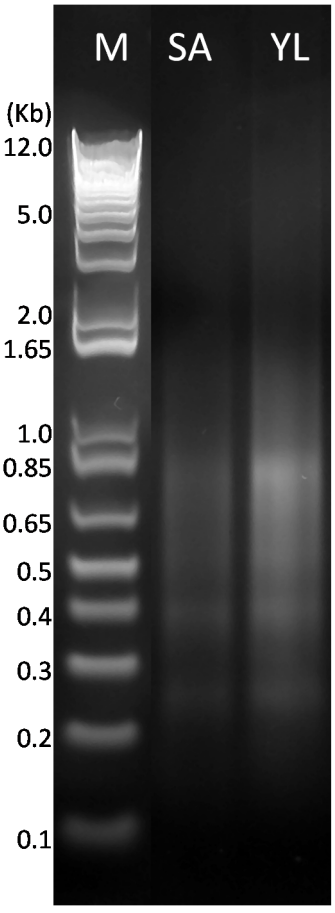

Figure 3-2. Agarose gel electrophoresis of first-strand cDNA products. First-strand cDNA samples, synthesized from the total RNA templates, were loaded on the standard agarose gel (1%) containing SYBR® Gold Nucleic Acid Gel Stain (Cat. #S11494; Invitrogen, Carlsbad, CA), and run in 1X TBE buffer, along with 1 Kb Plus DNA Ladder™ (Cat. #10787-018; Invitrogen, Carlsbad, CA). SA, shoot apex; YL, young leaf; M, size marker.

the young leaf total RNA appeared brighter on the gel, indicating a higher yield of first-strand cDNA products from the young leaf total RNA than the shoot apex total RNA in the reverse-transcriptase reactions. This result was confirmed when concentrations of the amino-modified cDNA samples were measured by spectrophotometry (Figure 3-3).

3.2 Labeling Efficiency of Amino-Modified cDNA

By comparing the amounts of fluorescently labeled cDNA to total amounts of amino-modified first-strand cDNA, labeling efficiency was assessed (Table 3-4 on page 58). As the total yield of amino-modified cDNA derived from shoot apex was lower than that from young leaf, the amounts of fluorescently labeled cDNA derived from shoot apex were also low regardless of which fluor was used. While the labeling efficiencies were significantly different between source tissue types, the difference between the two fluors was negligible.

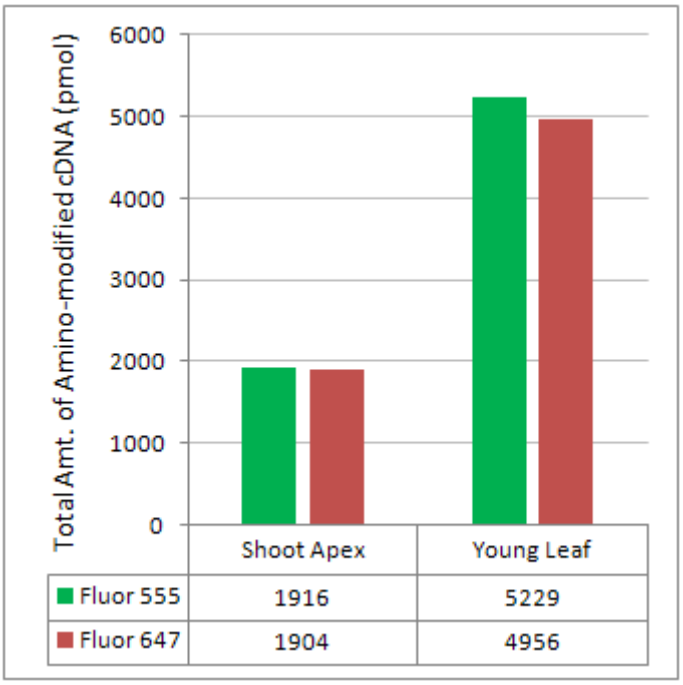

Figure 3-3. Total amounts of amino-modified cDNA. A_{260} and A_{320} for each of the purified target samples from the shoot apex and the young leaf were measured using a Beckman DU-600 spectrophotometer (Beckman, Fullerton, CA). The absorbance readings were converted into the total amounts of amino-modified cDNA in picomoles using the formula given in Equation 2-2 on page 40. The yields of amino-modified cDNA in the shoot apex sample were much lower than those in the young leaf, regardless the fluors used.

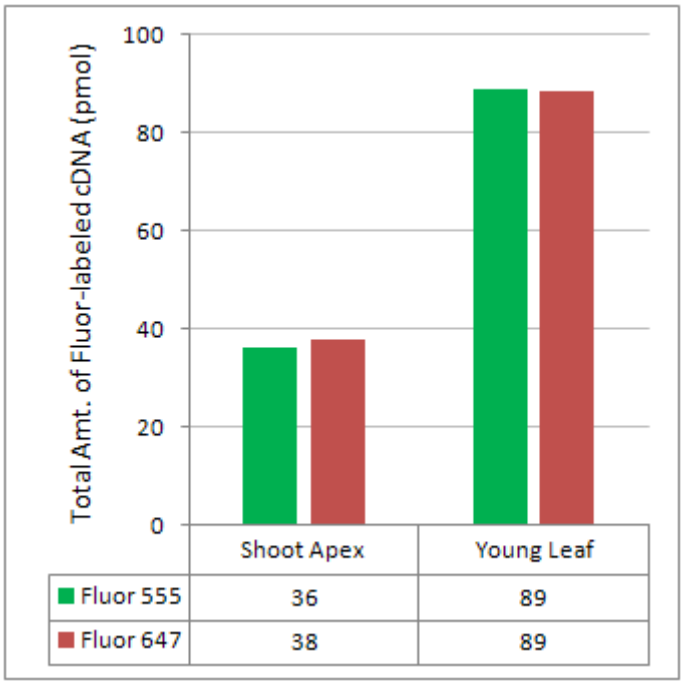

Figure 3-4. The amounts of fluorescently labeled cDNA. To calculate the total amounts of the fluorescently labeled cDNA in the purified target samples, absorbance were measured at 550 nm, 650 mn and 750 nm using a 'Multiple Wavelength Mode' in a Beckman DU-600 spectrophotometer (Beckman, Fullerton, CA). The amounts of cDNA targets labeled with Alexa® Fluor 555 and Alexa® Fluor 647 were converted into picomoles using the formulas given in Equation 2-4 and Equation 2-4 on page 40, respectively.

3.3 Scanned Arrays

The composite images of scanned microarrays were shown in Table 3-5 on page 59. The fluorescence intensities of the spots that were hybridized with cDNA targets derived from the shoot apex were low compared to those hybridized with cDNA targets from the young leaf, regardless of the fluorescence dye used. This was because there was a lower amount of fluorescently labeled cDNA from the shoot apex than from the leaf in the hybridization mixture.

3.4 Statistical Microarray Data Analysis

3.4.1 Log Transformation of Intensity Data

Among 12,288 spots on the composite image of each scanned array, intensity data were extracted from 11,255 spots for data analysis using GeneSpring GX10 software, excluding those

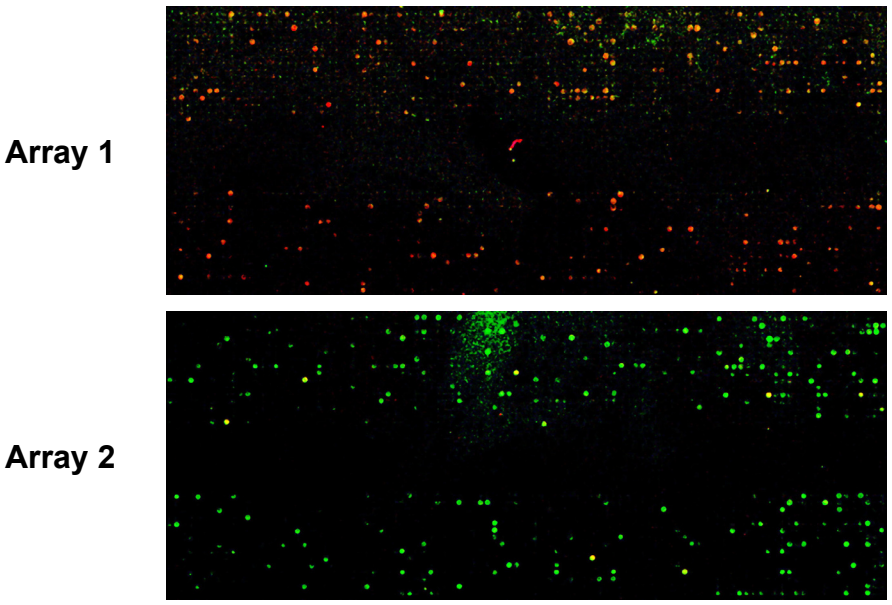

Figure 3-5. Portions of composite images of scanned arrays. Among the 32 blocks (8x4) of array spots, 8 blocks (2x4) are shown here. In array 1, cDNA targets derived from shoot apices were labeled with green dye (Alexa® Fluor 555) and cDNA targets derived from young leaves were labeled with red dye (Alexa® Fluor 647). In array 2, the dyes were swapped. The red fluorescence from the young leaf cDNA targets was more intense than the green from the shoot apex cDNA targets in array 1, where as the red fluorescence from the shoot apex cDNA targets was obscured by the higher intensity of green fluorescence from the young leaf cDNA targets in array 2, where the fluorophores were swapped. To prepare the images, each of two microarray slides was scanned twice; once for excitation of the green channel, Alexa® Fluor 555 and the second for the red channel, Alexa® Fluor 647. The images captured from each excitation channel were combined together to produce a composite image for each array.

regarded as missing values (Hovatta et al., 2005). Missing values included 336 empty spots that were marked as ‘BLANK’ in the GAL file, and 697 spots that were detected as ‘bad’, which might have contained imperfections and/or artifacts, such as scratches and dust particles. Among the 11,255 readable spots, 2,597 produced signals greater than background levels. The background-corrected mean spot intensity data were transformed to their $\log_2$ values and the distribution of spot intensity data became symmetrical. The effects of the log transformation are illustrated in Figure 3-6 on page 61.

3.4.2 Normalization of Log-transformed Data

Quantile normalization in GeneSpring GX resulted in standard distribution of the log-transformed data values. The data also underwent centralization, in which the distribution was moved so that it was centered over the expected mean, balancing the two channels to remove intensity-dependent variation due to dye-bias and/or tissue-specific labeling efficiency.

The effect of normalization was illustrated in the scatter plots (Figure 3-7 on page 63) and an MvA plot (Figure 3-8 on page 65). In the scatter plots, majority of the genes, which had similar expression levels in both tissue types appeared somewhere along the diagonal after normalization. MvA plot is a scatter plot of the difference (M) *versus* the average (A) of log spot intensity values between two samples:

$$M = \log_2(R/G) \qquad \text{(EQ. 3-1)}$$

$$A = \log_2(R*G)/2 \qquad \text{(EQ. 3-2)}$$

where R and G represent the fluorescence intensities in the red and green channels, respectively.

MvA plot is generally used to visualize the intensity ratios between red and green fluorescence in the experiments using two-color spotted arrays. It is useful to assess not only the relation between samples, but also quality by making it easy to identify the intensity dependent variation among low intensity spots. A common source of variation due to technical error in microarray data is incorrectly balanced photomultiplier tube (PMT) settings to compensate the differential excitation properties of the two channels during scanning, which results in a shift of the data from the x-axis (*M = 0*) of the ideal MvA plot (Petri *et al*., 2004). This random variation, which was caused by technical errors, was removed after screening the spots based on the statistical test criteria (described in the next section). After normalization, several descriptive statistics of the array data were represented graphically in a box plot, which is also called a box-whisker-plot.(Figure 3-9 on page 67).

Figure 3-6. The effect of the log transformation upon the distribution of the spot intensity values. The left four panels show the histogram of the background corrected mean spot intensity values without the log transformation. The spot intensity ranges spanned a very large interval and the distributions were left-ward skewed having a very long tail towards high spot intensity values. The right four panels show the distributions of the same values after the log transformation, in which the distribution of data became symmetrical and almost normal. The plots were generated in Microsoft Excel 2007 software.

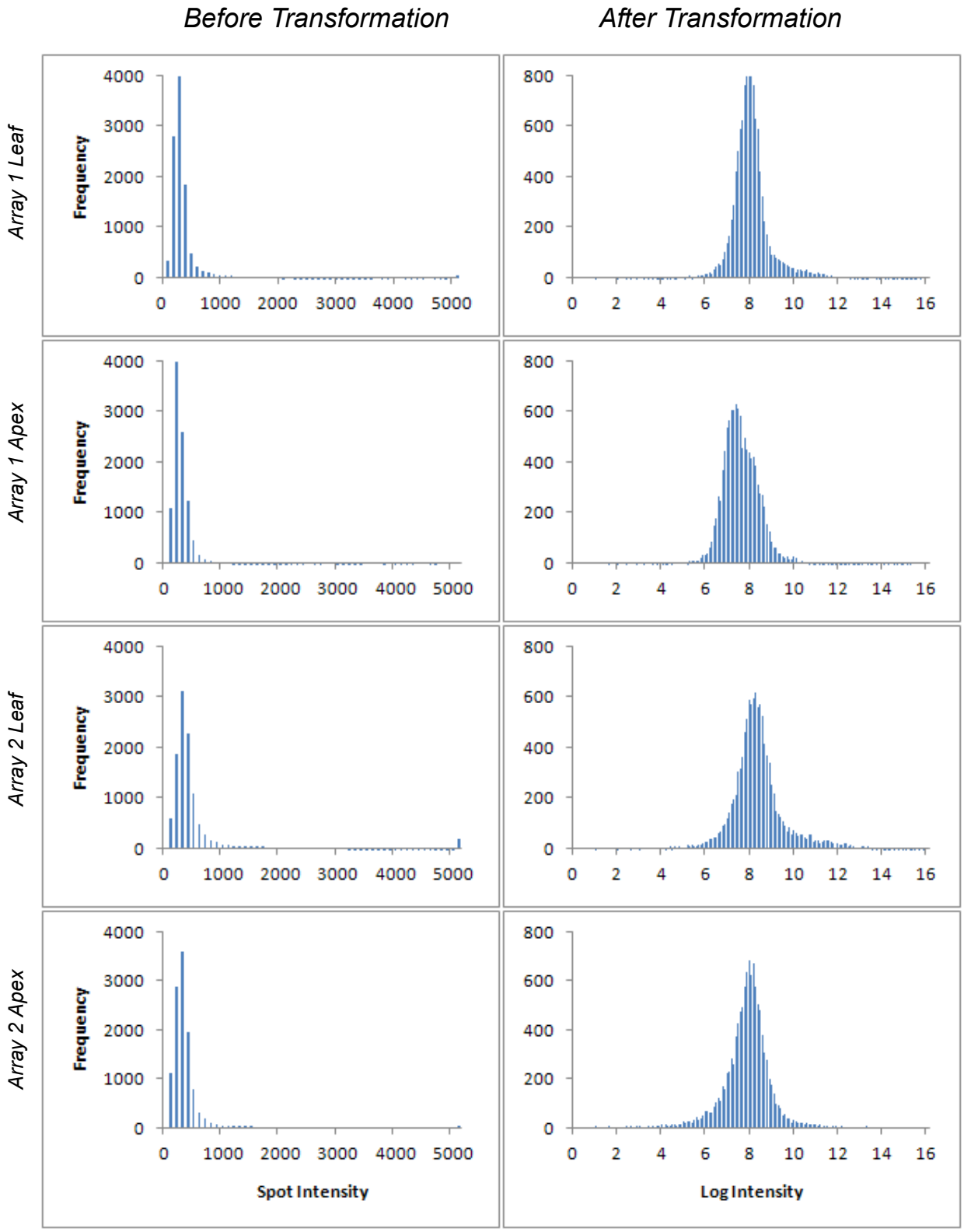
Before Transformation
After Transformation
Array 1 Leaf
Array 1 Apex
Array 2 Leaf
Array 2 Apex
Frequency
Spot Intensity
Log Intensity
0
1000
2000
3000
4000
5000
200
400
600
800
2
4
6
8
10
12
14
16

Figure 3-7. Scatter plots showing the effect of array spot intensity data normalization. The Upper panel represents the intensities from the shoot apex sample *vs.* the young leaf sample before normalization; and, the bottom panel, after normalization. The intensities from the young leaf sample are plotted on the horizontal axis, while those from the shoot apex sample are plotted on the vertical axis, after $\log_2$ transformation. Points above the diagonal (y = x) represent spots with higher intensities in the shoot apex whereas points below the diagonal represent spots higher in the young leaf. Intensity differences increase with distance from the diagonal line, reflecting the gene expression levels in the two tissue types. Before normalization, most spots appeared to have lower intensities in the shoot apex compared to the young leaf since most of the spots were plotted below the diagonal. However, when the data were normalized, most points moved toward the diagonal. The color legend indicates the approximate scale of $\log_2$ intensity level; blue is lower and red is higher. The two green lines above and below the y=0 diagonal line indicate the fold change, which is 2.0. Thus, the points that fall above the upper green line represent the genes that were preferentially expressed in the shoot apex than in the young leaf at 2-fold or more. Below the lower green line, are those expressed preferentially in the young leaf than in the shoot apex at 2-fold or more.

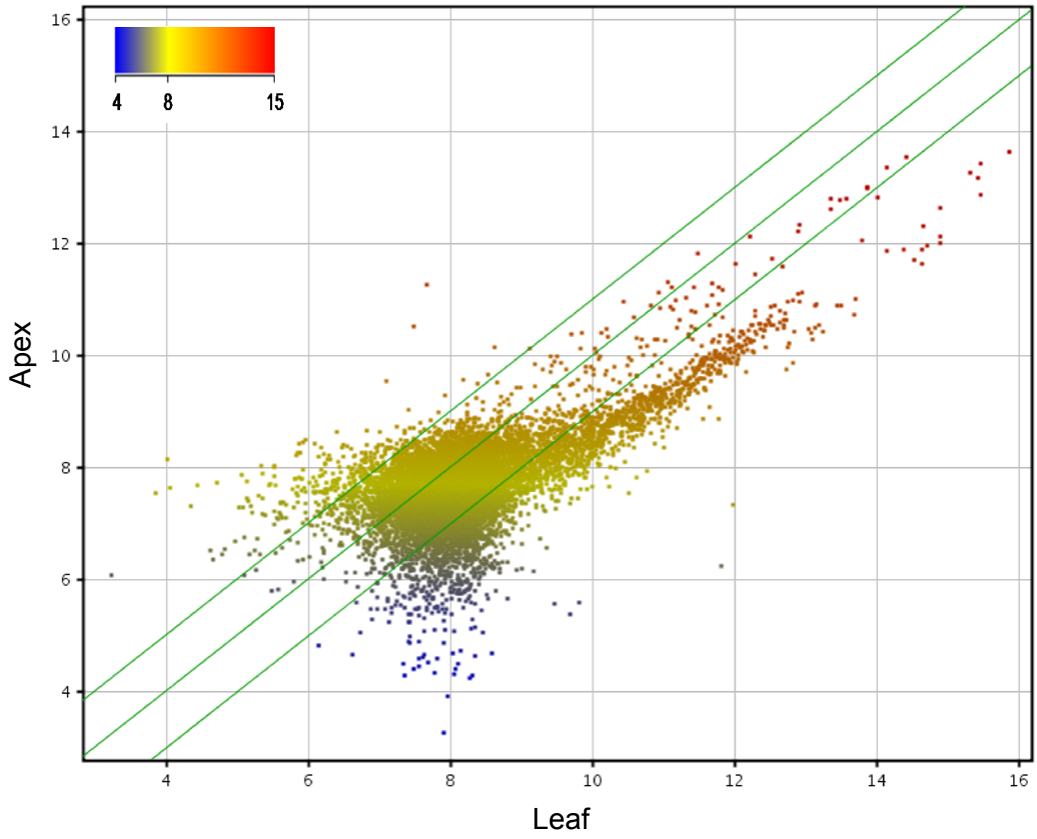
4
8
15
16
14
12
10
8
6
4
Apex
4
6
8
10
12
14
16
Leaf

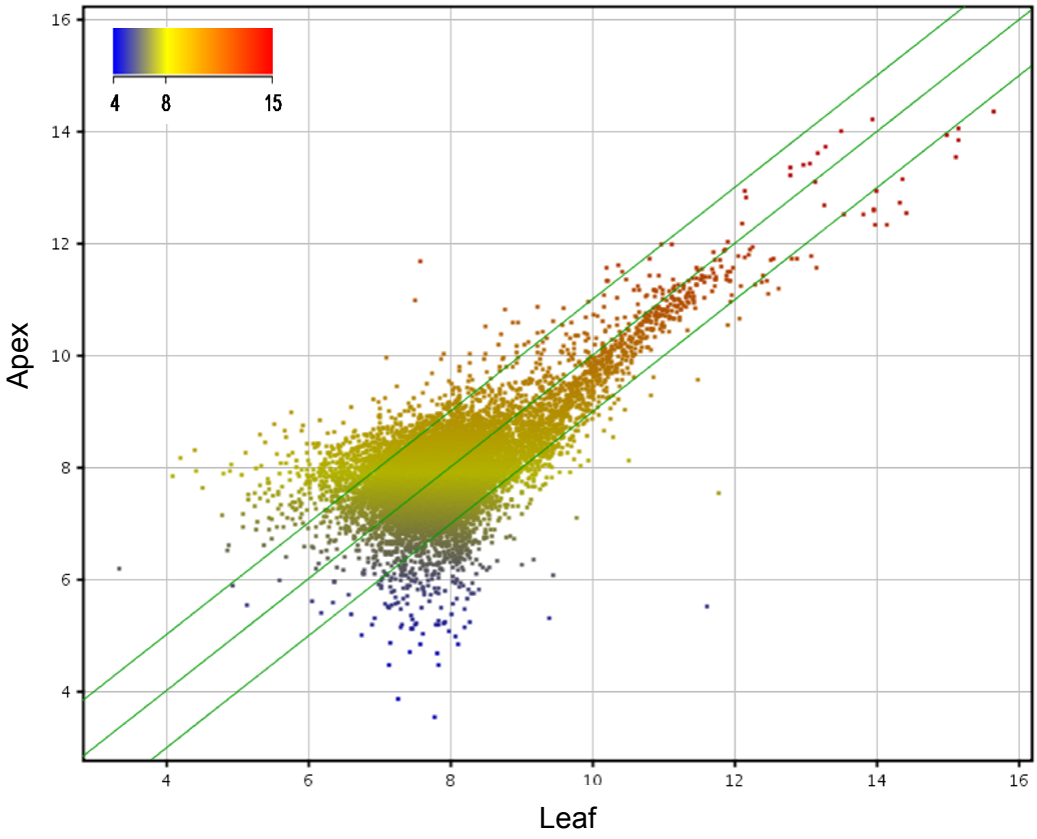
4
8
15
16
14
12
10
8
6
4
Apex
4
6
8
10
12
14
16
Leaf

Figure 3-8. MvA plot showing the effects of normalization. A distribution of spot intensity data was visualized on a MvA plot before (upper panel) and after normalization (lower panel). M on the vertical axis is the $\log_2$ transformed spot intensity ratio between two channels (shoot apex *vs*. young leaf), and A on the horizontal axis is the average spot intensity of the two channels after the $\log_2$ transformation. MvA plots reveal intensity dependent biases as well as extra variation at low intensity spots. In these MvA plots, which were generated in the GeneSpring GX 10 software, a high variation at low intensity spots was observed.

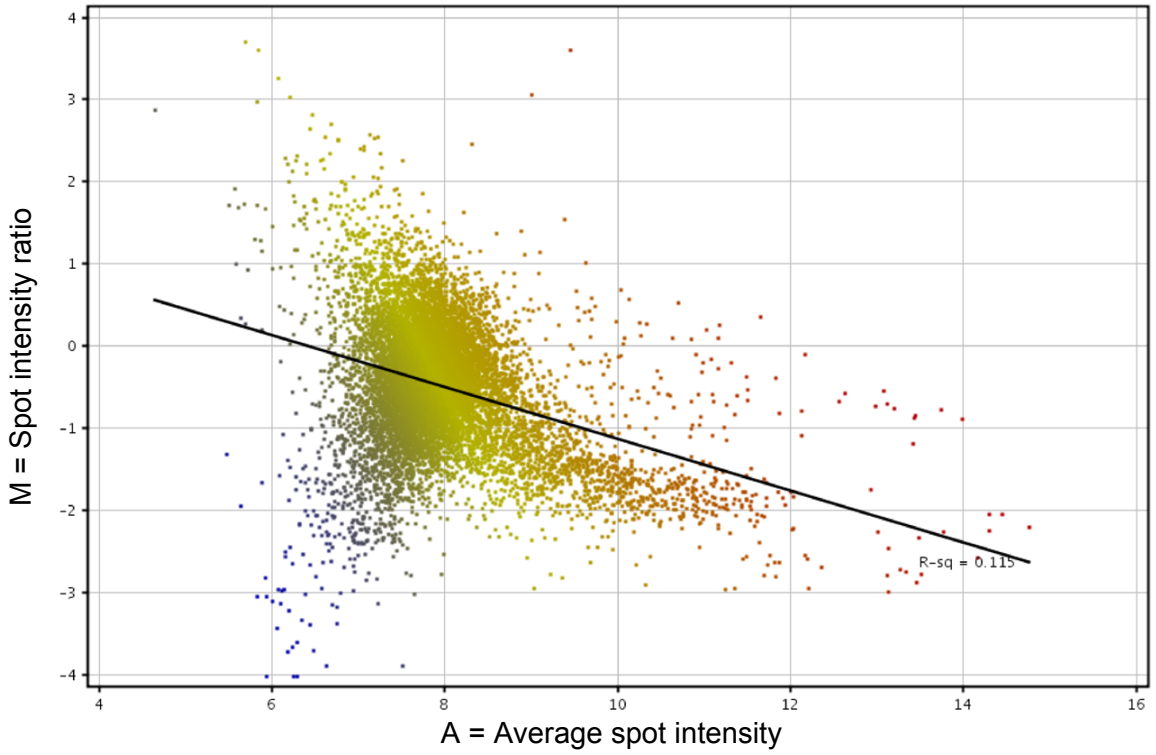
M = Spot intensity ratio
A = Average spot intensity
R-sq = 0.115
4
3
2
1
0
-1
-2
-3
-4
4
6
8
10
12
14
16

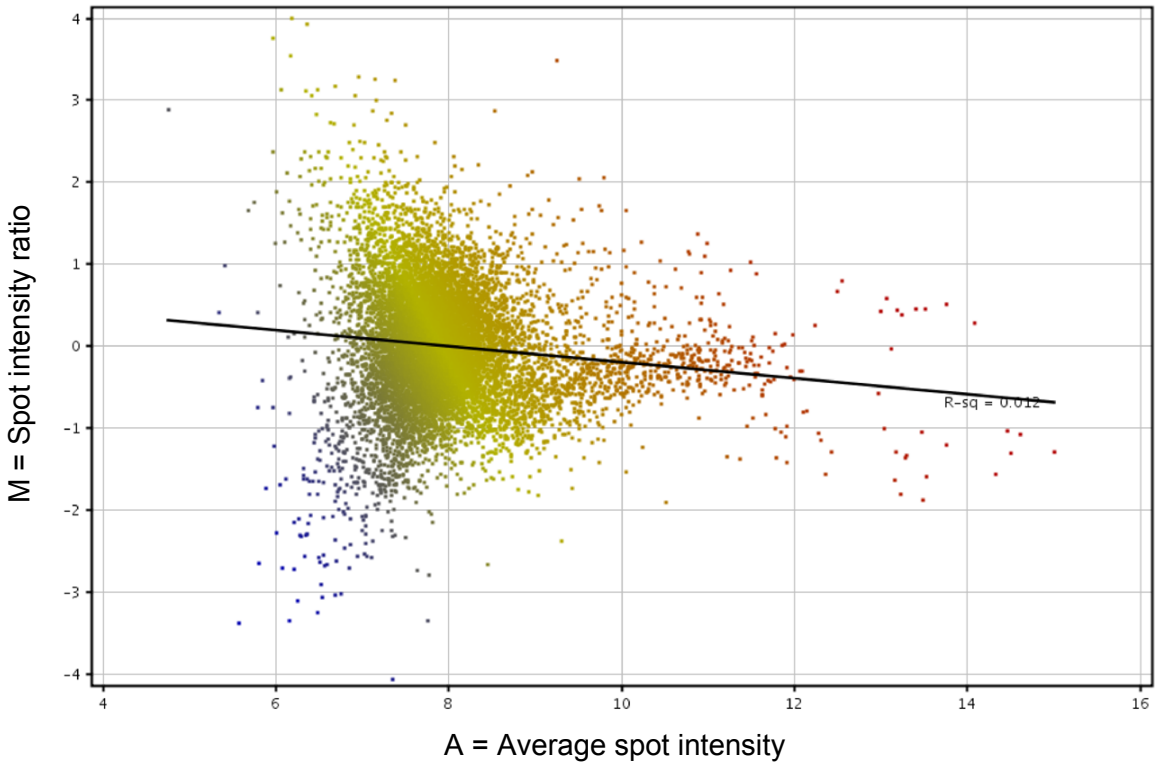
M = Spot intensity ratio
A = Average spot intensity
R-sq = 0.012
4
3
2
1
0
-1
-2
-3
-4
4
6
8
10
12
14
16

Figure 3-9. Box plot representing summary statistics of normalized spot intensity data. Each set of the box and tail represents each data set from four channels on the two microarrays. The upper and lower boundaries of the box show the location of the upper quartile (UQ) and lower quartile (LQ), which are the 75^{th} and 25^{th} percentiles, respectively. The central line in the box shows the position of the median (50^{th} percentile) of each data set. Thus, the box represents the interval that contains the central 50% of the data. The length of the tails, blue lines attached to UQ and LQ, are 1.5 times the interquartile distance (IQD). The data represented as red bars fall beyond [UQ+1.5 IQD] or [LQ-1.5 IQD] and are considered as outliers. By Quantile normalization, the median and the percentiles became uniform across the channels and arrays. The box plot was generated in the GeneSpring GX 10 software.

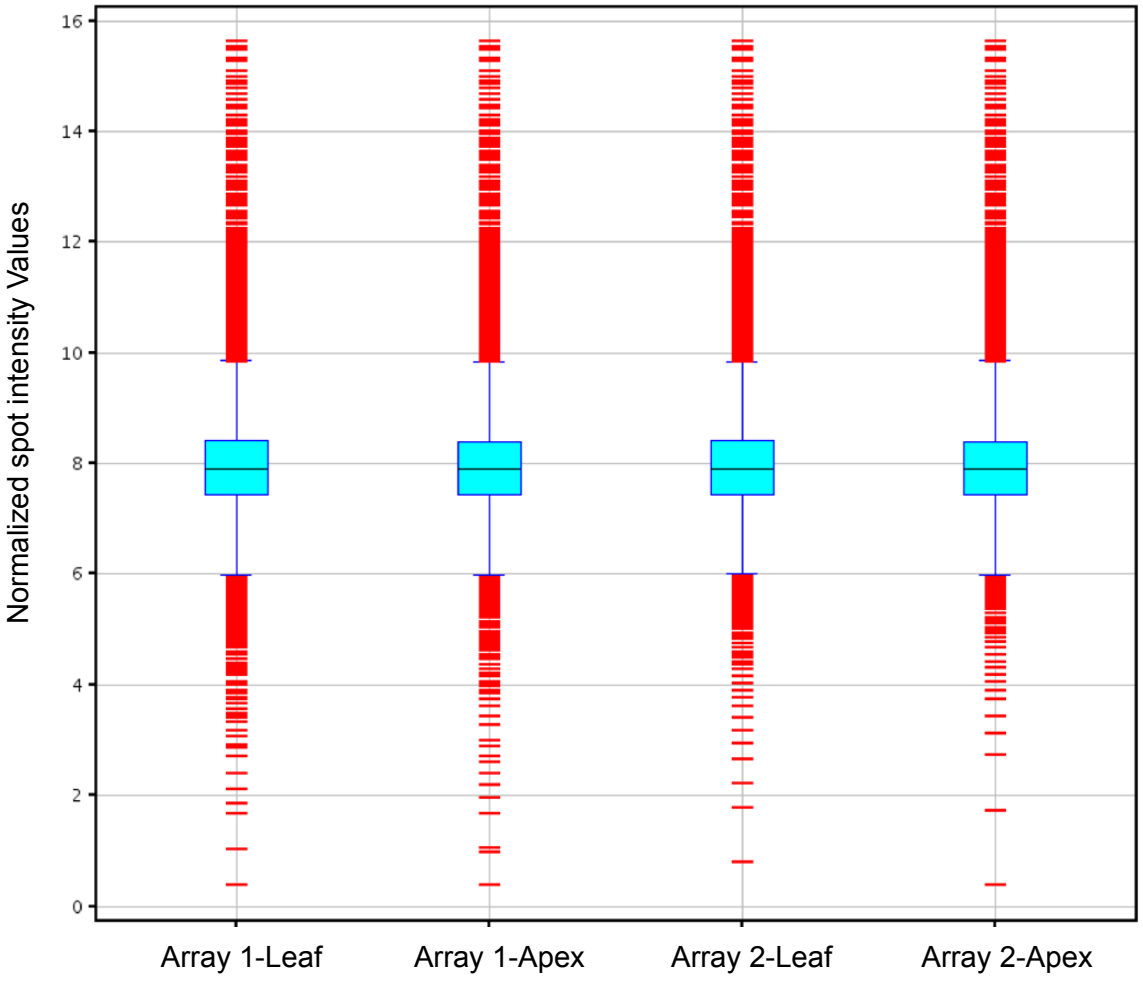
Normalized spot intensity Values
16
14
12
10
8
6
4
2
0
Array 1-Leaf
Array 1-Apex
Array 2-Leaf
Array 2-Apex

3.4.3 Filtering Differentially Expressed Genes

The results of the statistical test were represented in a ‘volcano’ plot (upper panel in Figure 3-10 on page 70) and a scatter plot (lower panel in Figure 3-10 on page 70), both illustrating the genes satisfying the following criteria:

1. statistical significance: filtered by unpaired t-test with p-value cutoff = 0.05 and Benjamini and Hochberge FDR correction applied.
2. biological significance: the $\log_2$ ratio in the spot intensity level between the two tissue types was greater than 1 (*i.e.*, fold ratio ≥ 2.0).

Under the given criteria, 174 genes were identified as being statistically differentially expressed two-fold or more when the transcriptomes of the shoot apex and the young leaf of *H. helix* cv. Goldheart were compared. Among them, 60 genes were preferentially expressed in the shoot apex, while 114 were preferentially expressed in the young leaf. A full list of the differentially expressed genes with expression level and fold ratio is presented in “Supplementary Data” (Table S-1 on page 121).

3.5 Verification of Expression Level

When the expression levels of the 60 shoot apex genes were explored using the e-Northern with Expression Browser, 55 genes were mapped in the data sets in the BAR and the AtGenExpress Consortium. Among them, 31 genes were confirmed to be expressed preferentially in the shoot apex (Table S-4 on page 142 in “Supplementary Data”). All of 103 young leaf genes had matches and 41 of them were confirmed to be expressed predominantly in the young leaf (Table S-5 on page 144 in “Supplementary Data”).

The *Arabidopsis* eFP Browser created 'electronic fluorescent pictographic' representations of expression patterns of the genes that were preferentially expressed in either type of tissue based on the AtGenExpress Consortium data (Goda *et al*., 2008; Kilian *et al*., 2007; Schmid *et al*., 2005; Winter *et al*., 2007). The representative output images from the eFP browser (Figure 3-11 on page 72) show the expression patterns of *AT2G22610* from the shoot apex and *AT3G62410* from the young leaf in developmental series.

Figure 3-10. A ‘volcano’ plot and a scatter plot showing differentially expressed genes. The volcano plot (upper panel) represents the genes that passed or failed the assigned criteria for screening. In the volcano plot the negative $\log_{10}$ of *p*-value [$-\log_{10}(p)$] was plotted against normalized log ratio [$\log_2(ratio)$]. Vertical green lines represent a 2-fold difference in the expression levels between the shoot apex and the young leaf tissues. Horizontal green line represents the t-test *p*-value of 0.05. Genes with large fold-differences and low *p*-values are easily identifiable graphically. The genes that were differentially expressed while satisfying the *p*-value cutoff 0.05 were shown in red and the remainder in grey. The red spots in the ‘volcano’ plot were also depicted in a scatter plot (lower panel). The spots above the upper diagonal represent the genes that are preferentially expressed in the shoot apex at 2-fold or more at 0.05 *p*-value cut-off, while those below the lower diagonal represent those were expressed predominantly in the leaf at the same criteria. The ‘volcano’ plot and the scatter plot were generated in the GeneSpring GX 10 software.

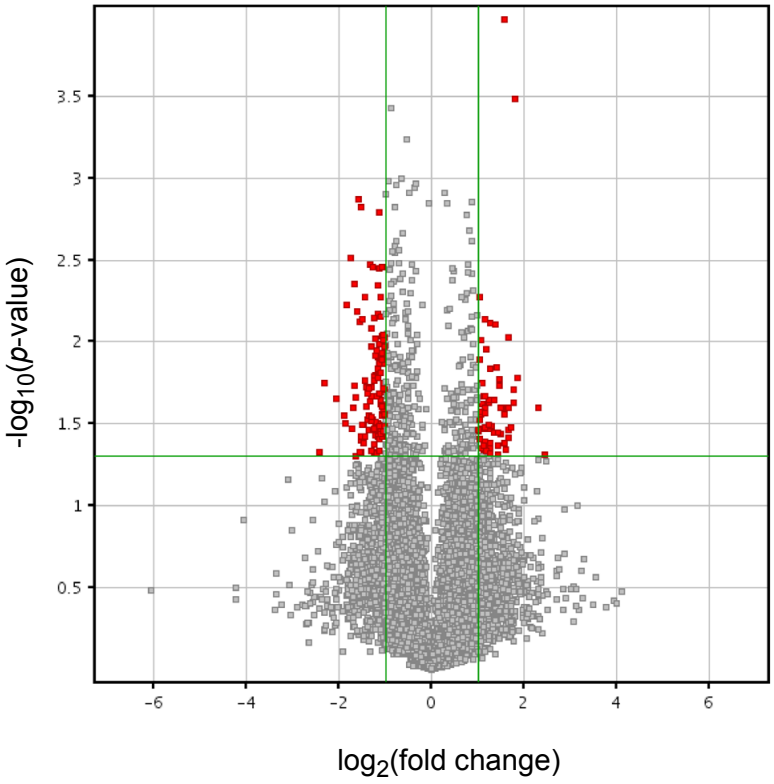
-log10(p-value)
log2(fold change)
3.5
3
2.5
2
1.5
1
0.5
-6
-4
-2
0
2
4
6

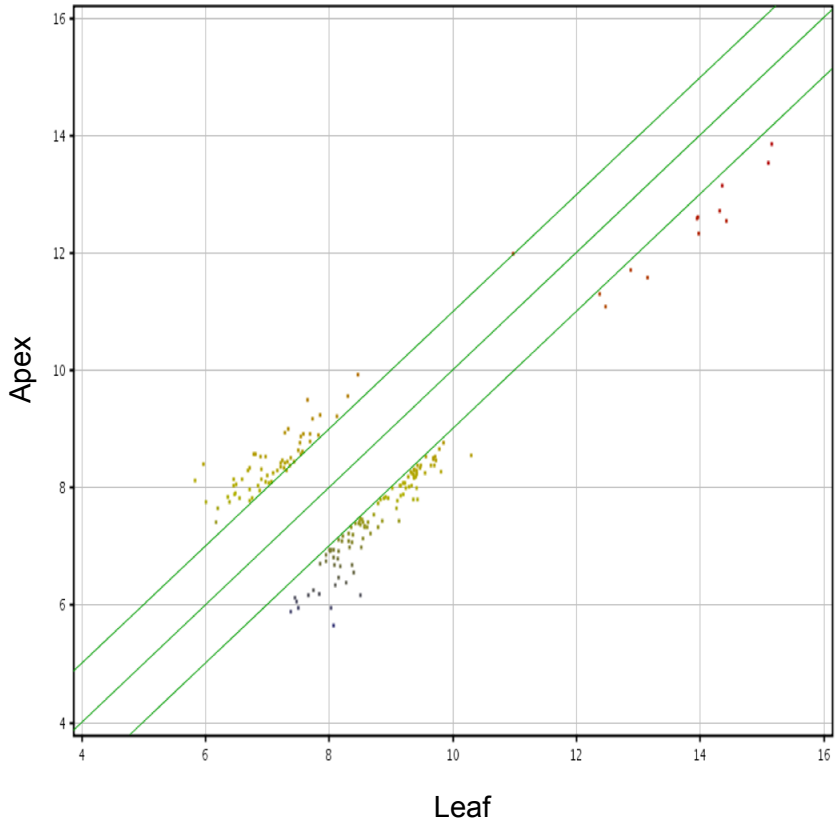
Apex
Leaf
16
14
12
10
8
6
4
4
6
8
10
12
14
16

Figure 3-11. The representative electronic fluorescent pictographs (eFPs). The upper and the lower panels show the changes in expression levels of the genes that are preferentially expressed in the shoot apex (*AT2G22610*) and in the young leaf (*AT3G62410*), respectively.

AT2G22610 encodes kinesin motor protein-related protein, which functions in ATP binding involved in microtubule-based movement. The gene product is located in the microtubule associated complex that are involved in cytoskeletal organization. *AT3G62410* encodes CP12-2, a small peptide found in the chloroplast stroma. It is thought to be involved in the formation of a complex with glyceraldehyde-3-phosphate dehydrogenase (GAPDH) and phosphoribulokinase (PRK) functioning in the Calvin cycle. Red indicates the highest expression level and blue the lowest.

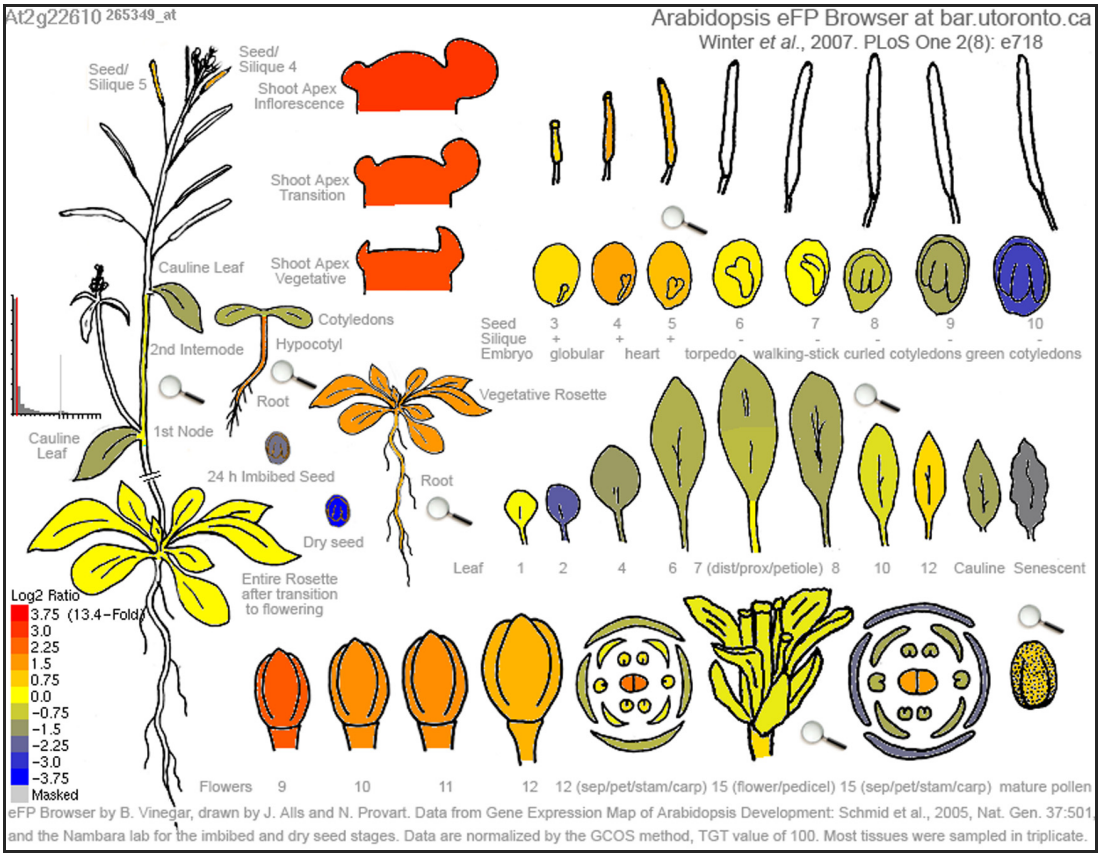
At2g22610 265349_at
Arabidopsis eFP Browser at bar.utoronto.ca
Winter et al., 2007. PLoS One 2(8): e718
Seed/ Silique 5
Seed/ Silique 4
Shoot Apex Inflorescence
Shoot Apex Transition
Shoot Apex Vegetative
Cauline Leaf
Cotyledons
Hypocotyl
2nd Internode
Root
1st Node
Cauline Leaf
24 h Imbibed Seed
Dry seed
Vegetative Rosette
Root
Entire Rosette after transition to flowering
Seed 3 4 5 6 7 8 9 10
Silique + + + - - - - -
Embryo globular heart torpedo walking-stick curled cotyledons green cotyledons
Leaf 1 2 4 6 7 (dist/prox/petiole) 8 10 12 Cauline Senescent
Flowers 9 10 11 12 12 (sep/pet/stam/carp) 15 (flower/pedicel) 15 (sep/pet/stam/carp) mature pollen
Log2 Ratio
3.75 (13.4-Fold)
3.0
2.25
1.5
0.75
0.0
-0.75
-1.5
-2.25
-3.0
-3.75
Masked
eFP Browser by B. Vinegar, drawn by J. Alls and N. Provart. Data from Gene Expression Map of Arabidopsis Development: Schmid et al., 2005, Nat. Gen. 37:501
and the Nambara lab for the imbibed and dry seed stages. Data are normalized by the GCOS method, TGT value of 100. Most tissues were sampled in triplicate.

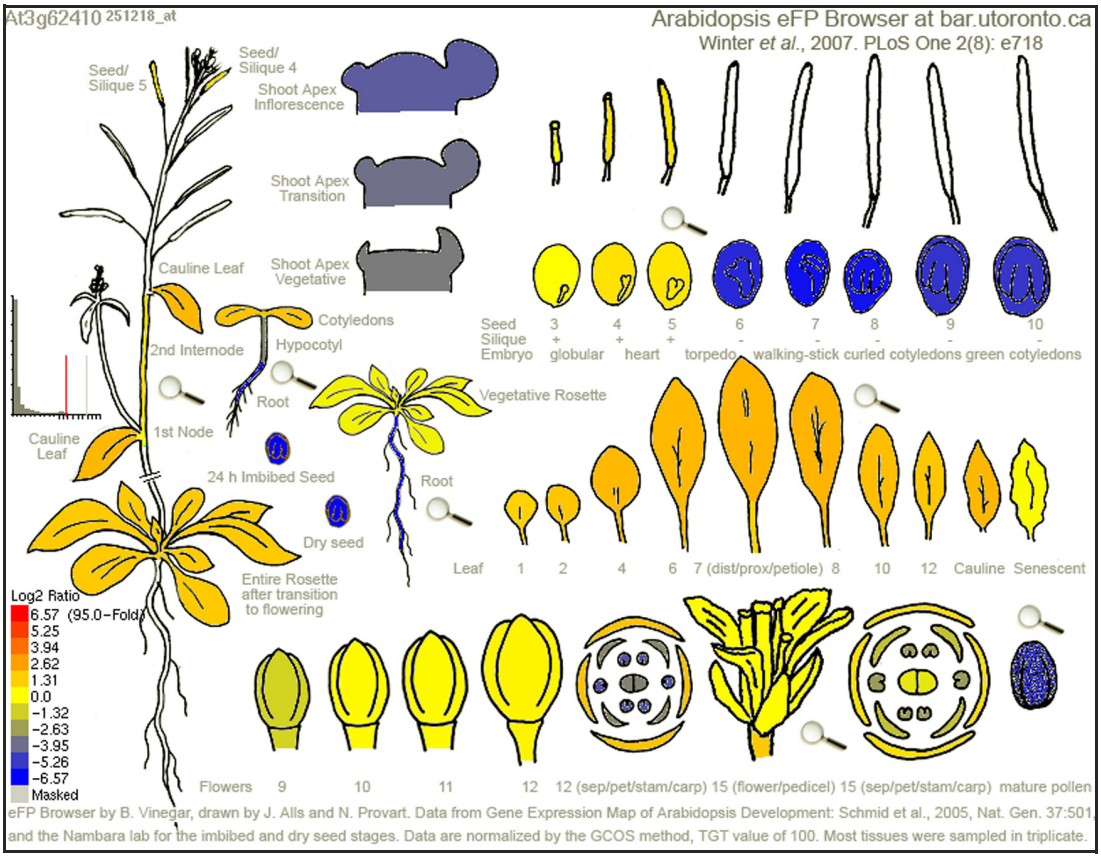
At3g62410 251218_at
Arabidopsis eFP Browser at bar.utoronto.ca
Winter et al., 2007. PLoS One 2(8): e718
Seed/ Silique 5
Seed/ Silique 4
Shoot Apex Inflorescence
Shoot Apex Transition
Shoot Apex Vegetative
Cauline Leaf
Cotyledons
Hypocotyl
2nd Internode
Root
1st Node
Cauline Leaf
24 h Imbibed Seed
Dry seed
Vegetative Rosette
Root
Entire Rosette after transition to flowering
Seed 3 4 5 6 7 8 9 10
Silique + + + - - - - -
Embryo globular heart torpedo walking-stick curled cotyledons green cotyledons
Leaf 1 2 4 6 7 (dist/prox/petiole) 8 10 12 Cauline Senescent
Flowers 9 10 11 12 12 (sep/pet/stam/carp) 15 (flower/pedicel) 15 (sep/pet/stam/carp) mature pollen
Log2 Ratio
6.57 (95.0-Fold)
5.25
3.94
2.62
1.31
0.0
-1.32
-2.63
-3.95
-5.26
-6.57
Masked
eFP Browser by B. Vinegar, drawn by J. Alls and N. Provart. Data from Gene Expression Map of Arabidopsis Development: Schmid et al., 2005, Nat. Gen. 37:501
and the Nambara lab for the imbibed and dry seed stages. Data are normalized by the GCOS method, TGT value of 100. Most tissues were sampled in triplicate.

3.6 Functional Analysis of Microarray Data

3.6.1 GO Slim Functional Classification

Genes that had unique AGI locus identifiers were categorized according to the GO slim to obtain a broad summary of gene types. The GO slim provided only high-level categories and its categorization scheme took all of the associated terms into account, which were often redundant. The results were generally uninformative. The gene counts associated with GO slim terms are based on the biological processes of the gene, the molecular functions of the gene product, and its cellular localization (Table S-2 on page 131 and Figure S-2 on page 127 in “Supplementary Data”).

3.6.2 Cluster Analysis

To identify and group the genes that were similarly expressed in each tissue type and infer any biological significance of the groups of genes, hierarchical and K-mean clustering analyses were carried out using GeneSpring GX. The hierarchical clustering dendrograms of the genes that are preferentially expressed in the shoot apex and the young leaf is presented in Figure S-4 on page 133 and Figure S-6 on page 137, respectively, in “Supplementary Data”. Also, the genes in each cluster were subjected to classification by GO slim functional categorization as in the previous section (“3.6.1 GO Slim Functional Classification”), and the results are shown in Figure S-5 on page 135 and Figure S-7 on page 139 in “Supplementary Data”.

There was no clear relationship between functional categories and clustering patterns of genes. When other distance methods were applied to the hierarchical clustering along with various parameters, the results were similar except for minor variations in the numbers of genes to fall in each cluster (data not shown). The K-mean clustering with various parameters revealed no significant patterns related to biological function of the genes (data not shown). Although the cluster analyses have been useful in general to identify patterns in gene expression in relation to their biological functions by grouping the similarly expressed genes (Drăghici, 2003), their usefulness was unclear in this study, where only two tissue types were compared: the shoot apex and the young leaf.

3.6.3 Manual Categorization of Gene Function

Since the TAIR GO slim scheme did not lead to a meaningful classification for the gene sets screened in this experiment, the genes were classified manually based on the functional categories provided in both TAIR GO slim and TAIR Gene Ontology as well as other protein databases as described in “2.9.2 Functional Annotation” on page 53 in “Materials and Methods”. To assign each gene to an appropriate category, the functional categories were grouped into a higher level category, divided into lower level categories, and/or combined into a category of the same level.

Excluding those that were not mapped to AGI (Arabidopsis Genome Initiative) locus identifiers, 163 genes represented by unique locus identifiers were categorized into 24 biological processes including ‘Unknown” (Figure 3-12 on page 76). Most genes that were preferentially expressed in one tissue type or the other were commonly involved in 15 biological processes, including ‘Unknown’. Meanwhile, there were 9 biological processes where the genes that were expressed only in one type of tissue were involved (Table 3-2). For example, in the cell cycle control/DNA repair, energy/respiration, carbohydrate metabolism, chlorophyll degradation and photosynthesis dark reaction were preferentially expressed in the young leaf. On the other hand, cytoskeletal organization and hormone metabolism were preferentially expressed in the shoot apex.

Table 3-2. Biological processes in which genes that were expressed in either type of tissue were involved.

Biological Process	Shoot Apex	Young Leaf	Locus Id
Cell cycle control/DNA Repair	-	3	AT1G18040, AT3G27010, AT5G41360
Cytoskeletal organization	3	-	AT1G64740, AT2G22610, AT5G20490
Energy/Respiration	-	2	AT1G53310, AT3G27380
Metabolism: Carbohydrate	-	2	AT1G09420, AT1G45130
Metabolism: Chlorophyll degradation	-	3	AT3G02450, AT3G44880, AT4G25650
Metabolism: Hormone	2	-	AT3G13730, AT5G05730
Photosynthesis, dark reaction	-	3	AT1G67090, AT3G62410, AT5G38430
Protein fate: sorting/targeting	1	-	AT5G05670
Response to biotic stimulus	-	2	AT3G09260, AT5G42500

Figure 3-12. Gene counts involved in manually categorized biological processes. The numbers of genes in each category are given in Table S-3 on page 141 in “Supplementary Data”. The manual categorization of the genes based on the TAIR GO slim, TAIR Gene Ontology and other protein databases (“2.9.2 Functional Annotation” on page 53 in “Materials and Methods”) revealed some of the biological processes, in which only genes that were preferentially expressed in either type of the tissue (shoot apex or young leaf) were involved. The shoot apex includes cytoskeletal organization, hormone metabolism, protein sorting/targeting, whereas the young leaf includes cell cycle control/DNA repair, energy/respiration, photosynthesis dark reaction, carbohydrate metabolism and chlorophyll degradation. Many genes, which were preferentially expressed in the shoot apex or in the young leaf, fell into the same functional categories, including photorespiration, photosynthesis light reaction, amino acid metabolism, lipid metabolism, protein translation, post-translational modification, protein folding, proteolysis, transcription and post-transcriptional processing, inter-/intra-cellular transportation and signal transduction. The genes categorized in ‘response to abiotic stimulus’ or ‘response to biotic stimulus’ have not been annotated in further detail. The ‘other metabolism’ and ‘other cellular process’ means that the particular gene is involved in a known biological process(es), but not included in this categorization. There were 29 genes (10 from the shoot apex and 19 from the young leaf) that have no annotated functions.

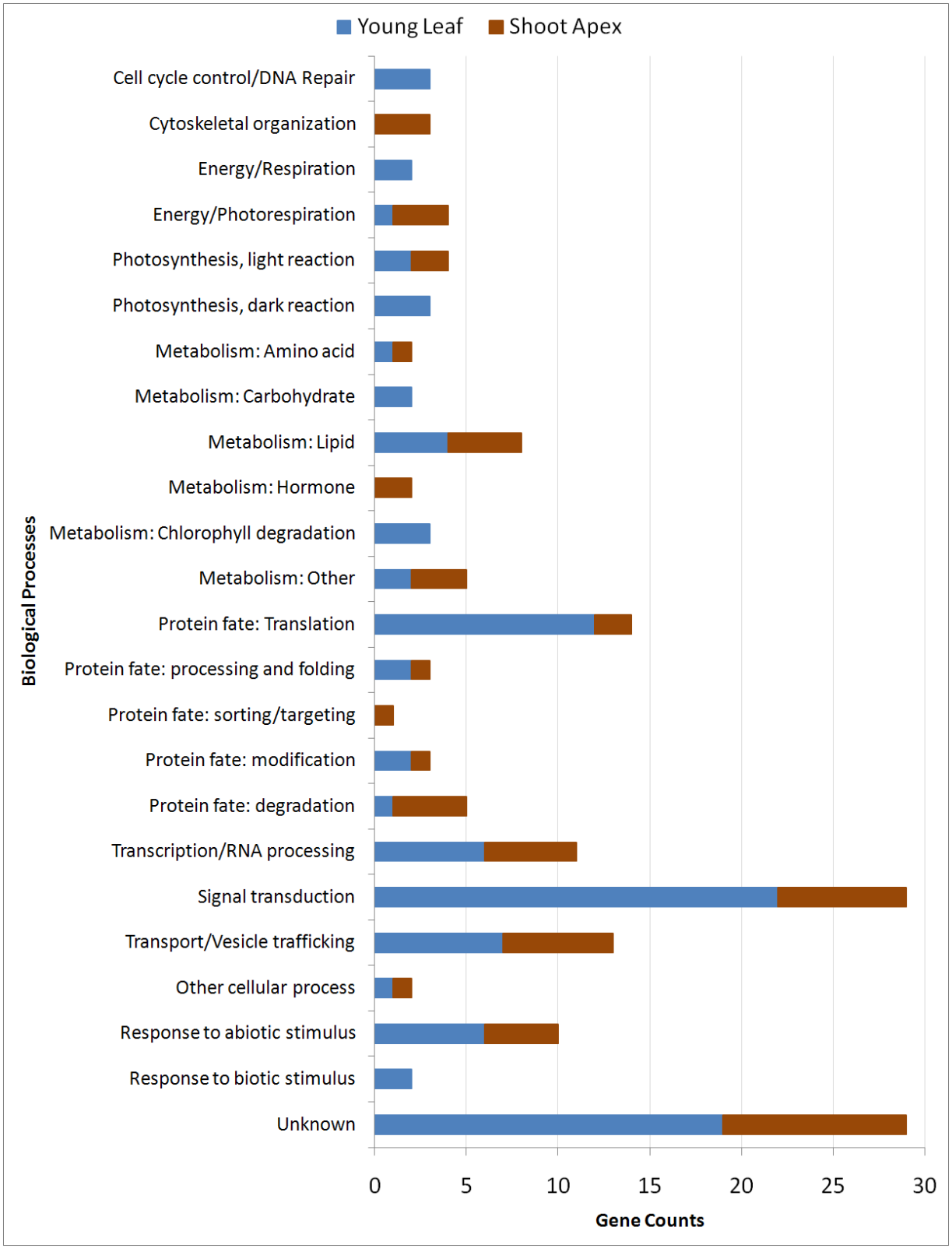
Young Leaf
Shoot Apex
Cell cycle control/DNA Repair
Cytoskeletal organization
Energy/Respiration
Energy/Photorespiration
Photosynthesis, light reaction
Photosynthesis, dark reaction
Metabolism: Amino acid
Metabolism: Carbohydrate
Metabolism: Lipid
Metabolism: Hormone
Metabolism: Chlorophyll degradation
Metabolism: Other
Protein fate: Translation
Protein fate: processing and folding
Protein fate: sorting/targeting
Protein fate: modification
Protein fate: degradation
Transcription/RNA processing
Signal transduction
Transport/Vesicle trafficking
Other cellular process
Response to abiotic stimulus
Response to biotic stimulus
Unknown
Biological Processes
0
5
10
15
20
25
30
Gene Counts

3.7 Pathway Analysis

The metabolic pathway analysis revealed some of the biologically meaningful inter-relations among the genes that were statistically differentially expressed in the shoot apex and in the young leaf, respectively. Fifty nine out of 60 the shoot apex gene products and 102 out of 103 young leaf gene products matched to the curated protein entities in the pathway database implemented in GeneSpring GX 10 software (Agilent Technologies Inc., 2008). There were no direct inter-relations among the matched gene products, except for the two gene products from the young leaf, namely EBF2 (EIN3-BINDING F-BOX PROTEIN 2) and SKP1, a component of the Skp1-Cullin-F-box-protein (SCF), which were encoded by *AT5G25350* and *AT1G75950*, respectively (Figure S-8 on page 146). When the relations were expanded so as to include the immediate neighbors of the curated gene products, a total of 30 gene products established one or more new relations: 9 from the shoot (Table 3-3) and 21 from the young leaf (Table 3-4 on page 79). The gene products from the shoot apex or the young leaf, which were thought to be involved in the regulatory pathways were discussed in the later chapter.

Diagrams showing the relations among the shoot apex gene products and other pathway entities were shown in Figure S-9 on page 147 in “Supplementary Data”. Their cellular localization were also provided in Figure S-10 on page 149 in “Supplementary Data”.

Table 3-3. Gene products of the shoot apex participating in one or more relations in the metabolic pathways.

Biological Process	Protein Name	Encoded by:
Energy: photorespiration	GLU1	AT5G04140
Transcription/RNA processing	ELF7	AT1G79730
	REF6	AT3G48430
	PCFS4	AT4G04885
Metabolism: hormone biosynthesis	CYP90D1	AT3G13730
	ASA1	AT5G05730
Translation	ERF1-1	AT5G47880
Response to abiotic stimuli	SAG21	AT4G02380
Transport, transmembrane	AST91	AT1G23090

Table 3-4. Gene products of the young leaf participating in one or more relations in the metabolic pathways.

Biological Process	Protein Name	Encoded by:
Cell cycle control	CDKD1;3	AT1G18040
Photosynthesis-dark reaction	CP12-2	AT3G62410
Photosynthesis-light reaction	FNR1	AT5G66190
Transcription/RNA processing	SIGA	AT1G64860
	SPL3	AT2G33810
	TAFII15	AT4G31720
Chlorophyll catabolic process	ACD1	AT3G44880
Ion homeostasis	CCH	AT3G56240
Protein Fate: folding	CPHSC70-2	AT5G49910
Protein Fate: translation	FBR12	AT1G26630
Response to abiotic stimuli	COR47	AT1G20440
Signal Transduction: hormone-mediated	RAP2.12	AT1G53910
Signal Transduction, hormone-mediated	ERF4	AT3G15210
Signal Transduction, in response to abiotic stimuli	STO	AT1G06040
	PHYA	AT1G09570
Signal Transduction, protein phosphorylation-mediated	PHOT1	AT3G45780
Signal Transduction, ubiquitin/protein ligase-mediated	SKP1	AT1G75950
	ATSR1	AT5G01820
	EBF2	AT5G25350
Transport, transmembrane	PIP1B	AT2G45960
Transport, vesicle-mediated	VSR1	AT3G52850

PART 4. DISCUSSION

4.1 Cross-species Hybridization

This study examined patterns of gene expression in the shoot apices and the young developing leaves of *H. helix* cv. Goldheart by comparing the transcriptome from one tissue type to the other. As is the case for non-model plant species, both genome sequence information and availability of prepared microarray platform are very limited for *H. helix*. To circumvent this limitation, a microarray-based heterologous hybridization analysis (cross-species hybridization or CSH) was carried out by hybridizing cDNA targets prepared from the shoot apices and the young leaves of *H. helix* cv. Goldheart onto *Arabidopsis thaliana* whole genome full-length cDNA microarrays.

In the microarray study using CSH, the primary technical challenge is the problem of sequence divergence between the species from which the probes on the microarray was prepared and the species providing the sample cDNA targets (Buckley, 2007). In the comparative genomics studies using CSH, where comparisons are made among samples prepared from different species, it is important to differentiate between actual differential gene expression and the bias due to sequence mismatches. In the study of heterologous hybridization using cDNA microarray that was generated from an African cichlid fish (*Astatotilapia burtoni* found in Lake Tanganyika) to examine expression patterns of seven other fish species ranging from closely related taxa to a very distantly related species, Renn *et al*. (2004) showed that gene expression profiles between species was more consistent for closely related ones (divergence time < 10 million years ago; Mya) than for intermediately related ones (divergence time ~65 Mya). For distantly related species (divergence time > 200 Mya), the consistency was even less, making it difficult to distinguish the differences among species from the effects of the sequence mismatches.

However, phylogenetic distance seems not necessarily a main criterion to determine the similarity required between the target and probe species in the microarray-based CSH studies, since phylogenetic distance might not exactly reflect the degree of divergence at the gene sequence level (Renn *et al*., 2004; Rutschmann, 2006). While the loss of overall hybridization signals due to the sequence divergence is inevitable in CSH, it has been indicated that the level of hybridization between targets and probes correlates better with the presence of orthologous than with random sequence similarity (Horvath, 2003), and sequence conservation among plant species is high enough to generate sufficient signals from the hybridized probes for global expression analysis (Fulton *et al*., 2002). In this study, sequence divergence between *H. helix* and *A. thaliana* did not add a bias since the two cDNA targets prepared from single species (*H. helix*)

were hybridized competitively against one another on the same probe set (*A. thaliana*). However, sequence divergence between target species (*H. helix*) and reference species (*A. thaliana*) likely influenced the effective size of the microarray. It could be expected that fewer features were detected in both the shoot apex and the young leaf samples from *H.helix* than the number of features that a single-species microarray could have detected in the samples from *A. thaliana* as shown in a study where CSH between *A. thaliana* and several distantly related species was used (Horvath, 2003).

4.2 Differential Hybridization between Shoot Apex and Young Leaves

In both the shoot apex and the young leaf samples from *H. helix*, labeled target cDNAs that hybridized onto the *A. thaliana* microarray probes above background were detected, and each type of tissue exhibited differential gene expression. Among 11,255 usable cDNA probes (with 'BLANK' and 'bad' spots excluded), 2,597 features produced signals that were greater than background levels, which constitutes 23% of total number of usable probes on the microarray. In a cross-species hybridization study, where a 11,522-element *Arabidopsis thaliana* microarray was hybridized with labeled cDNAs from shoot tip and mature leaf from several different distantly related species, such as leafy spurge, poplar and wild oat, 23 to 47% of the features on the array was detected above background (Horvath, 2003). Considering the phylogenetic distance between *H. helix* and *A. thaliana* and the use of tissue type, which was limited to shoot apices and young leaves at the very early developmental stage, 23% detection rate in this CSH experiment seemed to be within a reasonable range. Because the *A. thaliana* whole genome full-length cDNA microarray used in this study contained probes prepared from a variety of tissue types, including 1) etiolated seedlings, 2) roots, 3) rosette plants of various ages, 4) stems, flowers, and siliques at all stages from floral initiation to mature seeds (Newman *et al*., 1994), it is likely that the transcriptomes of the shoot apex and young leaf at early developmental stages represents only a small portion of the transcriptomes of the whole plant representing various developmental stages.

Among 2,597 hybridized features that produced signals above the threshold, a total of 174 genes (6.7% of the detected above background, or 1.4% of total array features) were found to be statistically significantly expressed by 2-fold or more at a *p*-value of 0.05 in the shoot apex or the young leaf. Among the total significantly differentially expressed genes, 60 were preferentially expressed in the shoot apex, and 114 were in the young leaf, perhaps reflecting tissue-specific differences in physiology and developmental processes. It was expected that many of the genes in the leaf primordia included in the shoot apex sample might have been expressed at similar

levels to those in the young leaf sample, which was in very early stage of the leaf development. Meanwhile, there were possibilities that the spot intensity levels of the features hybridized by the probes represented by the SAM-specific genes were not high enough above the background to be considered statistically significant due to the significantly smaller proportion of SAM tissue compared to the leaf primordia.

4.3 Functional Categories of Differentially Expressed Genes

A large portion of the gene products could be assigned to functional categories associated with basic biological processes. Genes that were preferentially expressed in either shoot apex or young leaf had multiple molecular functions and were involved in various biological processes occurring in most of the major cellular components, including chloroplasts, mitochondria, Golgi apparatus, endoplasmic reticulum, cytosol and plasma membrane. As the number of genes preferentially expressed in the young leaf was approximately twice higher than that in the shoot apex (114 *vs.* 60), the number of the genes participating in most functional categories were also similarly proportioned. Many of the detected genes, which were differentially expressed in either tissue, were predicted to have transcription/translation factor activities, various catalytic activities and binding function with other metabolic entities, which were involved in different biological processes, such as cell biogenesis, gene expression, energy generation, metabolism, signal transduction and transport. The common involvement in the major biological processes among the genes expressed differentially in either tissue types is reasonable given that both sample tissues were sharing similarities. The shoot apex sample contained not only shoot apical meristem but also leaf primordia that had already begun to differentiate into leaves, and the young leaf sample was only two plastochrons apart from the oldest leaf primordium in the shoot apex sample.

In spite of the overlapping characteristics of the two tissue types, the preferentially expressed genes in the two tissue samples differed in several respects. The genes that were expressed preferentially in the shoot apex represented transcripts that appeared to be more closely linked to cytoskeletal organization and phase change, whereas those in the young leaf appeared more related to cell and energy-related metabolism, such as photosynthesis dark reactions, aerobic respiration and carbohydrate catabolism. Perhaps the differences were a reflection of the transcription of the undifferentiated or less differentiated state of the shoot apex and the fully differentiated state of the young leaf.

4.4 Genes Involved in Regulatory Pathways In the Shoot Apex

The pathway analysis revealed some of the regulatory pathways that were expected to be occurring predominantly in the shoot apex.

4.4.1 Genes Involved in Phase Change

In the shoot apex, several gene products that are directly or indirectly involved in a signaling pathway, which delays flowering in *A. thaliana,* were detected, suggesting a similar signaling mechanism might be in operation for the prolonged vegetative state in *H. helix*. Changing from vegetative to reproductive growth phase in plants is a major developmental transition regulated by an integrated network of multiple signal transduction pathways that regulate the expression of genes associated with the transition of the vegetative SAM to floral/inflorescence meristem (Clouse, 2008; Simpson and Dean, 2002). Environmental and internal stimuli are mainly perceived and transduced by four genetic pathways: the autonomous, light-dependent, vernalization and gibberellin pathways (Roux *et al*., 2006). The autonomous pathway responds to internal developmental signals constitutively to control flowering (Putterill *et al*., 2004). The light-dependent pathway perceives changes in photoperiod, quality and intensity of irradiation for flowering (Schepens *et al*., 2004). The vernalization pathway is activated by exposure to long periods of cold before flowering (Henderson *et al*., 2003). The gibberellin (GA) pathway promotes flowering *via* the hormonal stimuli (Mutasa-Gottgens and Hedden, 2009). The notable aspect in this regulatory network is that all of these signal transduction pathways converge on a common set of integrator genes, such as LEAFY (LFY), FLOWERING TIME LOCUS T (FT) and SUPPRESSOR OF OVER-EXPRESSION OF CONSTANS 1(SOC1), which regulate the initiation of flowering via the action on the floral meristem identity genes (Bonnin *et al*., 2008; Roux *et al*., 2006). While signals from the photoperiod pathway are mediated through to the integrators by the floral activator CONSTANS (CO), signals from the autonomous and vernalization pathways are mediated by the floral repressor FLOWERING LOCUS C (FLC), a MADS-box transcriptional regulator (Henderson *et al*., 2003; Schepens *et al*., 2004). A prolonged cold treatment attenuates the expression level of FLC through a process known as vernalization and permits flowering to occur (Michaels and Amasino, 1999).

In this microarray analysis, two transcription factors that regulate the level of FLC were identified: RELATIVE OF EARLY FLOWERING 6 (REF6) and EARLY FLOWERING 7 (ELF7), which play a regulatory role in the brassinosteroids (BRs) and the autonomous signaling pathway, respectively (Figure 4-1 on page 84).

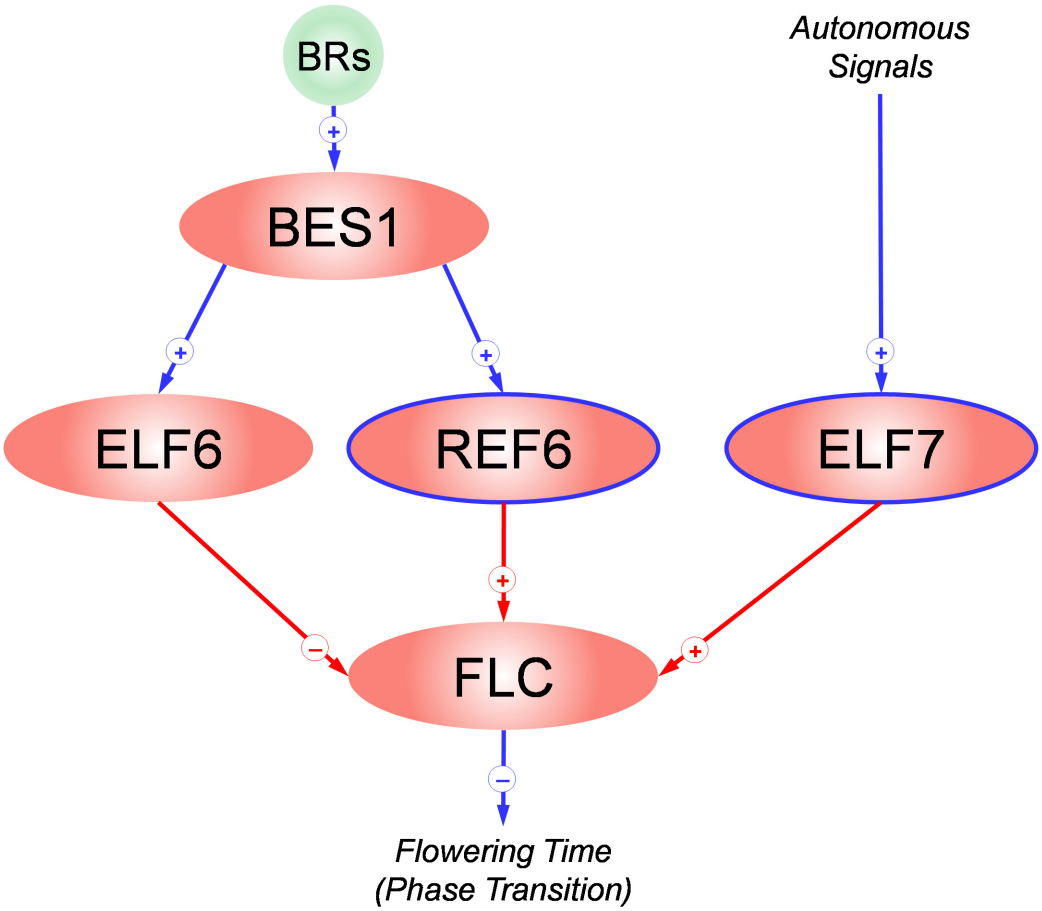

Figure 4-1. Signal transduction pathways involved in vegetative-floral transition occurring in the shoot apex. Plant steroid hormones brassinosteroids (BRs, in the green circle) signal through BES1, which positively regulates transcriptional regulators EARLY FLOWERING 6 (ELF6) and RELATIVE OF EARLY FLOWERING 6 (REF6). ELF6 and REF6 in turn regulate expression of FLOWERING LOCUS C (FLC) downstream of the pathway, thereby controlling flowering time. While ELF6 acts on FLC as a repressor, REF6 elevate FLC expression to levels that can delay flowering in plants that have not been vernalized. EFL7, which is a component of the autonomous signal pathway, elevates the expression of FLC as REF6 in the BRs-mediated pathway. See text for the details and references. Pink ovals represents gene products (transcription factors) with their protein name inside. Ovals with blue outline represents those expressed preferentially in the shoot apex, and ones without outline are those expressed constitutively in both the shoot apex and the young leaf, but associated only with those expressed preferentially in the shoot apex. Blue arrows indicate the direction of the signal transduction and the regulation with the arrow heads on the targets; red indicates the regulation of the gene expression. The plus (+) and minus (-) signs in the circles indicate positive and negative regulation, respectively.

While the hormonal signal directly regulates the integrator genes in the GA pathway of the flowering induction (Mutasa-Gottgens and Hedden, 2009), another class of plant hormones, the brassinosteroids (BRs), participate in the vernalization pathway *via* signaling through a cell surface receptor kinase, BRASSINOSTEROID INSENSITIVE 1-EXCESS MICROSPOROCYTES-SUPPRESSOR 1 (BRI1-EMS SUPPRESSOR 1 or BES1) (Domagalska *et al*., 2007). BES1 directly binds to target gene promoters, EARLY FLOWERING 6 (ELF6) and its closely related protein, RELATIVE OF EARLY FLOWERING 6 (REF6, encoded by *AT3G48430*) to activate or repress the expression of the gene and transduce BR-mediated responses (Yu *et al*., 2008). ELF6 and REF6, in spite of close similarity in their sequences, act differently in the regulation of flowering time. While ELF6 represses the expression level of FLC promoting floral transition, REF6 elevates the FLC level to delay the flowering time in *A. thaliana*. Ectopic expression studies and expression pattern analyses showed that ELF6 and REF6 have different cellular functions and are regulated differently (Noh *et al*., 2004). Another transcription factor that promotes the expression of FLC was detected in the shoot apex: EARLY FLOWERING 7 (ELF7, encoded by *AT1G79730*), which is a homolog of the component of yeast RNA polymerase II (Pol II), Paf1 (proteasome alpha subunit F-1) complex (He *et al*., 2004). While ELF6 acts on FLC as a repressor, ELF7 (as REF6) elevates FLC expression to the level that can delay flowering in *Arabidopsis* that have not been vernalized. Repression or elevation of FLC expression by ELF6 or REF6/ELF7 accompanies modifications of histone in FLC chromatin, implying that structural changes to the chromatin (chromatin remodeling) is necessary for the transcriptional regulation by this class of proteins (He *et al*., 2004; Noh *et al*., 2004).

Besides REF6, which is involved in the BR-mediated signal transduction pathway in flowering time, a cytochrome P450 (CYP90D1, encoded by *AT3G13730*) was also expressed preferentially in the shoot apex. Two cytochrome P450s, CYP90C1 and CYP90D1, participate in different steps of the BR biosynthesis pathway in *Arabidopsis thaliana*. While CYP90D1 catalyzes the oxidative reactions in the earlier phase of BR biosynthesis, CYP90C1, which is encoded by *ROTUNDIFOLIA3* (*ROT3*) gene, appears to play a role in an activation step in the BR pathway by converting typhasterol to castasterone (Kim *et al*., 2005a). In this microarray analysis, CYP90C1 was not co-expressed with CYP90D1 in the shoot apex. Considering the roles of REF6 and ELF7 elevating the expression level of the FLC, which directly suppresses the floral transition of the vegetative shoot *via* BR-mediated and autonomous signaling pathway, respectively, the activities of both transcription factors in the two different signaling pathways may coordinately play a role in sustaining the prolonged juvenility of the shoot, which is a characteristic of the *H. helix* plants.

4.4.2 Genes Involved in Cytoskeleton Organization

Genes that encode cytoskeletal components, such as Tubulin alpha-1 chain (TUA1, encoded by *AT1G64740*) and accessory proteins, Kinesin motor-related protein (encoded by *AT2G22610*) and Myosin-like protein XI K (AtXIK, encoded by *AT5G20490*), were preferentially expressed in the shoot apex, suggesting that the cytoskeleton-mediated cellular processes were occurring more actively than in the young leaf.

The shape and the growth of plant cells are greatly influenced by the organization of actin and microtubule (MT) cytoskeleton, of which activities are regulated by protein phosphorylation/ dephosphorylation (Baskin and Wilson, 1997; Camilleri *et al*., 2002). While actin filaments have important roles in the movement of organelles, microtubules play major roles for controlling the direction of cell expansion and determining cell polarity. (Mathur, 2004). Microtubules are the dimers of alpha- (TUA) and beta-tubulin (TUB), each binding a molecules of GTP. The binding site on the beta-chain is capable of exchanging GTP and GDP, which determines the stability of the microtubule dimer. While the dimer with beta-tubulin bound to GTP tends to assemble into microtubule, one bound to GDP tends to dissociate (Ludwig *et al*., 1988). Microtubules have been known to be closely associated with cell division and cell elongation and preferentially expressed in the meristematic cells that produce cortex (Uribe *et al*., 1998). In addition, TUA and TUB are detected in xylem and phloem tissues of stems indicating the involvement of microtubule during cellulose microfibril deposition in secondary walls as well (Oakley *et al*., 2007). The Kinesin motor-related protein, which is localized in the microtubule-associated complex, has a conserved microtubule-binding site in the motor domain and confers motor activity to microtubules when it binds ATP (Jiang *et al*, 2007). It is involved in microtubule-based movements, such as formation of the mitotic spindle and phragmoplast, vesicle traffic and other processes related to cytokinesis (Muller *et al*., 2006; Nishihama *et al*., 2002). This protein also plays a role in the morphogenesis of trichomes (Mathur and Chua, 2000; Oppenheimer *et al*., 1997). *Arabidopsis thaliana* myosin-like protein AtXIK has motor activity and is involved in rapid, myosin-driven organelle trafficking (*e.g.*, mitochondrion localization, peroxisome localization), which is required for the optimal plant growth (Peremyslov *et al*., 2008). It is also required for the morphogenesis of root hairs and trichomes on the stems and leaves (Ojangu *et al*., 2007).

In addition to the component of cytoskeleton and accessory motor proteins, two proteins, which are related to the enzymatic proteins acting on the phosphorylation and dephosphorylation of the cytoskeletal components were also detected in the shoot apex. *AT3G25800* encodes PROTEIN PHOSPHATASE 2A SUBUNIT A2 (PP2AA2), a serine/threonine-protein phosphatase 2A 65 kDa

regulatory subunit A2, which is one of three protein phosphatase 2A regulatory subunits functioning in the regulation of phosphorylation in signaling cascades (Slabas *et al*., 1994). The A subunit seems to negatively regulates the catalytic activity of PP2A (Zhou *et al*., 2004) and involved in cortical microtubule organization (Camilleri *et al*., 2002). *AT4G35750* encodes a putative Rho-GTPase-activating protein-related protein, which contains weak similarity to Rho-GTPase-Activating Protein 1 (RhoGAP1) (Jiang and Ramachandran, 2006). Proteins containing a RhoGAP motif catalyze the hydrolysis of GTP that is attached to Rho, and deactivate the regulator of the actin cytoskeleton (Gu *et al*., 2005). A RhoGAP has been shown to be important for sustaining polar growth of pollen tube in *Nicotiana tabacum* (Klahre and Kost, 2006), while one in *Arabidopsis* was shown to be involved in oxygen metabolism and H_2O_2 signaling (Baxter-Burrell *et al*., 2002).

Detection of the ethylene responsive gene which regulates auxin biosynthesis suggests a possible involvement of the cytoskeletal genes in the geotropic responses of the shoot apex. ANTHRANILATE SYNTHASE ALPHA 1 (ASA1, encoded by *AT5G05730*), together with ANTHRANILATE SYNTHASE BETA 1 (ASB1), is a key element in the regulation of auxin production and modulation between ethylene responses and auxin biosynthesis in *Arabidopsis*. Regulation of auxin production is mediated by the action of the ASA1 and ASB1 genes that respectively encode alpha- and beta-subunits of anthranilate synthase, the rate-limiting enzyme required for tryptophan biosynthesis (Stepanova *et al*., 2005). Up-regulation of ASA1 and ASB1 by ethylene results in the accumulation of auxin, whereas suppression of these genes prevents the ethylene-mediated auxin accumulation (Ivanchenko *et al*., 2008; Stepanova *et al*., 2005). Considering that the production of ethylene is promoted by gravity (Shi and Cline, 1992) and the role of the ethylene in modulation of gravitropic response (Madlung *et al*., 1999) through regulation of auxin production (Swarup *et al*., 2007), ASA1 could be involved in regulation of the cytoskeletal activities in response to the geotropic stimuli in *H. helix*. Since the cytoskeleton plays diverse roles in many cellular processes, precise roles of the gene products detected in the shoot apex of *H. helix* are not clear. However, considering the interactions between cytoskeleton and polar auxin distribution in response to external stimuli such as light and gravity (Godbolé *et al*., 2000; Muday and DeLong, 2001; Sun *et al*., 2004; Yamamoto and Kiss, 2002), they might be involved in the plagiotropism, a tendency to diverge from the vertical in response to stimuli, which is one the characteristics of shoot of the *H. helix* in the vegetative phase (Poethig, 1990).

4.5 Genes Involved in Regulatory Pathways In the Young Leaf

The microarray analysis and subsequent pathway analysis identified many regulatory genes that were preferentially expressed in the young leaf cells. They include genes that encode transcription factors and binding proteins with enzymatic activities that are involved in the signal transduction in response to ions, plant hormones or environmental stimuli; such as light (Figure 4-2 on page 89).

4.5.1 Genes Involved in Photomorphogenesis

PHOTOTROPIN1 (PHOT1, encoded by *AT3G45780*), also known as NON-PHOTOTROPIC HYPOCOTYL 1 (NPH1) or ROOT PHOTOTROPISM 1 (RPT1), is a plasma membrane-associated photoreceptor molecules mediating blue light-induced responses such as phototropism, chloroplast relocation, and stomatal opening as well as regulation of the rate of leaf expansion in *Arabidopsis* (Briggs and Christie, 2002; Chen *et al*., 2004). In plat leaves, phototropic responses play important roles for both the position and orientation of the leaf lamina to maximize the utilization of light for photosynthesis and to avoid damage from intense light. *Arabidopsis* PHOT1 contains a light activated serine-threonine kinase domain and autophosphorylates after binding chromophores (flavin mononucleotides) and subsequent light absorption (Christie *et al*., 1999). PHOT1 also phosphorylates the NPH3 protein, which is likely to be the first component in the signal transduction pathway downstream of PHO1.The RPT2, which contains a BTB/POZ (broad complex, tramtrack, bric-a-brac/pox virus and zinc finger) domain as NPH3, also transduces signals downstream of PHOT1 signaling pathway to induce the phototropic response (Galen *et al*., 2004; Inada *et al*., 2004; Motchoulski and Liscum, 1999). While NPH3 and RPT2 was constitutively expressed in both the shoot apex and the young leaf, two putative uncharacterized proteins (AT2G30600 and AT2G46260) containing a BTB/POZ domain were expressed preferentially in the young leaf. Proteins containing BTB/POZ interact cullin component functioning as a scaffold in the F-box-containing ubiquitin ligase E3 complexes, which subsequently regulate transcription factor family required for auxin-mediated signal transduction downstream of phototropic response (Weber *et al*., 2005; Weber and Hellmann, 2009). Two HEAT-repeat proteins, which possibly participate in auxin signaling in Arabidopsis by regulating assembly and disassembly of the SCF protein degradation (Cheng et al., 2004), were also preferentially expressed in the young leaf: AT1G64790 and AT2G36810.

PHYTOCHROME KINASE SUBSTRATE 1 (PKS1, encoded by *AT2G02950*) protein, which is a PHOT1 binding protein required for phototropic response, also binds with PHYTOCHROME A

Figure 4-2. Signal transduction pathways occurring in *H. helix* young leaf in response to light, hormone and salt stimuli. PHOT1 and PHYA are induced by blue light and red light, respectively. While red light inhibits blue light-induced phototropic response of PHOT1, PHYA regulates the intracellular distribution of PHOT1. NPH3 and RPT2 contain BTB/POZ domain, and are the upstream components in the regulation of phototropic responses. Two BTB/POZ domain-containing proteins (AT2G30600 and AT2G46260) and two HEAT-repeat proteins (AT1G64790 and AT2G36810) were preferentially expressed in the young leaf of *H. helix*. Both types of proteins may participate in auxin signaling in *Arabidopsis* by regulating assembly and disassembly of the SCF protein degradation. PKS1 is phosphorylated by a phytochrome kinase and negatively regulates phytochrome signaling. PKS1 also interacts with PHOT1 and NPH3 and may function in PHOT1-mediated phototropism. The expression of the EID1, which is a negatively acting component in the PHYA-dependent signaling pathway requires PHYA. COP1, which also requires PHYA for its expression, represses photomorphogenesis by promoting the ubiquitin-mediated proteolysis of positive regulators. COP1 also interacts with STO, suppressing the transcription of STO *via* TBP, a component of multisubunit transcription factor IID (TFIID; STG1) complex. NDPK2, which is an positive regulatory component upstream in the phytochrome signalling pathway, also interacts with AtSR1. A protein kinase (CIPK14 or AtSR1), which is induced by calcium ion and ABA, regulates the plant response to ABA and salt response in *Arabidopsis*.

The expression of TIR1 and ASK1 genes is regulated by auxin, and auxin response is mediated by the action of SCF(ASK1/TIR1), a SCF E3 ubiquitin ligase complex. While SCF(COI1) regulates signal transduction in response to JA, SCF(EBF2) regulates ethylene signaling pathway. Ethylene suppresses the action of SCF(EBF2) and the accumulation of EIN3 positively regulates the ethylene signaling. In the absence of ethylene, EIN3 is degraded by ubiquitin-mediated proteolysis by SCF(EBF2) suppressing ethylene-induced responses. While EIN3 is the substrate of SCF(EBF2), it is capable of an intricate modulation of EBF2 gene expression, fine-tuning the ethylene signaling. AtERF4 is a transcriptional repressor that modulates ethylene and ABA responses and JA-responsive defense. See text for the details and references.

The pink ovals with blue outlines are gene products that were expressed preferentially in the young leaf; those without outline were expressed constitutively in both the shoot apex and the young leaf, but associated only with those expressed preferentially in the young leaf. Circles in light green represent small molecules (hormones, ions) or environmental factors, such as light, which interact with the gene product(s). Double lobes colored in bright slate blue represent SCF complex with F-box component name in the parentheses. Grey boxes includes proteins containing specific functional domains, such as BOT/POZ, HEAT-repeat, GDSL lipase. The yellow diamond shapes represent biological responses downstream of the pathways. Arrows indicate activities of the entities, with arrow head on the target of the activity: blue, regulatory activity; red, gene expression; aqua, enzymatic activity. The circled + and - signs indicate positive and negative regulation on the target, respectively. The arrows without + or - sign indicates the direction of regulation without a specified activity of promoter or repressor. Orange lines without arrow heads represent the participation of the entities in non-directional binding activity or interaction.

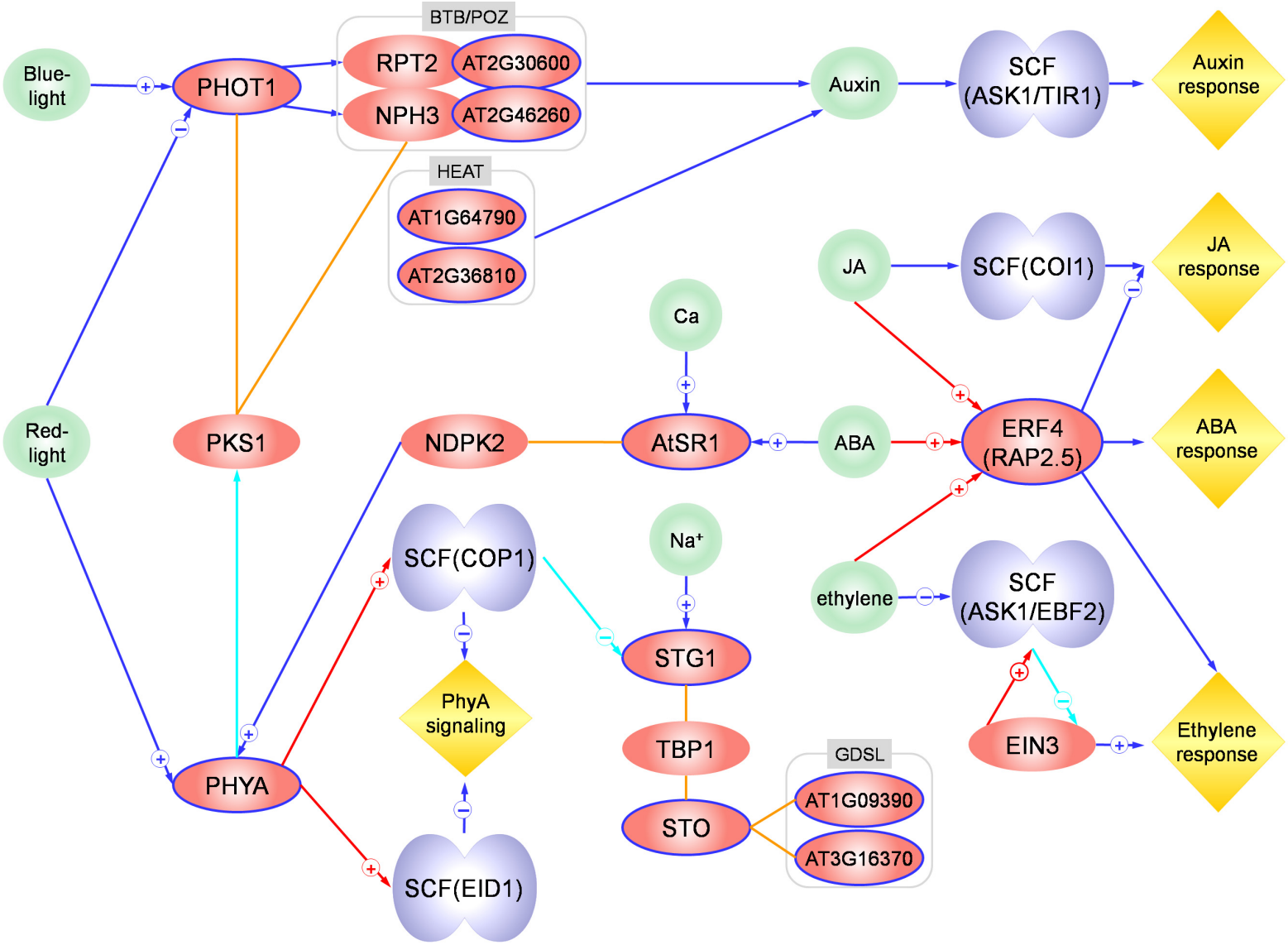
Blue-light
PHOT1
BTB/POZ
RPT2
AT2G30600
NPH3
AT2G46260
HEAT
AT1G64790
AT2G36810
Auxin
SCF (ASK1/TIR1)
Auxin response
JA
SCF(COI1)
JA response
Ca
Red-light
PKS1
NDPK2
AtSR1
ABA
ERF4 (RAP2.5)
ABA response
SCF(COP1)
Na+
ethylene
SCF (ASK1/EBF2)
PhyA signaling
STG1
TBP1
STO
GDSL
AT1G09390
AT3G16370
EIN3
Ethylene response
PHYA
SCF(EID1)

(PHYA, encoded by *AT1G09570*), another photoreceptor identified as one of the genes preferentially expressed in the young leaf. PHYA-dependent induction and phosphorylation of PKS1 by blue light suggest that PKS proteins may link two photoreceptors, phototropin and phytochrome, in phototropic responses (Fankhauser et al., 1999; Lariguet *et al*., 2006). Phytochrome A (phyA) is a cytoplasmic red/far-red light photoreceptor involved in the regulation of photomorphogenetic responses including gravitropism and phototropism (Correll *et al*., 2003) as well as de-etiolation of seedlings (Tepperman *et al*., 2006). PhyA functions as a homodimer, in which each subunit is bound to its own chromophore, and reversibly interconvertible by light. The Pr/Pr (inactive) form absorbs most strongly in the red region of the spectrum (peak absorbance at about 660 nm), and the Pfr/Pfr (active) form absorbs best in the far-red region (peak absorbance at around 730 nm). Absorption of red light by Pr/Pr dimer not only cause photoconversion to active Pfr/Pfr dimer, but also changes the subcellular location of the activated phyA, from cytosol to nucleus (Hiltbrunner *et al*., 2005; Rosler *et al*., 2007). Following light-triggered nuclear translocation, phyA regulates gene expression under continuous far-red light. PhyA in the Pr/Pr form controls the expression of a number of nuclear genes, including RuBisCO small subunit (RbcS), chlorophyll a/b binding protein, protochlorophyllide reductase, rRNA and others. It also regulates the expression of its own gene in a negative feedback mode (Kim *et al*., 2002; Ryu *et al*., 2005), and is involved in the inhibition of hypocotyl elongation, the promotion of greening, anthocyanin accumulation and flowering time regulation (Soh *et al*., 1998). PhyA acts as a positive regulator of phototropism by inhibiting gravitropism, and the optimal orientation of growth is determined by modulating the activities of the phototropin-promoting phototropism and the phytochrome- suppressing gravitropism (Lariguet and Fankhauser, 2004).

While photoconversion of Pr/Pr to Pfr/Pfr and subsequent nuclear translocation induce an array of morphogenetic responses, re-conversion of Pfr/Pfr to Pr/Pr negates the induction of those responses. Upon red light irradiation Pfr/Pfr in the nucleus is rapidly destabilized by E3 ubiquitin ligases that attache ubiquitin to the proteins, and subsequently degrade them. COP1 (CONSTITUTIVE PHOTOMORPHOGENIC 1) is an E3 ubiquitin ligase and suppresses photomorphogenesis by promoting the proteolysis of positively regulating transcription factors, thereby desensitizing phyA signals (Seo *et al*., 2003). It seems that FAR-RED ELONGATED HYPOCOTYL 1 (FHY1) and FAR-RED ELONGATED HYPOCOTYL 1-LIKE (FHL), which regulate the nuclear translocation of Pfr/Pfr, associate with and protects phyA from being recognized by COP1 and the subsequent ubiquitin-mediated proteolysis (Saijo *et al*., 2008). COP1 also interacts with STO (SALT TOLERANCE), another protein preferentially expressed in the young leaf

(discussed in the later section “4.5.3 Genes Expressed in Salt Response” on page 94). Like COP1, EMPFINDLICHER IM DUNKELROTEN LICHT 1 (EID1, encoded by *AT4G02440*), whose expression requires the presence of phyA (Buche *et al*., 2000), is a component of phyA-associated E3 ubiquitin ligase and functions as a phyA suppressor (Marrocco *et al*., 2006; Risseeuw *et al*., 2003). One of the key components of the E3 ubiquitin ligase that forms a complex with COP1 or EID1 and functions in ubiquitination and subsequent proteasomal degradation of phyA is *Arabidopsis* homolog of S-phase kinase-associated protein 1 (SKP1, encoded by *AT1G75950*). Together with CUL1, RING BOX1 (RBX1) and a F-box protein, SKP1 forms a SCF (Skp1-Cullin-F-box) E3 ubiquitin ligase complex. In the SCF complex, SKP1 functions as an adapter that associates CUL1 to the F-box protein, while F-box proteins delivers target proteins to a core that has ligase activity (Gagne *et al*., 2002). The SCF family of ubiquitin ligases targets diverse substrates for ubiquitin-dependent proteolysis, including transcription factors, signal transducers and cell cycle regulators. The functional specificity of this complex depends on the type of F-box protein (Tang *et al*., 2005). In *Arabidopsis*, almost 700 F-box proteins can be found suggesting that SCF E3 ubiquitin ligases may play a constitutive role in regulation of diverse biological processes in relation to plant physiology and development (Gagne et al., 2002).

While EID1 and COP1 function as negatively acting components in phyA-specific light signaling, NUCLEOSIDE DIPHOSPHATE KINASE 2 (NDPK2, encoded by *AT5G63310*), being activated by physical binding with phytochromes, is a positive regulatory component upstream of the phyA-mediated light signaling pathway in *Arabidopsis* (Choi *et al*., 1999; Shen *et al*., 2005). NDPK2 also interacts with a serine/threonine protein kinase, *Arabidopsis thaliana* Snf1-RELATED PROTEIN KINASE 3.15 (AtSR1), another salt tolerance-related protein preferentially expressed in the young leaf (discussed in the later section “4.5.3 Genes Expressed in Salt Response” on page 94).

4.5.2 Genes Expressed in Hormone Response

The F-box-containing proteins that participate in the formation of a SCF ubiquitin ligase complex also play a role in the ethylene signaling pathway *via* a transcription cascade involving the ETHYLENE-INSENSITIVE 3 (EIN3) and EIN3-BINDING F-BOX (EBF) protein families, which are plant-specific transcription factors. EBF1 and EBF2 proteins were shown to work coordinately in SCF complexes and degrade EIN3 to repress ethylene signaling (Gagne *et al*., 2004; Potuschak *et al*., 2003). EBF2 (encoded by *AT5G25350*), as a component of SCF E3 ubiquitin ligase complex, regulates the ethylene signaling cascade by modulating the stability of a key

transcription factor, EIN3 proteins, by means of the ubiquitination and subsequent proteasomal degradation of EIN3. Ethylene suppresses the proteolytic action SCF(EBF1/EBF2) on EIN3, and the accumulation of EIN3 proteins induces the ethylene-responsive gene expression (Potuschak *et al*., 2003). In the absence of ethylene, the level of EIN3 protein is extremely low because of SCF(EBF1/EBF2) complex that targets EIN3 for proteasome-mediated degradation (Olmedo *et al*., 2006). The mutant plants carrying the *ebf1* and *ebf2* accumulate the EIN3 protein in the absence of ethylene and show a constitutive ethylene response (Potuschak *et al*., 2003). While EIN3 is the substrate of SCF(EBF2), it is also capable of modulating the expression of *EBF2* gene, thereby fine-tune the ethylene signaling (Konishi and Yanagisawa, 2008). SCF(EBF1/EBF2) complex regulating ethylene signaling plays a role in embryogenesis and early postembryonic development, especially in cell elongation and division (Alonso and Stepanova, 2005).

While the SCF(EBF1/EBF2) complex regulates ethylene signaling pathway, another E3 ubiquitin ligase complex, SCF(TIR1), regulates auxin response (Dharmasiri *et al*., 2005). The SCF(TIR1) complex consists of ASK (*Arabidopsis* homolog of the yeast Skp1), AtCUL1 (*Arabidopsis thaliana* Cullin 1; *Arabidopsis* homolog of yeast Cdc53) and the F-box protein TIR1 (TRANSPORTER INHIBITOR RESPONSE 1) (Gray *et al*., 1999), which is the recognition component of the SCF complex coupled with the ubiquitin-proteasome proteolysis involved in auxin signaling (Walsh *et al*., 2006). In *Arabidopsis*, ASK proteins interact with F-box proteins with diverse binding specificities (Takahashi *et al*., 2004). The *Arabidopsis* SKP1 HOMOLOGUE 1 (ASK1, encoded by *AT1G75950*) is an essential component of the SCF ubiquitin ligase complex that recruits target proteins for degradation by the 26S proteasome (Wang *et al*., 2006). While a mutation in either ASK1 or TIR1 results in decreased auxin response, overexpression of TIR1 promotes auxin response, suggesting that SCF(ASK1/TIR1) is a controlling factor for auxin response (Gray *et al*., 1999). TIR1 has been shown to be also a receptor for the synthetic auxin IAA and 2,4-D (Walsh *et al*., 2006). Another SCF E3 ubiquitin ligase complex, SCF(COI1), which regulates signal transduction in response to jasmonates, was preferentially expressed in the young leaf. CORONATINE INSENSITIVE 1 (COI1, encoded by *AT2G39940*) associates with AtCUL1, AtRBX1, and either of the *Arabidopsis* SKP1 homologue proteins (ASK1 or ASK2) to assemble ubiquitin-ligase complexes, which are required for jasmonate (JA) response in *Arabidopsis* (Xu *et al*., 2002).

Another set of hormone-responsive transcription factors was expressed preferentially in the young leaf: RAP2.5 (also known as AtERF4, encoded by *AT3G15210*) and RAP2.12 (encoded by *AT1G53910*). RELATED TO APETALA 2 PROTEIN (RAP2) proteins are members of the AP2

(APETALA2)/EREBP (ethylene-responsive element binding proteins) transcription factor family, which are found exclusively in plants. AP2/EREBP family is divided into two subfamilies based on the number of AP2 domains included: AP2 and EREBP. The members of AP2 subfamily contain two AP2 domains, where as EREBPs contain only one AP2 domain. RAP2.5 and RAP2.12 belong to EREBP subfamily (Okamuro *et al*., 1997). AtERFs (*Arabidopsis* RAP2s) act as a transcriptional repressor binding to the GCC- box, which is found in the promoters of the genes related to pathogenesis (Fujimoto *et al*., 2000; Hao *et al*., 1998). The repression domain in AtERFs has the same motif as those in the plant zinc finger proteins that function as transcriptional repressors (Ohta *et al*., 2001). AtERFs are involved in the regulation of gene expression in response to stress by regulating components of stress signal transduction pathways, including other AtERFs. The expression of AtERF4 can be induced by abscisic acid (ABA), ethylene and jasmonic acid (JA), and it is suggested that AtERF4 is a transcriptional repressor that modulates ethylene and abscisic acid responses (Yang *et al*., 2005) and JA-responsive defense gene expression against the fungal pathogen *Fusarium oxysporum* (McGrath *et al*., 2005). Since the expression of AtERFs is regulated not only by ethylene but also by other signals from the ABA and the JA pathways, it is suggested that AtERFs function as transcription factors that integrate signals from multiple signaling pathways through transcriptional and post-transcriptional regulation (Shinshi, 2008).

4.5.3 Genes Expressed in Salt Response

In the young leaf of *H. helix*, calcium-interacting kinase was preferentially expressed. *Arabidopsis thaliana* SNF1-RELATED PROTEIN KINASE 3.15 (AtSR1, encoded by *AT5G01820*), also known as CBL-INTERACTING SERINE/THREONINE-PROTEIN KINASE 14 (CIPK14 or PKS24), has activity of serine/threonine protein kinase and is known to be involved in signal transduction in response to abiotic stimuli, such as abscisic acid, salt stress and exogenous calcium ion (Chikano *et al*., 2001; Nozawa *et al*., 2001). CIPKs belong to the sucrose non-fermenting-1 (SNF1)-related protein kinase subfamily 3 (SnRK3), interacting with calucineurin B-like proteins (CBL) (Hrabak *et al*., 2003; Nozawa *et al*, 2003). Calcineurin (CaN) is a Ca^{2+}- and calmodulin-dependent protein phosphatase (PP2B) that is an integral intermediate of a signal transduction pathway that modulates salt tolerance in yeast (Pardo *et al*., 1998). In plants, intracellular calcium signaling through a calcineurin-mediated pathway seems to convey beneficial effects of calcium in salt tolerance (Liu and Zhu, 1998). CIPKs specifically interact with the CBLs, which function as calcium sensors. When a CBL protein binds the regulatory NAF domain of CIPK protein, the kinase becomes activated in a calcium/calmodulin-dependent

manner (Albrecht *et al*., 2001). CIPK proteins play a key role in the salt-tolerance pathway that regulates the compartmentalization or sequestration of Na^+ in plant cells (Kim *et al*., 2007). CIPK proteins also facilitate salt export across membrane by interacting with the vacuolar H^+-ATPase and up-regulating its transport activity (Batelli *et al*., 2007). Exogenous calcium affects the transcription of an *Arabidopsis* CIPK gene, *AtSR1*, under abscisic acid and salt treatments, and it appears that calcium ions work upstream *AtSR1* to regulate the plant response to ABA and salt stress. It was shown that calcium-binding protein and protein kinase serve as the co-regulators in the regulation of plant responses to stresses, such as salt and ABA stimuli. (Qin et al., 2008). AtSR1 was also induced by metabolic sugars (Lee *et al*., 2005) and illumination of leaves (Nozawa *et al*, 2001), suggesting its involvement in multiple signal transduction pathways. AtSR1 also interacts with another kinase NDPK2 (encoded by *AT5G63310*), which has been shown to be involved in multiple signaling pathways including phytochrome and auxin signaling (described in the previous section on page 92). Interaction of AtSR1 with NDPK2, which also interacts with phytochrome A, suggests that AtSR1 and NDPK2 it could be a point of connection between salt stress and phytochrome-mediated signaling pathways in *Arabidopsis thaliana* (Verslues *et al*., 2007).

Another salt stress-related gene that was expressed preferentially in the young leaf of *H. helix* was SALT TOLERENCE (STO, encoded by *AT1G06040*), which is a putative transcription factor able to modulate Ca^{2+} signaling in yeast and confers salt tolerance to cells (Lippuner *et al*., 1996). STO interacts with COP1, which is a component of E3 ubiquitin ligase complex that acts as a suppressor of photomorphogenesis by controlling the degradation of positively acting transcription factors and their target gene expression (Ma *et al*., 2002), suggesting a possible link between a repressor of light-dependent signals and a downstream target of Ca^{2+} (Holm *et al*., 2001). COP1 actively suppresses the transcription of STO and destabilize the protein in the dark, whereas light promotes the accumulation of STO during the de-etiolation process, indicating that STO is also involved in light signaling (Indorf *et al*., 2007). STO also interacts with a GDSL lipase (encoded by *AT1G09390* or *AT3G16370*), a member of hydrolytic enzyme family containing GDSL-motif, a consensus catalytic residues glycine (G), aspartic acid (D), serine (S) and leucine (L) around the active site serine (Akoh *et al*., 2004). GDSL lipases, which have carboxylesterase activity acting on ester bonds, are involved in glycerol biosynthetic process and lipid metabolic process in the chloroplast stroma, and increase salt tolerance when overexpressed in yeast and transgenic plants (Naranjo *et al*., 2006). Sequence analysis indicates that GDSL lipases are functionally involved in multiple physiological processes including seed germination, flowering and defense

reactions against pathogenic organisms (Ling *et al*., 2006; Ling, 2008).

In the young leaf of *H. helix*, another salt stress-related gene was preferentially expressed: SALT TOLERANCE DURING GERMINATION 1 (STG1, encoded by *AT4G31720*). STG1 is a putative *Arabidopsis* TATA box-binding protein (TBP)-associated factor, which constitutes the transcription factor IID (TFIID) complex (Gao *et al*., 2006). The multisubunit protein complex TFIID is composed of a TATA binding protein (TBP) and a group of TBP-associated factors (TAFs), which are required for recognition of promoter and the nucleation of the RNA polymerase II transcriptional pre-initiation complex (Cler *et al*., 2009; Heard *et al*., 1993; Ozer *et al*., 1996). While overexpression of STG1 in *Arabidopsis* seeds improves salt tolerance during germination, loss-of-function mutant becomes more sensitive to salt stress, indicating that the transcription initiation factor is playing a role in the physiological response to salt toxicity in plants. In addition, the *stg1* mutant maintains a higher K^+/Na^+ ratio and accumulates than the wild-type under salt stress condition, suggesting that the STG1-related salt tolerance mechanism also involves the regulation of ion homeostasis (Gao *et al*., 2006). Both STO and STG1 interact with an H-protein promoter binding factor (HPPBF-1), also known as *Arabidopsis thaliana* TELOMERIC DNA-BINDING PROTEIN 1 (AtTBP1), which has a Myb telomeric DNA binding domain and its gene expression is induced by salt stress, suggesting STO, STG1 and HPPBF-1 together play a role in regulation of the response to salt stress (Nagaoka and Takano, 2003). However, since the *H. helix* plants used in this study were not under stress condition, detection of these salt stress-related genes expressed at a high level in the young leaf may indicate that their roles are not limited within salt stress-related signalling pathways. It appears that the actions of these stress-related genes are possibly involved in light-response signaling as well. This is similar to AtSR1, which interacts with light-signaling phytochrome A *via* the action of NDPK2. Also, STG1 is regulated by the proteolytic action of SCF(COP1), in which the expression of the COP1 protein component is positively regulated by the phytochrome A.

4.5.4 Genes Involved in Cell Proliferation

Microarray analysis detected genes expressed preferentially in the young leaf, which are involved in cell cycle control mediated by environmental or hormonal signals. *AT1G18040* encodes CYCLIN-DEPENDENT KINASE D1;3 (CDKD1;3), which is involved in activation of cell proliferation (Shimotohno *et al*., 2003). To become operative, CDKs bind specific cyclin partners, and the enzymatic activity of cyclin-CDK complexes is further regulated by the synthesis and degradation of cyclin subunits, binding to inhibitory proteins, and the phosphorylation of CDKs by

CDK-activating kinases (CAKs) (Morgan,1997). Two distinct classes of CAK have been identified in plants: CDKD and CDKF. CDKD is functionally similar to mammalian CAKs, whereas CDKF is a plant-specific CAK having unique enzymatic activities (Inzé and De Veylder, 2006). In *Arabidopsis*, CDKFs phosphorylate and activate CDKDs, suggesting that CDKD and CDKF are together components of a phosphorylation cascade involved in the control the cell cycle and transcription (Shimotohno *et al*., 2004; Umeda *et al*., 2005).

AT2G01450 encodes AtMPK17 (*Arabidopsis thaliana* MITOGEN-ACTIVATED PROTEIN KINASE 17), a member of mitogen-activated protein kinase (MAPK) family. This protein family has protein amino acid phosphorylation activity and constitute protein phosphorylation cascades that link various biotic and a biotic stimuli or hormonal signal to a wide range of cellular processes, including cell division and growth (MAPK Group, 2002). AtMPK4, one of *Arabidopsis* MAPKs, appears to promote salicylic acid-mediated defense and suppress jasmonic acid-induced responses (Petersen *et al*., 2000), whereas the tobacco ortholog of *Arabidopsis* MPK6, which is termed SIPK (salicylate-induced protein kinase), appears to positively regulate programmed cell death in response to pathogenic stress (Yang et al., 2001). Due to lack of MAPK mutant plants, probably because of their essential role in plant cell cycle, functions of most MAPKs in plant are largely unknown (Innes, 2001). And, the molecular function of the AtMPK17, which was preferentially expressed in *H. helix* young leaf, could not be precisely predicted. *AT3G27010* encodes a transcription factor TCP20, which belongs to a TCP (Teosinte-branched 1, Cycloidea, PCNA factor) transcription factor protein family. Members of this family contain a basic-helix-loop-helix (bHLH) domain involved in DNA binding. This protein specifically binds to sites in the promoter region of the PCNA (plant proliferating cellular nuclear antigen), an auxiliary protein of DNA polymerase δ, and the promoters of cyclin CYCB1;1 and ribosomal protein genes, regulating expression of cell cycle control and ribosomal genes (Kosugi and Ohashi, 1997; Trémousaygue *et al*., 2003). TCP20 is thought to link regulation of growth and cell division control pathways, by positively and negatively interacting with the promoters of cyclin CYB1;1 (Li *et al*., 2005a).

Along with the genes involved in cell cycle control, another gene which indicated an active cell growth in the young leaf was also detected. *AT2G06850* encodes XYLOGLUCAN ENDOTRANSGLUCOSYLASE/HYDROLASE 4 (AtXTH4 or XTH-4), which has hydrolase/ transferase activity on glycosyl bonds and catalyzes xyloglucan endohydrolysis (XEH) and/or endotransglycosylation (XET) (Rose *et al*., 2002). Xyloglucan is an essential polymer constituting the primary cell wall. The stands of xyloglucan bind firmly to the surface of individual cellulose microfibrils, and cross-linking them into a polysaccharide network of the cell wall. The XETs can

cleaves and religates xyloglucan strands, and thereby regulating the physical properties of the cell wall of growing tissues. The cleavage and re-ligation of xyloglucan strands are considered to play the major role in the course of wall expansion and, therefore, cell growth and differentiation (Nishitani and Tominaga, 1992), which are the major processes actively occurring in the young developing leaves. The members of xyloglucan endoxyloglucan transferase gene family are expressed differentially in response to environmental and hormonal stimuli, suggesting that cells may differentially recruit these cell wall-modifying enzymes, thereby change the properties of cell walls during development in response to the environmental condition (Xu *et al*., 1996). The endoxyloglucan transferase genes are known to be predominantly expressed in young developing tissues (Akamatsu *et al*., 1999).

4.5.5 Genes Involved in Carbon Assimilation

In the young leaf, genes involved in the organization of photosynthetic apparatus and carbon utilization by fixation of carbon dioxide appeared to be expressed preferentially to the shoot apex. RuBisCO (Ribulose Bisphosphate Carboxylase/Oxygenase), key enzyme in photosynthesis and photorespiration, catalyzes two types of reactions: the carboxylation and oxygenation of D-ribulose 1,5-bisphosphate. Both reactions occur competitively at the same active site and on the same substrate. Carboxylation reaction, the primary step in carbon dioxide fixation, yields two molecules of 3-phosphoglycerate (3-PGA) in the reductive photosynthetic carbon cycle, and the oxygenation reaction yields one molecule of 3-PGA and one of 2-phosphoglycolate in the oxidative photosynthetic carbon cycle (or photorespiratory carbon oxidation cycle). RuBisCO is a multi-protein enzyme, and the small subunit is encoded in nuclear DNA and translated on cytoplasmic ribosomes, while the large subunit is encoded in chloroplast DNA and translated on chloroplast ribosomes. The multigene family encoding the small subunit polypeptides of *Arabidopsis* RuBisCO consists of four genes and divided into two subfamilies based on DNA and amino acid sequence similarities (Krebbers *et al*., 1988). *AT1G67090* and *AT5G38430*, which were preferentially expressed in the young leaf of *H. helix*, encode RuBisCO small subunit (RbcS) 1A and 1B, respectively (Rutschow *et al*., 2008; Sawchuk *et al*., 2008).

AT3G62410 encodes CHLOROPLAST PROTEIN 12-2 (CP12-2), a small regulatory peptide found in the chloroplast stroma (Rutschow *et al*., 2008). It belongs to the CP12 gene family, which are playing a regulatory role in Calvin cycle. Two CP12 molecules act as scaffold elements, each interacts with glyceraldehyde-3-phosphate dehydrogenase (GAPDH) and phosphoribulokinase (PRK), respectively, to form a ternary supramolecular complex functioning in the Calvin cycle

(Marri, *et al*, 2005). CP12 has no enzymatic activity, but it changes conformation of the complex depending on redox conditions and effectively regulates the enzyme activities of GAPDH and PRK in the Calvin cycle (Marri, *et al*, 2005; Singh *et al*., 2008). *AT4G12800* encodes chloroplastic photosystem I reaction center subunit L (PSI-L), a structural constituent of photosystem I, which carries out the light reaction of photosynthesis (Ferro et al., 2003). *Arabidopsis thaliana* plants lacking the PSI-L subunit of photosystem I showed a decreased performance in photosynthesis in general (Lunde et al., 2003).

In the young leaf of *H. helix*, a chloroplast-targeted enzyme, ferredoxin-$NADP^+$-oxidoreductase (FNR), was expressed higher than in the shoot apex. In *Arabidopsis thaliana*, FNR exists as two isoforms, LEAF FNR1 (AtLFNR1) and AtLFNR2, which are encoded by the genes *AT5G66190* and *AT1G20020*, respectively. In the young leaf of *H. helix*, the AtLFNR1 was detected, but not AtLFNR2. Ferredoxin, located in the chloroplast stroma, transfers electrons to $NADP^+$ by way of FNR, attached to the chloroplast membrane. Ferredoxin and FNR form a complex and plays a key role in regulating the electron flow to modulate the production of ATP and reducing power. It is suggested that AtLFNR1 is involved in photosystem I-dependent cyclic electron flow, and required for membrane attachment of FNR (Lintala et al., 2007).

4.5.6 Genes Putatively Involved in Variegation Pattern Formation

Hedera helix cv. Goldheart has very stable and predictable variegation patterns with the white sectors appearing in the middle of the leaves. It is a chimeric variegation, where the mutation is localized in the cells of L3 layer of the shoot apical meristem, from which the middle section of the leaf tissue is derived (Tilney-Bassett, 1986). The white sectors are made of viable cells that have plastids arrested in thylakoid formation due to a mutation in nuclear gene (Manenti and Tedesco, 1971). For proper development of chloroplast in plants, both nuclear and chloroplastic transcripts are required to be accumulated to a certain level in the chloroplast. In the white sector of a variegated *A. thaliana*, the plastid accumulates normal levels of chloroplast transcripts, where as the expression of nuclear-encoded photosynthetic genes is substantially suppressed (Kato *et al*., 2007). In *A. thaliana*, membrane-anchored ATP-dependent metalloproteases, FtsHs, plays important roles in the formation of thylakoid membranes (Sakamoto *et al*., 2003) and the PSII repair cycle (Sakamoto *et al*., 2004). In *Arabidopsis thaliana* chloroplast, nine FtsH isomers are localized in thylakoid membranes as a heterocomplex formed by a pair of isomers, including FtsH1/5 and FtsH2/8 (Sakamoto *et al*., 2003; Yu *et al*., 2004; Zaltsman *et al*., 2005). Mutations in FtsH5 or FtsH2 in *Arabidopsis* result in variegation mutant *var1* or *var2* with green-and white-

sectored leaves (Yu *et al*., 2004; 2005), whereas in loss-of-function mutants of other chloroplast FtsH isomers do not show variegation phenotypes (Chen *et al*., 2000; Sakamoto *et al*., 2003). It is suggested that the leaf variegation in *Arabidopsis* is affected by the stable role of FtsH in the PSII repair cycle and the formation of thylakoid membranes, as well as the balance between the synthesis and degradation of chloroplast proteins (Miura *et al*., 2007).

Cross-species hybridization of *H. helix* targets onto *A. thaliana* microarray probes detected one of the FtsH protein isomers expressed preferentially in the young leaf of *H. helix*. *AT3G02450* encodes FtsH6 (FtsH protease 6), which is one of nine isomers of chloroplast-localized FtsH (Adam *et al*., 2001; Adam and Ostersetzer, 2001; Adam and Clarke, 2002). Its reported biochemical activities include degradation of unassembled chloroplastic complexes or oxidatively damaged and nonfunctional membrane proteins (Ostersetzer and Adam, 1997; Lindahl *et al*., 2000) as well as the light-harvesting complex II during high-light acclimation and senescence (García-Lorenzo *et al*., 2005; Żelisko *et al*., 2005). Two other gene products, which are involved in the degradation of chloroplastic proteins appeared to be preferentially expressed in the young leaf of *H. helix*. ACCELERATED CELL DEATH 1 (ACD1, encoded by *AT3G44880*) and ACCELERATED CELL DEATH 1-LIKE (ACD1-LIKE, encoded by *AT4G25650*) are *Arabidopsis thaliana* homologues of Pheophorbide alpha Oxygenase (PaO), an iron-containing, ferredoxin-dependent monooxygenase, which is involved in chloroplastic protein degradation (Tanaka *et al*., 2003). PaO plays a major role in metabolization of chlorophyll during senescence by cleaving the ring structure of pheophorbide alpha (Pruzinská *et al*., 2005). When the expression of ACD1 or ACD1-LIKE in the leaf is suppressed, the pheophorbide alpha, which is the degradation product of chlorophyll a, accumulates and causes cell death (Tanaka *et al*., 2003).

While the chlorophyll-lacking white sectors, which result from mutations in *FtsH* genes, are occurring randomly in the leaves of the *Arabidopsis* variegated mutants, the white sectors in the variegated leaves of *H. helix* cv. Goldheart are entirely composed of the cells, of which lineage can be traced back to the apical cells in the specific SAM layer (L3), which have the nuclear gene mutation. Thus, the *H. helix* homolog of *Arabidopsis thaliana* FtsH6, together with chloroplast proteolytic enzyme (PaO), which was also preferentially expressed in the young variegated leaves, may play a role in ‘cleaning up’ the unassembled or incomplete photosynthetic apparatus in the cells of the white sector.

SUMMARY

Transcriptomes from the shoot apex and the young leaf of *Hedera helix* cv. Goldheart were compared using a microarray-based cross-species hybridization technique. Fluorescently labeled target cDNAs from the shoot apex and the young leaf of *H. helix* were hybridized on *Arabidopsis thaliana* cDNA microarrays. Twenty-three percent of the EST (expressed sequence tag) spots on the *Arabidopsis* microarray were successfully hybridized to the mRNA transcripts from the *H. helix* shoot apices and young leaves with the fluorescence intensities above the background level. Considering the phylogenetic distance between the probe and the target species, the hybridization efficiency compared favorably to the published results from the heterologous hybridization experiments.

Among the genes that showed differential expression levels in the shoot apex or in the young leaf of *H. helix* satisfying the statistical criteria (*p* value cutoff = 0.05 with Benjamini and Hochberge FDR), 174 genes (60 in the shoot apex and 114 in the young leaf) were identified as being statistically differentially expressed two-fold or more when the transcriptomes of the shoot apex and the young leaf of *H. helix* cv. Goldheart were compared.

The preferentially expressed genes in the two tissue samples differed in several respects. The genes that were expressed preferentially in the shoot apex represented transcripts that appeared to be more closely linked to cytoskeletal organization and phase change, whereas those in the young leaf appeared more related to cell and energy-related metabolism, such as the photosynthesis dark reactions, aerobic respiration and carbohydrate catabolism. Perhaps the differences were a reflection of the transcription of the undifferentiated or less differentiated state of the shoot apex and the fully differentiated state of the young leaf. SAM-specific genes were not detected in this study. Probably, the spot intensity levels of the features hybridized by the probes represented by the SAM-specific genes were not high enough above the background to be considered statistically significant due to the significantly smaller proportion of SAM tissue compared to the leaf primordia. In addition, as many of the SAM-specific genes are regulatory components, they probably do not require abundant transtripts for thier functions.

To verify the functions of the genes, which were inferred based on the sequence similarity and annotated functions of their *Arabidopsis* homologs, subsequent studies are suggested: 1) genes identified in this study are to be sequenced to determine the level of homology; 2) expression domains of the genes to be localized in the tissue (*e.g. in situ* hybridization); 3) loss-/gain-of-function mutagenetic studies to identify the function of the gene of interest in *H. helix* plants.

REFERENCES

Adam, Z., I. Adamska, K. Nakabayashi, O. Ostersetzer, K. Haussuhl, A. Manuell, B. Zheng, O. Vallon, S.R. Rodermel, K. Shinozaki, and A.K. Clarke. 2001. Chloroplast and mitochondrial proteases in *Arabidopsis*. A proposed nomenclature. *Plant Physiol.* 125:1912-1918.

Adam, Z., and A.K. Clarke. 2002. Cutting edge of chloroplast proteolysis. *Trends Plant Sci.* 7:451-456.

Adam, Z., and O. Ostersetzer. 2001. Degradation of unassembled and damaged thylakoid proteins. *Biochem. Soc. Trans.* 29:427-430.

Adjaye, J., R. Herwig, D. Herrmann, W. Wruck, A. Benkahla, T.C. Brink, M. Nowak, J.W. Carnwath, C. Hultschig, H. Niemann, and H. Lehrach. 2004. Cross-species hybridisation of human and bovine orthologous genes on high density cDNA microarrays. *BMC Genomics*. 5:83.

Agilent Technologies Inc. 2008. *Agilent GeneSpring GX User Manual*. Agilent Technologies, Inc. Santa Clara, CA. (http://www.chem.agilent.com/Library/usermanuals/Public/GeneSpring-manual.pdf).

Akamatsu, T., Y. Hanzawa, Y. Ohtake, T. Takahashi, K. Nishitani, and Y. Komeda. 1999. Expression of endoxyloglucan transferase genes in *acaulis* mutants of *Arabidopsis*. *Plant Physiol.* 121:715-722.

Akoh, C.C., G.C. Lee, Y.C. Liaw, T.H. Huang, and J.F. Shaw. 2004. GDSL family of serine esterases/lipases. *Prog. Lipid Res.* 43:534-552.

Alba, R., Z. Fei, P. Payton, Y. Liu, S.L. Moore, P. Debbie, J. Cohn, M. D'Ascenzo, J.S. Gordon, J.K. Rose, G. Martin, S.D. Tanksley, M. Bouzayen, M.M. Jahn, and J. Giovannoni. 2004. ESTs, cDNA microarrays, and gene expression profiling: tools for dissecting plant physiology and development. *Plant J.* 39:697-714.

Albrecht, V., O. Ritz, S. Linder, K. Harter, and J. Kudla. 2001. The NAF domain defines a novel protein-protein interaction module conserved in $Ca2^{+}$-regulated kinases. *EMBO J.* 20:1051-1063.

Alonso, J.M., and A.N. Stepanova. 2005. Ethylene signaling pathway. *Sci. STKE*. 2005:cm3.

Anderson, M.L.M. 1995. Hybridization strategy. In: *Gene Probes: A Practical Approach*. Vol. 2. B.D. Hames and S.J. Higgins, Eds. IRL Press at Oxford University Press. Oxford, NY. 1-29.

Arabidopsis Genome Initiative. 2000. Analysis of the genome sequence of the flowering plant *Arabidopsis thaliana*. *Nature*. 408:796-815.

Bagnaresi, P., A. Moschella, O. Beretta, F. Vitulli, P. Ranalli, and P. Perata. 2008. Heterologous microarray experiments allow the identification of the early events associated with potato tuber cold sweetening. *BMC Genomics*. 9:176.

Ball, E. 1960. Sterile culture of the shoot apex of *Lupinus albus*. *Growth*. 24:91-110.

Ball, E.A. 1974. Experimental observations on the living shoot apex. *Rev. Cytol. et Biol. Vég.* 37:353-370.

Bar-Or, C., M. Bar-Eyal, T.Z. Gal, Y. Kapulnik, H. Czosnek, and H. Koltai. 2006. Derivation of species-specific hybridization-like knowledge out of cross-species hybridization results. *BMC Genomics*. 7:110.

Bar-Or, C., H. Czosnek, and H. Koltai. 2007a. Cross-species microarray hybridizations: a developing tool for studying species diversity. *Trends Genet.* 23:200-207.

Bar-Or, C., E. Novikov, A. Reiner, H. Czosnek, and H. Koltai. 2007b. Utilizing microarray spot characteristics to improve cross-species hybridization results. *Genomics*. 90:636-645.

Barton, M.K., and R.S. Poethig. 1993. Formation of the shoot apical meristem in *Arabidopsis thaliana*: an analysis of development in the wild type and in the shoot meristemless mutant. *Development*. 119:823-831.

Baskin, T.I., and J.E. Wilson. 1997. Inhibitors of protein kinases and phosphatases alter root morphology and disorganize cortical microtubules. *Plant Physiol.* 113:493-502.

Batelli, G., P.E. Verslues, F. Agius, Q. Qiu, H. Fujii, S. Pan, K.S. Schumaker, S. Grillo, and J.K. Zhu. 2007. SOS2 promotes salt tolerance in part by interacting with the vacuolar H^+-ATPase and upregulating its transport activity. *Mol. Cell. Biol.* 27:7781-7790.

Bäurle, I., and T. Laux. 2003. Apical meristems: the plant's fountain of youth. *Bioessays*. 25:961-970.

Baxter-Burrell, A., Z. Yang, P.S. Springer, and J. Bailey-Serres. 2002. RopGAP4-dependent Rop GTPase rheostat control of *Arabidopsis* oxygen deprivation tolerance. *Science*. 296:2026-2028.

Bayer, E., C. Thomas, and A. Maule. 2008. Symplastic domains in the *Arabidopsis* shoot apical meristem correlate with PDLP1 expression patterns. *Plant Signal. Behav.* 3:853-855.

Becher, M., I.N. Talke, L. Krall, and U. Kramer. 2004. Cross-species microarray transcript profiling reveals high constitutive expression of metal homeostasis genes in shoots of the zinc hyperaccumulator *Arabidopsis halleri*. *Plant J.* 37:251-268.

Benjamini, Y., and Y. Hochberg. 1995. Controlling the false discovery rate: a practical and powerful approach to multiple testing. *J. R. Stat. Soc. Series B Stat. Methodol.* 57:289-300.

Berardini, T.Z., S. Mundodi, L. Reiser, E. Huala, M. Garcia-Hernandez, P. Zhang, L.A. Mueller, J. Yoon, A. Doyle, G. Lander, N. Moseyko, D. Yoo, I. Xu, B. Zoeckler, M. Montoya, N. Miller, D. Weems, and S.Y. Rhee. 2004. Functional annotation of the *Arabidopsis* genome using controlled vocabularies. *Plant Physiol.* 135:745-755.

Bolstad, B.M., R.A. Irizarry, M. Astrand, and T.P. Speed. 2003. A comparison of normalization methods for high density oligonucleotide array data based on variance and bias. *Bioinformatics*. 19:185-193.

Bouche, N., and D. Bouchez. 2001. *Arabidopsis* gene knockout: phenotypes wanted. *Curr. Opin. Plant Biol.* 4:111-117.

Bowman, J.L., and S.K. Floyd. 2008. Patterning and polarity in seed plant shoots. *Annu. Rev. Plant Biol.* 59:67-88.

Brand, U., M. Grunewald, M. Hobe, and R. Simon. 2002. Regulation of *CLV3* expression by two homeobox genes in Arabidopsis. *Plant Physiol.* 129:565-575.

Brand, U., M. Hobe, and R. Simon. 2001. Functional domains in plant shoot meristems. *Bioessays*. 23:134-141.

Briggs, W.R., and J.M. Christie. 2002. Phototropins 1 and 2: versatile plant blue-light receptors. *Trends Plant Sci.* 7:204-210.

Brown, J.A.M., J.P. Miksche, and H.H. and Smith. 1964. An analysis of ^{3}H-thymidine distribution throughout the vegetative meristem of *Arabidopsis thaliana* (L.) Heynh. *Radiat. Bot.* 4:107-113.

Brunstein, F.C., and D.K. Yamaguchi. 1992. The oldest known Rocky Mountain bristlecone pines (*Pinus aristata* Engelm.). *Arct. Alp. Res.*:253-256.

Buche, C., C. Poppe, E. Schafer, and T. Kretsch. 2000. *eid1*: a new *Arabidopsis* mutant hypersensitive in phytochrome A-dependent high-irradiance responses. *Plant Cell*. 12:547-558.

Büche, C., C. Poppe, E. Schafer, and T. Kretsch. 2000. eid1: a new Arabidopsis mutant hypersensitive in phytochrome A-dependent high-irradiance responses. *Plant Cell*. 12:547-558.

Buckley, B.A. 2007. Comparative environmental genomics in non-model species: using heterologous hybridization to DNA-based microarrays. *J. Exp. Biol.* 210:1602-1606.

Buvat, R. 1952. Structure, évolution et fonctionnement du méristeme apical de quelques dicotylédones. *Ann. Sci. Nat. Botan. et. Biol. Vgtale, IIe Sr.* 13:199-300.

Buvat, R. 1955. Le méristème apical de la tige. *Annê. Biol.* 31:595-656.

Byrne, M.E., J. Simorowski, and R.A. Martienssen. 2002. *ASYMMETRIC LEAVES1* reveals *knox* gene redundancy in *Arabidopsis*. *Development*. 129:1957-1965.

Camilleri, C., J. Azimzadeh, M. Pastuglia, C. Bellini, O. Grandjean, and D. Bouchez. 2002. The *Arabidopsis TONNEAU2* gene encodes a putative novel protein phosphatase 2A regulatory subunit essential for the control of the cortical cytoskeleton. *Plant Cell*. 14:833-845.

Carles, C.C., and J.C. Fletcher. 2003. Shoot apical meristem maintenance: the art of a dynamic balance. *Trends Plant Sci.* 8:394-401.

Castilho, P.C., B.A. Buckley, G. Somero, and B.A. Block. 2009. Heterologous hybridization to a complementary DNA microarray reveals the effect of thermal acclimation in the endothermic bluefin tuna (*Thunnus orientalis*). *Mol. Ecol.*

Chen, M., Y. Choi, D.F. Voytas, and S. Rodermel. 2000. Mutations in the *Arabidopsis VAR2* locus cause leaf variegation due to the loss of a chloroplast FtsH protease. *Plant J.* 22:303-313.

Chen, M., J. Chory, and C. Fankhauser. 2004. Light signal transduction in higher plants. *Annu. Rev. Genet.* 38:87-117.

Cheng, Y., X. Dai, and Y. Zhao. 2004. AtCAND1, a HEAT-repeat protein that participates in auxin signaling in *Arabidopsis*. *Plant Physiol.* 135:1020-1026.

Cheng, Y., G. Qin, X. Dai, and Y. Zhao. 2007. NPY1, a BTB-NPH3-like protein, plays a critical role in auxin-regulated organogenesis in *Arabidopsis*. *Proc. Natl. Acad. Sci. U.S.A.* 104:18825-18829.

Chikano, H., M. Ogawa, Y. Ikeda, N. Koizumi, T. Kusano, and H. Sano. 2001. Two novel genes encoding SNF-1 related protein kinases from *Arabidopsis thaliana*: differential accumulation of *AtSR1* and *AtSR2* transcripts in response to cytokinins and sugars, and phosphorylation of sucrose synthase by AtSR2. *Mol. Gen. Genet.* 264:674-681.

Choi, G., H. Yi, J. Lee, Y.K. Kwon, M.S. Soh, B. Shin, Z. Luka, T.R. Hahn, and P.S. Song. 1999. Phytochrome signalling is mediated through nucleoside diphosphate kinase 2. *Nature*. 401:610-613.

Christie, J.M., M. Salomon, K. Nozue, M. Wada, and W.R. Briggs. 1999. LOV (light, oxygen, or voltage) domains of the blue-light photoreceptor phototropin (nph1): binding sites for the chromophore flavin mononucleotide. *Proc. Natl. Acad. Sci. U.S.A.* 96:8779-8783.

Clark, S.E. 1997. Organ formation at the vegetative shoot meristem. *Plant Cell*. 9:1067-1076.

Clark, S.E., S.E. Jacobsen, J.Z. Levin, and E.M. Meyerowitz. 1996. The *CLAVATA* and *SHOOT MERISTEMLESS* loci competitively regulate meristem activity in *Arabidopsis*. *Development*. 122:1567-1575.

Clark, S.E., M.P. Running, and E.M. Meyerowitz. 1993. *CLAVATA1*, a regulator of meristem and flower development in *Arabidopsis*. *Development*. 119:397-418.

Clark, S.E., R.W. Williams, and E.M. Meyerowitz. 1997. The *CLAVATA1* gene encodes a putative receptor kinase that controls shoot and floral meristem size in *Arabidopsis*. *Cell*. 89:575-585.

Clement-Ziza, M., D. Gentien, S. Lyonnet, J.P. Thiery, C. Besmond, and C. Decraene. 2009. Evaluation of methods for amplification of picogram amounts of total RNA for whole genome expression profiling. *BMC Genomics*. 10:246.

Cler, E., G. Papai, P. Schultz, and I. Davidson. 2009. Recent advances in understanding the structure and function of general transcription factor TFIID. *Cell. Mol. Life Sci.* 66:2123-2134.

Clouse, S.D. 2008. The molecular intersection of brassinosteroid-regulated growth and flowering in *Arabidopsis*. *Proc. Natl. Acad. Sci. U.S.A.* 105:7345-7346.

Clowes, F.A.L. 1961. Apical meristems. In: *Botanical Monographs*. Blackwell Scientific Publications. Oxford. 217 p.

Correll, M.J., K.M. Coveney, S.V. Raines, J.L. Mullen, R.P. Hangarter, and J.Z. Kiss. 2003. Phytochromes play a role in phototropism and gravitropism in *Arabidopsis* roots. *Adv. Space Res.* 31:2203-2210.

Corson, G., and E. Gifford. 1969. Histochemical studies of the shoot apex of *Datura stramonium* during transition to flowering. *Phytomorphol.* 19:189-196.

Cutter, E.G. 1965. Recent experimental studies of the shoot apex and shoot morphogenesis. *Bot. Rev.* 31:7-113.

Dharmasiri, N., S. Dharmasiri, D. Weijers, E. Lechner, M. Yamada, L. Hobbie, J.S. Ehrismann, G. Jurgens, and M. Estelle. 2005. Plant development is regulated by a family of auxin receptor F box proteins. *Dev. Cell*. 9:109-119.

Doerner, P. 1999. Shoot meristems: Intercellular signals keep the balance. *Curr. Biol.* 9:R377-380.

Domagalska, M.A., F.M. Schomburg, R.M. Amasino, R.D. Vierstra, F. Nagy, and S.J. Davis. 2007. Attenuation of brassinosteroid signaling enhances *FLC* expression and delays flowering. *Development*. 134:2841-2850.

Drăghici, S. 2003. *Data Analysis Tools for DNA Microarrays*. Chapman & Hall/CRC. Boca Raton. 517 pp.

Dudoit, S., Y.H. Yang, M.J. Callow, and T.P. Speed. 2002. Statistical methods for identifying differentially expressed genes in replicated cDNA microarray experiments. *Stat. Sin.* 12:111-139.

Dudoit, S., and M.J. van der Laan. 2007. *Multiple Testing Procedures And Applications To Genomics*. Springer. New York; London.

Eddy, S.F., and K.B. Storey. 2007. Comparative Molecular Physiological Genomics. In: *Environmental Genomics*. C.C. Martin and C.C. Martin, Eds. Humana Press. Totowa, NJ. 81-110.

Emrich, S.J., W.B. Barbazuk, L. Li, and P.S. Schnable. 2007. Gene discovery and annotation using LCM-454 transcriptome sequencing. *Genome Res.* 17:69-73.

Endrizzi, K., B. Moussian, A. Haecker, J.Z. Levin, and T. Laux. 1996. The *SHOOT MERISTEMLESS* gene is required for maintenance of undifferentiated cells in *Arabidopsis* shoot and floral meristems and acts at a different regulatory level than the meristem genes *WUSCHEL* and *ZWILLE*. *Plant J.* 10:967-979.

Evans, M.M., and M.K. Barton. 1997. Genetics of angiosperm shoot apical meristem development. *Annu. Rev. Plant Physiol. Plant Mol. Biol.* 48:673-701.

Evenari, M. 1989. The history of research on white-green variegated plants. *Bot. Rev.* 55:106-139.

Ewens, W.J., and G.R. Grant. 2005. Gene expression, microarrays, and multiple testing. In: *Statisical Methods in Bioinformatics: An Introduction*. Springer-Verlag. New York, NY. 430-474.

Fankhauser, C., K.C. Yeh, J.C. Lagarias, H. Zhang, T.D. Elich, and J. Chory. 1999. PKS1, a substrate phosphorylated by phytochrome that modulates light signaling in *Arabidopsis*. *Science*. 284:1539-1541.

Fei, Z., X. Tang, R.M. Alba, J.A. White, C.M. Ronning, G.B. Martin, S.D. Tanksley, and J.J. Giovannoni. 2004. Comprehensive EST analysis of tomato and comparative genomics of fruit ripening. *Plant J.* 40:47-59.

Ferro, M., D. Salvi, S. Brugiere, S. Miras, S. Kowalski, M. Louwagie, J. Garin, J. Joyard, and N. Rolland. 2003. Proteomics of the chloroplast envelope membranes from *Arabidopsis thaliana*. *Mol. Cell. Proteomics*. 2:325-345.

Fletcher, J.C. 2002. Coordination of cell proliferation and cell fate decisions in the angiosperm shoot apical meristem. *Bioessays*. 24:27-37.

Fletcher, J.C., U. Brand, M.P. Running, R. Simon, and E.M. Meyerowitz. 1999. Signaling of cell fate decisions by *CLAVATA3* in *Arabidopsis* shoot meristems. *Science*. 283:1911-1914.

Fletcher, J.C., and E.M. Meyerowitz. 2000. Cell signaling within the shoot meristem. *Curr. Opin. Cell Biol.* 3:23-30.

Foster, A.S. 1938. Structure and growth of the shoot apex in *Ginkgo biloba*. *Bull. Torrey Bot. Club*. 65:531-556.

Francis, D. 1992. The cell cycle in plant development. *New Phytol.* 122:1-20.

Fujimoto, S.Y., M. Ohta, A. Usui, H. Shinshi, and M. Ohme-Takagi. 2000. *Arabidopsis* ethylene-responsive element binding factors act as transcriptional activators or repressors of GCC box-mediated gene expression. *Plant Cell*. 12:393-404.

Fulton, T.M., R. Van der Hoeven, N.T. Eannetta, and S.D. Tanksley. 2002. Identification, analysis, and utilization of conserved ortholog set markers for comparative genomics in higher plants. *Plant Cell*. 14:1457-1467.

Gagne, J.M., B.P. Downes, S.H. Shiu, A.M. Durski, and R.D. Vierstra. 2002. The F-box subunit of the SCF E3 complex is encoded by a diverse superfamily of genes in *Arabidopsis*. *Proc. Natl. Acad. Sci. U.S.A.* 99:11519-11524.

Gagne, J.M., J. Smalle, D.J. Gingerich, J.M. Walker, S.D. Yoo, S. Yanagisawa, and R.D. Vierstra. 2004. *Arabidopsis* EIN3-binding F-box 1 and 2 form ubiquitin-protein ligases that repress ethylene action and promote growth by directing EIN3 degradation. *Proc. Natl. Acad. Sci. U.S.A.* 101:6803-6808.

Galen, C., J. Huddle, and E. Liscum. 2004. An experimental test of the adaptive evolution of phototropins: blue-light photoreceptors controlling phototropism in *Arabidopsis thaliana*. *Evolution*. 58:515-523.

Gallois, J.L., C. Woodward, G.V. Reddy, and R. Sablowski. 2002. Combined SHOOT MERISTEMLESS and WUSCHEL trigger ectopic organogenesis in *Arabidopsis*. *Development*. 129:3207-3217.

Gao, X., F. Ren, and Y.T. Lu. 2006. The *Arabidopsis* mutant *stg1* identifies a function for TBP-associated factor 10 in plant osmotic stress adaptation. *Plant Cell Physiol.* 47:1285-1294.

García-Lorenzo, M., A. Żelisko, G. Jackowski, and C. Funk. 2005. Degradation of the main Photosystem II light-harvesting complex. *Photochem. Photobiol. Sci.* 4:1065-1071.

Gifford, E. 1954. The shoot apex in angiosperms. *Bot. Rev.* 20:477-529.

Gisel, A., S. Barella, F.D. Hempel, and P.C. Zambryski. 1999. Temporal and spatial regulation of symplastic trafficking during development in *Arabidopsis thaliana* apices. *Development*. 126:1879-1889.

Glantz, S.A. 2005. *Primer of Biostatistics*. McGraw-Hill Medical Pub. New York. 520 pp.

Goda, H., E. Sasaki, K. Akiyama, A. Maruyama-Nakashita, K. Nakabayashi, W. Li, M. Ogawa, Y. Yamauchi, J. Preston, K. Aoki, T. Kiba, S. Takatsuto, S. Fujioka, T. Asami, T. Nakano, H. Kato, T. Mizuno, H. Sakakibara, S. Yamaguchi, E. Nambara, Y. Kamiya, H. Takahashi, M.Y. Hirai, T. Sakurai, K. Shinozaki, K. Saito, S. Yoshida, and Y. Shimada. 2008. The AtGenExpress hormone and chemical treatment data set: experimental design, data evaluation, model data analysis and data access. *Plant J.* 55:526-542.

Godbolé, R., W. Michalke, P. Nick, and a.R. Hertel. 2000. Cytoskeletal drugs and gravity-induced lateral auxin transport in rice coleoptiles. *Plant Biol. (Stuttg)*. 2:176-181.

Goff, S.A., D. Ricke, T.H. Lan, G. Presting, R. Wang, M. Dunn, J. Glazebrook, A. Sessions, P. Oeller, H. Varma, D. Hadley, D. Hutchison, C. Martin, F. Katagiri, B.M. Lange, T. Moughamer, Y. Xia, P. Budworth, J. Zhong, T. Miguel, U. Paszkowski, S. Zhang, M. Colbert, W.L. Sun, L. Chen, B. Cooper, S. Park, T.C. Wood, L. Mao, P. Quail, R. Wing, R. Dean, Y. Yu, A. Zharkikh, R. Shen, S. Sahasrabudhe, A. Thomas, R. Cannings, A. Gutin, D. Pruss, J. Reid, S. Tavtigian, J. Mitchell, G. Eldredge, T. Scholl, R.M. Miller, S. Bhatnagar, N. Adey, T. Rubano, N. Tusneem, R. Robinson, J. Feldhaus, T. Macalma, A. Oliphant, and S. Briggs. 2002. A draft sequence of the rice genome (*Oryza sativa* L. ssp. *japonica*). *Science*. 296:92-100.

Gray, W.M., J.C. del Pozo, L. Walker, L. Hobbie, E. Risseeuw, T. Banks, W.L. Crosby, M. Yang, H. Ma, and M. Estelle. 1999. Identification of an SCF ubiquitin-ligase complex required for auxin response in *Arabidopsis thaliana*. *Genes Dev.* 13:1678-1691.

Groß-Hardt, R., and T. Laux. 2001. Shoots and buds. In: *Encyclopedia of Life Sciences*. John Wiley & Sons, Ltd. Chichester. 1-3.

Gu, Y., Y. Fu, P. Dowd, S. Li, V. Vernoud, S. Gilroy, and Z. Yang. 2005. A Rho family GTPase controls actin dynamics and tip growth via two counteracting downstream pathways in pollen tubes. *J. Cell Biol.* 169:127-138.

Han, I.S., T.S. Tseng, W. Eisinger, and W.R. Briggs. 2008. Phytochrome A regulates the intracellular distribution of phototropin 1-green fluorescent protein in *Arabidopsis thaliana*. *Plant Cell*. 20:2835-2847.

Hanstein, J.v. 1868. Die Scheitelzellgruppe im Vegetationspunkt der Phanerogamen. *Festschrift der Niederrheinischen Gesellschaft für Natur- und Heilkunde*:109-134.

Hao, D., M. Ohme-Takagi, and A. Sarai. 1998. Unique mode of GCC box recognition by the DNA-binding domain of ethylene-responsive element-binding factor (ERF domain) in plant. *J. Biol. Chem.* 273:26857-26861.

He, Y., M.R. Doyle, and R.M. Amasino. 2004. PAF1-complex-mediated histone methylation of *FLOWERING LOCUS C* chromatin is required for the vernalization-responsive, winter-annual habit in *Arabidopsis*. *Genes Dev.* 18:2774-2784.

Heard, D.J., T. Kiss, and W. Filipowicz. 1993. Both *Arabidopsis* TATA binding protein (TBP) isoforms are functionally identical in RNA polymerase II and III transcription in plant cells: evidence for gene-specific changes in DNA binding specificity of TBP. *EMBO J.* 12:3519-3528.

Henderson, I.R., C. Shindo, and C. Dean. 2003. The need for winter in the switch to flowering. *Annu. Rev. Genet.* 37:371-392.

Hiltbrunner, A., A. Viczian, E. Bury, A. Tscheuschler, S. Kircher, R. Toth, A. Honsberger, F. Nagy, C. Fankhauser, and E. Schafer. 2005. Nuclear accumulation of the phytochrome A photoreceptor requires FHY1. *Curr. Biol.* 15:2125-2130.

Hobe, M., U. Brand, R. Waites, and R. Simon. 2001. Control of cell fate in plant meristems. *Novartis Found. Symp.* 237:235-243; Discussion 243-247.

Holm, M., C.S. Hardtke, R. Gaudet, and X.W. Deng. 2001. Identification of a structural motif that confers specific interaction with the WD40 repeat domain of *Arabidopsis* COP1. *EMBO J.* 20:118-127.

Horvath, D.P., R. Schaffer, M. West, and E. Wisman. 2003. *Arabidopsis* microarrays identify conserved and differentially expressed genes involved in shoot growth and development from distantly related plant species. *Plant J.* 34:125-134.

Hovatta, I., K. Kimppa, A. Lehmussola, J. Saharinen, and P. Tiikkainen. 2005. *DNA Microarray Data Analysis*. CSC-Scientific Computing Ltd. Helsinki, Finland. (http://www.csc.fi/english/research/sciences/bioscience/books/microarraybook2nd).

Hrabak, E.M., C.W. Chan, M. Gribskov, J.F. Harper, J.H. Choi, N. Halford, J. Kudla, S. Luan, H.G. Nimmo, M.R. Sussman, M. Thomas, K. Walker-Simmons, J.K. Zhu, and A.C. Harmon. 2003. The *Arabidopsis* CDPK-SnRK superfamily of protein kinases. *Plant Physiol.* 132:666-680.

Hudson, A., and J. Goodrich. 1997. Plant meristems: cell signalling keeps the balance. *Curr. Biol.* 7:R427-429.

Hughes, T.R., M. Mao, A.R. Jones, J. Burchard, M.J. Marton, K.W. Shannon, S.M. Lefkowitz, M. Ziman, J.M. Schelter, M.R. Meyer, S. Kobayashi, C. Davis, H. Dai, Y.D. He, S.B. Stephaniants, G. Cavet, W.L. Walker, A. West, E. Coffey, D.D. Shoemaker, R. Stoughton, A.P. Blanchard, S.H. Friend, and P.S. Linsley. 2001. Expression profiling using microarrays fabricated by an ink-jet oligonucleotide synthesizer. *Nat. Biotechnol.* 19:342-347.

Hunter, S., R. Apweiler, T.K. Attwood, A. Bairoch, A. Bateman, D. Binns, P. Bork, U. Das, L. Daugherty, L. Duquenne, R.D. Finn, J. Gough, D. Haft, N. Hulo, D. Kahn, E. Kelly, A. Laugraud, I. Letunic, D. Lonsdale, R. Lopez, M. Madera, J. Maslen, C. McAnulla, J. McDowall, J. Mistry, A. Mitchell, N. Mulder, D. Natale, C.

Orengo, A.F. Quinn, J.D. Selengut, C.J. Sigrist, M. Thimma, P.D. Thomas, F. Valentin, D. Wilson, C.H. Wu, and C. Yeats. 2009. InterPro: the integrative protein signature database. *Nucleic Acids Res.* 37:D211-215.

Huson, D.H., D.C. Richter, C. Rausch, T. Dezulian, M. Franz, and R. Rupp. 2007. Dendroscope: An interactive viewer for large phylogenetic trees. *BMC Bioinf*. 8:460.

Inada, S., M. Ohgishi, T. Mayama, K. Okada, and T. Sakai. 2004. RPT2 is a signal transducer involved in phototropic response and stomatal opening by association with phototropin 1 in *Arabidopsis thaliana*. *Plant Cell*. 16:887-896.

Indorf, M., J. Cordero, G. Neuhaus, and M. Rodriguez-Franco. 2007. Salt tolerance (STO), a stress-related protein, has a major role in light signalling. *Plant J.* 51:563-574.

Innes, R.W. 2001. Mapping out the roles of MAP kinases in plant defense. *Trends Plant Sci.* 6:392-394.

Invitrogen Life Technologies. 2004. *SuperScript™ Indirect cDNA Labeling System - For generating fluorescently labeled cDNA to use in microarray screening (Catalog nos. L1014-01, L1014-02, and L1014-03)*. Invitrogen Life Technologies. Carlsbad, CA. (http://tools.invitrogen.com/content/sfs/manuals/superscriptindirectcdnalabeling_man.pdf).

Inzé, D., and L. De Veylder. 2006. Cell cycle regulation in plant development. *Annu. Rev. Genet.* 40:77-105.

Irish, V.F. 1991. Cell lineage in plant development. *Curr. Opin. Cell Biol.* 3:983-987.

Irish, V.F., and I.M. Sussex. 1992. A fate map of the *Arabidopsis* embryonic shoot apical meristem. *Development*. 115:745-753.

Ivanchenko, M.G., G.K. Muday, and J.G. Dubrovsky. 2008. Ethylene-auxin interactions regulate lateral root initiation and emergence in *Arabidopsis thaliana*. *Plant J.* 55:335-347.

Jiang, S., M. Li, T. Xu, D. Ren, and G. Liu. 2007. Two kinesins from *Arabidopsis*, KatB and KatC, have a second microtubule-binding site in the tail domain. *J. Biochem. Mol. Biol.* 40:44-52.

Jiang, S.Y., and S. Ramachandran. 2006. Comparative and evolutionary analysis of genes encoding small GTPases and their activating proteins in eukaryotic genomes. *Physiol. Genomics*. 24:235-251.

Kang, J., G. Zhang, G. Bonnema, Z. Fang, and X. Wang. 2008. Global analysis of gene expression in flower buds of *Ms-cd1 Brassica oleracea* conferring male sterility by using an *Arabidopsis* microarray. *Plant Mol. Biol.* 66:177-192.

Kassahn, K.S. 2008. Microarrays for comparative and ecological genomics: beyond single-species applications of array technologies. *J. Fish Biol.* 72:2407-2434.

Kato, Y., E. Miura, R. Matsushima, and W. Sakamoto. 2007. White leaf sectors in *yellow variegated2* are formed by viable cells with undifferentiated plastids. *Plant Physiol.* 144:952-960.

Kayes, J.M., and S.E. Clark. 1998. *CLAVATA2*, a regulator of meristem and organ development in *Arabidopsis*. *Development*. 125:3843-3851.

Kerstetter, R.A., and S. Hake. 1997. Shoot meristem formation in vegetative development. *Plant Cell*. 9:1001-1010.

Kilian, J., D. Whitehead, J. Horak, D. Wanke, S. Weinl, O. Batistic, C. D'Angelo, E. Bornberg-Bauer, J. Kudla, and K. Harter. 2007. The AtGenExpress global stress expression data set: protocols, evaluation and model data analysis of UV-B light, drought and cold stress responses. *Plant J.* 50:347-363.

Kim, B.G., R. Waadt, Y.H. Cheong, G.K. Pandey, J.R. Dominguez-Solis, S. Schultke, S.C. Lee, J. Kudla, and S. Luan. 2007. The calcium sensor CBL10 mediates salt tolerance by regulating ion homeostasis in *Arabidopsis*. *Plant J.* 52:473-484.

Kim, D.H., J.G. Kang, S.S. Yang, K.S. Chung, P.S. Song, and C.M. Park. 2002. A phytochrome-associated protein phosphatase 2A modulates light signals in flowering time control in *Arabidopsis*. *Plant Cell*. 14:3043-3056.

Kim, G.T., S. Fujioka, T. Kozuka, F.E. Tax, S. Takatsuto, S. Yoshida, and H. Tsukaya. 2005a. CYP90C1 and CYP90D1 are involved in different steps in the brassinosteroid biosynthesis pathway in *Arabidopsis thaliana*. *Plant J.* 41:710-721.

Kim, I., K. Kobayashi, E. Cho, and P.C. Zambryski. 2005b. Subdomains for transport via plasmodesmata corresponding to the apical-basal axis are established during *Arabidopsis* embryogenesis. *Proc. Natl. Acad. Sci. U.S.A.* 102:11945-11950.

Kirk, J.T.O., and R.A.E. Tilney-Bassett. 1978. *The Plastids: Their Chemistry, Structure, Growth and Inheritance*. Elsevier/North Holland Biomedical Press. Amsterdam, New York. 960 pp.

Klahre, U., and B. Kost. 2006. Tobacco RhoGTPase ACTIVATING PROTEIN1 spatially restricts signaling of RAC/Rop to the apex of pollen tubes. *Plant Cell*. 18:3033-3046.

Konishi, M., and S. Yanagisawa. 2008. Ethylene signaling in *Arabidopsis* involves feedback regulation via the elaborate control of *EBF2* expression by EIN3. *Plant J.* 55:821-831.

Kosugi, S., and Y. Ohashi. 1997. PCF1 and PCF2 specifically bind to cis elements in the rice proliferating cell nuclear antigen gene. *Plant Cell*. 9:1607-1619.

Krebbers, E., J. Seurinck, L. Herdies, A.R. Cashmore, and M.P. Timko. 1988. Four genes in two diverged subfamilies encode the ribulose-1,5-bisphosphate carboxylase small subunit polypeptides of *Arabidopsis thaliana*. *Plant Mol. Biol.* 11:745-759.

Lariguet, P., H.E. Boccalandro, J.M. Alonso, J.R. Ecker, J. Chory, J.J. Casal, and C. Fankhauser. 2003. A growth regulatory loop that provides homeostasis to phytochrome a signaling. *Plant Cell*. 15:2966-2978.

Lariguet, P., and C. Fankhauser. 2004. Hypocotyl growth orientation in blue light is determined by phytochrome A inhibition of gravitropism and phototropin promotion of phototropism. *Plant J.* 40:826-834.

Lariguet, P., I. Schepens, D. Hodgson, U.V. Pedmale, M. Trevisan, C. Kami, M. de Carbonnel, J.M. Alonso, J.R. Ecker, E. Liscum, and C. Fankhauser. 2006. PHYTOCHROME KINASE SUBSTRATE 1 is a phototropin 1 binding protein required for phototropism. *Proc. Natl. Acad. Sci. U.S.A.* 103:10134-10139.

Laufs, P., J. Dockx, J. Kronenberger, and J. Traas. 1998a. *MGOUN1* and *MGOUN2*: two genes required for primordium initiation at the shoot apical and floral meristems in *Arabidopsis thaliana*. *Development*. 125:1253-1260.

Laufs, P., O. Grandjean, C. Jonak, K. Kieu, and J. Traas. 1998b. Cellular parameters of the shoot apical meristem in *Arabidopsis*. *Plant Cell*. 10:1375-1390.

Laux, T., K.F. Mayer, J. Berger, and G. Jurgens. 1996. The *WUSCHEL* gene is required for shoot and floral meristem integrity in *Arabidopsis*. *Development*. 122:87-96.

Lawit, S.J., K. O'Grady, W.B. Gurley, and E. Czarnecka-Verner. 2007. Yeast two-hybrid map of *Arabidopsis* TFIID. *Plant Mol. Biol.* 64:73-87.

Lee, E.J., H. Iai, H. Sano, and N. Koizumi. 2005. Sugar responsible and tissue specific expression of a gene encoding AtCIPK14, an *Arabidopsis* CBL-interacting protein kinase. *Biosci., Biotechnol. Biochem.* 69:242-245.

Lenhard, M., G. Jurgens, and T. Laux. 2002. The *WUSCHEL* and *SHOOTMERISTEMLESS* genes fulfil complementary roles in *Arabidopsis* shoot meristem regulation. *Development*. 129:3195-3206.

Li, C., T. Potuschak, A. Colon-Carmona, R.A. Gutierrez, and P. Doerner. 2005a. *Arabidopsis* TCP20 links regulation of growth and cell division control pathways. *Proc. Natl. Acad. Sci. U.S.A.* 102:12978-12983.

Li, L., J. Roden, B.E. Shapiro, B.J. Wold, S. Bhatia, S.J. Forman, and R. Bhatia. 2005b. Reproducibility, fidelity, and discriminant validity of mRNA amplification for microarray analysis from primary hematopoietic cells. *J. Mol. Diagn.* 7:48-56.

Li, Q., C. Fraley, R.E. Bumgarner, K.Y. Yeung, and A.E. Raftery. 2005c. Donuts, scratches and blanks: robust model-based segmentation of microarray images. *Bioinformatics*. 21:2875-2882.

Lindahl, M., C. Spetea, T. Hundal, A.B. Oppenheim, Z. Adam, and B. Andersson. 2000. The thylakoid FtsH protease plays a role in the light-induced turnover of the photosystem II D1 protein. *Plant Cell*. 12:419-431.

Ling, H. 2008. Sequence analysis of GDSL lipase gene family in *Arabidopsis thaliana*. *Pak. J. Biol. Sci.* 11:763-767.

Ling, H., J. Zhao, K. Zuo, C. Qiu, H. Yao, J. Qin, X. Sun, and K. Tang. 2006. Isolation and expression analysis of a GDSL-like lipase gene from *Brassica napus* L. *J. Biochem. Mol. Biol.* 39:297-303.

Lintala, M., Y. Allahverdiyeva, H. Kidron, M. Piippo, N. Battchikova, M. Suorsa, E. Rintamaki, T.A. Salminen, E.M. Aro, and P. Mulo. 2007. Structural and functional characterization of ferredoxin-$NADP^+$-oxidoreductase using knock-out mutants of *Arabidopsis*. *Plant J.* 49:1041-1052.

Lippuner, V., M.S. Cyert, and C.S. Gasser. 1996. Two classes of plant cDNA clones differentially complement yeast calcineurin mutants and increase salt tolerance of wild-type yeast. *J. Biol. Chem.* 271:12859-12866.

Liu, J., and J.K. Zhu. 1998. A calcium sensor homolog required for plant salt tolerance. *Science*. 280:1943-1945.

Long, J.A., and M.K. Barton. 1998. The development of apical embryonic pattern in *Arabidopsis*. *Development*. 125:3027-3035.

Long, J.A., E.I. Moan, J.I. Medford, and M.K. Barton. 1996. A member of the *KNOTTED* class of homeodomain proteins encoded by the *STM* gene of *Arabidopsis*. *Nature*. 379:66-69.

Lucas, W.J. 1995. Plasmodesmata: intercellular channels for macromolecular transport in plants. *Curr. Opin. Cell Biol.* 7:673-680.

Ludwig, S.R., D.G. Oppenheimer, C.D. Silflow, and D.P. Snustad. 1988. The α1-tubulin gene of *Arabidopsis thaliana*: primary structure and preferential expression in flowers. *Plant Mol. Biol.* 10:311-321.

Lunde, C., P.E. Jensen, L. Rosgaard, A. Haldrup, M.J. Gilpin, and H.V. Scheller. 2003. Plants impaired in state transitions can to a large degree compensate for their defect. *Plant Cell Physiol.* 44:44-54.

Lyndon, R.F. 1970a. Planes of cell division and growth in the shoot apex of *Pisum*. *Ann. Bot. (Lond)*. 34:19-28.

Lyndon, R.F. 1970b. Rates of cell division in the shoot apical meristem of *Pisum*. *Ann. Bot. (Lond)*. 34:1-17.

Lyndon, R.F. 1998. *The Shoot Apical Meristem: Its Growth and Development*. Cambridge University Press. Cambridge, UK; New York. 277 pp.

Lyndon, R.F., and M.E. Cunninghame. 1986. Control of shoot apical development via cell division. *Symp. Soc. Exp. Biol.* 40:233-255.

Ma, L., Y. Gao, L. Qu, Z. Chen, J. Li, H. Zhao, and X.W. Deng. 2002. Genomic evidence for COP1 as a repressor of light-regulated gene expression and development in *Arabidopsis*. *Plant Cell*. 14:2383-2398.

Madlung, A., F.J. Behringer, and T.L. Lomax. 1999. Ethylene plays multiple nonprimary roles in modulating the gravitropic response in tomato. *Plant Physiol.* 120:897-906.

Manenti, G., and G. Tedesco. 1971. Ultrastructure and pigments of ivy (*Hedera helix* L.) varieties with green and variegated leaves. *Caryologia*. 30:163-176.

MAPK Group. 2002. Mitogen-activated protein kinase cascades in plants: a new nomenclature. *Trends Plant Sci.* 7:301-308.

Marri, L., F. Sparla, P. Pupillo, and P. Trost. 2005. Co-ordinated gene expression of photosynthetic glyceraldehyde-3-phosphate dehydrogenase, phosphoribulokinase, and CP12 in *Arabidopsis thaliana*. *J. Exp. Bot.* 56:73-80.

Marrocco, K., Y. Zhou, E. Bury, M. Dieterle, M. Funk, P. Genschik, M. Krenz, T. Stolpe, and T. Kretsch. 2006. Functional analysis of EID1, an F-box protein involved in phytochrome A-dependent light signal transduction. *Plant J.* 45:423-438.

Mathur, J. 2004. Cell shape development in plants. *Trends Plant Sci.* 9:583-590.

Mathur, J., and N.H. Chua. 2000. Microtubule stabilization leads to growth reorientation in *Arabidopsis* trichomes. *Plant Cell*. 12:465-477.

Mayer, C.-D., and C. Glasbey. 2005. Statistical methods in microarray gene expression data analysis. In: *Probabilistic Modeling in Bioinformatics and Medical Informatics*. D. Husmeier, R. Dybowski, and S. Roberts, Eds. Springer-Verlag. London. 211-238.

Mayer, K.F., H. Schoof, A. Haecker, M. Lenhard, G. Jurgens, and T. Laux. 1998. Role of *WUSCHEL* in regulating stem cell fate in the *Arabidopsis* shoot meristem. *Cell*. 95:805-815.

McGrath, K.C., B. Dombrecht, J.M. Manners, P.M. Schenk, C.I. Edgar, D.J. Maclean, W.R. Scheible, M.K. Udvardi, and K. Kazan. 2005. Repressor- and activator-type ethylene response factors functioning in jasmonate signaling and disease resistance identified via a genome-wide screen of *Arabidopsis* transcription factor gene expression. *Plant Physiol.* 139:949-959.

Medford, J.I. 1992. Vegetative apical meristems. *Plant Cell*. 4:1029-1039.

Mewes, H.W., S. Dietmann, D. Frishman, R. Gregory, G. Mannhaupt, K.F. Mayer, M. Munsterkotter, A. Ruepp, M. Spannagl, V. Stumpflen, and T. Rattei. 2008. MIPS: analysis and annotation of genome information in 2007. *Nucleic Acids Res.* 36:D196-201.

Meyerowitz, E.M. 1997. Genetic control of cell division patterns in developing plants. *Cell*. 88:299-308.

Michaels, S.D., and R.M. Amasino. 1999. *FLOWERING LOCUS C* encodes a novel MADS domain protein that acts as a repressor of flowering. *Plant Cell*. 11:949-956.

Miura, E., Y. Kato, R. Matsushima, V. Albrecht, S. Laalami, and W. Sakamoto. 2007. The balance between protein synthesis and degradation in chloroplasts determines leaf variegation in *Arabidopsis yellow variegated* mutants. *Plant Cell*. 19:1313-1328.

Molecular Devices Inc. 2001. GenePix® File Formats. In: *http://www.moleculardevices.com/pages/software/gn_genepix_file_formats.html*.

Moore, S., P. Payton, M. Wright, S. Tanksley, and J. Giovannoni. 2005. Utilization of tomato microarrays for comparative gene expression analysis in the Solanaceae. *J. Exp. Bot.* 56:2885-2895.

Morgan, D.O. 1997. Cyclin-dependent kinases: engines, clocks, and microprocessors. *Annu. Rev. Cell Dev. Biol.* 13:261-291.

Motchoulski, A., and E. Liscum. 1999. *Arabidopsis* NPH3: A NPH1 photoreceptor-interacting protein essential for phototropism. *Science*. 286:961-964.

Muday, G.K., and A. DeLong. 2001. Polar auxin transport: controlling where and how much. *Trends Plant Sci.* 6:535-542.

Muller, S., S. Han, and L.G. Smith. 2006. Two kinesins are involved in the spatial control of cytokinesis in *Arabidopsis thaliana*. *Curr. Biol.* 16:888-894.

Mutasa-Gottgens, E., and P. Hedden. 2009. Gibberellin as a factor in floral regulatory networks. *J. Exp. Bot.* 60:1979-1989.

Nagaoka, S., and T. Takano. 2003. Salt tolerance-related protein STO binds to a Myb transcription factor homologue and confers salt tolerance in *Arabidopsis*. *J. Exp. Bot.* 54:2231-2237.

Nagarajan, R. 2003. Intensity-based segmentation of microarray images. *IEEE Trans. Med. Imaging.* 22:882-889.

Naranjo, M.A., J. Forment, M. Roldan, R. Serrano, and O. Vicente. 2006. Overexpression of *Arabidopsis thaliana LTL1*, a salt-induced gene encoding a GDSL-motif lipase, increases salt tolerance in yeast and transgenic plants. *Plant, Cell Environ.* 29:1890-1900.

Newman, T., F.J. de Bruijn, P. Green, K. Keegstra, H. Kende, L. McIntosh, J. Ohlrogge, N. Raikhel, S. Somerville, M. Thomashow, and et al. 1994. Genes galore: a summary of methods for accessing results from large-scale partial sequencing of anonymous *Arabidopsis* cDNA clones. *Plant Physiol.* 106:1241-1255.

Ni, J., and S.E. Clark. 2006. Evidence for functional conservation, sufficiency, and proteolytic processing of the CLAVATA3 CLE domain. *Plant Physiol.* 140:726-733.

Nishihama, R., T. Soyano, M. Ishikawa, S. Araki, H. Tanaka, T. Asada, K. Irie, M. Ito, M. Terada, H. Banno, Y. Yamazaki, and Y. Machida. 2002. Expansion of the cell plate in plant cytokinesis requires a kinesin-like protein/MAPKKK complex. *Cell*. 109:87-99.

Nishitani, K., and R. Tominaga. 1992. Endo-xyloglucan transferase, a novel class of glycosyltransferase that catalyzes transfer of a segment of xyloglucan molecule to another xyloglucan molecule. *J. Biol. Chem.* 267:21058-21064.

Noh, B., S.H. Lee, H.J. Kim, G. Yi, E.A. Shin, M. Lee, K.J. Jung, M.R. Doyle, R.M. Amasino, and Y.S. Noh. 2004. Divergent roles of a pair of homologous jumonji/zinc-finger-class transcription factor proteins in the regulation of *Arabidopsis* flowering time. *Plant Cell*. 16:2601-2613.

Nozawa, A., N. Koizumi, and H. Sano. 2001. An *Arabidopsis* SNF1-related protein kinase, AtSR1, interacts with a calcium-binding protein, AtCBL2, of which transcripts respond to light. *Plant Cell Physiol.* 42:976-981.

Nozawa, A., Y. Sawada, T. Akiyama, N. Koizumi, and H. Sano. 2003. Variable interactions between sucrose non-fermented 1-related protein kinases and regulatory proteins in higher plants. *Biosci., Biotechnol. Biochem.* 67:2533-2540.

Nuwaysir, E.F., W. Huang, T.J. Albert, J. Singh, K. Nuwaysir, A. Pitas, T. Richmond, T. Gorski, J.P. Berg, J. Ballin, M. McCormick, J. Norton, T. Pollock, T. Sumwalt, L. Butcher, D. Porter, M. Molla, C. Hall, F. Blattner, M.R. Sussman, R.L. Wallace, F. Cerrina, and R.D. Green. 2002. Gene expression analysis using oligonucleotide arrays produced by maskless photolithography. *Genome Res.* 12:1749-1755.

Nygaard, V., M. Holden, A. Loland, M. Langaas, O. Myklebost, and E. Hovig. 2005. Limitations of mRNA amplification from small-size cell samples. *BMC Genomics*. 6:147.

Oakley, R.V., Y.S. Wang, W. Ramakrishna, S.A. Harding, and C.J. Tsai. 2007. Differential expansion and expression of α- and β-tubulin gene families in *Populus*. *Plant Physiol.* 145:961-973.

Ohta, M., K. Matsui, K. Hiratsu, H. Shinshi, and M. Ohme-Takagi. 2001. Repression domains of class II ERF transcriptional repressors share an essential motif for active repression. *Plant Cell*. 13:1959-1968.

Ohtsu, K., M.B. Smith, S.J. Emrich, L.A. Borsuk, R. Zhou, T. Chen, X. Zhang, M.C. Timmermans, J. Beck, B. Buckner, D. Janick-Buckner, D. Nettleton, M.J. Scanlon, and P.S. Schnable. 2007. Global gene expression analysis of the shoot apical meristem of maize (*Zea mays* L.). *Plant J.* 52:391-404.

Ojangu, E.L., K. Jarve, H. Paves, and E. Truve. 2007. *Arabidopsis thaliana* myosin XIK is involved in root hair as well as trichome morphogenesis on stems and leaves. *Protoplasma*. 230:193-202.

Okamuro, J.K., B. Caster, R. Villarroel, M. Van Montagu, and K.D. Jofuku. 1997. The AP2 domain of APETALA2 defines a large new family of DNA binding proteins in *Arabidopsis*. *Proc. Natl. Acad. Sci. U.S.A.* 94:7076-7081.

Olmedo, G., H. Guo, B.D. Gregory, S.D. Nourizadeh, L. Aguilar-Henonin, H. Li, F. An, P. Guzman, and J.R. Ecker. 2006. *ETHYLENE-INSENSITIVE5* encodes a 5'-->3' exoribonuclease required for regulation of the EIN3-targeting F-box proteins EBF1/2. *Proc. Natl. Acad. Sci. U.S.A.* 103:13286-13293.

Oppenheimer, D.G., M.A. Pollock, J. Vacik, D.B. Szymanski, B. Ericson, K. Feldmann, and M.D. Marks. 1997. Essential role of a kinesin-like protein in *Arabidopsis* trichome morphogenesis. *Proc. Natl. Acad. Sci. U.S.A.* 94:6261-6266.

Ostersetzer, O., and Z. Adam. 1997. Light-stimulated degradation of an unassembled Rieske FeS protein by a thylakoid-bound protease: the possible role of the FtsH protease. *Plant Cell*. 9:957-965.

Ozer, J., A.H. Bolden, and P.M. Lieberman. 1996. Transcription factor IIA mutations show activator-specific defects and reveal a IIA function distinct from stimulation of TBP-DNA binding. *J. Biol. Chem.* 271:11182-11190.

Pardo, J.M., M.P. Reddy, S. Yang, A. Maggio, G.H. Huh, T. Matsumoto, M.A. Coca, M. Paino-D'Urzo, H. Koiwa, D.J. Yun, A.A. Watad, R.A. Bressan, and P.M. Hasegawa. 1998. Stress signaling through Ca^{2+}/calmodulin-dependent protein phosphatase calcineurin mediates salt adaptation in plants. *Proc. Natl. Acad. Sci. U.S.A.* 95:9681-9686.

Pariset, L., G. Chillemi, S. Bongiorni, V.R. Spica, and A. Valentini. 2009. Microarrays and high-throughput transcriptomic analysis in species with incomplete availability of genomic sequences. *New Biotechnol.* 25:272-279.

Pease, A.C., D. Solas, E.J. Sullivan, M.T. Cronin, C.P. Holmes, and S.P. Fodor. 1994. Light-generated oligonucleotide arrays for rapid DNA sequence analysis. *Proc. Natl. Acad. Sci. U.S.A.* 91:5022-5026.

Peremyslov, V.V., A.I. Prokhnevsky, D. Avisar, and V.V. Dolja. 2008. Two class XI myosins function in organelle trafficking and root hair development in *Arabidopsis*. *Plant Physiol.* 146:1109-1116.

PerkinElmer Life Sciences Inc. 2002. *ScanArray Express Microarray Analysis System User Manual*. PerkinElmer Life Sciences Inc. Shelton, CT. 173 pp.

Petersen, M., P. Brodersen, H. Naested, E. Andreasson, U. Lindhart, B. Johansen, H.B. Nielsen, M. Lacy, M.J. Austin, J.E. Parker, S.B. Sharma, D.F. Klessig, R. Martienssen, O. Mattsson, A.B. Jensen, and J. Mundy. 2000. *Arabidopsis* MAP kinase 4 negatively regulates systemic acquired resistance. *Cell*. 103:1111-1120.

Petri, A., J. Fleckner, and M.W. Matthiessen. 2004. Array-A-Lizer: a serial DNA microarray quality analyzer. *BMC Bioinformatics*. 5:12.

Pilkington, M. 1929. The regeneration of the stem apex. *New Phytol.* 28:37-53.

Plantefol, L. 1947. Hélice foliare, point végétatif et stéle chez les dicotylédones. La notion d'anneau initial. *Rev. Gén. Bot.* 54:49-80.

Poethig, S. 1989. Genetic mosaics and cell lineage analysis in plants. *Trends Genet.* 5:273-277.

Poethig, S. 1990. Phase change and the regulation of shoot morphogenesis in plants. *Science*. 250:923-930.

Popham, R.A., and A.P. Chan. 1950. Zonation in the vegetative stem tp of *Chrysanthemum morifolium* Bailey. *Am. J. Bot.* 37:476-484.

Potuschak, T., E. Lechner, Y. Parmentier, S. Yanagisawa, S. Grava, C. Koncz, and P. Genschik. 2003. EIN3-dependent regulation of plant ethylene hormone signaling by two *Arabidopsis* F box proteins: EBF1 and EBF2. *Cell*. 115:679-689.

Prokhnevsky, A.I., V.V. Peremyslov, and V.V. Dolja. 2008. Overlapping functions of the four class XI myosins in *Arabidopsis* growth, root hair elongation, and organelle motility. *Proc. Natl. Acad. Sci. U.S.A.* 105:19744-19749.

Pruzinská, A., G. Tanner, S. Aubry, I. Anders, S. Moser, T. Muller, K.H. Ongania, B. Krautler, J.Y. Youn, S.J. Liljegren, and S. Hörtensteiner. 2005. Chlorophyll breakdown in senescent *Arabidopsis* leaves.

Characterization of chlorophyll catabolites and of chlorophyll catabolic enzymes involved in the degreening reaction. *Plant Physiol.* 139:52-63.

Putterill, J., R. Laurie, and R. Macknight. 2004. It's time to flower: the genetic control of flowering time. *Bioessays*. 26:363-373.

Qiagen. 2001. *RNeasy® Midi/Maxi Handbook*. Qiagen. Valencia, CA. 108 pp.

Qin, Y., L.i. X, M. Guo, K. Deng, J. Lin, D. Tang, X. Guo, and X. Liu. 2008. Regulation of salt and ABA responses by CIPK14, a calcium sensor interacting protein kinase in *Arabidopsis*. *Sci. China C. Life Sci.* 51:391-401.

Raghavan, C., E.K. Ong, M.J. Dalling, and T.W. Stevenson. 2006. Regulation of genes associated with auxin, ethylene and ABA pathways by 2,4-dichlorophenoxyacetic acid in *Arabidopsis*. *Funct. Integr. Genomics*. 6:60-70.

Reddy, G.V., and E.M. Meyerowitz. 2005. Stem-cell homeostasis and growth dynamics can be uncoupled in the *Arabidopsis* shoot apex. *Science*. 310:663-667.

Renn, S.C., N. Aubin-Horth, and H.A. Hofmann. 2004. Biologically meaningful expression profiling across species using heterologous hybridization to a cDNA microarray. *BMC Genomics*. 5:42.

Rinne, P.L., P.M. Kaikuranta, and C. van der Schoot. 2001. The shoot apical meristem restores its symplasmic organization during chilling-induced release from dormancy. *Plant J.* 26:249-264.

Rinne, P.L., and C. van der Schoot. 1998. Symplasmic fields in the tunica of the shoot apical meristem coordinate morphogenetic events. *Development*. 125:1477-1485.

Risseeuw, E.P., T.E. Daskalchuk, T.W. Banks, E. Liu, J. Cotelesage, H. Hellmann, M. Estelle, D.E. Somers, and W.L. Crosby. 2003. Protein interaction analysis of SCF ubiquitin E3 ligase subunits from *Arabidopsis*. *Plant J.* 34:753-767.

Rogers, S.O. 1980. *The Shoot Apex*. University of Oregon. Eugene, Oregon USA.

Rogers, S.O., and H.T. Bonnett. 1989. Evidence for apical initial cells in the vegetative shoot apex of *Hedera helix* cv. Goldheart. *Am. J. Bot.* 76:539-545.

Rose, J.K., J. Braam, S.C. Fry, and K. Nishitani. 2002. The XTH family of enzymes involved in xyloglucan endotransglucosylation and endohydrolysis: current perspectives and a new unifying nomenclature. *Plant Cell Physiol.* 43:1421-1435.

Rosler, J., I. Klein, and M. Zeidler. 2007. *Arabidopsis fhl/fhy1* double mutant reveals a distinct cytoplasmic action of phytochrome A. *Proc. Natl. Acad. Sci. U.S.A.* 104:10737-10742.

Roux, F., P. Touzet, J. Cuguen, and V. Le Corre. 2006. How to be early flowering: an evolutionary perspective. *Trends Plant Sci.* 11:375-381.

Rueda, L., and L. Qin. 2004. An improved clustering-based approach for DNA microarray image segmentation. In: *Image Analysis and Recognition: International Conference, ICIAR 2004*. Iciar, A. Campilho, and M. Kamel, Eds. pp. 17-24. Springer-Verlag. Berlin, Heidelberg. September 29-October 1, 2004, Porto, Portugal.

Rueda, L., and L. Qin. 2005. A new method for DNA microarray image segmentation. In: *International Conference on Image Analysis and Recognition, ICIAR 2005, LNCS 3656*. M. Kamel and A. Campilho, Eds. pp. 886-893. Springer-Verlag. Berlin, Heidelberg. September 2005, Toronto, Canada.

Russell, S., L.A. Meadows, and R.R. Russell. 2009. Chapter 4. Sample collection and labeling. In: *Microarray Technology In Practice*. Elsevier/Academic Press. Amsterdam; Boston. 71-100.

Rutschmann, F. 2006. Molecular dating of phylogenetic trees: A brief review of current methods that estimate divergence times. *Divers. Distrib.* 12:35-48.

Rutschow, H., A.J. Ytterberg, G. Friso, R. Nilsson, and K.J. van Wijk. 2008. Quantitative proteomics of a chloroplast *SRP54* sorting mutant and its genetic interactions with *CLPC1* in *Arabidopsis*. *Plant Physiol.* 148:156-175.

Ryu, J.S., J.I. Kim, T. Kunkel, B.C. Kim, D.S. Cho, S.H. Hong, S.H. Kim, A.P. Fernandez, Y. Kim, J.M. Alonso, J.R. Ecker, F. Nagy, P.O. Lim, P.S. Song, E. Schafer, and H.G. Nam. 2005. Phytochrome-specific type 5 phosphatase controls light signal flux by enhancing phytochrome stability and affinity for a signal transducer. *Cell*. 120:395-406.

Saijo, Y., D. Zhu, J. Li, V. Rubio, Z. Zhou, Y. Shen, U. Hoecker, H. Wang, and X.W. Deng. 2008. *Arabidopsis* COP1/SPA1 complex and FHY1/FHY3 associate with distinct phosphorylated forms of phytochrome A in balancing light signaling. *Mol. Cell*. 31:607-613.

Sakamoto, W. 2003. Leaf-variegated mutations and their responsible genes in *Arabidopsis thaliana*. *Genes Genet. Syst.* 78:1-9.

Sakamoto, W., E. Miura, Y. Kaji, T. Okuno, M. Nishizono, and T. Ogura. 2004. Allelic characterization of the leaf-variegated mutation *var2* identifies the conserved amino acid residues of FtsH that are important for ATP hydrolysis and proteolysis. *Plant Mol. Biol.* 56:705-716.

Satina, S., A. Blakeslee, and A. Avery. 1940. Demonstration of the three germ layers in the shoot apex of Datura by means of induced polyploidy in periclinal chimeras. *Am. J. Bot.* 27:895-905.

Satina, S., and A.F. Blakeslee. 1941. Periclinal chimeras in *Datura stramonium* in relation to development of leaf and flower. *Am. J. Bot.* 28:862-871.

Sawchuk, M.G., T.J. Donner, P. Head, and E. Scarpella. 2008. Unique and overlapping expression patterns among members of photosynthesis-associated nuclear gene families in *Arabidopsis*. *Plant Physiol.* 148:1908-1924.

Schena, M. 2003. Microarray Surfaces. In: *Microarray Analysis*. Wiley-Liss. Hoboken, NJ. 95-120.

Schena, M., D. Shalon, R.W. Davis, and P.O. Brown. 1995. Quantitative monitoring of gene expression patterns with a complementary DNA microarray. *Science*. 270:467-470.

Schepens, I., P. Duek, and C. Fankhauser. 2004. Phytochrome-mediated light signalling in *Arabidopsis*. *Curr. Opin. Plant Biol.* 7:564-569.

Schmid, M., T.S. Davison, S.R. Henz, U.J. Pape, M. Demar, M. Vingron, B. Scholkopf, D. Weigel, and J.U. Lohmann. 2005. A gene expression map of *Arabidopsis thaliana* development. *Nat. Genet.* 37:501-506.

Schmidt, A. 1924. Histologische Studien an phanerogamen Vegetationspunkten. *Bot. Arch. (Berlin)*. 8:345-404.

Schoof, H., M. Lenhard, A. Haecker, K.F. Mayer, G. Jurgens, and T. Laux. 2000. The stem cell population of *Arabidopsis* shoot meristems in maintained by a regulatory loop between the *CLAVATA* and *WUSCHEL* genes. *Cell*. 100:635-644.

Schulman, E. 1958. Bristlecone pine, oldest known living thing. *Natl. Geogr. Mag.* 113:354-372.

Scofield, S., and J.A. Murray. 2006. The evolving concept of the meristem. *Plant Mol. Biol.* 60:V-VII.

Seo, H.S., J.Y. Yang, M. Ishikawa, C. Bolle, M.L. Ballesteros, and N.H. Chua. 2003. LAF1 ubiquitination by COP1 controls photomorphogenesis and is stimulated by SPA1. *Nature*. 423:995-999.

Shen, Y., J.I. Kim, and P.S. Song. 2005. NDPK2 as a signal transducer in the phytochrome-mediated light signaling. *J. Biol. Chem.* 280:5740-5749.

Shi, L., and M. Cline. 1992. Shoot Inversion-induced Ethylene Production in the *Diageotropica* Tomato Mutant. *Ann. Bot. (Lond)*. 69:119-122.

Shimotohno, A., S. Matsubayashi, M. Yamaguchi, H. Uchimiya, and M. Umeda. 2003. Differential phosphorylation activities of CDK-activating kinases in *Arabidopsis thaliana*. *FEBS Lett.* 534:69-74.

Shimotohno, A., C. Umeda-Hara, K. Bisova, H. Uchimiya, and M. Umeda. 2004. The plant-specific kinase CDKF;1 is involved in activating phosphorylation of cyclin-dependent kinase-activating kinases in *Arabidopsis*. *Plant Cell*. 16:2954-2966.

Shinshi, H. 2008. Ethylene-regulated transcription and crosstalk with jasmonic acid. *Plant Sci.* 175:18-23.

Silk, W.K., and R.O. Erickson. 1979. Kinematics of plant growth. *J. Theor. Biol.* 76:481-501.

Simpson, G.G., and C. Dean. 2002. *Arabidopsis*, the Rosetta stone of flowering time? *Science*. 296:285-289.

Sineshchekov, V., and C. Fankhauser. 2004. PKS1 and PKS2 affect the phyA state in etiolated *Arabidopsis* seedlings. *Photochem. Photobiol. Sci.* 3:608-611.

Singh, P., D. Kaloudas, and C.A. Raines. 2008. Expression analysis of the *Arabidopsis CP12* gene family suggests novel roles for these proteins in roots and floral tissues. *J. Exp. Bot.* 59:3975-3985.

Slabas, A.R., A.P. Fordham-Skelton, D. Fletcher, J.M. Martinez-Rivas, R. Swinhoe, R.R. Croy, and I.M. Evans. 1994. Characterisation of cDNA and genomic clones encoding homologues of the 65 kDa regulatory subunit of protein phosphatase 2A in *Arabidopsis thaliana*. *Plant Mol. Biol.* 26:1125-1138.

Soh, M.S., S.H. Hong, H. Hanzawa, M. Furuya, and H.G. Nam. 1998. Genetic identification of FIN2, a far red light-specific signaling component of *Arabidopsis thaliana*. *Plant J.* 16:411-419.

Steeves, T.A. 2006. The shoot apical meristem: an historical perspective. *Can. J. Botany.* 84:1-5.

Steeves, T.A., and I.M. Sussex. 1989. *Patterns in Plant Development*. Cambridge University Press. Cambridge, UK; New York. 388 pp.

Stepanova, A.N., J.M. Hoyt, A.A. Hamilton, and J.M. Alonso. 2005. A Link between ethylene and auxin uncovered by the characterization of two root-specific ethylene-insensitive mutants in *Arabidopsis*. *Plant Cell*. 17:2230-2242.

Stewart, R.N. 1970. Determination of number and mitotic activity of shoot apical initial cells by analysis of mericlinal chimeras. *Am. J. Bot.* 57:816.

Sun, H., S. Basu, S.R. Brady, R.L. Luciano, and G.K. Muday. 2004. Interactions between auxin transport and the actin cytoskeleton in developmental polarity of *Fucus distichus* embryos in response to light and gravity. *Plant Physiol.* 135:266-278.

Sussex, I., and D. Rosenthal. 1973. Differential ^{3}H-thymidine labeling of nuclei in the shoot apical meristem of *Nicotiana*. *Bot. Gaz.* 134:295-301.

Swarup, R., P. Perry, D. Hagenbeek, D. Van Der Straeten, G.T. Beemster, G. Sandberg, R. Bhalerao, K. Ljung, and M.J. Bennett. 2007. Ethylene upregulates auxin biosynthesis in *Arabidopsis* seedlings to enhance inhibition of root cell elongation. *Plant Cell*. 19:2186-2196.

Szymkowiak, E.J., and I.M. Sussex. 1996. What chimeras can tell us about plant development. *Annu. Rev. Plant Physiol. Plant Mol. Biol.* 47:351-376.

Takahashi, N., H. Kuroda, T. Kuromori, T. Hirayama, M. Seki, K. Shinozaki, H. Shimada, and M. Matsui. 2004. Expression and interaction analysis of *Arabidopsis Skp1*-related genes. *Plant Cell Physiol.* 45:83-91.

Tan, P.K., T.J. Downey, E.L. Spitznagel, Jr., P. Xu, D. Fu, D.S. Dimitrov, R.A. Lempicki, B.M. Raaka, and M.C. Cam. 2003. Evaluation of gene expression measurements from commercial microarray platforms. *Nucleic Acids Res.* 31:5676-5684.

Tanaka, R., M. Hirashima, S. Satoh, and A. Tanaka. 2003. The *Arabidopsis-accelerated cell death* Gene *ACD1* is involved in oxygenation of pheophorbide α: Inhibition of the pheophorbide α oxygenase activity does not lead to the "Stay-Green" phenotype in *Arabidopsis*. *Plant Cell Physiol.* 44:1266-1274.

Tang, X., S. Orlicky, Q. Liu, A. Willems, F. Sicheri, and M. Tyers. 2005. Genome-wide surveys for phosphorylation-dependent substrates of SCF ubiquitin ligases. *Methods Enzymol.* 399:433-458.

Tepperman, J.M., Y.S. Hwang, and P.H. Quail. 2006. phyA dominates in transduction of red-light signals to rapidly responding genes at the initiation of *Arabidopsis* seedling de-etiolation. *Plant J.* 48:728-742.

The Gene Ontology Consortium, M. Ashburner, C.A. Ball, J.A. Blake, D. Botstein, H. Butler, J.M. Cherry, A.P. Davis, K. Dolinski, S.S. Dwight, J.T. Eppig, M.A. Harris, D.P. Hill, L. Issel-Tarver, A. Kasarskis, S. Lewis, J.C. Matese, J.E. Richardson, M. Ringwald, G.M. Rubin, and G. Sherlock. 2000. Gene ontology: tool for the unification of biology. *Nat. Genet.* 25:25-29.

The UniProt Consortium. 2009. The Universal Protein Resource (UniProt) 2009. *Nucleic Acids Res.* 37:D169-174.

Tilney-Bassett, R.A.E. 1986. *Plant Chimeras*. E. Arnold. London, UK; Baltimore, MD. 199 pp.

Tooke, F., and N. Battey. 2003. Models of shoot apical meristem function. *New Phytol.* 159:37-52.

Toufighi, K., S.M. Brady, R. Austin, E. Ly, and N.J. Provart. 2005. The Botany Array Resource: e-Northerns, Expression Angling, and promoter analyses. *Plant J*. 43:153-163.

Trémousaygue, D., L. Garnier, C. Bardet, P. Dabos, H. C., and B. Lescure. 2003. Internal telomeric repeats and 'TCP domain' protein-binding sites co-operate to regulate gene expression in *Arabidopsis thaliana* cycling cells. *Plant J.* 33:957-966.

Trotochaud, A.E., T. Hao, G. Wu, Z. Yang, and S.E. Clark. 1999. The CLAVATA1 receptor-like kinase requires CLAVATA3 for its assembly into a signaling complex that includes KAPP and a Rho-related protein. *Plant. Cell*. 11:393-406.

Twyman, R.M. 2003. Growth and development: Molecular biology of development. In: *Encyclopedia of Applied Plant Sciences*. B. Thomas, D.J. Murphy, and B.G. Murray, Eds. Elsevier Academic. Amsterdam, Boston. 539-549.

Umeda, M., A. Shimotohno, and M. Yamaguchi. 2005. Control of cell division and transcription by cyclin-dependent kinase-activating kinases in plants. *Plant Cell Physiol.* 46:1437-1442.

Uribe, X., M.A. Torres, M. Capellades, P. Puigdomenech, and J. Rigau. 1998. Maize α-tubulin genes are expressed according to specific patterns of cell differentiation. *Plant Mol. Biol.* 37:1069-1078.

Veit, B. 2006. Stem cell signalling networks in plants. *Plant Mol. Biol.* 60:793-810.

Verslues, P.E., G. Batelli, S. Grillo, F. Agius, Y.S. Kim, J. Zhu, M. Agarwal, S. Katiyar-Agarwal, and J.K. Zhu. 2007. Interaction of SOS2 with nucleoside diphosphate kinase 2 and catalases reveals a point of connection between salt stress and H_2O_2 signaling in *Arabidopsis thaliana*. *Mol. Cell. Biol.* 27:7771-7780.

Walbot, V. 1996. Sources and consequences of phenotypic and genotypic plasticity in flowering plants. *Trends Plant Sci.* 1:27-32.

Walsh, T.A., R. Neal, A.O. Merlo, M. Honma, G.R. Hicks, K. Wolff, W. Matsumura, and J.P. Davies. 2006. Mutations in an auxin receptor homolog *AFB5* and in *SGT1b* confer resistance to synthetic picolinate auxins and not to 2,4-dichlorophenoxyacetic acid or indole-3-acetic acid in *Arabidopsis*. *Plant Physiol.* 142:542-552.

Wang, X., W. Ni, X. Ge, J. Zhang, H. Ma, and K. Cao. 2006. Proteomic identification of potential target proteins regulated by an ASK1-mediated proteolysis pathway. *Cell Res.* 16:489-498.

Wardlaw, C.W. 1957. The reactivity of the apical meristem as ascertained by cytological and other techniques. *New Phytol.* 56:221-229.

Weber, H., A. Bernhardt, M. Dieterle, P. Hano, A. Mutlu, M. Estelle, P. Genschik, and H. Hellmann. 2005. *Arabidopsis* AtCUL3a and AtCUL3b form complexes with members of the BTB/POZ-MATH protein family. *Plant Physiol.* 137:83-93.

Weber, H., and H. Hellmann. 2009. *Arabidopsis thaliana* BTB/ POZ-MATH proteins interact with members of the ERF/AP2 transcription factor family. *FEBS J.*

Weeraratna, A.T., and D.D. Taub. 2007. Microarray data analysis. In: *Microarray Data Analysis: Methods and Applications*. M.J. Korenberg, Ed. Humana Press. Totowa, NJ. 1-16.

Wetmore, R.H. 1953. The use of in vitro cultures in the investigation of growth and differentiation in vascular plants. *Brookhaven Symp. Biol.* 6:22-38; discussion, 38-40.

Wilfinger, W.W., K. Mackey, and P. Chomczynski. 1997. Effect of pH and ionic strength on the spectrophotometric assessment of nucleic acid purity. *BioTechniques*. 22:474-476, 478-481.

Williams, L., and J.C. Fletcher. 2005. Stem cell regulation in the *Arabidopsis* shoot apical meristem. *Curr. Opin. Plant Biol.* 8:582-586.

Winter, D., B. Vinegar, H. Nahal, R. Ammar, G.V. Wilson, and N.J. Provart. 2007. An "electronic fluorescent pictograph" browser for exploring and analyzing large-scale biological data sets. *PLoS One*. 2:e718.

Wu, S., C. Wang, and H. Yan. 2005. Mean shift and morphology based segmentation scheme for DNA microarray images. In: *Advances in Intelligent Computing: International Conference on Intelligent Computing, ICIC 2005*. D.-S. Huang, X.-P. Zhang, and G.-B. Huang, Eds. pp. 41-50. Springer-Verlag. Berlin, New York. August 23-26, 2005, Hefei, China.

Xie, M., M. Tataw, and G. Venugopala Reddy. 2009. Towards a functional understanding of cell growth dynamics in shoot meristem stem-cell niche. *Semin. Cell Dev. Biol.* 20:1126-1133.

Xu, L., F. Liu, E. Lechner, P. Genschik, W.L. Crosby, H. Ma, W. Peng, D. Huang, and D. Xie. 2002. The SCF(COI1) ubiquitin-ligase complexes are required for jasmonate response in *Arabidopsis*. *Plant Cell*. 14:1919-1935.

Xu, W., P. Campbell, A.K. Vargheese, and J. Braam. 1996. The *Arabidopsis XET*-related gene family: environmental and hormonal regulation of expression. *Plant J.* 9:879-889.

Yamamoto, K., and J.Z. Kiss. 2002. Disruption of the actin cytoskeleton results in the promotion of gravitropism in inflorescence stems and hypocotyls of *Arabidopsis*. *Plant Physiol.* 128:669-681.

Yang, K.Y., Y. Liu, and S. Zhang. 2001. Activation of a mitogen-activated protein kinase pathway is involved in disease resistance in tobacco. *Proc. Natl. Acad. Sci. U.S.A.* 98:741-746.

Yang, M., Y. Hu, M. Lodhi, W.R. McCombie, and H. Ma. 1999. The *Arabidopsis SKP1-LIKE1* gene is essential for male meiosis and may control homologue separation. *Proc. Natl. Acad. Sci. U.S.A.* 96:11416-11421.

Yang, Y.H., and N.P. Thorne. 2003. Normalization for two-color cDNA microarray data. In: *Statistics and Science: A Festschrift for Terry Speed*. D.R. Goldstein, Ed. Institute of Mathematical Statistics. Beachwood, Ohio. 403-418.

Yang, Z., L. Tian, M. Latoszek-Green, D. Brown, and K. Wu. 2005. *Arabidopsis* ERF4 is a transcriptional repressor capable of modulating ethylene and abscisic acid responses. *Plant Mol. Biol.* 58:585-596.

Yu, F., S. Park, and S.R. Rodermel. 2004. The *Arabidopsis FtsH* metalloprotease gene family: interchangeability of subunits in chloroplast oligomeric complexes. *Plant J.* 37:864-876.

Yu, F., S. Park, and S.R. Rodermel. 2005. Functional redundancy of AtFtsH metalloproteases in thylakoid membrane complexes. *Plant Physiol.* 138:1957-1966.

Yu, J., S. Hu, J. Wang, G.K. Wong, S. Li, B. Liu, Y. Deng, L. Dai, Y. Zhou, X. Zhang, M. Cao, J. Liu, J. Sun, J. Tang, Y. Chen, X. Huang, W. Lin, C. Ye, W. Tong, L. Cong, J. Geng, Y. Han, L. Li, W. Li, G. Hu, J. Li, Z. Liu, Q. Qi, T. Li, X. Wang, H. Lu, T. Wu, M. Zhu, P. Ni, H. Han, W. Dong, X. Ren, X. Feng, P. Cui, X. Li, H. Wang, X. Xu, W. Zhai, Z. Xu, J. Zhang, S. He, J. Xu, K. Zhang, X. Zheng, J. Dong, W. Zeng, L. Tao, J. Ye, J. Tan, X. Chen, J. He, D. Liu, W. Tian, C. Tian, H. Xia, Q. Bao, G. Li, H. Gao, T. Cao, W. Zhao, P. Li, W. Chen, Y. Zhang, J. Hu, S. Liu, J. Yang, G. Zhang, Y. Xiong, Z. Li, L. Mao, C. Zhou, Z. Zhu, R. Chen, B. Hao, W. Zheng, S. Chen, W. Guo, M. Tao, L. Zhu, L. Yuan, and H. Yang. 2002. A draft sequence of the rice genome (*Oryza sativa* L. ssp. *indica*). *Science*. 296:79-92.

Yu, X., L. Li, M. Guo, J. Chory, and Y. Yin. 2008. Modulation of brassinosteroid-regulated gene expression by Jumonji domain-containing proteins ELF6 and REF6 in *Arabidopsis*. *Proc. Natl. Acad. Sci. U.S.A.* 105:7618-7623.

Zaltsman, A., N. Ori, and Z. Adam. 2005. Two types of FtsH protease subunits are required for chloroplast biogenesis and Photosystem II repair in *Arabidopsis*. *Plant Cell*. 17:2782-2790.

Żelisko, A., M. García-Lorenzo, G. Jackowski, S. Jansson, and C. Funk. 2005. AtFtsH6 is involved in the degradation of the light-harvesting complex II during high-light acclimation and senescence. *Proc. Natl. Acad. Sci. U.S.A.* 102:13699-13704.

Zhai, J.Y. 2001. Making GenePix Array List (GAL) files. In: *Application Note: Genomics*. Axon Instruments, Inc. Union City, CA. (http://www.moleculardevices.com/pdfs/GenePix_Pro_AppNote_Making_GAL_Files.pdf).

Zhou, H.W., C. Nussbaumer, Y. Chao, and A. DeLong. 2004. Disparate roles for the regulatory A subunit isoforms in *Arabidopsis* protein phosphatase 2A. *Plant Cell*. 16:709-722.

SUPPLEMENTARY DATA

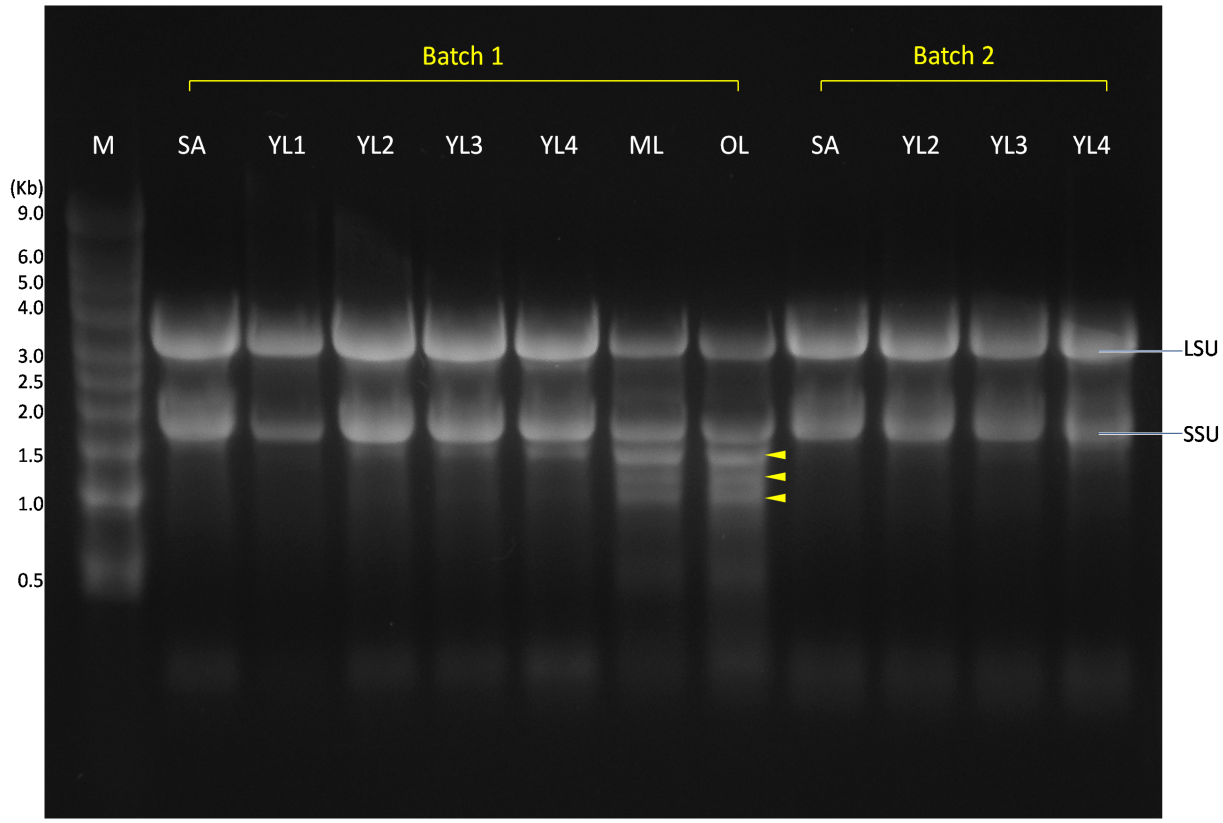

Figure S-1. Formaldehyde denaturing agarose gel electrophoresis of total RNA. Total RNA samples from two extraction batches were loaded on the formaldehyde denaturing agarose gel (1.2%) containing SYBR® Green II RNA Gel Stain (0.1 µl/ml; Cat. #S7564; Invitrogen, Carlsbad, CA), and run in 1X MOPS buffer along with RNA Millennium™ Size Markers (Cat. #7151; Ambion, Austin, TX) (M). Batch 1 includes shoot apex (SA), young leaf 1 through 4 (YL1-YL4), mature leaf (ML) and old leaf (OL), and batch 2 contains SA, YL2, YL3 and YL4. In all samples, bands of large subunit (LSU) rRNA and small subunit (SSU) rRNA are clearly visible, and the LSU bands are significantly brighter than SSU ones, indicating the total RNA extracts are intact. In the samples of ML and OL, the smaller ribosomal RNAs (yellow arrow heads) are observed. However, they become less visible, the younger is the leaf, and hardly visible in samples of SA and YL1. These small ribosomal RNAs are presumably from plastids and mitochondria, but could be the fragments from the broken-down large subunits. In latter case, it dose not necessarily mean the integrity of the RNA products have been compromised, since the bands are reasonably distinctive.

Table S-1. Normalized expression levels and fold ratios of statistically differentially expressed genes in the shoot apex and the young leaf.

Tissue, Expressed in:	Locus Id[a]	GenBank Accession	Expression Level (Normalized Log_2 Value)		Fold Ratio
			Shoot Apex	Young Leaf	
Shoot apex	AT1G04290	N38084	8.43	7.20	2.34
Shoot apex	AT1G09390	AA042309	7.84	6.35	2.80
Shoot apex	AT1G10140	T76366	7.82	6.54	2.43
Shoot apex	AT1G19690	T42600	9.00	7.33	3.18
Shoot apex	AT1G23090	N96564	9.94	8.45	2.79
Shoot apex	AT1G47860	R65207	8.35	6.70	3.14
Shoot apex	AT1G56140	T46398	7.92	6.48	2.71
Shoot apex	AT1G58080	T42357	8.42	7.28	2.21
Shoot apex	AT1G61690	R65048	8.36	7.20	2.23
Shoot apex	AT1G64740	T43389	8.07	6.48	2.99
Shoot apex	AT1G66180	R30258	8.91	7.57	2.54
Shoot apex	AT1G70850	R90370	8.52	7.37	2.22
Shoot apex	AT1G70900	T21553	9.19	7.73	2.75
Shoot apex	AT1G79040	N64965	8.26	7.08	2.27
Shoot apex	AT1G79730	W43382	8.62	7.56	2.08
Shoot apex	AT2G01100	R65004	7.90	6.46	2.70
Shoot apex	AT2G02160	H37017	9.25	7.84	2.65
Shoot apex	AT2G03480	N96755	7.76	6.00	3.39
Shoot apex	AT2G04160	R65329	8.09	7.01	2.10
Shoot apex	AT2G05070	N65841	8.04	6.84	2.28
Shoot apex	AT2G16280	N65624	8.11	7.06	2.07
Shoot apex	AT2G22610	N96076	7.76	6.37	2.62
Shoot apex	AT2G26640	T88116	8.33	6.90	2.70
Shoot apex	AT2G27730	N96894	8.16	6.90	2.39
Shoot apex	AT2G31440	AA042199	9.56	8.30	2.39
Shoot apex	AT2G38730	R90624	8.80	7.67	2.17
Shoot apex	AT2G41060	T44669	7.78	6.70	2.11
Shoot apex	AT2G42030	N38456	8.29	6.67	3.07
Shoot apex	AT2G47760	T43898	8.64	7.49	2.22
Shoot apex	AT3G03070	AA040947	8.57	6.80	3.41
Shoot apex	AT3G13080	T22571	8.41	5.95	5.50
Shoot apex	AT3G13730	R30379	8.92	7.68	2.36
Shoot apex	AT3G15360	AA041000	8.05	6.45	3.03

Table S-1. *(Cont'd)* Normalized expression levels and fold ratios of statistically differentially expressed genes in the shoot apex and the young leaf.

Tissue, Expressed in:	Locus Id[a]	GenBank Accession	Expression Level (Normalized Log_2 Value)		Fold Ratio
			Shoot Apex	Young Leaf	
Shoot apex	AT3G20320	N65377	7.95	6.86	2.13
Shoot apex	AT3G23660	T43752	8.53	6.88	3.14
Shoot apex	AT3G23750	T75836	7.64	6.19	2.74
Shoot apex	AT3G25800	N96135	8.30	7.30	2.00
Shoot apex	AT3G29000	T22328	8.94	7.27	3.18
Shoot apex	AT3G45730	R90055	8.31	7.15	2.22
Shoot apex	AT3G48430	T20781	7.98	6.71	2.42
Shoot apex	AT4G02380	H37120	8.47	7.23	2.36
Shoot apex	AT4G04885	T46431	8.58	7.53	2.07
Shoot apex	AT4G15570	N65040	8.22	6.99	2.34
Shoot apex	AT4G17340	T44758	8.58	6.77	3.51
Shoot apex	AT4G22120	T45917	9.51	7.64	3.63
Shoot apex	AT4G27652	T20758	8.90	7.81	2.12
Shoot apex	AT4G28260	T76283	8.16	6.45	3.26
Shoot apex	AT4G35750	T42554	8.53	6.96	2.96
Shoot apex	AT5G04140	T44042	8.15	6.58	2.97
Shoot apex	AT5G05670	T42371	9.23	8.12	2.16
Shoot apex	AT5G05730	N65620	7.83	6.75	2.11
Shoot apex	AT5G20490	T45160	8.45	7.31	2.20
Shoot apex	AT5G40200	T21425	8.46	7.43	2.04
Shoot apex	AT5G45510	N65552	8.78	7.52	2.39
Shoot apex	AT5G47880	N38610	8.35	7.26	2.12
Shoot apex	AT5G52510	H36280	8.11	6.97	2.20
Shoot apex	AT5G57490	T76108	7.43	6.16	2.41
Shoot apex	AT5G61270	T21699	8.88	7.53	2.53
Shoot apex	AT5G65540	N96308	8.38	7.35	2.03
Shoot apex	ATMG00020	N95849	11.99	10.96	2.04
Young leaf	AT1G03290	H36966	8.38	9.48	2.14
Young leaf	AT1G06040	H36917	8.54	9.56	2.02
Young leaf	AT1G09420	N37552	11.72	12.86	2.21
Young leaf	AT1G09570	W43836	7.82	8.94	2.16
Young leaf	AT1G10040	T46432	5.97	7.48	2.85
Young leaf	AT1G10290	W43823	8.20	9.36	2.23

Table S-1. *(Cont'd)* Normalized expression levels and fold ratios of statistically differentially expressed genes in the shoot apex and the young leaf.

Tissue, Expressed in:	Locus Id[a]	GenBank Accession	Expression Level (Normalized Log_2 Value)		Fold Ratio
			Shoot Apex	Young Leaf	
Young leaf	AT1G14710	N96674	6.18	7.66	2.79
Young leaf	AT1G17340	W43750	6.95	8.06	2.15
Young leaf	AT1G18040	T43700	7.79	9.09	2.45
Young leaf	AT1G20440	T45106	7.12	8.14	2.03
Young leaf	AT1G21750	T42754	8.20	9.40	2.29
Young leaf	AT1G26630	W43100	7.08	8.37	2.43
Young leaf	AT1G27510	N65787	7.80	8.83	2.03
Young leaf	AT1G36730	H36042	8.38	9.42	2.04
Young leaf	AT1G45130	T42360	7.15	8.54	2.62
Young leaf	AT1G48440	T46290	7.34	8.56	2.33
Young leaf	AT1G48540	W43535	8.54	9.70	2.23
Young leaf	AT1G53310	W43501	8.26	9.54	2.41
Young leaf	AT1G53910	T41899	8.09	9.19	2.14
Young leaf	AT1G60890	N37920	8.66	9.78	2.15
Young leaf	AT1G62480	R65450	7.17	8.21	2.04
Young leaf	AT1G64790	AA042471	7.85	8.90	2.06
Young leaf	AT1G64860	T88387	8.00	9.01	2.01
Young leaf	AT1G66940	T44206	8.52	9.68	2.22
Young leaf	AT1G67090	AA042318	6.18	8.49	4.97
Young leaf	AT1G73190	H37171	8.28	9.79	2.85
Young leaf	AT1G75630	AA041170	7.74	8.79	2.07
Young leaf	AT1G75950	AA041150	13.15	14.34	2.29
Young leaf	AT2G01450	N96333	6.07	7.47	2.63
Young leaf	AT2G06850	T21988	6.98	8.32	2.52
Young leaf	AT2G14170	R90227	6.68	8.17	2.80
Young leaf	AT2G18110	N97130	7.10	8.30	2.30
Young leaf	AT2G22720	N97072	7.41	8.53	2.16
Young leaf	AT2G24400	H37493	8.00	9.23	2.34
Young leaf	AT2G26080	T43739	7.23	8.66	2.70
Young leaf	AT2G30505	T43338	8.29	9.41	2.16
Young leaf	AT2G30600	W43672	6.95	8.00	2.07
Young leaf	AT2G33810	W43355	7.45	8.52	2.09
Young leaf	AT2G36810	W43407	8.32	9.36	2.05

Table S-1. *(Cont'd)* Normalized expression levels and fold ratios of statistically differentially expressed genes in the shoot apex and the young leaf.

Tissue, Expressed in:	Locus Id[a]	GenBank Accession	Expression Level (Normalized Log_2 Value)		Fold Ratio
			Shoot Apex	Young Leaf	
Young leaf	AT2G40150	H37615	7.89	9.19	2.47
Young leaf	AT2G44410	H37336	7.55	8.71	2.22
Young leaf	AT2G45140	N65366	7.49	8.49	2.00
Young leaf	AT2G45960	H76521	8.77	9.84	2.10
Young leaf	AT2G46260	T20881	7.81	9.42	3.05
Young leaf	AT3G02450	T46384	5.90	7.37	2.77
Young leaf	AT3G03120	H77070	7.32	8.60	2.41
Young leaf	AT3G03920	N65654	7.37	8.50	2.18
Young leaf	AT3G05560	T88520	8.50	9.67	2.24
Young leaf	AT3G09260	N65420	12.55	14.42	3.65
Young leaf	AT3G09830	N95900	7.43	8.85	2.67
Young leaf	AT3G15210	N65389	8.22	9.41	2.26
Young leaf	AT3G16370	N37598	7.10	8.20	2.13
Young leaf	AT3G20410	N96718	8.26	9.32	2.07
Young leaf	AT3G26780	T21648	6.93	8.00	2.10
Young leaf	AT3G27010	R84108	8.17	9.36	2.28
Young leaf	AT3G27380	T76709	7.34	8.34	2.00
Young leaf	AT3G41768	N37617[b]	12.59	13.95	2.55
Young leaf	AT3G41768	N38563[b]	11.58	13.14	2.95
Young leaf	AT3G43800	T43130	6.94	8.03	2.12
Young leaf	AT3G44880	N37395	7.40	8.42	2.01
Young leaf	AT3G44890	R30312	6.34	8.08	3.35
Young leaf	AT3G45780	W43664	6.79	8.13	2.54
Young leaf	AT3G48780	R64760	8.27	9.32	2.06
Young leaf	AT3G52850	N96879	6.69	8.08	2.62
Young leaf	AT3G53430	T42421[c]	5.95	8.02	4.19
Young leaf	AT3G53430	T75791[c]	5.81	8.12	4.95
Young leaf	AT3G53430	W43275[c]	8.38	9.69	2.47
Young leaf	AT3G56240	H76196	8.22	9.35	2.18
Young leaf	AT3G61415	N38071	8.55	10.28	3.32
Young leaf	AT3G62290	T46252	7.35	8.56	2.30
Young leaf	AT3G62410	T45735	8.33	9.46	2.17
Young leaf	AT4G02930	T46137	6.27	7.74	2.77

Table S-1. *(Cont'd)* Normalized expression levels and fold ratios of statistically differentially expressed genes in the shoot apex and the young leaf.

Tissue, Expressed in:	Locus Id[a]	GenBank Accession	Expression Level (Normalized Log_2 Value)		Fold Ratio
			Shoot Apex	Young Leaf	
Young leaf	AT4G12360	T42221	8.25	9.41	2.23
Young leaf	AT4G12800	AA042646	6.19	7.83	3.12
Young leaf	AT4G14350	H76719	7.23	8.30	2.10
Young leaf	AT4G16670	H76174	8.39	9.63	2.36
Young leaf	AT4G17486	H36563	6.38	8.26	3.68
Young leaf	AT4G17830	T45601	11.10	12.46	2.56
Young leaf	AT4G25650	T88375	7.34	8.78	2.72
Young leaf	AT4G26060	T76182	6.70	7.84	2.19
Young leaf	AT4G28080	AA042475	6.55	8.39	3.58
Young leaf	AT4G30390	T76400	8.48	9.72	2.36
Young leaf	AT4G31720	H76292	7.86	9.14	2.43
Young leaf	AT4G32780	T42550	6.13	7.44	2.47
Young leaf	AT4G36440	T88343	7.81	9.34	2.88
Young leaf	AT4G37520	H76577	7.20	8.38	2.26
Young leaf	AT5G01820	W43158	6.75	7.94	2.27
Young leaf	AT5G09530	T22771	6.99	8.51	2.87
Young leaf	AT5G14030	T88470	7.45	8.48	2.04
Young leaf	AT5G16130	T43999	8.18	9.27	2.11
Young leaf	AT5G25350	N38266	12.62	13.95	2.52
Young leaf	AT5G26740	AA042683	6.83	8.06	2.35
Young leaf	AT5G26742	N95880	7.44	9.12	3.21
Young leaf	AT5G35690	N95870	8.29	9.36	2.10
Young leaf	AT5G38430	H77160[d]	8.05	9.13	2.11
Young leaf	AT5G38430	N65749[d]	7.41	8.62	2.30
Young leaf	AT5G38430	T43328[d]	6.47	8.14	3.16
Young leaf	AT5G40170	N65076	8.04	9.14	2.14
Young leaf	AT5G41360	T76410	7.82	8.88	2.09
Young leaf	AT5G42500	R89967	7.65	9.08	2.69
Young leaf	AT5G43280	T43247	6.92	8.14	2.34
Young leaf	AT5G48480	AA067454	8.08	9.21	2.19
Young leaf	AT5G49910	T43623	8.05	9.32	2.41
Young leaf	AT5G53460	N95884	8.01	9.41	2.63
Young leaf	AT5G58620	H36962	6.86	7.94	2.12

Table S-1. *(Cont'd)* Normalized expression levels and fold ratios of statistically differentially expressed genes in the shoot apex and the young leaf.

Tissue, Expressed in:	Locus Id[a]	GenBank Accession	Expression Level (Normalized Log_2 Value)		Fold Ratio
			Shoot Apex	Young Leaf	
Young leaf	AT5G59850	N96893	8.03	9.28	2.37
Young leaf	AT5G66190	T46002	5.65	8.07	5.33
Young leaf	ATCG00950	AA042713	12.34	13.96	3.08
Young leaf	no match	N37911	13.54	15.10	2.93
Young leaf	in	R30010	7.39	8.46	2.10
Young leaf	TAIR	T46184	6.69	8.36	3.16
Young leaf	database[e]	N37896	11.31	12.36	2.06
Young leaf		T20605	13.85	15.15	2.45
Young leaf		H77104	12.72	14.31	3.00

[a.] Among 114 EST spots representing genes preferentially expressed in the young leaf, 8 GenBank accession numbers were mapped to 3 AGI locus identifiers. Every EST representing genes that were preferentially expressed in the shoot apex had a unique corresponding AGI locus identifier.

[b.] Two ESTs (N37617, N38563) were mapped to AT3G41768.

[c.] Three ESTs (T42421, T75791, W43275) were mapped to AT3G53430.

[d.] Three ESTs (H77160, N65749, T43328) were mapped to AT5G38430.

[e.] There were 6 ESTs that were mapped to no AGI locus identifiers. Thus, 103 ESTs from the young leaf sample and 60 ESTs from the shoot apex sample were considered for the functional annotation.

Figure S-2. Graphical view of gene counts in GO slim functional categories for all genes expressed differentially in the shoot apex and the young leaf. One hundred sixty three genes matching to unique AGI locus identifiers at TAIR database were categorized based on GO slim keywords: biological processes (top panel), in which the genes are involved; molecular functions (middle), which the genes have; cellular components (bottom), in which the gene products are acting. Most of the genes were associated more than one functional categories.

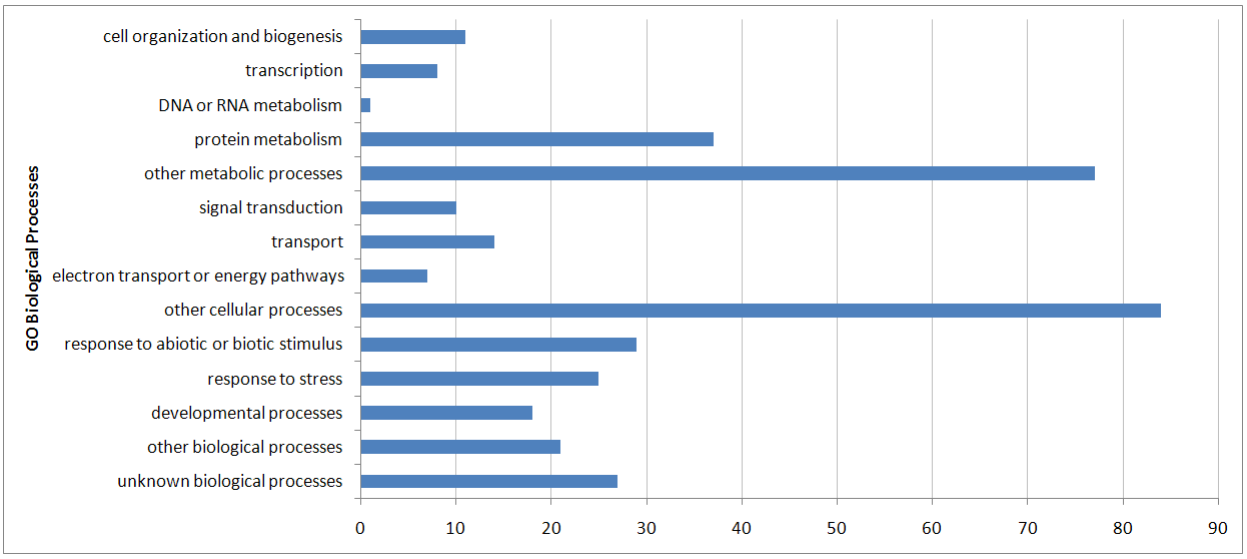
GO Biological Processes
cell organization and biogenesis
transcription
DNA or RNA metabolism
protein metabolism
other metabolic processes
signal transduction
transport
electron transport or energy pathways
other cellular processes
response to abiotic or biotic stimulus
response to stress
developmental processes
other biological processes
unknown biological processes
0
10
20
30
40
50
60
70
80
90

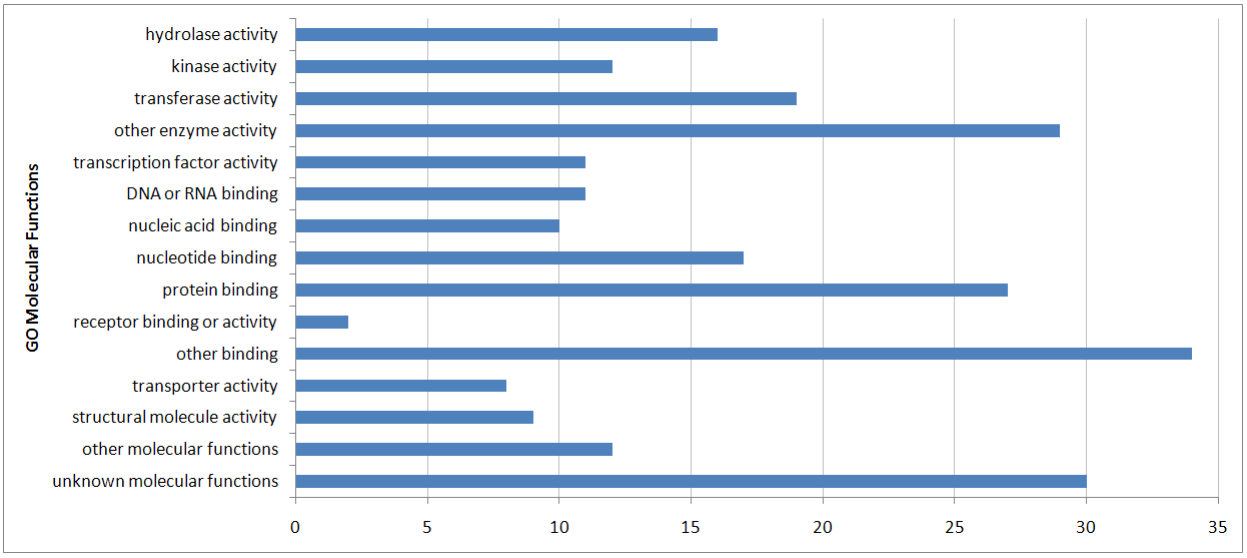
GO Molecular Functions
hydrolase activity
kinase activity
transferase activity
other enzyme activity
transcription factor activity
DNA or RNA binding
nucleic acid binding
nucleotide binding
protein binding
receptor binding or activity
other binding
transporter activity
structural molecule activity
other molecular functions
unknown molecular functions
0
5
10
15
20
25
30
35

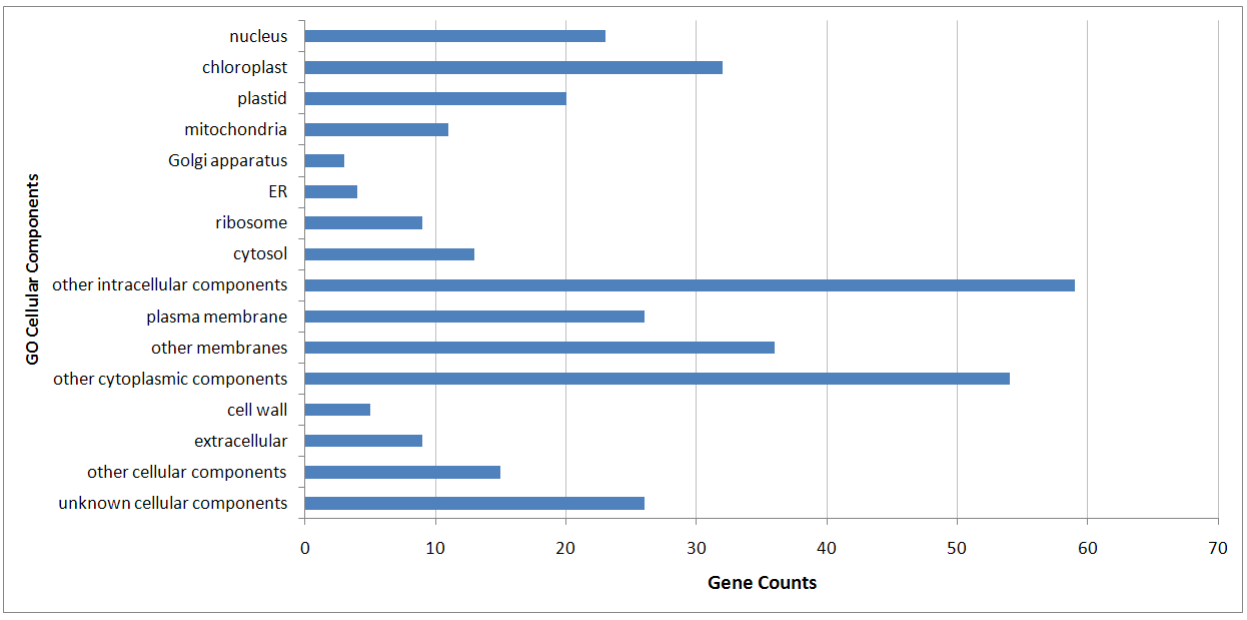
GO Cellular Components
nucleus
chloroplast
plastid
mitochondria
Golgi apparatus
ER
ribosome
cytosol
other intracellular components
plasma membrane
other membranes
other cytoplasmic components
cell wall
extracellular
other cellular components
unknown cellular components
0
10
20
30
40
50
60
70
Gene Counts

Figure S-3. Comparison of gene counts in GO slim functional categories between tissue types. Genes that were expressed differentially in the shoot apex and the young leaf were categorized separately and the gene counts in each functional category were compared between the shoot apex and the young leaf. As the total number of genes preferentially expressed in the young leaf was much higher than those in the shoot apex (103 *vs*. 60), the ratios of gene counts in the functional categories were similarly proportionated in general. Among those preferentially expressed in the shoot apex, no genes were involved in the biological process of 'DNA or RNA metabolism' or had 'receptor binding or receptor activity'.

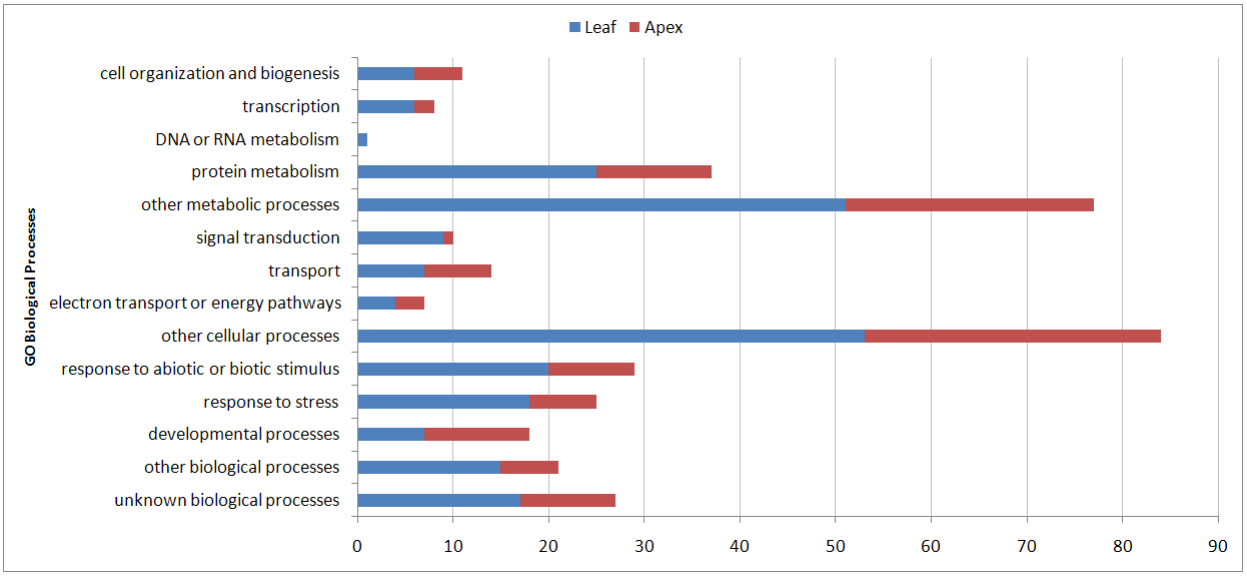
Leaf
Apex
GO Biological Processes
cell organization and biogenesis
transcription
DNA or RNA metabolism
protein metabolism
other metabolic processes
signal transduction
transport
electron transport or energy pathways
other cellular processes
response to abiotic or biotic stimulus
response to stress
developmental processes
other biological processes
unknown biological processes
0
10
20
30
40
50
60
70
80
90

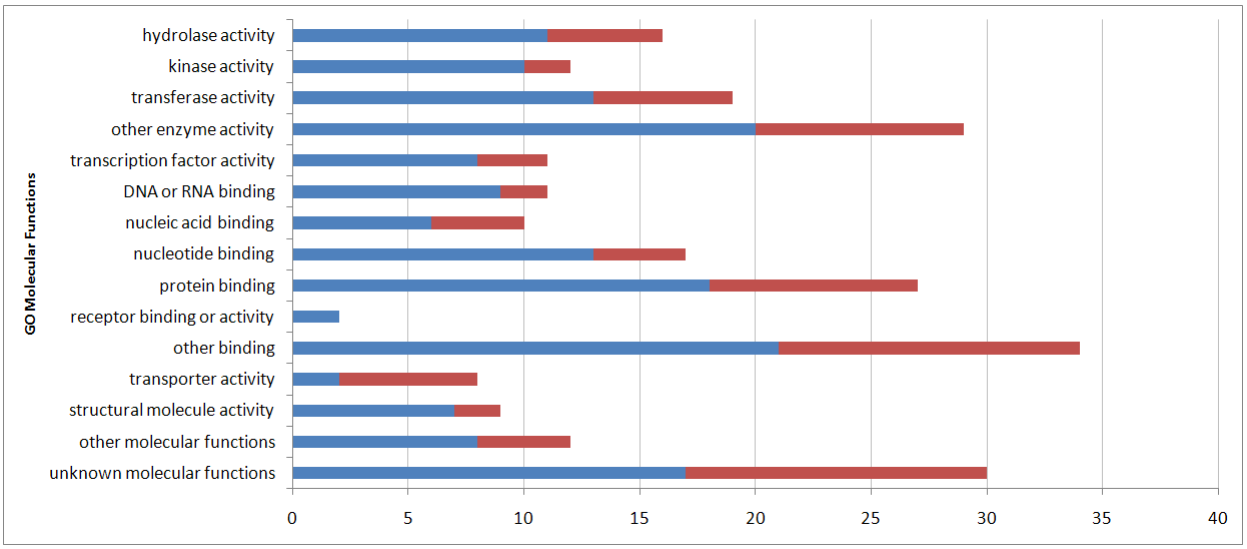
GO Molecular Functions
hydrolase activity
kinase activity
transferase activity
other enzyme activity
transcription factor activity
DNA or RNA binding
nucleic acid binding
nucleotide binding
protein binding
receptor binding or activity
other binding
transporter activity
structural molecule activity
other molecular functions
unknown molecular functions
0
5
10
15
20
25
30
35
40

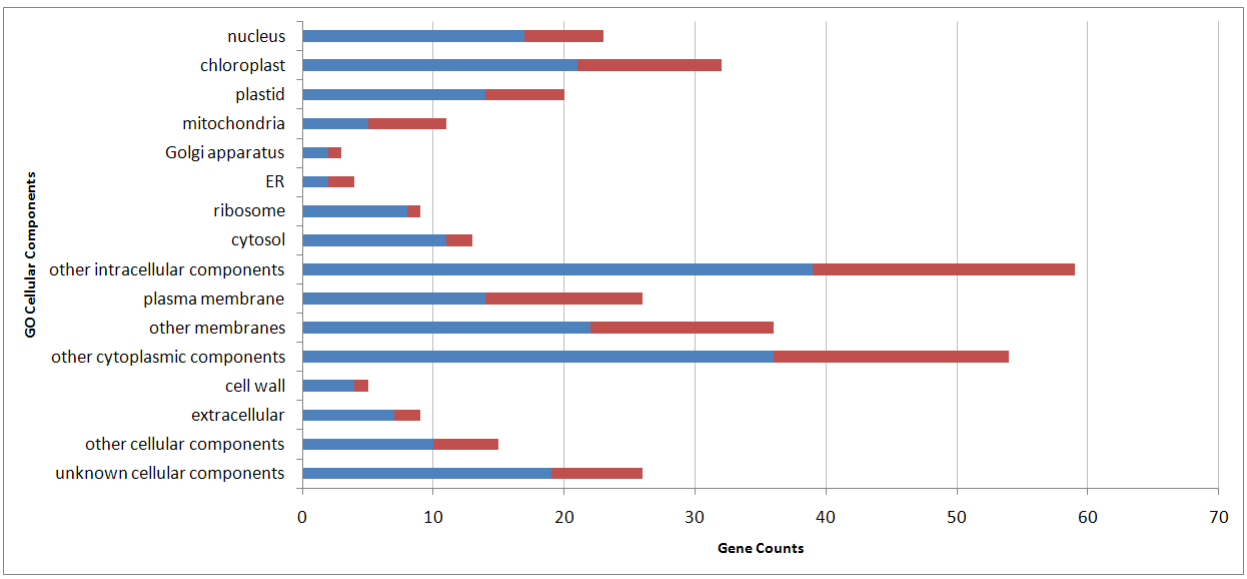
GO Cellular Components
nucleus
chloroplast
plastid
mitochondria
Golgi apparatus
ER
ribosome
cytosol
other intracellular components
plasma membrane
other membranes
other cytoplasmic components
cell wall
extracellular
other cellular components
unknown cellular components
0
10
20
30
40
50
60
70
Gene Counts

Table S-2. The numbers of genes and annotations associated with each functional category in GO slim.

Keyword Category	Functional Category	Gene Count		Annotation Count	
		Shoot apex	Young leaf	Shoot apex	Young leaf
GO Cellular Component	other intracellular components	21	39	34	75
	other cytoplasmic components	19	36	26	61
	other membranes	13	22	18	27
	plasma membrane	12	14	12	16
	chloroplast	11	21	21	43
	unknown cellular components	8	19	8	19
	nucleus	6	15	6	17
	plastid	6	14	11	27
	mitochondria	6	5	8	5
	other cellular components	4	10	4	11
	ribosome	2	8	3	13
	extracellular	2	7	2	7
	ER	2	2	2	2
	cytosol	1	6	1	8
	cell wall	1	4	1	5
	Golgi apparatus	1	2	1	4
GO Molecular Function	unknown molecular functions	14	17	14	17
	other binding	8	13	9	13
	other enzyme activity	8	18	8	20
	transferase activity	6	11	6	11
	protein binding	6	14	6	14
	transporter activity	6	2	8	2
	hydrolase activity	5	10	7	12
	other molecular functions	4	7	4	8
	transcription factor activity	3	7	3	7
	structural molecule activity	3	7	3	7
	DNA or RNA binding	2	6	3	6
	kinase activity	2	10	2	14
	nucleic acid binding	2	4	2	4
	nucleotide binding	0	8	0	8
	receptor binding or activity	0	2	0	3
GO Biological Process	other cellular processes	30	53	42	71
	other metabolic processes	26	50	31	60
	protein metabolism	12	25	13	26

Table S-2. *(Cont'd)* The numbers of genes and annotations associated with each functional category in

Keyword Category	Functional Category	Gene Count		Annotation Count	
		Shoot apex	Young leaf	Shoot apex	Young leaf
	developmental processes	11	6	19	9
	unknown biological processes	10	16	10	16
	response to abiotic or biotic stimulus	9	21	13	43
	response to stress	8	19	11	27
	transport	7	7	8	11
	other biological processes	6	14	6	17
	cell organization and biogenesis	6	6	9	7
	transcription	2	6	2	7
	electron transport or energy pathways	2	4	2	4
	signal transduction	1	9	1	10
	DNA or RNA metabolism	0	1	0	1

Figure S-4. Hierarchical cluster analysis of genes expressed preferentially in the shoot apex. Expression levels were transformed to log base 2 and subjected to Euclidian distance linkage clustering in GeneSpring GX 10 software to identify and group the genes that were similarly up-regulated in the shoot apex and infer any biological significance of the groups of genes. In the dendrogram, 60 genes were grouped into four major clusters (0 to 3) based on the branching patterns, which were indications of similarities in the expression level. At the first level of branching, the cluster 3, which was represented by single gene (N95849), was separated from the all of the other genes in the list. At the second level, cluster 2, which had 17 genes, clearly branched from others by their high expression levels. At the third level, clusters 1 and 2 were separated, consisting of 18 and 24 genes, respectively. When each cluster of genes was subjected to classification by GO functional categories, there was no clear relationship between functional categories and clustering of genes (See Figure S-5 on page 135). While the genes of cluster 0 were represented in most functional categories, those in other clusters were represented in limited numbers of the functional categories. This probably was due to the small number of genes in those clusters, rather than the nature of the genes in the cluster. Color indicates magnitude of expression levels for the denoted genes (red, higher; blue, lower).

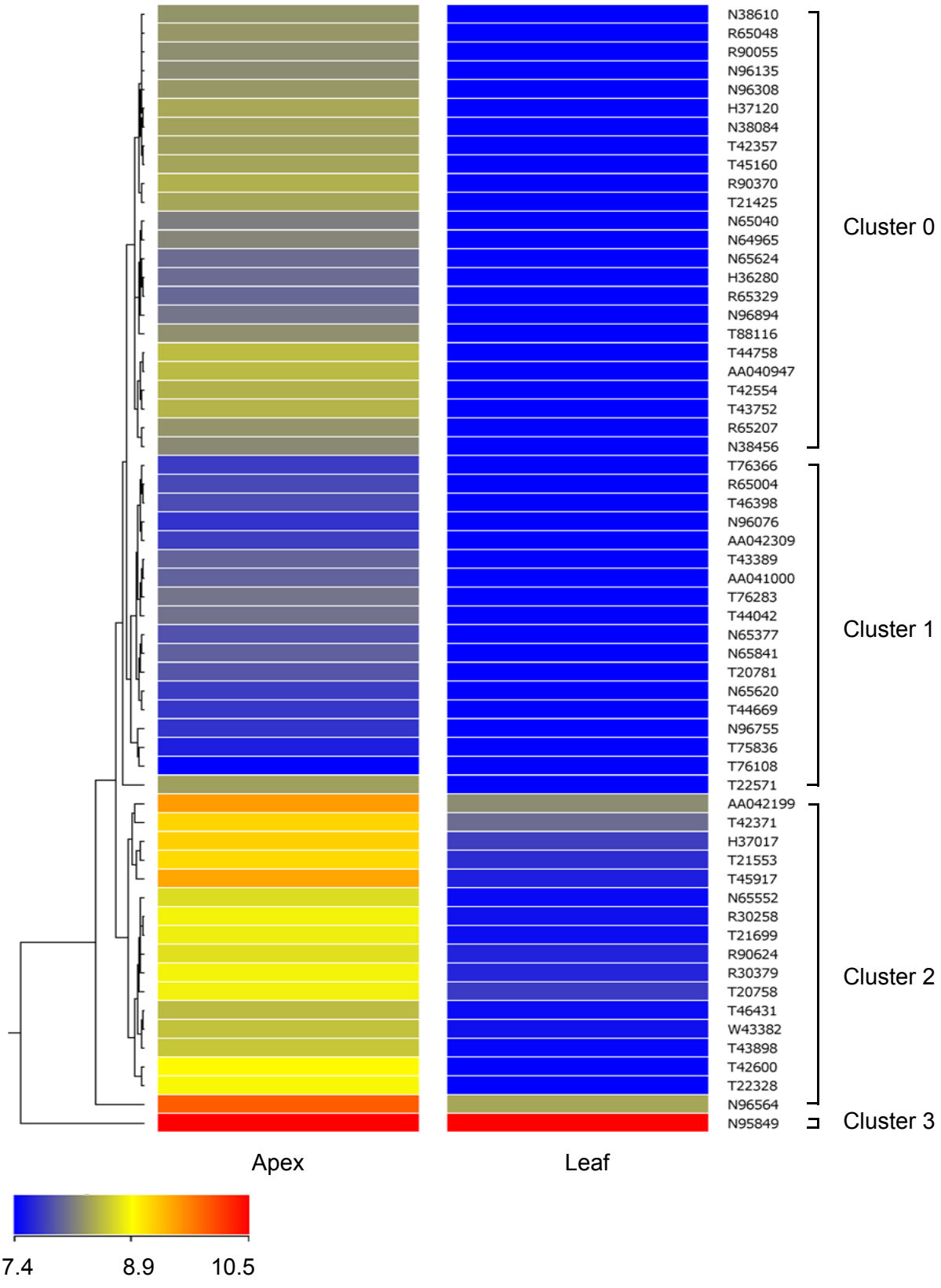
N38610
R65048
R90055
N96135
N96308
H37120
N38084
T42357
T45160
R90370
T21425
N65040
N64965
N65624
H36280
R65329
N96894
T88116
T44758
AA040947
T42554
T43752
R65207
N38456
T76366
R65004
T46398
N96076
AA042309
T43389
AA041000
T76283
T44042
N65377
N65841
T20781
N65620
T44669
N96755
T75836
T76108
T22571
AA042199
T42371
H37017
T21553
T45917
N65552
R30258
T21699
R90624
R30379
T20758
T46431
W43382
T43898
T42600
T22328
N96564
N95849
Cluster 0
Cluster 1
Cluster 2
Cluster 3
Apex
Leaf
7.4
8.9
10.5

Figure S-5. GO slim functional categorization of genes expressed higher in shoot apex by hierarchical clustering. The hierarchical clustering applied to the gene set expressed preferentially in the shoot apex did not appear to lead to a meaningful functional categorization

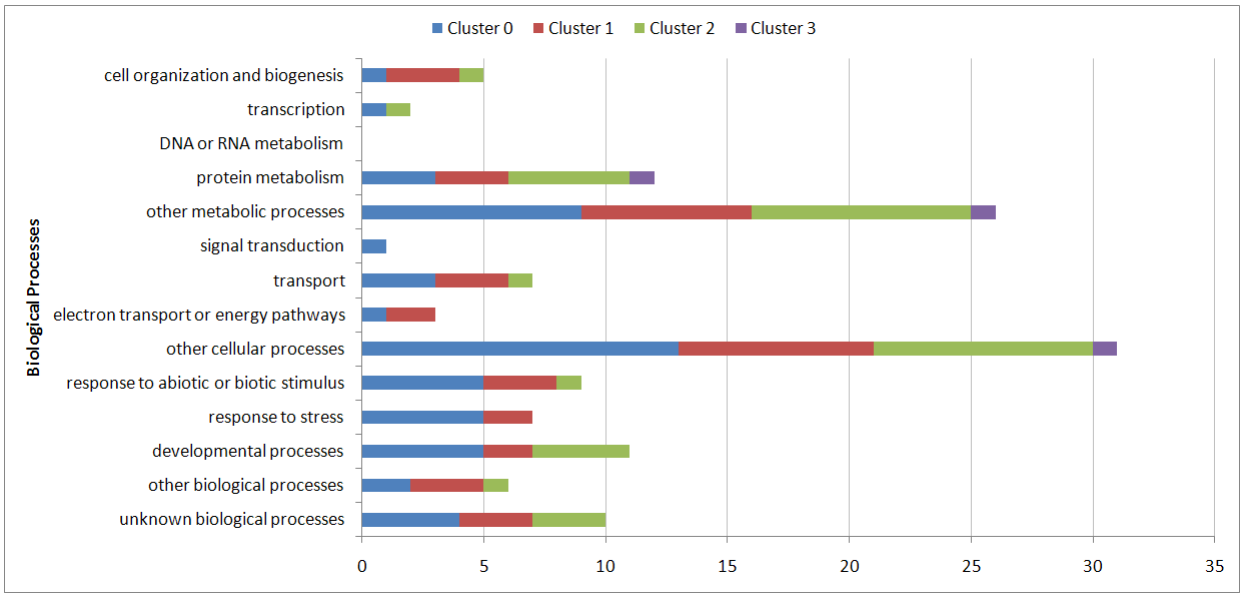
Cluster 0
Cluster 1
Cluster 2
Cluster 3
Biological Processes
cell organization and biogenesis
transcription
DNA or RNA metabolism
protein metabolism
other metabolic processes
signal transduction
transport
electron transport or energy pathways
other cellular processes
response to abiotic or biotic stimulus
response to stress
developmental processes
other biological processes
unknown biological processes
0
5
10
15
20
25
30
35

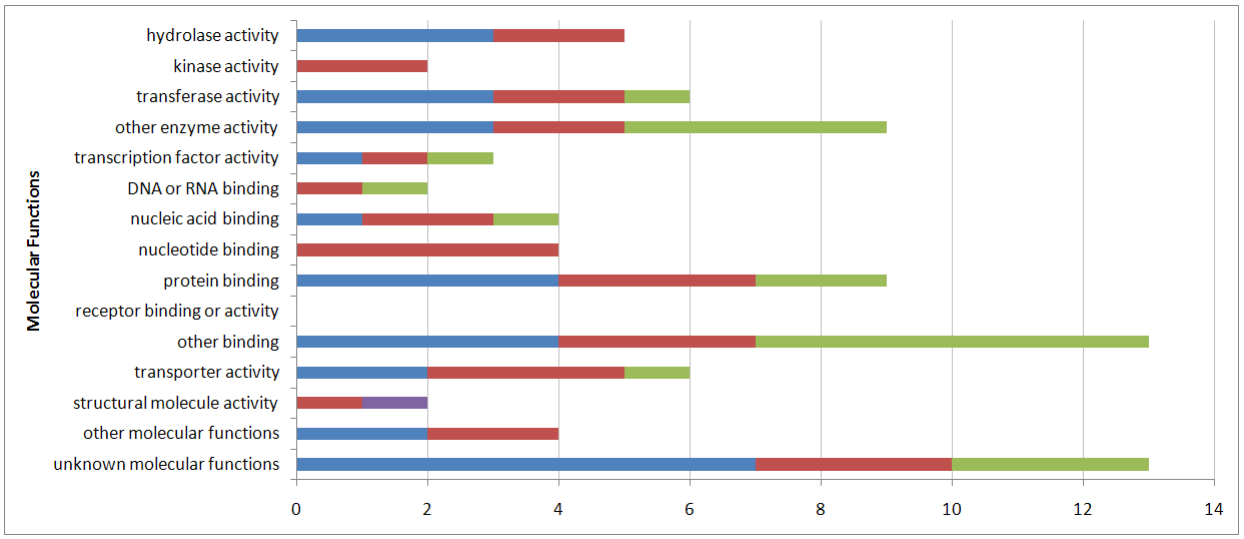
Molecular Functions
hydrolase activity
kinase activity
transferase activity
other enzyme activity
transcription factor activity
DNA or RNA binding
nucleic acid binding
nucleotide binding
protein binding
receptor binding or activity
other binding
transporter activity
structural molecule activity
other molecular functions
unknown molecular functions
0
2
4
6
8
10
12
14

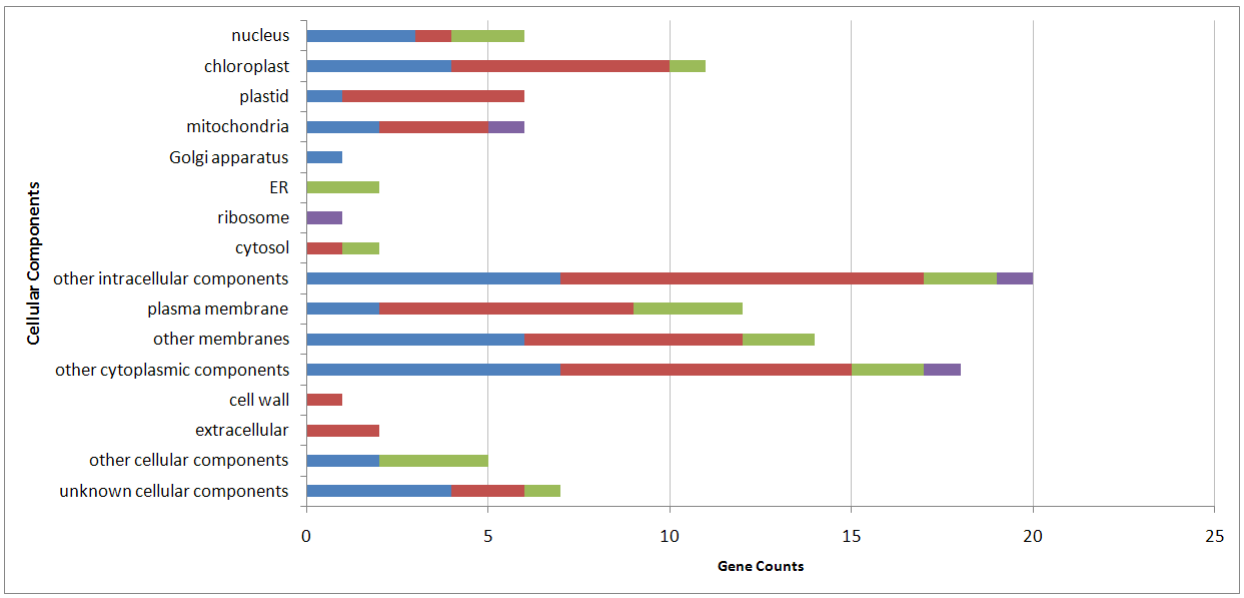
Cellular Components
nucleus
chloroplast
plastid
mitochondria
Golgi apparatus
ER
ribosome
cytosol
other intracellular components
plasma membrane
other membranes
other cytoplasmic components
cell wall
extracellular
other cellular components
unknown cellular components
0
5
10
15
20
25
Gene Counts

Figure S-6. Hierarchical cluster analysis of genes expressed preferentially in the young leaf. Expression levels were transformed and subjected to Euclidian distance linkage clustering as with those in the shoot apex (See Figure S-4 on page 133). In the dendrogram, 114 genes were grouped into three major clusters (0 to 2). At the first level of branching, the cluster 2, including 12 genes, was clearly branched from others by high expression levels of the genes (red). At the second level, clusters 1 and 2 were separated, consisting of 48 and 54genes, respectively. When each cluster of genes was subjected to classification by GO functional categories, there was no clear relationship between functional categories and clustering of genes (See Figure S-7 on page 139).

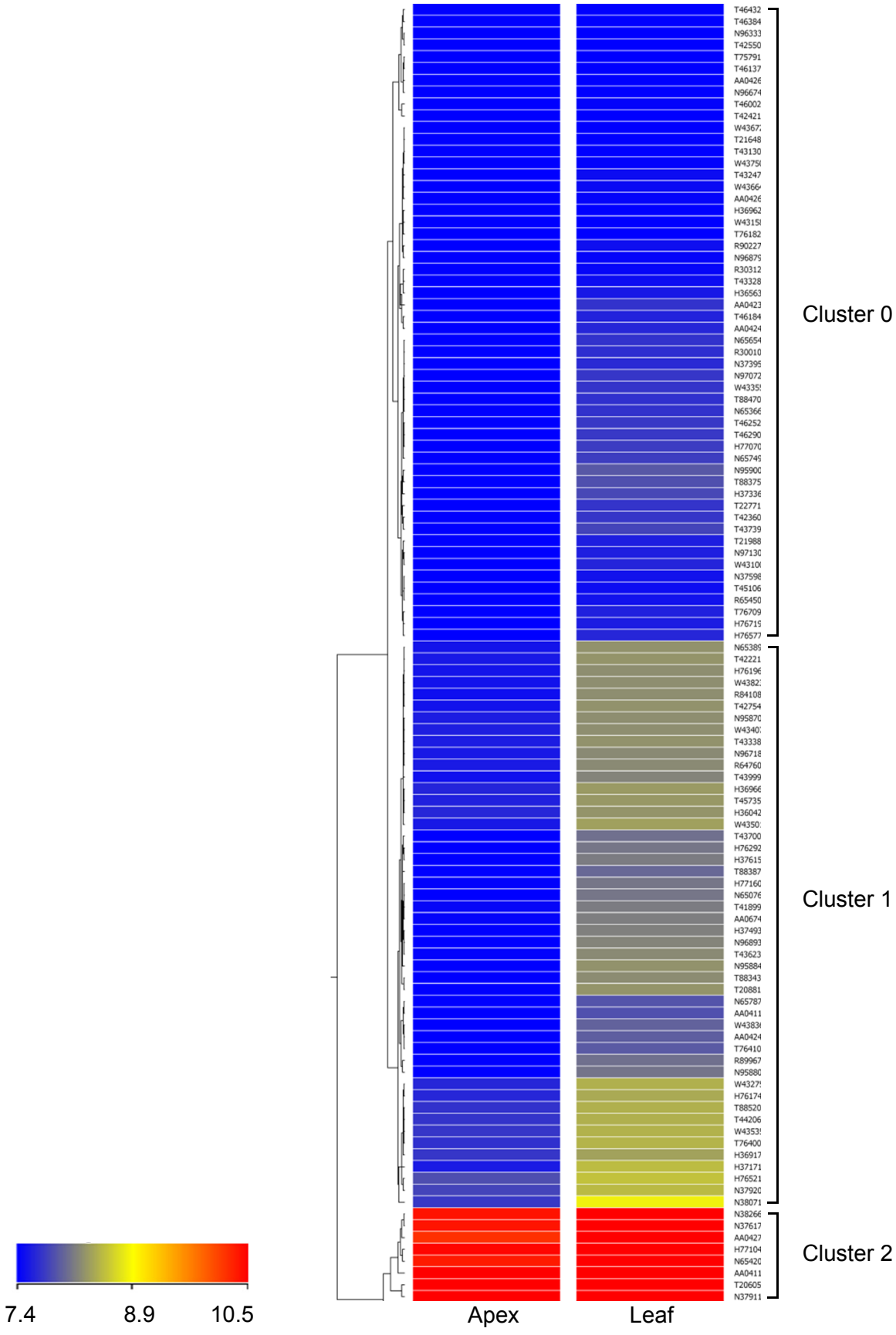
Cluster 0
Cluster 1
Cluster 2
7.4
8.9
10.5
Apex
Leaf

Figure S-7. GO slim functional categorization of genes expressed higher in the young leaf by hierarchical clustering. The hierarchical clustering applied to the gene set expressed preferentially in the young leaf did not appear to lead to a meaningful functional categorization.

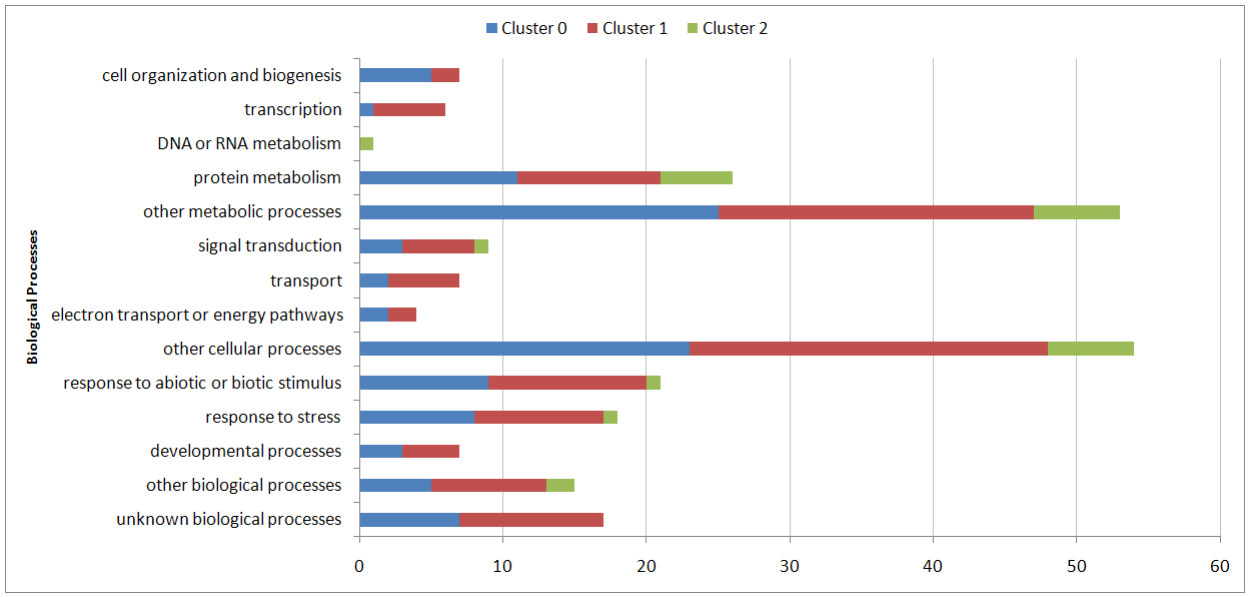
Cluster 0
Cluster 1
Cluster 2
Biological Processes
cell organization and biogenesis
transcription
DNA or RNA metabolism
protein metabolism
other metabolic processes
signal transduction
transport
electron transport or energy pathways
other cellular processes
response to abiotic or biotic stimulus
response to stress
developmental processes
other biological processes
unknown biological processes
0
10
20
30
40
50
60

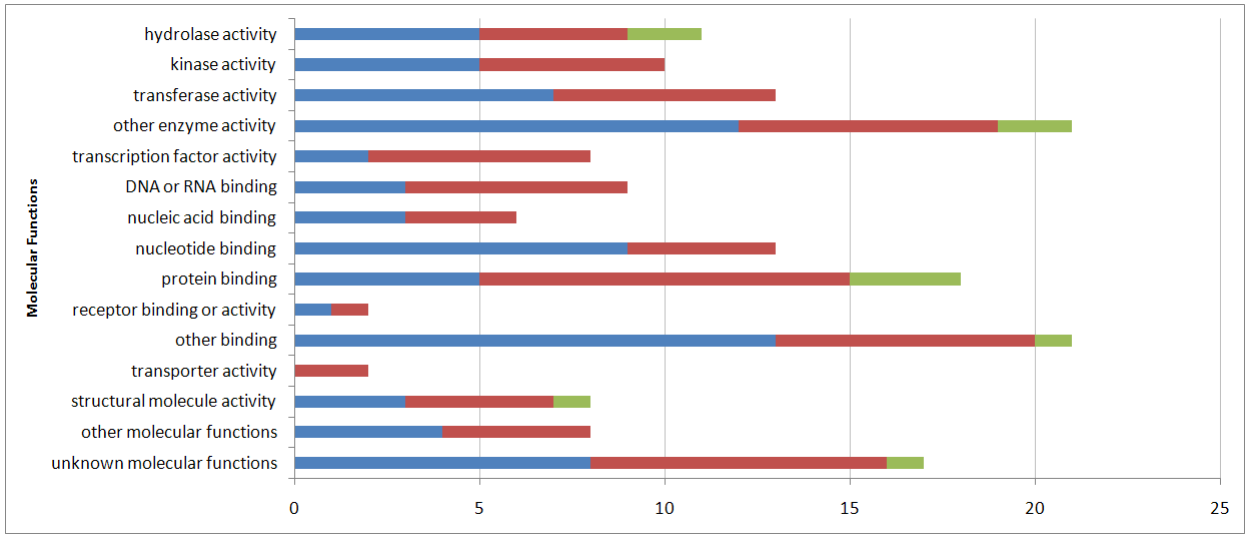
Molecular Functions
hydrolase activity
kinase activity
transferase activity
other enzyme activity
transcription factor activity
DNA or RNA binding
nucleic acid binding
nucleotide binding
protein binding
receptor binding or activity
other binding
transporter activity
structural molecule activity
other molecular functions
unknown molecular functions
0
5
10
15
20
25

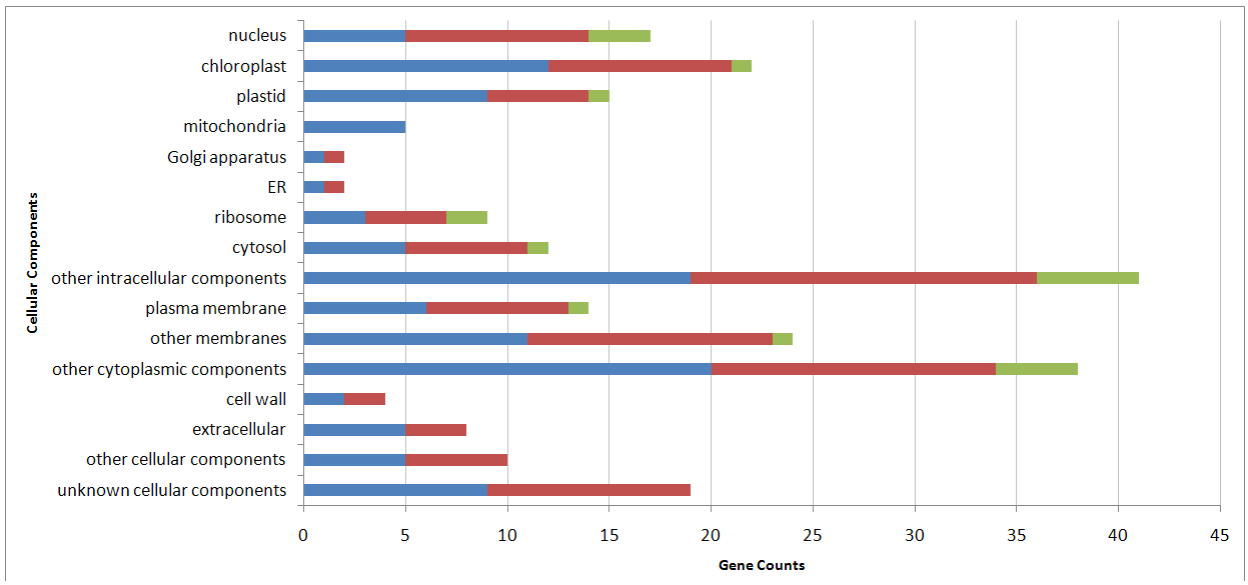
Cellular Components
nucleus
chloroplast
plastid
mitochondria
Golgi apparatus
ER
ribosome
cytosol
other intracellular components
plasma membrane
other membranes
other cytoplasmic components
cell wall
extracellular
other cellular components
unknown cellular components
0
5
10
15
20
25
30
35
40
45
Gene Counts

Table S-3. Number of genes involved in biological processes categorized manually.

Biological Process	Expressed higher in Shoot Apex	Expressed higher in Young Leaf
Cell cycle control/DNA Repair	0	3
Cytoskeletal organization	3	0
Energy/Respiration	0	2
Energy/Photorespiration	3	1
Photosynthesis, light reaction	2	2
Photosynthesis, dark reaction	0	3
Metabolism: Amino acid	1	1
Metabolism: Carbohydrate	0	2
Metabolism: Lipid	4	4
Metabolism: Hormone	2	0
Metabolism: Chlorophyll degradation	0	3
Metabolism: Other	3	2
Protein fate: Translation	2	12
Protein fate: processing and folding	1	2
Protein fate: sorting/targeting	1	0
Protein fate: modification	1	2
Protein fate: degradation	4	1
Transcription/RNA processing	5	6
Signal transduction	7	22
Transport/Vesicle trafficking	6	7
Other cellular process	1	1
Response to abiotic stimulus	4	6
Response to biotic stimulus	0	2
Unknown	10	19
Total	**60**	**103**

Table S-4. Expression levels of genes identified as preferentially expressed in the shoot apex by Expression Browser.

AGI Locus	Shoot Apex	Leaf 1 & 2	Affymetrix Annotation
AT4G35750	0.45	0.42	253163_at| Rho-GTPase-activating protein-related|
AT4G28260	0.68	0.64	253805_at| unknown protein|
AT5G52510	0.70	0.43	248366_at| scarecrow-like transcription factor 8 (SCL8)|
AT1G61690	0.71	0.59	264423_at| phosphoinositide binding|
AT3G13080	0.79	0.74	259937_s_at| MRP3__ATMRP3; ATPase, coupled to transmembrane movement of substances / chlorophyll catabolite transporter/ glutathione S-conjugate-exporting ATPase|
AT1G56140	0.91	0.60	262082_s_at| leucine-rich repeat family protein / protein kinase family protein|
AT5G47880	0.92	0.86	248749_at| ERF1-1 (EUKARYOTIC RELEASE FACTOR 1-1); translation release factor|
AT3G25800	0.97	0.67	259408_at| PDF1_PR 65__PP2AA2 (PROTEIN PHOSPHATASE 2A SUBUNIT A2); protein phosphatase type 2A regulator|
AT3G03070	1.08	1.06	258846_at| NADH-ubiquinone oxidoreductase-related|
AT3G23660	1.12	0.92	258097_at| transport protein, putative|
AT2G27730	1.13	0.61	266206_at| unknown protein|
AT1G70850	1.14	0.59	262260_at| MLP34 (MLP-LIKE PROTEIN 34)|
AT2G01100	1.18	0.49	262204_at| unknown protein|
AT2G41060	1.22	0.70	267050_at| RNA recognition motif (RRM)-containing protein|
AT2G31440	1.30	0.80	263247_at| protein binding|
AT5G65540	1.34	0.94	247171_at| unknown protein|
AT1G09390	1.36	1.01	264501_at| GDSL-motif lipase/hydrolase family protein|
AT5G57490	1.39	1.07	247923_at| VDAC4 (VOLTAGE DEPENDENT ANION CHANNEL 4); voltage-gated anion channel|
AT5G05730	1.40	1.24	250738_at| AMT1_TRP5_WEI2__ASA1 (ANTHRANILATE SYNTHASE ALPHA SUBUNIT 1); anthranilate synthase|
AT2G03480	1.41	0.72	265715_s_at| dehydration-responsive protein-related|
AT2G02160	1.41	0.97	266121_at| zinc finger (CCCH-type) family protein|
AT2G26640	1.56	1.46	267606_at| KCS11 (3-KETOACYL-COA SYNTHASE 11); acyl transferase/ catalytic/ transferase, transferring acyl groups other than amino-acyl groups|
AT1G19690	1.67	1.52	261147_at| binding / catalytic/ coenzyme binding|
AT1G79730	1.74	0.69	261347_at| ELF7 (EARLY FLOWERING 7)|
AT2G38730	1.79	1.15	266411_at| peptidyl-prolyl cis-trans isomerase, putative / cyclophilin, putative / rotamase, putative|
AT4G22120	1.93	0.74	254340_at| early-responsive to dehydration protein-related / ERD protein-related|
AT4G15570	1.95	0.70	245529_at| MAA3 (MAGATAMA 3)|
AT5G05670	2.19	0.61	250768_at| signal recognition particle binding|

Table S-4. *(Cont'd)* Expression levels of genes identified as preferentially expressed in the shoot apex by Expression Browser.

AGI Locus	Shoot Apex	Leaf 1 & 2	Affymetrix Annotation
AT5G40200	2.43	0.90	249396_at| DegP9 (DegP protease 9); catalytic/ protein binding / serine-type endopeptidase/ serine-type peptidase|
AT1G47860	3.33	1.13	261729_s_at|
AT2G22610	6.24	0.96	265349_at| kinesin motor protein-related

Table S-5. Expression levels of genes identified as preferentially expressed in the young leaf by Expression Browser.

AGI Locus	Shoot Apex	Leaf 1 & 2	Affymetrix Annotation
AT2G33810	0.07	0.20	267460_at| SPL3 (SQUAMOSA PROMOTER BINDING PROTEIN-LIKE 3); DNA binding / transcription factor|
AT3G62410	0.08	2.37	251218_at| CP12-2; protein binding|
AT1G20440	0.21	0.43	259570_at| RD17__COR47 (COLD-REGULATED 47)|
AT4G26060	0.29	0.52	253992_at| unknown protein|
AT4G25650	0.34	1.43	254021_at| ACD1-LIKE (ACD1-LIKE); 2 iron, 2 sulfur cluster binding / electron carrier/ oxidoreductase|
AT1G03290	0.35	0.45	264362_at| unknown protein|
AT3G44880	0.44	0.97	246335_at| LLS1_PAO__ACD1 (ACCELERATED CELL DEATH 1); iron-sulfur cluster binding / pheophorbide a oxygenase|
AT4G12360	0.48	1.17	254837_at| protease inhibitor/seed storage/lipid transfer protein (LTP) family protein|
AT5G40170	0.53	1.98	249393_at| AtRLP54 (Receptor Like Protein 54); kinase/ protein binding|
AT5G25350	0.55	0.88	246935_at| EBF2 (EIN3-BINDING F BOX PROTEIN 2); protein binding|
AT4G30390	0.57	0.66	253637_at| unknown protein|
AT4G17830	0.60	0.71	254690_at| peptidase M20/M25/M40 family protein|
AT5G66190	0.62	3.10	247131_at| ATLFNR1__FNR1 (FERREDOXIN-NADP(+)-OXIDORE-DUCTASE 1); NADPH dehydrogenase/ electron transporter, transferring electrons within the cyclic electron transport pathway of photosynthesis/ electron transporter, transferring electrons within the noncyclic electron transp|
AT1G17340	0.66	1.26	261060_at| phosphoinositide phosphatase family protein|
AT3G43800	0.68	1.94	252712_at| ATGSTU27 (GLUTATHIONE S-TRANSFERASE TAU 27); glutathione transferase|
AT2G45960	0.71	1.30	266927_at| ATHH2_PIP1;2_TMP-A__PIP1B (NAMED PLASMA MEM-BRANE INTRINSIC PROTEIN 1B); water channel|
AT1G75630	0.72	0.84	262924_s_at| AVA-P4; ATPase|
AT5G26740	0.76	0.88	246843_at| unknown protein|
AT3G03120	0.77	0.87	258876_at| ATARFB1C (ADP-ribosylation factor B1C); GTP binding|
AT3G09830	0.81	1.09	258650_at| protein kinase, putative|
AT4G14350	0.82	1.01	245608_at| protein kinase family protein|
AT3G15210	0.91	1.23	257053_at| ATERF-4_ATERF4_RAP2.5__ERF4 (ETHYLENE RESPONSIVE ELEMENT BINDING FACTOR 4); DNA binding / protein binding / transcription factor/ transcription repressor|
AT2G26080	0.91	1.87	266892_at| AtGLDP2 (Arabidopsis thaliana glycine decarboxylase P-protein 2); ATP binding / glycine dehydrogenase (decarboxylating)|
AT4G12800	0.92	2.32	254790_at| PSAL (photosystem I subunit L)|
AT1G64860	0.93	3.29	262879_at| RPOD1_SIG1_SIG2_SIGB__SIGA (SIGMA FACTOR A); DNA binding / DNA-directed RNA polymerase/ sigma factor/ transcrip-tion factor|

Table S-5. *(Cont'd)* Expression levels of genes identified as preferentially expressed in the young leaf by Expression Browser.

AGI Locus	Shoot Apex	Leaf 1 & 2	Affymetrix Annotation
AT1G06040	0.95	1.48	260956_at| STO (SALT TOLERANCE); DNA binding / protein binding / transcription factor/ zinc ion binding|
AT3G16370	0.96	2.17	259375_at| GDSL-motif lipase/hydrolase family protein|
AT4G28080	0.96	4.99	253849_at| binding|
AT1G27510	0.99	1.53	264437_at| INVOLVED IN: response to singlet oxygen; LOCATED IN: thylakoid membrane; EXPRESSED IN: 22 plant structures; EXPRESSED DURING: 13 growth stages; BEST Arabidopsis thaliana protein match is: EX1 (EXECUTER1) (TAIR:AT4G33630.2); Has 213 Blast hits to 208 proteins in 76 species: Archae - 0; Bacteria - 13; Metazoa - 63; Fungi - 31; Plants - 69; Viruses - 0; Other Eukaryotes - 37 (source: NCBI BLink).|
AT1G09570	1.03	1.18	264508_at| FHY2_FRE1_HY8__PHYA (PHYTOCHROME A); G-protein coupled photoreceptor/ protein histidine kinase/ red or far-red light photoreceptor/ signal transducer|
AT2G01450	1.04	1.08	266348_at| ATMPK17; MAP kinase|
AT3G45780	1.18	3.40	252543_at| JK224_NPH1_RPT1__PHOT1 (PHOTOTROPIN 1); FMN binding / blue light photoreceptor/ kinase/ protein binding / protein serine/ threonine kinase|
AT2G30600	1.31	3.13	267523_at| BTB/POZ domain-containing protein|
AT1G73190	1.40	2.12	260088_at| ALPHA-TIP__TIP3;1; water channel|
AT3G02450	1.46	1.85	258494_at| cell division protein ftsH, putative|
AT2G24400	1.56	1.68	265683_at| auxin-responsive protein, putative / small auxin up RNA (SAUR_D)|
AT2G06850	1.65	1.78	266215_at| EXT__EXGT-A1 (ENDOXYLOGLUCAN TRANSFERASE); hydrolase, acting on glycosyl bonds / xyloglucan:xyloglucosyl transferase|
AT2G40150	1.66	1.68	263386_at| INVOLVED IN: biological process unknown; EXPRESSED IN: 21 plant structures; EXPRESSED DURING: 13 growth stages; CONTAINS InterPro DOMAIN/s: Protein of unknown function DUF231, plant (InterPro:IPR004253); BEST Arabidopsis thaliana protein match is: ESK1 (ESKIMO 1) (TAIR:AT3G55990.1); Has 712 Blast hits to 693 proteins in 16 species: Archae - 0; Bacteria - 0; Metazoa - 0; Fungi - 0; Plants - 712; Viruses - 0; Other Eukaryotes - 0 (source: NCBI BLink).|
AT3G44890	1.69	4.39	246339_at| RPL9 (RIBOSOMAL PROTEIN L9); structural constituent of ribosome|
AT5G49910	1.86	3.07	248582_at| HSC70-7__CPHSC70-2EAT SHOCK PROTEIN 70-2 (CHLOROPLAST HEAT SHOCK PROTEIN 70-2); ATP binding / unfolded protein binding

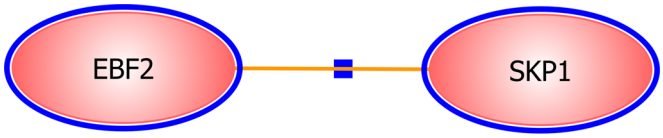

Figure S-8. A pathway diagram showing a direct relation between EBF2 and SKP1. Among 102 protein products of the young leaf, only EBF2 and SKP1 had a direct interaction. EIN3-BINDING F-BOX PROTEIN 2 (EBF2, encoded by At5g25350) is a component of F-box protein complex involved in ubiquitin-dependent protein catabolic process in response to ethylene stimulus. SKP1, Arabidopsis SKP1 homolog encoded by At1g75950, is a SCF ubiquitin-protein ligase interacting with UFO protein and regulate negatively DNA recombination. Orange line with blue square indicates these two proteins participate in binding.

Figure S-9. The relations among the shoot apex gene products involved in metabolic pathways. The pink ovals with blue overlay are proteins that have been curated in the pathway databases; those without overlay are the immediately neighboring entities that interact with those proteins. The yellow diamond shape indicates the biological process and green circle indicates a small molecule interacting with the gene product, which is sulfide in this case. The entities pointed by the arrow heads are the targets of regulation. The circled + and - sings indicates positive and negative regulation on the target, respectively.

The protein EARLY FLOWERING 7 (ELF7, encoded by AT1G79730) acts as a positive regulator for FLOWERING LOCUS C (FLC). The elevated FLC expression, which is the characteristic of nonvernalized winter annuals, requires ELF7 and ELF8, that are homologs of components of the Paf1 (RNA polymerase II associated factor 1) complex of *Saccharomyces cervisiae* (He *et al*., 2004). The yeast Paf1 complex, composed of Paf1, Ctr9, Cdc73, Rtf1, and Leo1, associates with RNA polymerase II at promoters and in the actively transcribed portions of mRNA genes (Porter *et al*., 2005). Meanwhile, EARLY FLOWERING 6 (REF6, encoded by AT3G48430) plays role as an FLC repressor in the FCL-dependent pathway, which is one of the pathways controlling flowering in Arabidopsis thaliana (Noh *et al*., 2004).

The eukaryote RELEASE FACTOR 1 (eRF1, encoded by AT5G47880) is one of two polypeptide chain release factors on the ribosome, which govern termination of translation in eukaryotes. The eRF1 promotes stop-codon-dependent hydrolysis of peptidyl-tRNA, and the eukaryote RELEASE FACTOR 3 (eRF3) interacts with eRF1 and stimulates eRF1 activity in the presence of GTP. In ribosomes, uncoupling of the peptidyl-tRNA and GTP hydrolyses are mediated by the formation of the ternary eRF1-eRF3-GTP complex (Frolova *et al*., 1996).

CYP90D1 (CYTOCHROME P450, FAMILY 90, SUBFAMILY D, POLYPEPTIDE 1; encoded by AT3G13730) is involved in brassinosteroid biosynthesis pathway (Kim *et al*., 2005a) and synthesis of dhurrin, a tyrosine derived cyanogenic glucoside (Keilsen *et al*., 2008).

AST91 (SULFATE TRANSPOTER 91, encoded by AST91) up-regulates key reactions of sulfate reduction as well as of cysteine, methionine and glutathione synthesis, but none of the known sulfur-deficiency induced sulfate transporter genes (Jost *et al*., 2005).

ASA1 (ANTHRANILATE SYNTHASE alpha1 gene (AT5G05730) encodes alpha-subunits of anthranilate synthase, a rate-limiting enzyme of Trp biosynthesis. Up-regulation of ASA1 by ethylene stimulus results in the accumulation of auxin, whereas loss-of-function mutation in this gene prevents the ethylene-stimulated auxin biosynthesis (Ivanchenko *et al*., 2008; Stepanova *et al*., 2005).

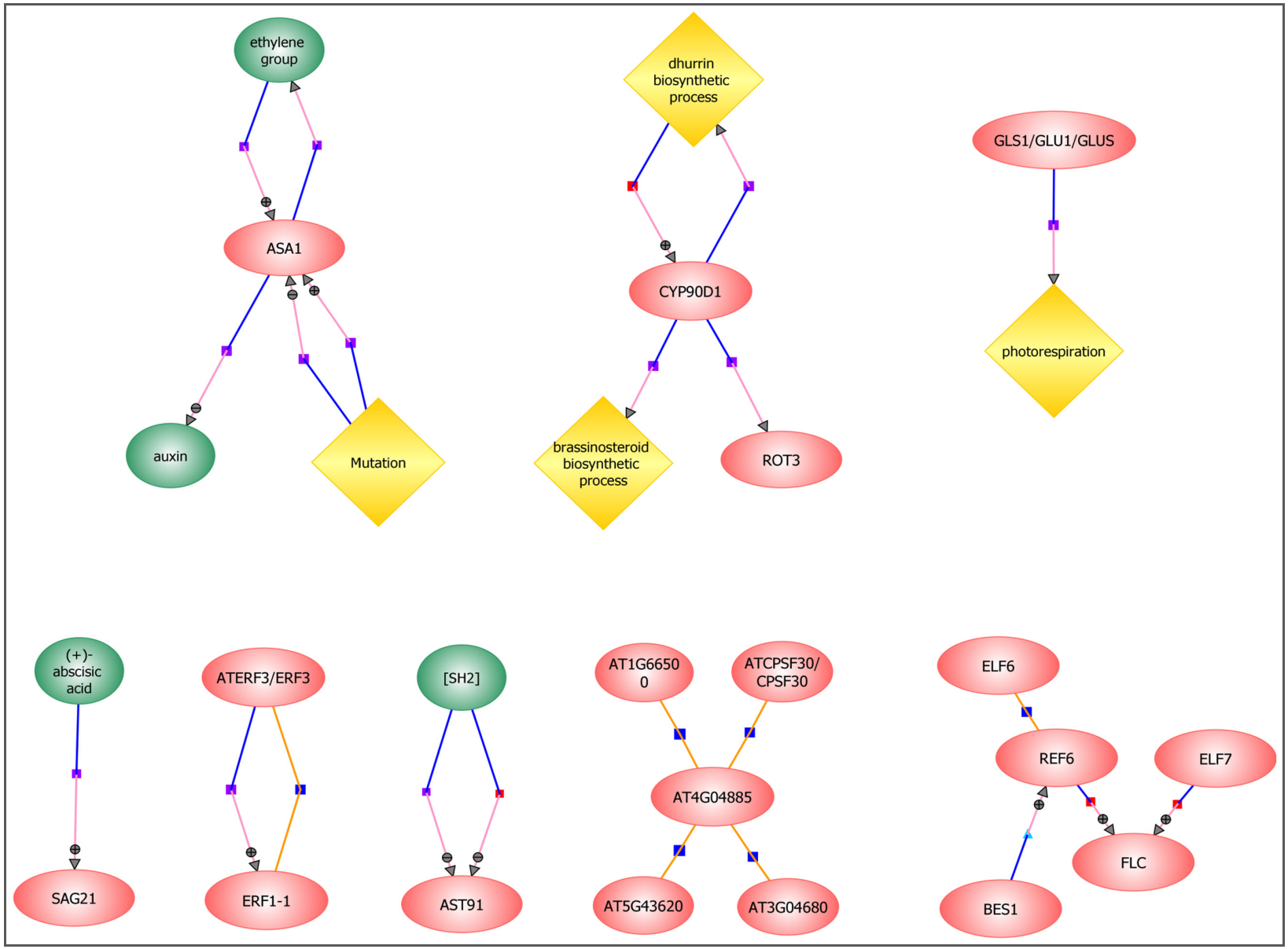
ethylene group
ASA1
auxin
Mutation
dhurrin biosynthetic process
CYP90D1
brassinosteroid biosynthetic process
ROT3
GLS1/GLU1/GLUS
photorespiration
(+)-abscisic acid
SAG21
ATERF3/ERF3
ERF1-1
[SH2]
AST91
AT1G66500
ATCPSF30/CPSF30
AT4G04885
AT5G43620
AT3G04680
ELF6
REF6
ELF7
FLC
BES1

Figure S-10. Localization of the shoot apex gene products in the cellular components. Four proteins were localized in the mitochondria (AT2G03480, AT2G27730, AT3G03070 and AT5G57490) and three were in the chloroplasts (AT1G19690, PSBR and TGD2). In the endoplasmic reticulum, two gene products were identified: AT2G47760 and AT5G05670. Another 2 proteins, AT1G56140 and AT3G23750, were localized in the plasma membrane. AT3G23660 localized in the Golgi apparatus, and three (FIF7, BES1, AT3G04680) in the nucleus. Among 46 cytosol-located gene products, nine had relations with other entities (previously shown in Figure S-9 on page 147). The pink ovals with blue overlay are proteins that were expressed preferentially in the young leaf; those without overlay are the immediately neighboring entities that interact with those proteins. The yellow diamond shape indicates the biological process and green circle indicates a small molecule interacting with the gene product, such as hormones and ions, or environmental factors, such as light. Arrow heads indicate the targets of regulation. The circled + and - sings indicates positive and negative regulation on the target, respectively. Lines without arrow heads represent binding activity between the two entities

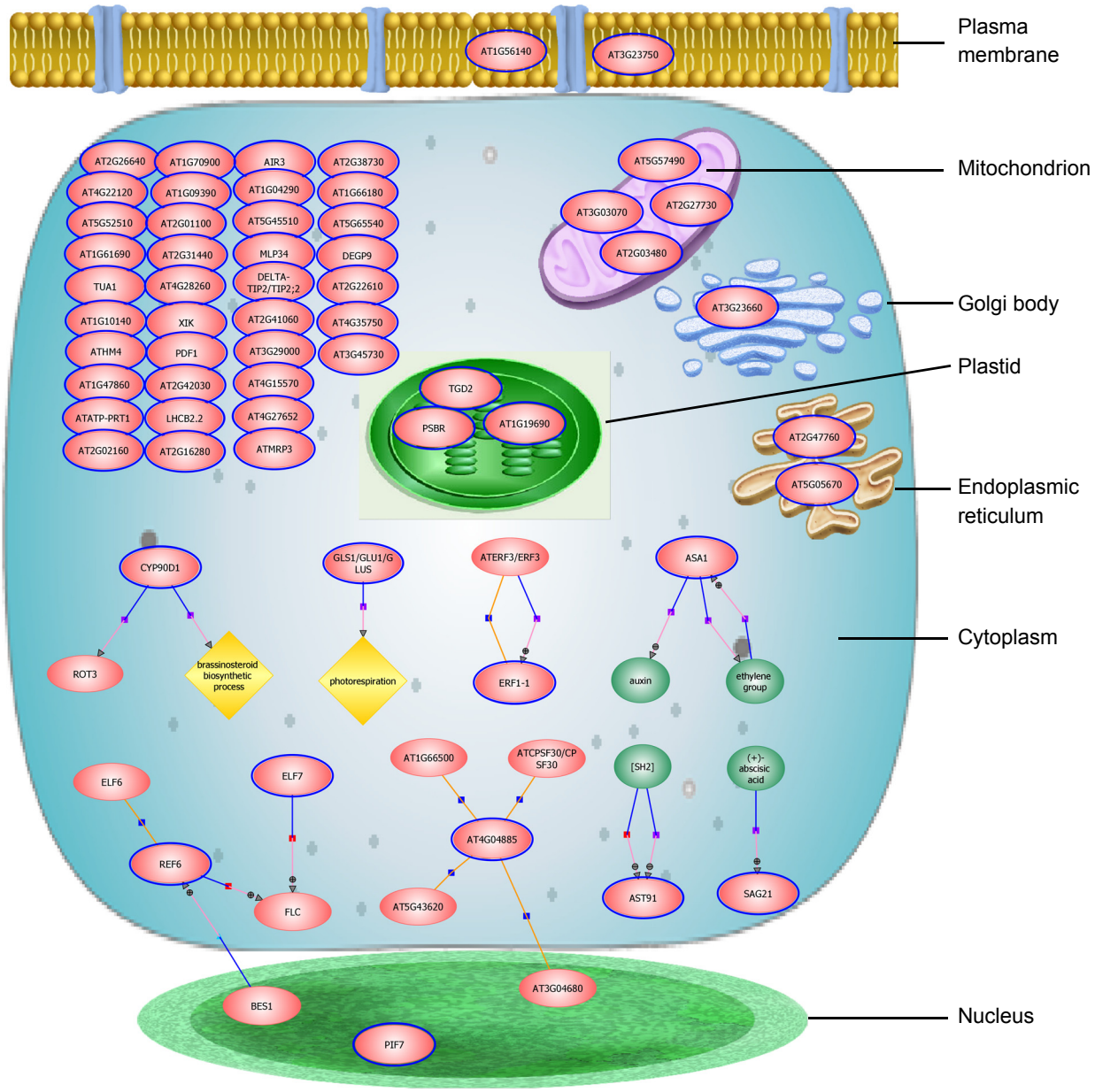
Plasma membrane
Mitochondrion
Golgi body
Plastid
Endoplasmic reticulum
Cytoplasm
Nucleus
AT1G56140
AT3G23750
AT2G26640
AT1G70900
AIR3
AT2G38730
AT4G22120
AT1G09390
AT1G04290
AT1G66180
AT5G52510
AT2G01100
AT5G45510
AT5G65540
AT1G61690
AT2G31440
MLP34
DEGP9
TUA1
AT4G28260
DELTA-TIP2/TIP2;2
AT2G22610
AT1G10140
XIK
AT2G41060
AT4G35750
ATHM4
PDF1
AT3G29000
AT3G45730
AT1G47860
AT2G42030
AT4G15570
ATATP-PRT1
LHCB2.2
AT4G27652
AT2G02160
AT2G16280
ATMRP3
AT5G57490
AT3G03070
AT2G27730
AT2G03480
AT3G23660
TGD2
PSBR
AT1G19690
AT2G47760
AT5G05670
CYP90D1
GLS1/GLU1/GLUS
ATERF3/ERF3
ASA1
ROT3
brassinosteroid biosynthetic process
photorespiration
ERF1-1
auxin
ethylene group
ELF6
ELF7
AT1G66500
ATCPSF30/CPSF30
[SH2]
(+)-abscisic acid
REF6
AT4G04885
FLC
AT5G43620
AST91
SAG21
BES1
AT3G04680
PIF7